Organic Carbon Pools in Permafrost-Affected Soils of Siberian Arctic Regions

Dissertation

zur Erlangung des Doktorgrades

der Naturwissenschaften im Fachbereich Geowissenschaften

der Universität Hamburg

vorgelegt von

Sebastian Zubrzycki

aus

Starogard in Polen

Hamburg 2013

Als Dissertation angenommen vom Fachbereich Geowissenschaften der Universität Hamburg

auf Grund der Gutachten von Prof. Dr. Eva-Maria Pfeiffer

und Prof. Dr. Lars Kutzbach

Hamburg, den 23.01.2013

Prof. Dr. Christian Betzler

Leiter des Fachbereichs Geowissenschafen

Contents

I. Summary

Permafrost-affected soils of the Lena River Delta (Northern Siberia) and its hinterland are characterized by a high diversity. The three main soil groups of the permafrost-affected soils, which are organic-rich Histels, cryoturbated Turbels and mineral and non-cryoturbated Orthels, include a large variety of subgroups. This variability formed while time, temperature, and water saturation strongly slowed the soil-forming processes. These diverse North-Siberian soils have been only scarcely investigated by soil scientists so far, although they play a major role in global long-term carbon sequestration. Permafrost-affected soils started to attract broader attention since increasing knowledge about the carbon storage of these soils has been coupled with future climate trend projections indicating the potential of a positive feedback loop of warming when the predicted release of "permafrost carbon" will increase the greenhouse effect. Despite their small thickness of few decimetres, these soils and their carbon storage might play an important role in affecting the future climate when one considers the projected increases of temperature and recent models of the active layer depth development. The question if they are still sequestering carbon is still controversially discussed and will have different answers for different permafrost regions.

Approaches to determine the carbon source and sink functions of permafrost-affected soils require robust knowledge of the recent carbon storage of these soils, which is where this thesis begins. Here the author provides the first robust estimates of the carbon storage of the modern, Holocene geomorphologic units of the Lena River Delta as well as estimates of the carbon stocks of the seasonally thawed layer from a latitudinal transect in Northeast-Siberia extending from the Lena River Delta into its hinterland. For the area of the Lena River Delta, he also reports total nitrogen stocks.

The Lena River Delta, which is the largest delta in the Arctic, extends over an area of 32,000 km² and likely holds the major part of the soil organic carbon mass stored in the seven major deltas in the northern permafrost regions. The geomorphologic units of the Lena River Delta, which were formed by true deltaic sedimentation processes are a Holocene river terrace and active – still regularly flooded – floodplains. Their mean soil organic carbon stocks for the upper 1 m of soils were estimated at 29 kg m^{-2} ± 10 kg m^{-2} and at 14 kg m^{-2} ± 7 kg m^{-2},

respectively. For the depth of 1 m, the total soil organic carbon storage of the Holocene river terrace was estimated at 121 Tg ± 43 Tg, and the soil organic carbon storage of the active floodplains was estimated at 120 Tg ± 66 Tg. The mass of soil organic carbon stored within the observed seasonally thawed active layer was estimated at about 127 Tg assuming an average maximum active layer depth of 50 cm. The soil organic carbon mass that is stored in the perennially frozen ground below the average maximum active layer, which is excluded from intense biogeochemical exchange with the atmosphere, was estimated at 113 Tg. The mean nitrogen stocks for the upper 1 m of soils were estimated at 1.2 kg m^{-2} ± 0.4 kg m^{-2} for the Holocene river terrace and 0.9 kg m^{-2} ± 0.4 kg m^{-2} for the active floodplain levels, respectively. For the depth of 1 m, the total nitrogen storage of the river terrace was estimated at 4.8 Tg ± 1.5 Tg, and the total nitrogen storage of the floodplains at 7.7 Tg ± 3.6 Tg. Considering the projections for deepening the seasonally thawed active layer up to 120 cm in the Lena River Delta region within the 21st century, these large carbon and nitrogen stocks could become increasingly available for decomposition and mineralization processes.

Twelve sites along a north-south latitudinal transect in Siberia were investigated to classify the soils and to determine their soil organic carbon stocks in the top 30 cm of the seasonally thawed layer, which was shallower compared to the intensive delta study mentioned above. There was a distinct arrangement into three groups of increasing soil organic carbon stocks along the transect with decreasing latitude. The greatest stocks, with mean values of 24 kg m^{-2} ± 9 kg m^{-2} were identified for the southern group of forest tundra and taiga sites on the ancient Central Siberian Plateau. The soils of Lena River Delta's first and third river terraces had stocks of on average 12 kg m^{-2} ± 3 kg m^{-2} whereas the sand-dominated north-western part of the delta, the second river terrace, stored only 4 kg m^{-2} ± 2 kg m^{-2} in the top 30 cm of the soils. The climatological gradient with changing vegetation productivity and different parent materials result in varying pedogenetic processes and were identified as key controls on the soil organic carbon stocks.

Using the linear increase of the cumulative soil organic stock size with increasing soil depth determined for the investigated Lena River Delta soils in a regression model, the organic carbon stocks of soils investigated within the latitudinal transect are likely to reach up to 80 kg m^{-2} within a depth of 100 cm. The results of the pilot study encourage continuing the

organic carbon quantification studies within this region to gain a more detailed knowledge about the soils of the unique and various landscapes of Northeast-Siberia.

Zusammenfassung

Die von Permafrost beeinflussten Böden des nordostsibirischen Lenadeltas und seines Hinterlandes sind durch eine sehr hohe Diversität charakterisiert. Die drei Bodenhauptgruppen der von Permafrost beeinflussten Böden, die organikreichen Histels, die kryoturbierten Turbels und die mineralischen und nicht-kryoturbierten Orthels, umfassen eine große Variabilität an untergeordneten Bodeneinheiten. Diese Variabilität entstand, obwohl Zeit, Temperatur und Wassersättigung die bodenbildenden Prozesse stark verlangsamten. Diese diversen, von Permafrost beeinflussten sibirischen Böden wurden bisher nur unzureichend bodenwissenschaftlich untersucht, obwohl sie bei der globalen Langzeit-Kohlenstoff-Sequestrierung eine entscheidende Rolle spielen. Sie gewannen erst an Bedeutung als das wachsende Wissen über die Kohlenstoffvorräte dieser Böden im Zusammenhang mit den aktuellen Projektionen zum zukünftigen, globalen Klima betrachtet wurden. Diese könnten in einem sich selbst verstärkenden Kreislauf resultieren, wenn freigesetzter „Permafrost-Kohlenstoff“ den Treibhauseffekt verstärken würde. Obwohl nur wenige Dezimeter mächtig, werden diese Böden mit ihren Vorräten an Kohlenstoff möglicherweise eine entscheidende Rolle bei der Entwicklung des zukünftigen Klimas spielen, wenn die aktuellen Projektionen zum Temperaturanstieg und die aktuellen Modelle zur Entwicklung der Mächtigkeit der saisonalen Auftauschicht betrachtet werden. Die Frage, ob diese Böden immer noch Kohlenstoff sequestrieren, wird noch kontrovers diskutiert und wird wahrscheinlich unterschiedliche Antworten aus unterschiedlichen permafrost-beeinflussten Regionen liefern.

Ansätze zur Beantwortung der Frage nach einer Kohlenstoff-Quellen- und Kohlenstoff-Senkenfunktion der von Permafrost beeinflussten Böden brauchen belastbares Wissen über die rezenten Kohlenstoffvorräte dieser Böden. Und genau hier setzt diese Arbeit an. Der Autor liefert eine erste robuste Abschätzung der Kohlenstoffvorräte in den modernen holozänen geomorphologischen Einheiten des Lenadeltas und darüber hinaus eine Abschätzung der Kohlenstoffgehalte in der saisonalen Auftauschicht entlang eines Nordsüd-Transekts im Nordosten Sibiriens, welcher sich vom Lenadelta bis zu seinem Hinterland erstreckt. Für den Bereich des Lenadeltas werden auch die Stickstoffvorräte geschätzt.

Das Lenadelta, das größte arktische Delta, erstreckt sich über eine Fläche von 32.000 km² und speichert wahrscheinlich einen Großteil des Gesamtkohlenstoffvorrats der sieben größten Deltas der nördlichen permafrostbeeinflussten Regionen. Zu den geomorphologischen Einheiten des Lenadeltas, welche durch echte fluviatile Sedimentationsprozesse entstanden sind, gehören die holozäne Flussterrasse und aktive Überflutungsebenen. Ihr mittlerer Gehalt an organischem Kohlenstoff im oberen Meter des Bodens wurde auf 29 kg m^{-2} ± 10 kg m^{-2} beziehungsweise auf 14 kg m^{-2} ± 7 kg m^{-2} geschätzt. Für die Tiefe von einem Meter liefert die Schätzung einen Kohlenstoffvorrat in der holozänen Flussterrasse von 121 Tg ± 43 Tg. Die aktiven Überflutungsebenen speichern 120 Tg ± 66 Tg. Der Kohlenstoffvorrat der beobachteten saisonalen Auftauschicht wurde auf circa 127 Tg geschätzt, wenn eine durchschnittliche maximale Tiefe von 50 cm angenommen wird. Der Kohlenstoffvorrat, welcher im Permafrost unter der Auftauschicht gespeichert vorliegt und nicht von intensiven biogeochemischen Austauschprozessen mit der Atmosphäre beeinflusst wird, wurde auf 113 Tg geschätzt. Die mittleren Stickstoffgehalte im ersten Meter der Böden wurden auf 1,2 kg m^{-2} ± 0,4 kg m^{-2} für die holozäne Flussterrasse und auf 0,9 kg m^{-2} ± 0,4 kg m^{-2} für die aktiven Überflutungsebenen geschätzt. Für die Tiefe von einem Meter beträgt der Vorrat des Gesamtstickstoffs der Flussterrasse 4,8 Tg ± 1,5 Tg und der Überflutungsebene 7,7 Tg ± 3,6 Tg. Unter den Annahmen der Projektionen der Entwicklung der Mächtigkeit der saisonalen Auftauschicht wird diese bis zu 120 cm im Bereich des Lenadeltas im 21. Jahrhundert erreichen. Demzufolge würden die großen Kohlenstoff- und Stickstoffvorräte verstärkt für Abbau- und Mineralisationsprozesse verfügbar sein.

Zwölf Standorte entlang eines Nordsüd-Transekts im Nordosten Sibiriens wurden untersucht, um die Böden zu klassifizieren und ihre Gehalte an organischem Kohlenstoff in den oberen 30 cm der saisonalen Auftauschicht zu quantifizieren. Die Auftauschicht dieser Gebiete war im Mittel nicht so tief wie die, der intensiven Studie im Lenadelta. Bei der Betrachtung der Gehalte des organischen Kohlenstoffs wurde eine Anordnung in drei Gruppen offensichtlich. Innerhalb dieser Gruppen nahm der Kohlenstoffgehalt bei abnehmender nördlicher Breite zu. Die höchsten Gehalte wurden an den südlichsten Standorten, nämlich der Waldtundra und Taiga des geologisch alten Zentralsibirischen Plateaus identifiziert. Sie betrugen im Mittel 24 kg m^{-2} ± 9 kg m^{-2}. Die Böden der ersten und dritten Flussterrasse des Lenadeltas wiesen

mittlere Kohlenstoffgehalte von 12 kg m^{-2} ± 3 kg m^{-2} auf, wohingegen die Böden des sanddominierten nordwestlichen Teils des Deltas, der zweiten Flussterrasse, nur 4 kg m^{-2} ± 2 kg m^{-2} in den oberen 30 cm beherbergten. Der klimatische Gradient mit sich ändernder Produktivität der Vegetation und unterschiedliches Ausgangsmaterial mit variierenden pedogenetischen Prozessen wurden als die Schlüsselprozesse identifiziert, welche die Höhe der Kohlenstoffgehalte steuern.

Unter Zuhilfenahme der kumulierten Gehalte an organischem Kohlenstoff der intensiven Bodenstudie im Lenadelta, welche mit zunehmender Profiltiefe annähernd linear steigen und unter Anwendung des dazugehörigen Regressionsmodells, beträgt der Gehalt des organischen Kohlenstoffs der im Nordsüd-Transekt untersuchten Böden möglicherweise bis zu 80 kg m^{-2} innerhalb der oberen 100 cm der Böden. Die Ergebnisse dieser Pilotstudie verdeutlichen die Bedeutung der Fortführung der Quantifizierungsstudien der Kohlenstoffgehalte dieser Regionen. Diese werden zur Vergrößerung des Wissens über die Böden der einzigartigen und mannigfaltigen Landschaften Nordost-Sibiriens beitragen sowie deren Bedeutung für globale Kohlenstoff-Flussbilanzen detaillierter darstellen.

II. List of Tables

III. List of Figures

IV. List of Symbols and Abbreviations

A_f	degree of activity
bhp	brake horsepower
BS	base saturation
CEC	cation exchange capacity
cvg	coverage
d	day
dB(A)	A-weighted decibels
DEM	digital elevation model
EC	electrical conductivity
Gt	Gigatonn
h	hour
IC	inorganic carbon
KA5	German key for soil classification (Bodenkundliche Kartieranleitung)
kyr	thousand years
LOI	loss on ignition
M	mole

N	number
NCSCD	Northern Circumpolar Soil Carbon Database
n.d.	not determined
OC	organic carbon
Pg	Petagram
R	Pearson product-moment correlation coefficient
rpm	rotation per minute
S	Siemens
SC	soil complex
SD	standard deviation
SE	standard error
SEE	standard error of the estimate
SIPRE	Snow-Ice-Permafrost-Research-Establishment
SOC	soil organic carbon
Tg	Teragram
UTM	Universal Transverse Mercator
WGS	World Geodetic System

1. Introduction

Permafrost-affected soils have accumulated enormous pools of organic matter during the Quaternary Period (Harden *et al.* 1992, Smith *et al.* 2004, Zimov *et al.* 2006a, Gorham *et al.* 2007). The area occupied by permafrost-affected soils amounts to more than 8.6 million km^2, which is about 27 % of all land areas north 50° N (Jones *et al.* 2010). Due to these facts, permafrost-affected soils are considered as one of the most important cryosphere elements within the climate system. Due to the cryopedogenic processes that form these particular soils and the overlying vegetation that is adapted to the arctic climate, organic matter has accumulated to the extent that today there might be up to 1024 Pg (1 Pg = 10^{15} g = 1 Gt) of soil organic carbon stored within the uppermost three meters of ground (Tarnocai *et al.* 2009). Progressive climate change has already been observed, and with projected polar amplification (Lembke *et al.* 2007), permafrost-affected soils will undergo fundamental property changes (Anisimov and Nelson 1997, McGuire *et al.* 2009, Grosse *et al.* 2011, Koven *et al.* 2011). As an essential effect of these changes, higher turnover and mineralization rates of the organic matter are expected to result in an increased climate-relevant trace gas release to the atmosphere (Dutta *et al.* 2006, Wagner *et al.* 2007, Khvorostyanov *et al.* 2008, Schuur *et al.* 2009). Beer (2008) assumed this organic matter mobilisation to likely result in a positive feedback loop of warming when the increased release of methane and carbon dioxide from thawed permafrost-affected soils will enhance the greenhouse effect. Therefore, permafrost regions with their particular soils potentially could trigger an important tipping point of the global climate system (Lenton and Schellnhuber 2010), with additional political and social implications. However, the question of whether permafrost regions are already a carbon source (Oechel *et al.* 1993, Zimov *et al.* 1997, Oechel *et al.* 2000) or even still accumulate carbon (Corradi *et al.* 2005, Kutzbach *et al.* 2007, van der Molen *et al.* 2007) could not be satisfactorily answered until today.

To answer this question, it is necessary to find a suitable small-scale approach and subsequent techniques to upscale the results. With this work, the author has done a first step to answer the question on the carbon sink and source function of permafrost-affected soils. The extensive soil investigations continuing the long-term research done within the frame of Russian-German cooperation projects will fill a knowledge gap caused by a long-lasting neglect of

considerable areas of Russia in terms of soil cover. Around 70 % of the land area of Russia was not taken into account when a national Soviet soil classification key was developed in 1977. No permafrost-affected soils were included (Anon 1986).

The presented soil mapping and soil property results indicate a large diversity of permafrost-affected soils developing in the severe environments of the Siberian Arctic. These soils develop within a shallow layer of 30...50 cm thickness that thaws annually for only few weeks during the summer period. The soil survey results serve as a basis for following investigations describing in detail the stocks of soil organic carbon and total nitrogen of extensive areas in the arctic. Such descriptions are necessary to assess especially the carbon storage of the permafrost layers, where the carbon is currently excluded from biogeochemical cycles.

This work provides new insights into the stocks of carbon and nitrogen. An increased focus on this subject, especially in underrepresented Siberian regions, could contribute to more robust estimations of the soil organic carbon pool of permafrost regions as well as to better understanding of the carbon sink and source functions of permafrost-affected soils. The most up-to-date carbon storage estimates show that the storage of organic matter in the northern circumpolar permafrost regions is high at 496 Pg of carbon within the uppermost one meter of ground and up to 1024 Pg within the uppermost three meters (Tarnocai *et al.* 2009). The data resulting in these estimates are not well distributed over the entire circumpolar permafrost regions since especially soil carbon pool data from Siberia are scarce. The author of this thesis provides new data and enhanced estimates for underrepresented regions of the Russian Arctic. Although the area occupied by the main arctic deltas as mentioned by Walker (1998) amounts only to 77,000 km² which is just around 1 % of the total area of arctic and alpine tundra of 7.4 10^6 km^2 according to Loveland *et al.* (2000), the contribution of these deltas to the total soil organic carbon pool within the permafrost-underlain areas is high due to the estimated large thickness of their deposits (Tarnocai *et al.* 2009). The size of the delta investigated in the context of this work amounts to 32,000 km² and is the largest arctic delta. Hence, the results and estimates derived in this region have a large importance for the entire arctic delta regions. The results of this study will be integrated into Northern Circumpolar Soil Carbon Database (Tarnocai *et al.* 2007, Hugelius *et al.* 2012) improving its quality.

1.1 Aims and objectives

Primary objectives of the presented thesis are directed to the above described open questions about the permafrost-affected soils and the portions of carbon and nitrogen stored within the perennially frozen layers that are currently excluded from the biogeochemical cycles. Important elements of this work are: (1) soil mapping of not yet investigated areas of the Lena River Delta's oldest terrace of Middle and Late Pleistocene age and (2) soil investigations along a latitudinal transect in Northeast-Siberia, (3) core and outcrop sampling of soils at representative sites of the investigated areas as well as analyses of their chemical and physical properties, (4) collection and analyses of frozen one-meter soil cores drilled by a new permafrost auger (5) and calculations of soil organic carbon (SOC) stocks and total nitrogen (TN) stocks for all collected cores. (6) Storage estimations of SOC and TN for the areas of deltaic origin in the Lena River Delta using remote sensing information complete this work.

1.2 Chapter overview

The study was written in the form of four main chapters representing independent but successive work packages. The presented chapters partly have been published or are prepared for publication (Tab. 1). Overlapping statements and repetition of general information may occur due to the article-like structure.

The chapter 2 "Permafrost-Affected Soils and their Carbon Pools – State-of-the-Art" is devoted to provide a broad and detailed background description for the following studies at the same time. In this chapter, definitions are clarified, and the current state of research is discussed providing an overview of permafrost-affected soils and their carbon-related functions. In the comprehensive chapter 3 "Diversity of Permafrost-Affected Soils in Northern Siberia", a detailed description of the manifold permafrost-affected soils investigated in Northeast-Sibera is given. Detailed soil investigations are the matter of the following chapters. In chapter 4 "Soil Organic Carbon and Nitrogen Stocks in the Lena River Delta", the attention is devoted to the quantification of the important stocks of organic carbon

and total nitrogen on Samoylov Island and to provide a carbon and nitrogen storage estimate for the deltaic areas of the Lena River Delta.

Table 1: Overview of publications presented within this thesis.

Tab. 1: Übersicht der in dieser Arbeit präsentierten Publikationen.

Publication	Remarks	Chapter
Zubrzycki, S., Kutzbach, L., and Pfeiffer, E.-M. 2012: Böden in Permafrostgebieten der Arktis als Kohlenstoffsenke und Kohlenstoffquelle. Polarforschung 81(1): 33-46.	slightly modified version, original in german	Chapter 2
Zubrzycki, S., Kutzbach, L., Grosse, G., Desyatkin, A., and Pfeiffer, E.-M. 2013: Organic Carbon and Total Nitrogen Stocks in Soils of the Lena River Delta. Biogeosciences, 10, 3507-3524, doi:10.5194/bg-10-3507-2013.	modified version	Chapter 4
Zubrzycki, S. 2012: Drilling frozen soils in Siberia. Polarforschung 81(2): 151-153.	modified version	Chapter 4.3.1
Zubrzycki, S., Kutzbach, L., Vakhrameeva, P., and Pfeiffer, E.-M. 2012: Variability of Soil Organic Carbon Stocks of Different Permafrost Soils: Initial Results from a North-South Transect in Siberia. In: Hinkel, K.M. (Eds.) Proceedings of the 10th International Conference on Permafrost. Salekhard, pp. 485-490.	slightly modified version	Chapter 5

Chapter 5 “Soil Organic Carbon in the Active Layer in Soils from a Latitudinal Transect” provides first insights to the carbon stocks within the seasonally thawed layer of different permafrost-affected soils of three different geomorphic and vegetational units of Northeast-Siberia. The chapter 6 “Synthesis and conclusions” is giving an overall recapitulation of the study results, and points to selected open questions where future research work may be directed to.

1.3 Authors’ contribution

Because of the multidisciplinary character of the investigations, several co-authors contributed to the published papers (Tab. 1). As first author, Sebastian Zubrzycki designed the studies, reviewed the relevant literature, collected the samples and the data, conducted all analyses and interpretation of the data, coordinated and wrote the publications, and created most of the figures. The publication based on chapter 2 was critically reviewed and discussed

by the co-authors. Additionally, E.-M. Pfeiffer provided photographs for Figure 1. L. Kutzbach provided information for Table 3 as well as Figure 10, Figure 11, and Figure 13. Chapter 4 was critically reviewed and discussed by the co-authors. G. Grosse provided the Landsat-7 ETM+ and WorldView-1 remote sensing imagery of the Lena River Delta as well as the accuracy assessment of the satellite image classification. A. Desyatkin partly contributed to the sample collection. The co-authors of the paper, based on chapter 5, provided helpful reviews. P. Vakhramaeeva, in addition, provided the names of the described sites. These site names were also used in chapter 3.

2. Permafrost-Affected Soils and their Carbon Pools – State-of-the-Art

2.1 Introduction

In wide areas of the high latitudes of Northern Europe, Greenland, Canada, Alaska and Russia, a particular group of soils has developed during the Quaternary whose diversity is based primarily on special cryopedogenetic processes within the pedosphere of our Earth system. Among the most important cryopedogenetic processes are the cryogenic weathering (frost wedging), ice segregation and accumulation (by increased freezing on of water on existing ice lenses), cryoturbation (mixing of soils by repeated freezing and thaw and, consequently, expansion and contraction processes), cryometamorphosis (transformation of soil structures due to ice), gelifluction (slow, wide-area downflow of soil material of the thaw layer on slopes with an inclination of > 2 °), frost heave, frost sorting (material dislocation caused by the increase in volume during the freezing of water) and frost crack formation (due to the contraction of the frozen soil at very low temperatures) (Fig. 1).

The areas of the northern hemisphere underlain by permafrost extend over almost 23 million km^2, approximately one quarter of their total land surface (Baranov 1959, Shi 1988, Zhang 1999, 2003, French 2007). They are called permafrost areas if their subsurface soils and sediments maintain temperatures of 0 °C or below during two consecutive years (van Everdingen 1998) (see Fig. 2A). Under this definition, the ground water - if it contains many dissolved substances or is held in fine pores – can also exist in liquid form in permafrost. In order to unambiguously demarcate permafrost from the supra permafrost above it, the term *cryotic* (temperature < 0 °C) was introduced (French 2007). In addition to this point of view, which focuses on the ground temperature regime and designates the boundary of the ground that is permanently below 0 °C as the so-called permafrost table, there is another point of view that focuses on the thaw-freeze cycle. This distinguishes, in the upper ground area, the seasonal thaw layer from the underlying permanently frozen ground (Fig. 2B).

A spatial differentiation of the permafrost areas is based on the portion of the areas on top of the permafrost in relation to the total surface of an area in continuous, discontinuous, and

sporadic and isolated permafrost. In addition to the high latitudes of the northern hemisphere, permafrost and permafrost-affected soils are also found in the mountains of the earth and the ice-free areas of Antarctica; there, however, only in small portions of the surface (0.35 % of Antarctica) (Bockheim 1995, Vieira *et al.* 2010). The Antarctic permafrost-affected soils represent special, extremely cold and salt-rich habitats (Bockheim 1979, 2002, Bockheim and McLeod 2008).

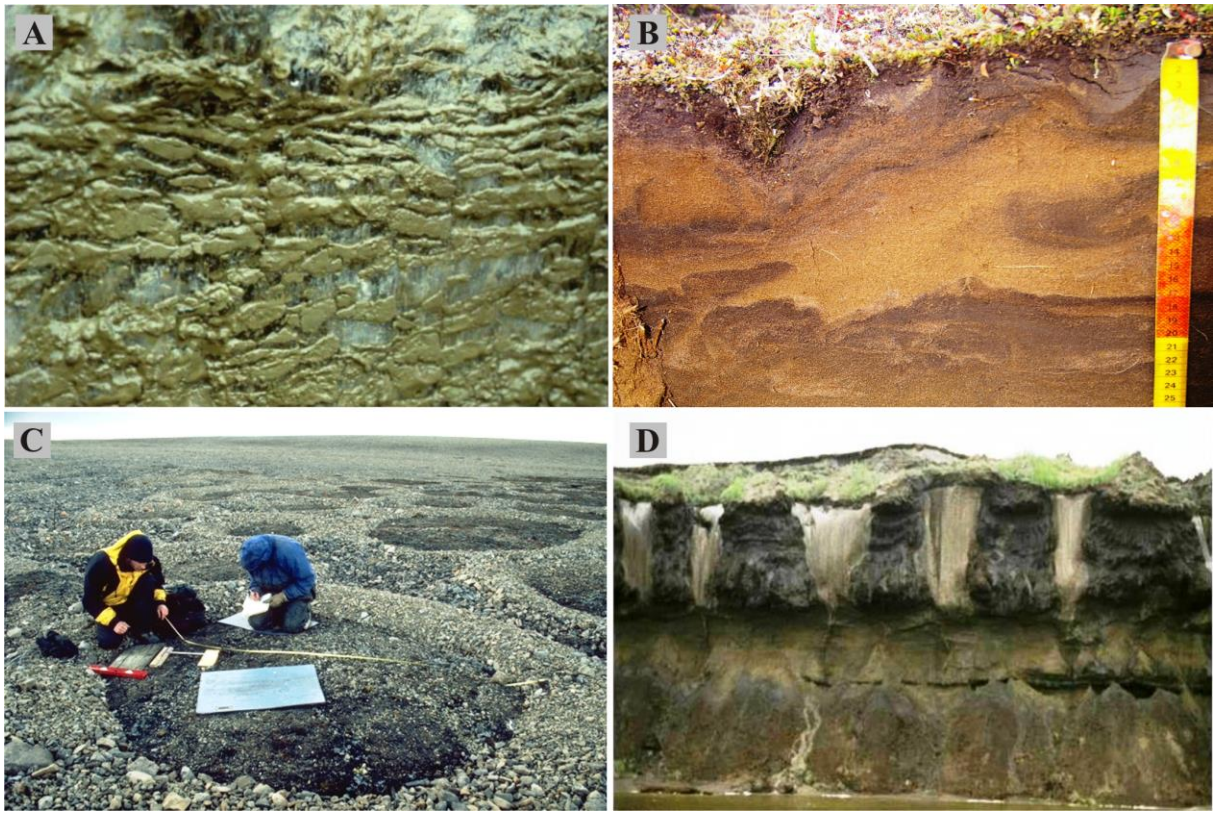

Figure 1: Results of cryopedogenic processes in permafrost. A = Segregated ice, Lena River Delta, Siberia 2007. B = Cryoturbation in the top soil of a Gelisol (Typic Psammoturbel), Arga Complex, northwestern Lena River Delta, Siberia 2009. C = Sorted circles (frost patterns) formed by frost sorting, Brøgger Peninsula, Spitsbergen, 1999. D = Ice wedges, cliff exposure at the Olenyokskaya Channel, Lena River Delta, Siberia 2007. A, B, D own photos, C Julia Boike.

Fig. 1: Ergebnisse kryopedogenetischer Prozesse im Permafrost. A = Segregationseis, Lena-Delta, Sibirien 2007. B = Kryoturbation im Oberboden eines Gelisols (*Typic Psammoturbel*), Arga-Komplex, nordwestliches Lena-Delta, Sibirien 2009. C = Sortierte Kreise als eine Form von Frostmustern, die durch Frostsortierung entstehen, Brøggerhalbinsel, Spitzbergen, 1999. D = Eiskeile, aufgeschlossen an einem Kliff im Olenyokskaya Kanal, Lena-Delta, Sibirien 2007. Aufnahmen: A, B, D eigene Bilder, C Julia Boike.

The extension of the terrestrial permafrost areas does not entirely correspond to the extension of the permafrost-affected soils. These soils form their own class or reference group of the highest category in the various international soil systematics.

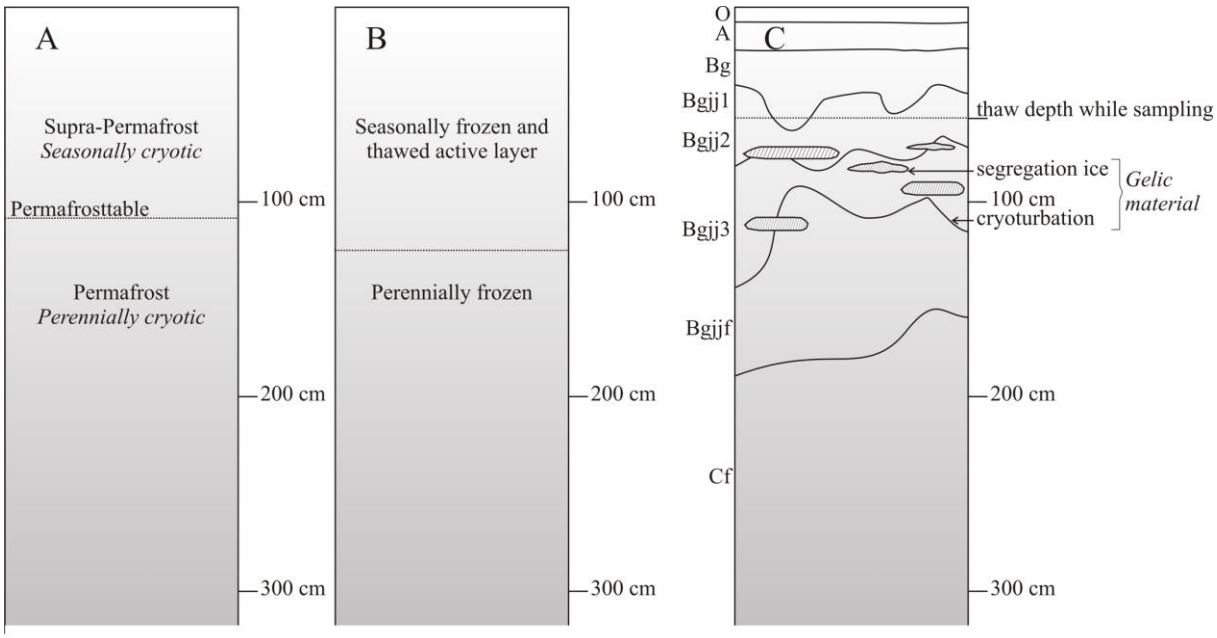

Figure 2: Schematic view of properties of permafrost-affected soils. A = The soil-thermal properties. The permafrost table divides the supra-permafrost (temperature can temporarily be higher than 0 °C within two consecutive years) and the permafrost (temperature is at least two consecutive years lower than 0 °C). B = the freeze-thaw-regime of the soils with the seasonally frozen and thawed active layer and the subjacent perennially frozen soil. C = Example of a permafrost-affected soil profile. Cryoturbation and segregated ice (*gelic* material according to US Soil Taxonomy (Soil Survey Staff 2010)) are indicated.

Fig. 2: Schematische Darstellung der Eigenschaften Permafrost beeinflusster Böden. A = Bodenthermische Eigenschaften. Die Permafrosttafel trennt den Supra-Permafrost (Temperatur kann über zwei Jahre hinweg zeitweise über 0 °C liegen) vom Permafrost (Temperatur liegt mindestens zwei Jahre kontinuierlich unter 0 °C). B = Gefrier-Tau-Regime der Böden mit der saisonal zeitweise gefrorenen und zeitweise getauten Bodenschicht und dem darunterliegenden permanent gefrorenen Boden. C = Beispiel für ein Profil eines Permafrost beeinflussten Bodens mit angedeuteter Kryoturbation und Segregationseis (*gelic* material nach US Soil Taxonomy (Soil Survey Staff 2010)).

In current use are primarily the American classification system "Keys to Soil Taxonomy" (Soil Survey Staff 2010) with the so-called Gelisols (from Latin *gelus* = ice) as permafrost-

affected soil class (Fig. 3 and Fig. 4), and the international reference system of the "WRB: World Reference Base for Soil Resources" of the international Food and Agriculture Organization (FAO 2007) with the Cryosol group (from Greek κρύος (*cryos*) = cold). The diagnostic horizons, or characteristics, of these soils are the existence of permafrost in the uppermost meter of the soil, or clear cryoturbation characteristics and/or segregation ice (*gelic* material according to US Soil Taxonomy (Soil Survey Staff 2010)) in the active layer of the soil above the permafrost present within a depth of 2 meters (Fig. 2 and Fig. 4). An advantage of using both of these systems is the easy comparability of the various national and international studies on permafrost-affected soils.

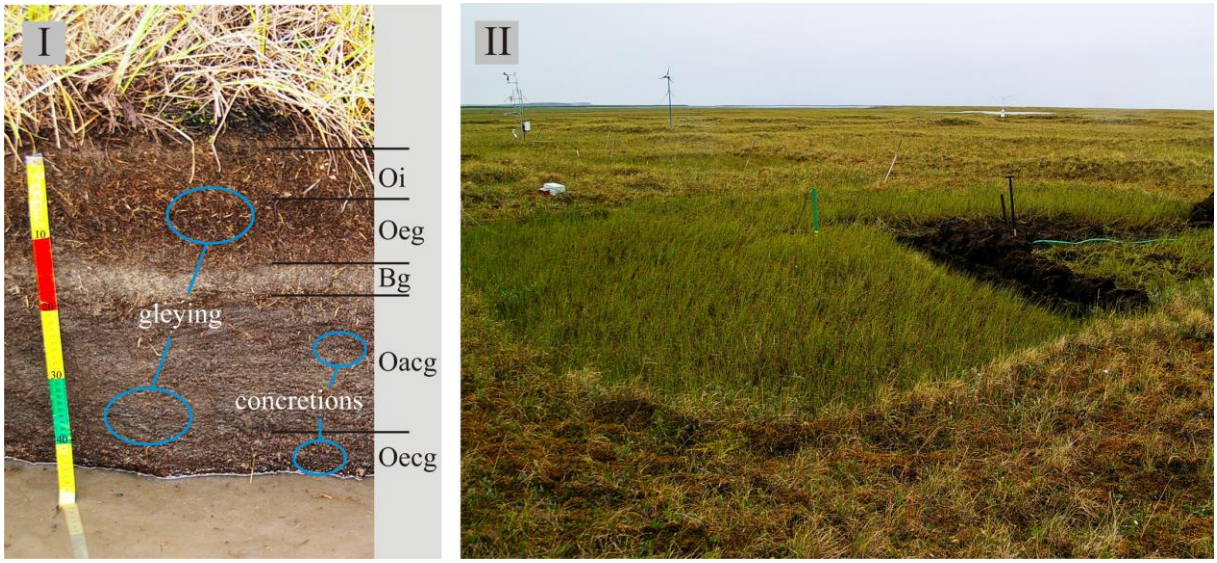

Figure 3: A non cryoturbated organic dominated permafrost-affected soil, *Typic Historthel* (I) and the study area it is from (II) – Samoylov Island, central Lena River Delta, Siberia 2007. Historthel = **Great Group:** Hist = **greek ιστός (histos) = tissue (plant);** **Suborder:** orth = **Orthels are soils with little or no cryoturbation and except polygons, patterned ground is leaking;** **Order:** el = **formative element of Gelisols = lat. Gelu = frost, coldness.** **"O" and "B" indicate soil horizons. "O" indicates an organic matter-dominated horizon that has formed at the soil surface. It consists of undecomposed or partially decomposed litter (i.e., needles, twigs, moss, and lichens). "B" indicates a subsurface horizon that has formed below an "O" or "A" horizon. It shows the obliteration of all or much of the parent soil material structure. It can be characterized by many qualifiers. Examples are gleying properties (suffix "g") described as formation of grey, greenish and bluish spots caused by reduced iron. Iron reduction occurs when soils are water-saturated for long periods. In this case the soil parent material consists of fluvial sands that were deposited during a flood in the study area. Suffixes "i", "e" and "a" classify the O**

horizon's organic matter in "slightly", intermediately" and "highly" decomposed. The existence of iron and/or manganese concretions is indicated by suffix "c".

Fig. 3: Ein nicht kryoturbierter, von organischem Material dominierter, Permafrost beeinflusster Boden, ein „*Typic Historthel*" (I) und das Arbeitsgebiet (II) Insel Samoylov, zentrales Lena-Delta, Sibirien 2007, aus dem er stammt. Historthel = **Great Group:** Hist = **griechisch ιστός (histos) = Gewebe (Pflanzen).** **Suborder:** orth = **Orthels sind Böden, die wenig oder gar nicht kryoturbiert und außer polygonalen keine weiteren Frostmuster aufweisen.** **Order:** el = **formatives Element der Gelisole = lat. Gelu = Frost, Kälte.** **„O" und „B" bezeichnen Bodenhorizonte. „O" bezeichnet einen von organischer Substanz dominierten Bodenhorizont, der an der Bodenoberfläche entstanden ist. Er bestehet aus nichtzersetzter oder teilweise zersetzter Streu (i.e. Blätter, Nadeln, Zweige, Moose, Flechten). „B" bezeichnet einen Unterbodenhorizont, welcher unter einem „O-" oder „A-" Horizont gebildet wird und eine deutliche Veränderung gegenüber dem Ausgangsgestein zeigt. Er kann durch viele Merkmale gekennzeichnet sein. Ein Beispiel ist die Vergleyung (Suffix „g"), die graue, grünliche oder bläuliche Flecken durch reduziertes Eisen verursacht. Das Eisen wird reduziert, wenn der Boden lange Zeit wassergesättigt ist. In diesem Fall besteht er aus fluviatilen Sanden; diese wurden bei einer Überflutung des Untersuchungsgebietes abgelagert. Die Suffixe „i", „e" und „a" unterteilen die organische Substanz des O-Horizonts in „schwach", „fortgeschritten" und „stark" zersetzte. Das Vorhandensein von Eisen- und/oder Mangankonkretionen wird mit dem Suffix „c" gekennzeichnet.**

In the Russian classification systems, permafrost-affected soils with cryoturbation and cryometamorphosis, widespread on Russian land, are treated as Cryozems in a separate soil class. All other soils of these areas without these two characteristics are allocated to other soil classes with the additional mention of the subjacent permafrost (such as *alluvisol* with underlying permafrost (Shishov *et al*. 2004)). Alternatively, permafrost is included as a state of soils and their specifications (Elovskaya 1987). In Germany, permafrost-affected soils only exist as relictic or fossil remnants of periglacial soil formations. In the current German soil classification (AG Boden 2005), they are not described independently, but can be counted as paleo soils (such as recent *podzol* on top of cryoturbated nonsorted circles). Remnants of these soils are occasionally described in connection with the periglacial layers (AG Boden 2005, Altermann *et al*. 2008). The spatial extension of the gelisols or cryosols north of the fiftieth degree latitude covers 27 % of the land mass (Jones *et al*. 2010) and corresponds to approx. 8.6 million km^2. The permafrost-affected soils (here *cryosols* according to the WRB, FAO 2007) are combined with other important soil types of these latitudes such as *podzols*

(acidified soils, 15 %), *leptosols* (hard rock soils, 8 %) and *cambisols* (brunified soils, 8 %) (Jones *et al*. 2010), (see Fig. 5)

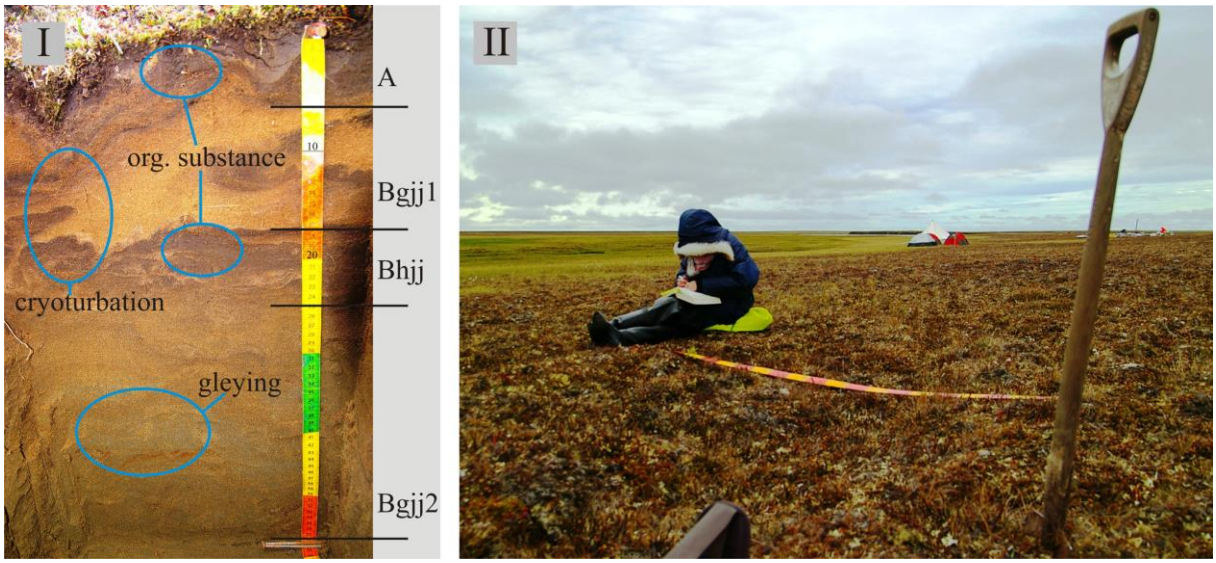

Figure 4: A sand-dominated and cryoturbated permafrost-affected soil, *Typic Psammoturbel* (I) and the study area it is from (II) the Arga Complex, northwestern Lena River Delta, Siberia 2009. Psammoturbel = **Great Group:** Psamm(o) = **greek ἄμμος (psamm) = sand; Suborder:** turb = **lat. Turbatio = disturbance; Order:** el = **formative element of Gelisols = lat. Gelu = frost, coldness. "A" and "B" indicate soil horizons. "A" indicates a mineral horizon that has formed at the surface or below an organic horizon. It has accumulated humified organic matter that is mixed with the mineral fraction. "B" indicates subsurface horizons (see Fig. 3). Within this profile there are several B horizons with different properties. The suffix "h" indicates an illuvial accumulation of organic matter or sesquioxides and "jj" stands for cryoturbated horizons. Suffix "g" is explained in the caption of Figure 3.**

Fig. 4: Ein sanddominierter und kryoturbat verwürgter Permafrost beeinflusster Boden, ein „*Typic Psammoturbel*" (I) und das Arbeitsgebiet (II), Arga-Komplex im nordwestlichen Lena-Delta (Sibirien 2009), aus dem er stammt. Psammoturbel = **Great Group:** Psamm(o) = **griechisch ἄμμος (psamm) = Sand. Suborder:** turb = **lat. Turbatio = Unordnung, Störung. Order:** el = **formatives Element der Gelisole = lat. Gelu = Frost, Kälte. „A" und „B" bezeichnen Bodenhorizonte. „A" bezeichnet einen Mineralbodenhorizont, der an der Bodenoberfläche oder unter einem organischen Auflagehorizont gebildet wurde. Er hat humifizierte organische Substanz akkumuliert, welche in die Mineralfraktion eingearbeitet ist. „B" bezeichnet Unterbodenhorizonte (vgl. Fig. 3). In diesem Profil finden sich mehrere B-Horizonte mit unterschiedlichen Merkmalen. Das Suffix „h" zeigt, dass im Bodenhorizont eine natürliche Anreicherung von organischer Substanz oder von Sesquioxiden stattgefunden hat und „jj" bezeichnet kryoturbierte Horizonte. Das Suffix „g" beschreibt eine Vergleyung (vgl. Fig. 3).**

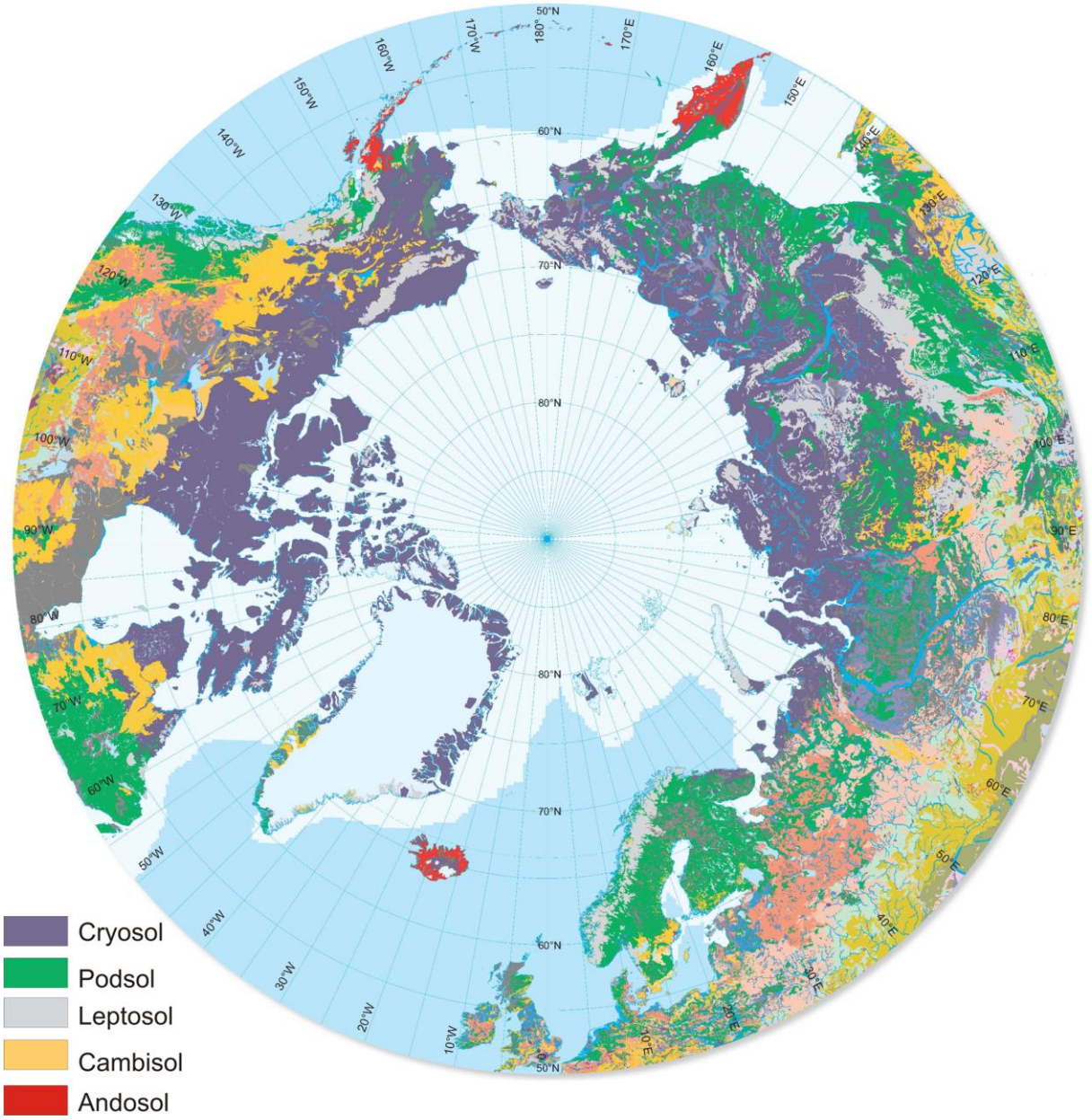

Figure 5: Soil map of territories above 50° N (JONES *et al.* 2010). The legend represents soils dominating this area and *Andosols* that developed from volcanic ash and are prevalent in Iceland, Kamchatka and Alaska. Soil classification according to the World Reference Base for Soil Resources (FAO 2007).

Fig. 5: Bodenkarte der Gebiete nördlich 50° N (JONES *et al.* 2010). Die Legende zeigt die diesen Raum dominierenden Böden sowie die auf Island, Kamtschatka und Alaska weit verbreiteten Vulkanascheböden, die *Andosole*. Bodenklassifikation nach der World Reference Base for Soil Resources (FAO 2007).

The properties and the spatial distribution of the permafrost-affected soils within the various countries were collected by Tarnocai (2004) und Smith and Veldhuis (2004) for Canada, by Ping *et al*. (2004a) for Alaska, by Goryachkin and Ignatenko (2004), Naumov (2004), Karavaeva (2004), Sokolov *et al*. (2004) and Gracheva (2004) for the diverse and extensive areas of Russia, by Maximovich (2004) for Mongolia and by Ping *et al*. (2004b) for China and published as a book titled "Cryosols Permafrost-Affected Soils" by Kimble (2004). The book contains a comprehensive description of the research into permafrost-affected soils and their history, as well as the spatial distribution of these soils along with their properties. It not only addresses the discussion of the various national and international classification systems, but also the potential uses as settlement areas, agricultural land, and as supplier of natural resources. "Permafrost Soils" by Margesin (2009) is a comprehensive book focusing on the biology of permafrost-affected soils. Aspects such as biodiversity and bioactivity (e.g. Ozerskaya *et al*. 2009, Panikov 2009), the effect of global warming (e.g. Wagner and Liebner 2009) and the problems of pollutant accumulation in permafrost area (e.g. Barnes and Chuvilin 2009) are covered in this book.

2.2 Permafrost-affected soils as carbon stores

The low average temperatures and the extreme annual temperature differences in the permafrost areas have led to a considerable accumulation of organic matter in the Quaternary. The biomass, newly formed during the short summer phase, is initially accumulated after die-off in the uppermost active layer of the soil. Due to the annually recurring accumulation of organic matter – and often also fluvial or aeolian sedimentation of mineral matter – can lead to an upward shift of the soil surface as well as of the surface of the permanently frozen layer, so that gradually more and more organic matter is incorporated. Cryoturbation also leads to the inclusion of organic matter in deeper soil horizons. Another process is the relocation of organic matter in dissolved state and its precipitation and deposition above the permafrost table, where it was able to accumulate over millennia due to the very low temperatures and low decay rates. The permafrost-affected soils, therefore, are relevant carbon sinks, effective over long periods of time (Post *et al*. 1982, Corradi *et al*. 2005, Kutzbach *et al*. 2007, van der

Molen *et al.* 2007). The sink function occurred primarily via the soils near the surface which incorporate the biomass of the typical arctic climate-adapted tundra vegetation after its die-off as litter in their carbon sink. According to current estimates, 1024 Pg of organic carbon are stored in permafrost-affected soils down to a depth of 3 m (Tarnocai *et al.* 2009). Adding the deep-reaching sediments rich in organic carbon of the Yedoma landscapes and arctic deltas, the total estimates of the organic carbon stored in permafrost areas amount to about 1670 Pg (Tarnocai *et al.* 2009). These estimates were based on the Northern Circumpolar Soil Carbon Database (NCSCD, Tarnocai *et al.* 2007), the most comprehensive currently available database on organic carbon in permafrost-affected soils, which currently is being updated (Hugelius *et al.* 2012). But even the information in this database is still fraught with great uncertainties at the present time. When looking closely at the distribution of the sites considered so far, it becomes apparent that when evaluating the reliability of the soil data stored in the database (100 % = "reliable," 0 % = "unreliable," according to Kuhry *et al.* (2010)), the arctic delta areas and the Yedoma landscapes with ice-rich permafrost sediments in Siberia (Fig. 6), based on the very sketchy and difficult-to-access data situation regarding permafrost-affected soils of this region until now, can only be assessed with a reliability of less than 33 %. The areas of the North American region, on the other hand, are very well represented with up to 80 % (Kuhry *et al.* 2010). This can be attributed to the above-average number of published soil studies in these regions. In publications of recent years, some ambiguities were apparent in the estimates of the carbon quantities stored in the permafrost-affected soils. These stemmed, on the one hand, from the unbalanced distribution of existing soil study data, and on the other hand, the widely varying definitions of the respective research objects. The number of publications on carbon contents in permafrost-affected soils is manageable (Tab. 2). Using the two most-cited publications, Post *et al.* (1982) and Tarnocai *et al.* (2009), as examples, these different points of view are easily illustrated: while Post *et al.* (1982), in the course of a global determination of the carbon pools of all lifezones, only consider 48 soil profiles in arctic tundra areas to a depth of 100 cm, Tarnocai *et al.* (2009) combined and updated the pedological results of existing studies from permafrost regions (e.g. Zimov *et al.* 2006b, Schuur *et al.* 2008) and supplemented them with their own data. More than 400 soil profiles were evaluated, and the pool of organic carbon for various studies

objects such as the permafrost-affected soils to a depth of 3 m, the arctic delta areas (up to 50 m depth) or the Yedoma landscapes (up to 25 m depth) were calculated.

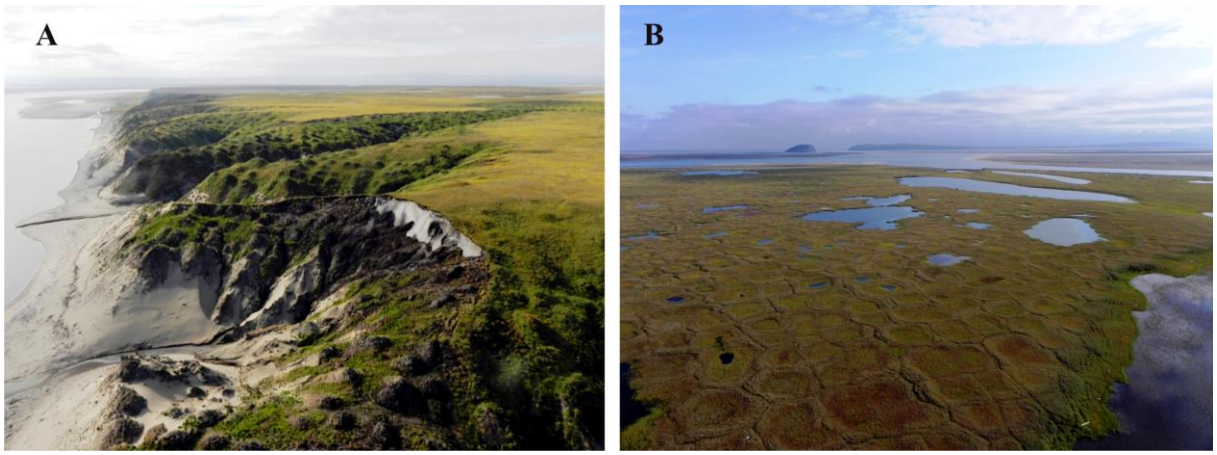

Figure 6: Examples of underrepresented landscapes in the Northern Circumpolar Soil Carbon Database (NCSCD). A = Yedoma landscape of Kurungnakh Island; an erosional river cliff with exposed ice-rich sediments. B = Polygonal tundra of Samoylov Island. Both islands are located in the Lena River Delta in northeastern Siberia. Photos 2010.

Fig. 6: Beispiele von in der „Northern Circumpolar Soil Carbon Database" (NCSCD) unterrepräsentierten Landschaften. A = Yedoma-Landschaft der Insel Kurungnakh im Lena-Delta; Aufschluss eisreicher Sedimente eines Fluss-Erosionskliffs. B = Polygonale Tundra der Insel Samoylov im Lena-Delta. Aufnahmen 2010.

Looking at the results compiled in Table 2, one will notice that the study results can be divided into two main groups: the results to a depth of 30 cm and those to 100 cm. Another group comprises carbon studies that limit their sampling to the active layer that is further defined (depths of 20 cm up to 50 cm) or only to certain soil horizons. All study results show that the permafrost-affected soils store a lot of carbon per soil surface. The carbon pool fluctuates between 4 kg m^{-2} and 24 kg m^{-2} for the upper 30 cm of the soils. When the authors looked at variously defined depths of the thaw soils on the day of sampling, the carbon pool was between 13 kg m^{-2} and 29 kg m^{-2}. The results of the studies that examined the carbon pool up to a depth of 100 cm vary between 4 kg m^{-2} and 69 kg m^{-2} (Tab. 2). Furthermore, these data reveal the very high fluctuation range of the results from different permafrost regions.

Table 2: Overview of carbon studies from different permafrost regions. Only results related to the permafrost-affected soils are presented. This list shows only some examples and is not intended to be exhaustive. SOC = soil organic carbon.

Tab. 2: Eine Übersicht von Kohlenstoff-Studien in unterschiedlichen Permafrostregionen. Dargestellt sind Teilergebnisse der genannten Studien zu Permafrost beeinflussten Böden. Diese Liste zeigt nur einige Beispiele und erhebt keinen Anspruch auf Vollständigkeit. SOC = Boden eigener organischer Kohlenstoff.

Sampling depth AUTHORS	SOC-Pool kg m^{-2} (min)	SOC-Pool kgm^{-2} (max)	Mass SOC Pg	Study sites as described in publication
depth 0-30 cm				
STOLBOVOI 2002	11.6	13.3	62	Russia
TARNOCAI *et al.* 2009			191	Northern permafrost regions
HUGELIUS *et al.* 2010		16.3		Tulemalu Lake, central Canadian Arctic
SEE CHAPTER 5.4, PAGE 130	4.0	24.0		N-S-Transect (73.5°- 69.5° N) along the Lena River, Siberia
active layer depth				
OECHEL AND BILLINGS 1992	13.0	29.0	55	Tundra
TARNOCAI AND BALLARD 1994	21.7	26.2		Canadian Arctic / Subarctic
ORLOV *et al.* 1996		14.5	59	Russia
NADELHOFFER *et al.* 1997		20.3		Alaska
GUNDELWEIN *et al.* 2007		14.5		Labaz Lake, Taymyr-Peninsula
depth 0-100 cm				
POST *et al.* 1982		21.8	192	Tundra
TARNOCAI AND SMITH 1992	4.0	63.0		Canada
MATSUURA AND YEFREMOV 1995	11.0	20.0		Russia
ROZHKOV *et al.* 1996			116	Tundra and northern Taiga in Russia
PING *et al.* 1997	31.4	69.2		Tundra in Alaska
STOLBOVOI 2002	16.6	26.9	107	Russia
TARNOCAI *et al.* 2003	25.6	59.2	268	Northern permafrost regions
POST 2006		14.2		Tundra
GUNDELWEIN *et al.* 2007		30.7		Labaz Lake, Taymyr-Peninsula
PING *et al.* 2008		34.8	98	North American Arctic region
TARNOCAI *et al.* 2009	22.6	66.6	496	Northern permafrost regions
HUGELIUS *et al.* 2010		33.8		Tulemalu Lake, central Canadian Arctic
BLISS AND MAURSETTER 2010		54.5	38	Gelisols of Alaska
PING *et al.* 2010	12.6	50.9		Discontinuous, warm permafrost, boreal forests in Alaska
SEE CHAPTER 4.4.2, PAGE 105	6.6	48.0		Samoylov Island, Lena River Delta, Siberia
depth 0-300 cm				
TARNOCAI *et al.* 2009	159.2	358.2	1024	Northern permafrost regions
depth > 300 cm				
TARNOCAI *et al.* 2009		65.0	241	arctic deltas

AUTHORS	OC (min) %wt	OC (max) %wt	Mass SOC Pg	Study sites as described in publication
ZIMOV *et al.* 2006a		2.6	500	Yedoma-landscapes in North Siberia
ZIMOV *et al.* 2006b		2.38	450	Yedoma-landscapes in North Siberia
TARNOCAI *et al.* 2009		2.6	407	Yedoma-landscapes in North Siberia
SCHIRRMEISTER *et al.* 2011a	1	17	250 - 375	20 coastal exposures in North Siberia

Looking at the data of current literature on total mass of organic carbon in the permafrost areas (Tab. 2), the problematic aspect of comparability becomes obvious. The results of the studies refer to very different surfaces in terms of size. The studied surfaces may be countries, regions or even vegetation units. Despite the difficult comparability, the results of these studies illustrate that the total pool of the permafrost-affected soils' organic carbon is very high at 1024 Pg (Tarnocai *et al.* 2009) and exceeds the mass of carbon of the entire global vegetation biomass or the atmosphere of 650 Pg and 750 Pg (IPCC 2007), respectively. The carbon quantities stored in permafrost-affected soils are therefore to be considered one of the most important factors for the understanding and function of the cryosphere within the climate system. Permafrost-affected soils with their special carbon dynamics are very sensitive to environmental and climatic changes due to their temperature dependence. It can be assumed – for the past as well as for the present – that global and regional environmental and climatic changes, as well as the dynamics of soil carbon in permafrost areas interact and will continue to interact with one another via physical and biogeochemical feedback mechanisms (McGuire *et al.* 2009, Grosse *et al.* 2011). With the currently predicted climate warming and its particularly strong effects in the arctic regions (Lembke *et al.* 2007), and the concurrent local and regional decline and degradation of permafrost (Anisimov and Nelson 1997), the properties of permafrost-affected soils will undergo a fundamental change.

Warming within the permafrost areas can lead to an augmentation of the thickness of the seasonal active layer in the upper soil (Fig. 2 and Fig. 7) and to a change in its hydrological site conditions (Koven *et al.* 2011). This leads to an increased microbial decay of the organic matter and a more intensive release of the climate-relevant trace gases carbon dioxide, methane and nitrogen oxide (Dutta *et al.* 2006, Wagner *et al.* 2007, Khvorostyanov *et al.* 2008, Schuur *et al.* 2009).

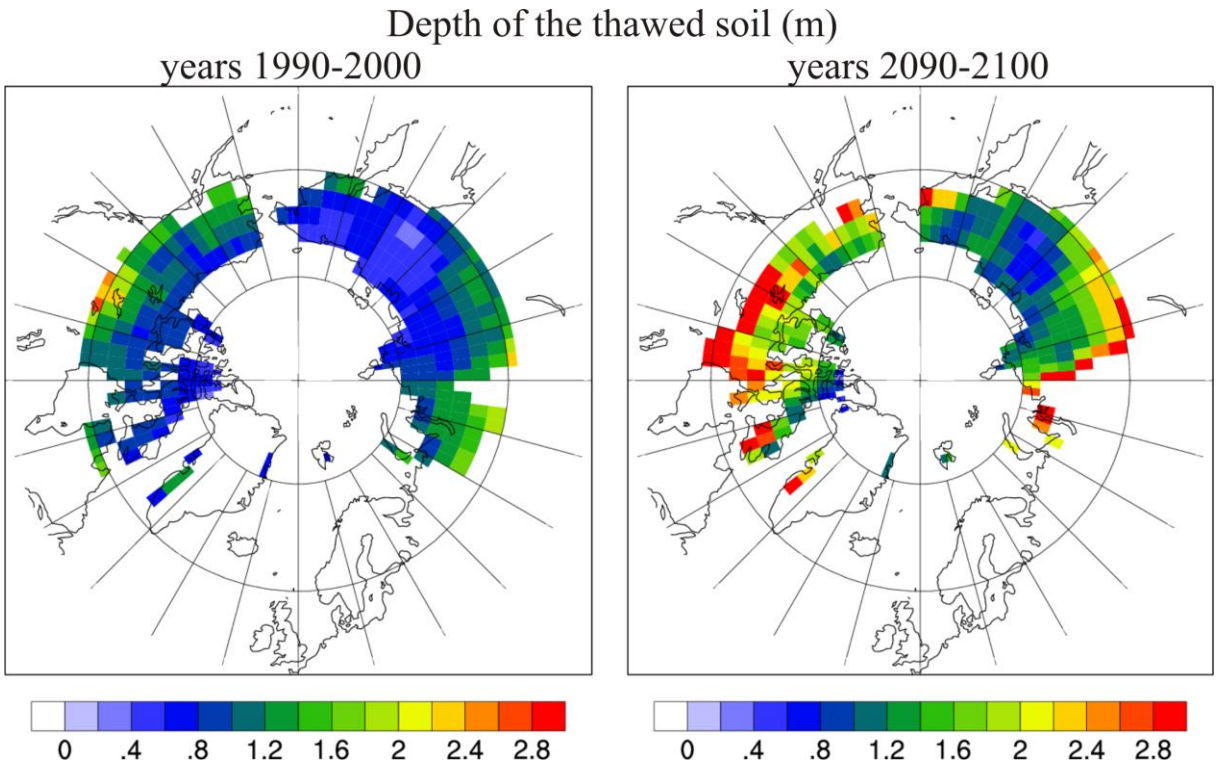

Figure 7: The modelled maximum depth of the seasonally thawed soil, the active layer, in meters for the period 1990...2000 and 2090...2100. White cells indicate areas where no permafrost within 50 m depth was calculated. (Koven *et al.* 2011, ©2011 PNAS), excerpt.

Fig. 7: Die modellierte maximale Mächtigkeit des saisonalen Auftaubodens in Metern für die Jahre 1990...2000 und die Jahre 2090...2100. Weiße Zellen stehen für Gebiete, für die kein Permafrost innerhalb der oberen 50 m berechnet wurde. (Koven *et al.* 2011, ©2011 PNAS), Auszug.

In other words, if the current warming of the arctic climate is the cause of an increased decline in the extent of the permafrost areas, which in turn leads to an increased release of greenhouse gases in the Earth's atmosphere, a further rise in temperatures on a global scale, but also in the permafrost areas themselves must be expected (Fig. 8).

These processes show the positive feedback effects in permafrost landscapes or in the cryosphere of our Earth system that are not yet sufficiently considered in the climate models relating to temperature projection. Because of these complex effects, the permafrost areas in particular represent an important possible tipping element of the global climate system, relevant even for politics and society (Lenton and Schellnhuber 2010). A tipping element is

considered to consist of those components of the Earth system that can essentially and irrevocably be altered under loads beyond critical limits (Lenton and Schellnhuber 2010). Whether the soils of the permafrost areas already act as carbon sources (Oechel *et al.* 1993, Zimov *et al.* 1997, Oechel *et al.* 2000) or still accumulate carbon (Corradi *et al.* 2005, Kutzbach *et al.* 2007, van der Molen *et al.* 2007) is not yet clear and has to be assessed differently on a regional scale.

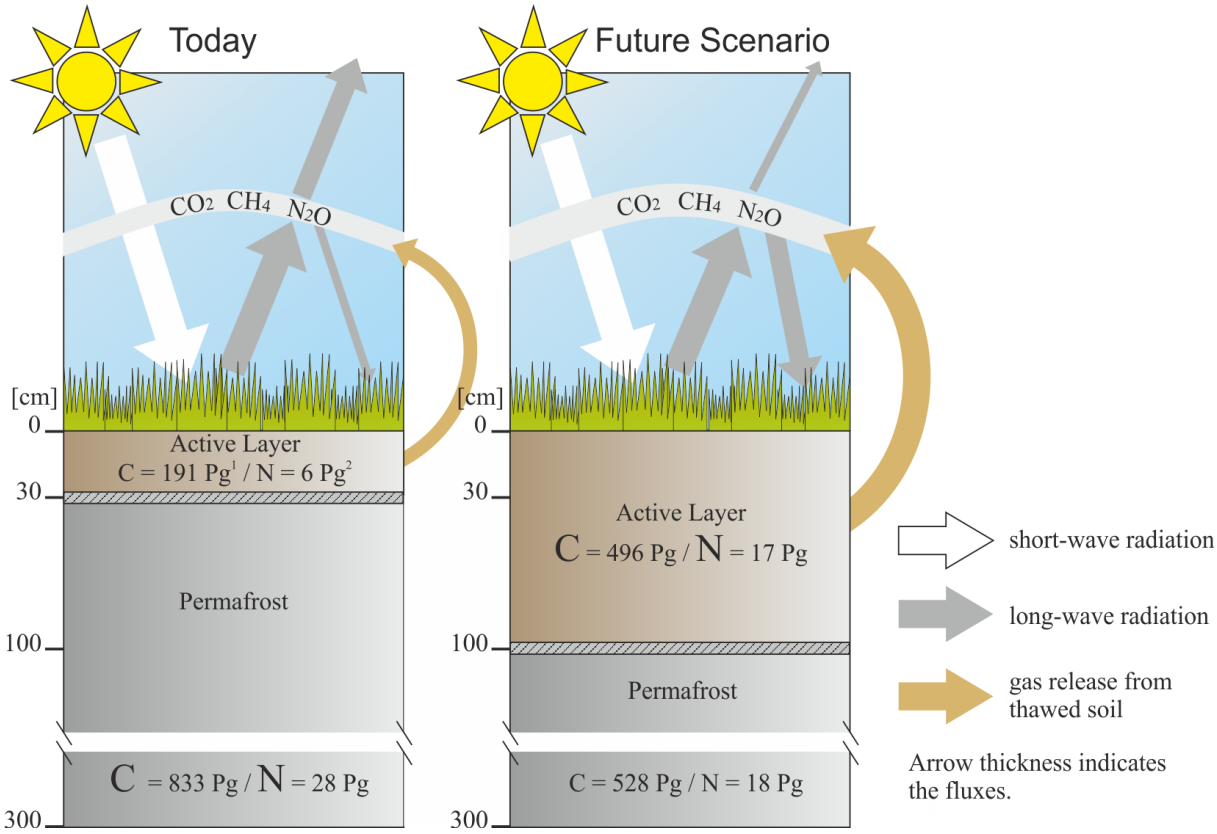

Figure 8: Schematic illustration of the carbon and nitrogen dynamic feedbacks and the climate-driven changes within the permafrost-affected soils. C-pools (Tarnocai *et al.* 2009), N-pools calculated using the C/N ratio of 30. Figure according to Beer (2009).

Fig. 8: Schematische Darstellung zur Rückkopplung der Kohlenstoff- und Stickstoffdynamik und den klimabedingten Änderungen in Permafrost beeinflussten Böden. C-pools (Tarnocai *et al.* 2009), N-pools unter Zuhilfenahme des C/N-Verhältnisses von 30 kalkuliert. Nach Beer (2009).

The complexity of these carbon source/sink functions of the permafrost-affected soils is not yet sufficiently understood. There is a lack of measurements, as well as robust, adequately

validated modelled projections and predictions to make reliable prognoses for the development of the carbon dynamics of permafrost-affected soils in the warming climate system (McGuire *et al.* 2009).

2.3 Current level of knowledge of the carbon pool in permafrost-affected soils in Russian Arctic

Because of the particular relevance of the cryosphere and especially the terrestrial permafrost for climate system research, the number of published scientific articles focusing on the carbon pool in the permafrost regions has dramatically increased during the past five years compared to the last 20 years (Fig. 9).

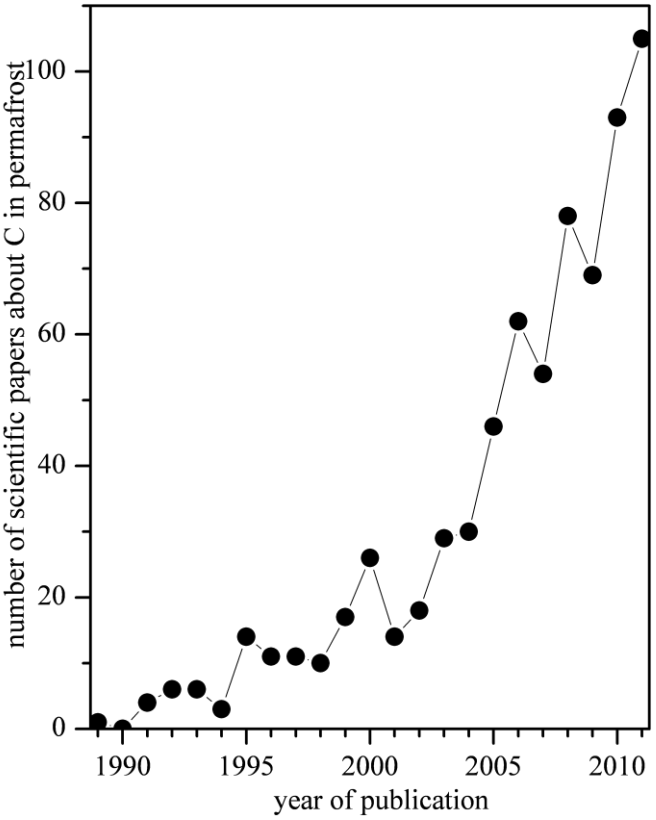

Figure 9: Number of scientific papers published between 1989 and 2011 as a result of a search for the keywords „permafrost + carbon“ in Web of Knowledge (www.webofknowledge.com).

Fig. 9: Anzahl wissenschaftlicher Artikel in den Jahren 1989 bis 2011 als Ergebnis einer Recherche nach den Schlüsselbegriffen „permafrost + carbon“ bei Web of Knowledge (www.webofknowledge.com).

The largest part of these published articles deals with the North American region. In recent years however, areas of the Eurasian permafrost – especially in the Russian region - have also been increasingly studied in detail. The data of these small research areas can only be used reliably so far for local upscaling of the carbon quantities. Special permafrost phenomena such as ice and organic-rich sediments of the Yedoma landscapes, which have until now been largely neglected, were increasingly being studied (Zimov *et al.* 2006a).

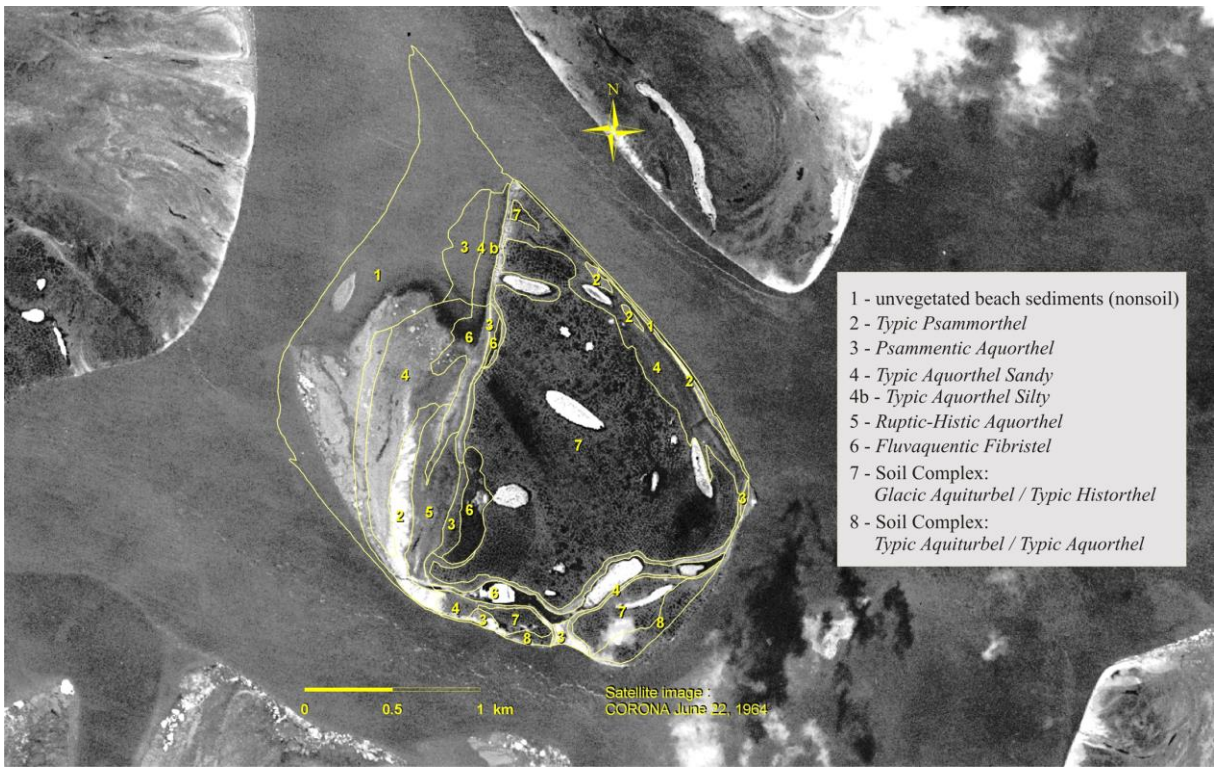

Figure 10: A soil map of Samoylov Island as a result of long-term soil research within this area of the Lena River Delta. Generated from data by Pfeiffer *et al.* 2000 and 2002 (see Sanders *et al.* 2010). Soil classification according to the US Soil Taxonomy (Soil Survey Staff 2010). The plotted coast line from July, 1964 points out the high coastal dynamics within the beach and floodplain in the western part of island.

Fig. 10: Bodenkarte der Insel Samoylov im Lena-Delta als Ergebnis langjähriger Bodenforschung in dieser Region. Erstellt aus Daten von Pfeiffer *et al.* 2000 und 2002 (vgl. Sanders *et al.* 2010). Bodenklassifikation nach der US Soil Taxonomy (Soil Survey Staff 2010). Der eingetragene Küstenverlauf vom Juli 1964 verdeutlicht die hohe Küstendynamik der Strandflächen und Überflutungsebenen im Westen der Insel.

The near-surface soils of the permafrost areas of North Siberia have long played a large role in the study of carbon pools and greenhouse gas emissions by Russian scientists and, since the 1990s, by large German-Russian cooperation projects. In addition to the classic soil survey with its genesis and distribution in permafrost areas (Krasuk 1927, Ivanova 1965 and 1971, Karavaeva 1969, Targulyan 1971, Elovskaya *et al.* 1979, Desyatkin and Teterina 1991, Pfeiffer 1998, Pfeiffer *et al.* 2000, Pfeiffer *et al.* 2002) (for examples see Fig. 3, Fig. 4, Fig. 10 and Fig. 11), numerous physicochemical properties and processes of permafrost-affected soils were also studied (e.g. Pfeiffer and Jansen 1992, Okoneshnikova 1994, Pfeiffer *et al.* 1997, Fiedler *et al.* 2004, Kutzbach *et al.* 2004, Desyatkin and Desyatkin 2006, Zubrzycki *et al.* 2008, Sanders *et al.* 2010) (for examples see Fig. 11, Fig. 12, Fig. 13 and Tab. 3).

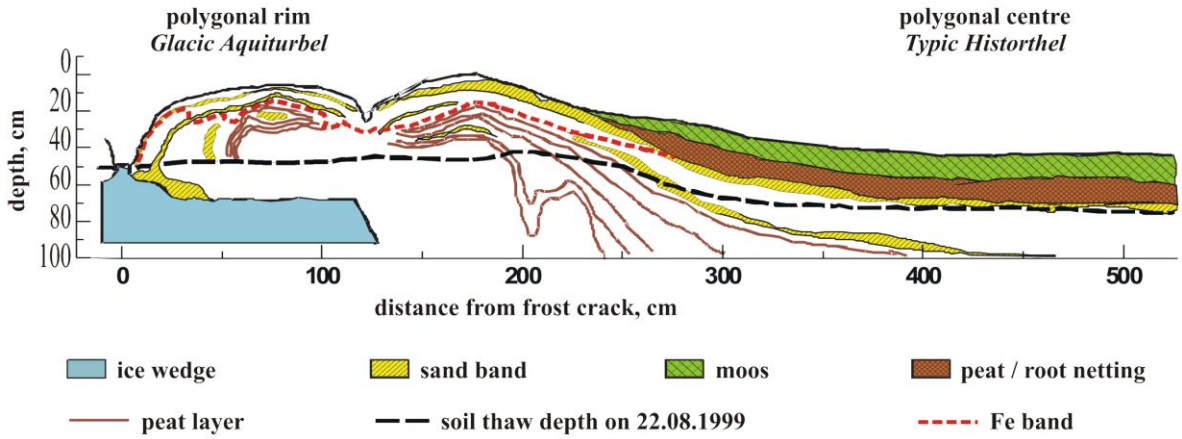

Figure 11: Cross section of a low centred polygon with a surface depression above the ice wedge and another one at the ice wedge's end. Soils that have developed in this polygon are a *Glacic Aquiturbel* at the polygon rim above the ice wedge and a *Typic Historthel* in the polygon centre. Scheme compiled from field observations of 22.08.1999.

Fig. 11: Querschnitt durch ein „low-centred" Polygon" mit einer Oberflächeneinsenkung über dem Eiskeil und einer weiteren Einsenkung am Rande des Eiskeils. Böden, die sich in diesem Polygon gebildet haben, sind im Polygonrand über dem Eiskeil ein „*Glacic Aquiturbel*" und im Polygonzentrum ein „*Typic Historthel*". Schema nach Feldaufnahmen vom 22.08.1999.

The turnover of organic matter in the soil and the associated formation of greenhouse gases in moist tundra areas of Eurasia were also researched on a small scale as part of field campaigns (e.g. Wüthrich *et al.* 1999, Rivkina *et al.* 2007, Knoblauch *et al.* 2008, Wagner *et al.* 2009,

Liebner *et al.* 2011, Shcherbakova *et al.* 2011). The emissions of greenhouse gases were initially captured in the North Siberian Lena delta starting in 2000 via small-scale closed chamber measurements (Kutzbach *et al.* 2004, Sachs *et al.* 2010) and later expanded by Eddy-Covariance measurements (Kutzbach *et al.* 2007, Sachs *et al.* 2008, Wille *et al.* 2008). The seasonally averaged methane emissions determined via closed chamber measurements lay between 4.3 and 28 mg CH_4 m^{-2} d^{-1} (Kutzbach *et al.* 2004), and between 4.9 und 100 mg CH_4 m^{-2} d^{-1} (Sachs *et al.* 2010). The Eddy-Covariance measurements provided results on the order of magnitude of 0.01 to 0.55 g CO_2 h^{-1} m^{-2} for releasing carbon dioxide by respiration processes (Kutzbach *et al.* 2007). The methane flows amounted to 18.7 to 30 mg CH_4 m^{-2} d^{-1} for averaged daily emissions within the measuring period (Sachs *et al.* 2008, Wille *et al.* 2008).

Table 3: Chemical properties of two exemplary soil profiles (see Fig. 11 and Fig. 13) with their horizons according to the US Soil Taxonomy (Soil Survey Staff 2010), horizon depth, texture, hydromorphology, pH value, organic carbon content in weight percent, C/N ratio and rooting.

Tab. 3: Chemische Eigenschaften zweier Beispielbodenprofile (vgl. Fig. 11 und Fig. 13) mit Angaben zur Horizontbezeichnung nach der US Soil Taxonomy (Soil Survey Staff 2010), zur Tiefe der einzelnen Horizonte, zur Textur, zu den Hydromorphieverhältnissen, zum pH-Wert, zum Gehalt an organischem Kohlenstoff in Gewichtsprozent, zum C/N-Verhältnis und zur Durchwurzelung.

Glacic Aquiturbel – Polygonal Rim of a „low-centred“ ice wedge polygon							
Horizon	Depth (cm)	Texture	red. conditions	pH	OC	C/N	Roots
Ajj	0-12	Loamy sand	No	5.9	1.8	21	Many
Bjjg1	12-15	Sandy loam	No	6.2	2.2	21	Frequent
Bjjg2	15-47	Loam	Yes	5.5	2.9	24	Frequent
Bjjgf	47-70	Loam	Yes	6.0	3.0	20	None
Typic Historthel – Polygonal Centre of a „low-centred“ ice wedge polygon							
Horizon	Depth (cm)	Texture	red. conditions	pH	OC	C/N	Roots
Oi	0-11	Peat	No	5.0	22.1	43	Few
OeBg	11-26	Peat + Sand	Yes	4.8	12.6	35	Many
Bg	26-31	Sand	Yes	4.8	2.1	> 100	Frequent
Bgf	31-64	Sandy loam	Yes	5.0	4.2	30	None

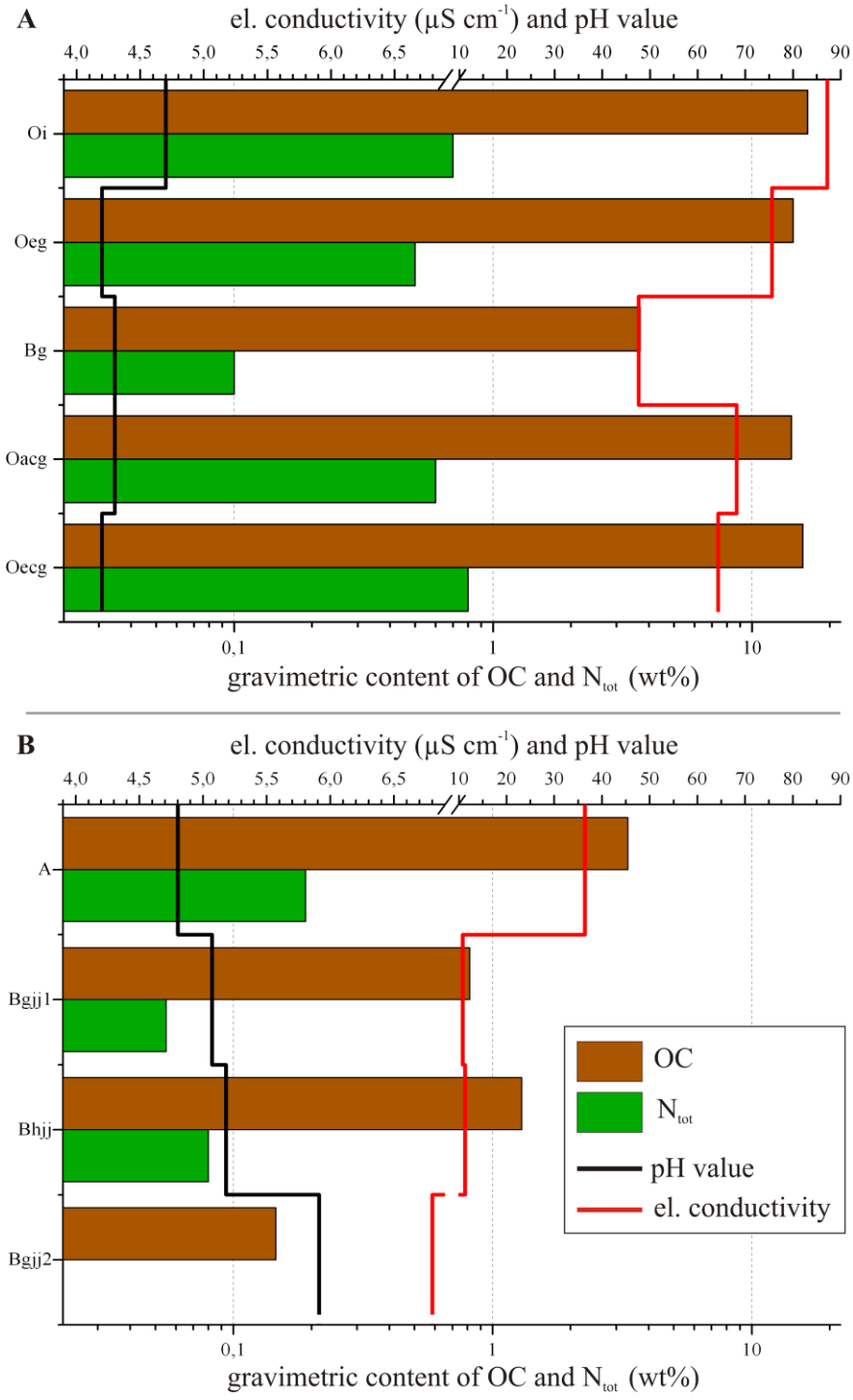

Figure 12: Chemical analyses of in Figure 3 and Figure 4 presented permafrost-affected soils. A = Chart for *Typic Historthel*. B = Chart for *Typic Psammoturbel*. For better comparison, both charts use the same scaling. The upper scale is for the pH value and electrical conductivity (µS cm^{-1}). Both properties were measured in a soil suspension of the soil sample and water. The scale at the bottom represents the contents of carbon and nitrogen (%wt).

Fig. 12: Chemische Analysen der in Figure 3 und Figure 4 vorgestellten Permafrost beeinflussten Böden. A = Diagramm für den „*Typic Historthel*“. B = Diagramm für den „*Typic Psammoturbel*“. Beide Graphen sind für eine einfache Vergleichbarkeit gleich skaliert. Die obere Skala gilt für den pH Wert und die elektrische Leitfähigkeit (µS cm^{-1}). Beide Eigenschaften wurden in einer Bodensuspension aus Bodenprobe und Wasser gemessen. Die untere Skala gilt den Elementgehalten von Kohlenstoff und Stickstoff (Gew.-%).

First English-language works on the survey of the carbon quantities in the permafrost-affected soils of the Siberian Arctic also exist (Gundelwein *et al.* 2007, see chapter 5, page 125). Their results determined for small area of Siberia are comparable to those of other areas (see Tab. 2). It also becomes apparent, however, that inaccuracies can occur in global extrapolations if the data situation from the individual regions is insufficient (see chapter 5.5, page 134). The carbon pools are not only recorded in the Siberian Arctic, but also in the European-Russian Arctic by means of field work, and extrapolated onto larger areas via remote sensing methods (Mazhitova *et al.* 2003, Hugelius and Kuhry 2009, Hugelius *et al.* 2011).

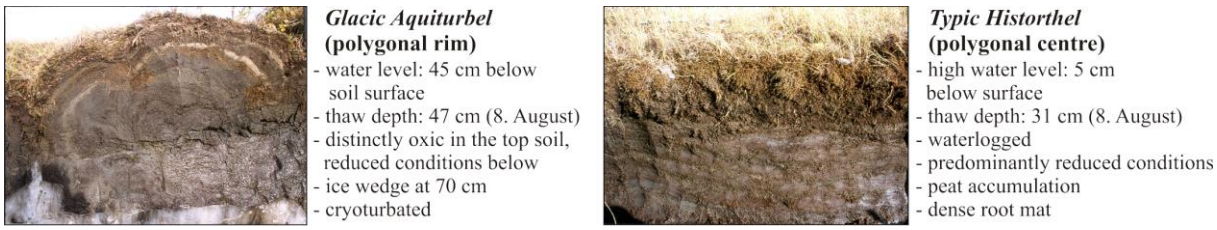

Figure 13: Two examples of permafrost-affected soils from Samoylov Island with a brief description of soil properties. The presented soil complex consisting of *Glacic Aquiturbels* and *Typic Historthels* dominates the soils of this island in the Lena River Delta (see Fig. 10).

Fig. 13: Beispiele Permafrost beeinflusster Böden auf der Insel Samoylov im Lena-Delta mit Kurzbeschreibung der Bodeneigenschaften. Der dargestellte Bodenkomplex – bestehend aus *Glacic Aquiturbels* und *Typic Historthels* – dominiert die Böden der Insel (vgl. Fig. 10).

In addition to the above studies limited to 1 m through 3 m of the carbon pools in the permafrost-affected soils, the study of special permafrost phenomena such as the sediments of the Yedoma landscapes is important. The studies of Siberian regions show that these sediments have a high gravimetric carbon content which, however, is subject to strong

fluctuations depending on the studied site. It is usually between 1 %wt and 4 %wt, but can also reach values of up to 17 %wt in the case of peaty layers (Zimov *et al.* 1997, Zimov *et al.* 2006a, Zimov *et al*. 2006b, Schirrmeister *et al.* 2011a).

2.4 Research requirements

A significant number of new data records on soils and the quantities of carbon stored in them from the under-represented areas of the circumpolar regions – especially the Siberian Arctic – is necessary to update the Northern Circumpolar Soil Carbon Database (Kuhry *et al.* 2010). This can only be achieved by combining measuring fieldwork with modelling work for the permafrost areas, primarily for the Eurasian and especially for the Siberian region. Because of the sketchy data situation, special focus should be directed not only to the delta deposits, the ice-rich sediments of the Yedoma landscapes (see Tarnocai *et al.* 2009), but also to the permafrost-affected soils of the hilly and mountainous regions. The more comprehensive data basis is necessary for a better understanding of the interactions between the particular climate, soil and vegetation conditions in the permafrost areas. From this information conclusions will be able to be drawn regarding the factors of the processes occurring today or the future remobilization of the labile organic carbon of the permafrost-affected soils. For future research projects it is important to reach high interdisciplinarity among the researchers in one area, because only the synthesis of the various research approaches and their results can lead to an improved understanding of the permafrost-affected soils and their carbon dynamics.

Since not only the size of the carbon pool in permafrost-affected soils varies regionally (McGuire *et al.* 2009), its recent carbon source and sink function is also different from region to region. And since field research cannot be carried out everywhere with sufficient intensity, large-scale thematic soil-type maps should initially be drawn up on a regional basis. These results, gathered from fieldwork and shown in maps, may serve as the basis for future extrapolations of various element fluxes. With the help of high-resolution vegetation and soil-type maps of underrepresented areas containing soil texture and hydrology, more accurate estimates of the carbon pool of the circumpolar permafrost region can be performed using GIS-analyses (compare to Hugelius 2012). To this end, many already existing soil and

sediment samples could be reanalyzed. Afterwards, new work areas can be targeted to fill the research gaps.

Data on the carbon pools and processes in the permafrost areas, obtained via targeted field and lab work, can be integrated into new and more reliable models. Through the synergistic and interdisciplinary collaboration of measurement and modelling permafrost researchers, it will be possible to model the development of these vast areas with their enormous quantities of potentially labile organic carbon and facilitate prognoses regarding possible greenhouse gas emissions from permafrost-affected soils. These, in turn, will lead to new, more realistic future projections of global temperature development and reduce the current uncertainty surrounding the significance of the cryosphere, including the carbon pools in permafrost-affected soils, for the climate system.

3. Diversity of Permafrost-Affected Soils in Northern Siberia

3.1 Introduction

Permafrost, which is soil or rock material maintaining temperatures of 0 °C or below during at least two consecutive years (van Everdingen 1998) is widespread in the northern hemisphere. The areas underlain by permafrost extend over almost 23 million km^2, approximately one quarter of their total northern land surface (Baranov 1959, Shi 1988, Zhang 1999, 2003, French 2007). Within the huge permafrost-underlain areas a large number of various soils types could develop. Beside the - per definition - "permafrost soils": Gelisols (Soil Survey Staff 2010) or Cryosols (FAO 2007) there is a diversity of soils types in the circumpolar region. In the Soil Atlas of the Northern Circumpolar Region Jones *et al*. (2010) described 24 different soil groups in the area above 50° N, whereupon 12 of these soil groups cover more than 1 % of the regarded soil area. However, with coverage of 27 % Cryosols are the dominant group followed by podzols (15 %), leptosols (8 %) and cambisols (8 %) (Jones *et al*. 2010).

Permafrost with its features affects the characteristics of the soils developing in the overlying layer, the so-called supra-permafrost that answers to the seasonally thawed active layer. Though the period for active pedogenesis is limited to few weeks during the arctic summer, the diversity of soils developing in these regions is high. This diversity results from cryogenic processes (Ping *et al*. 1998) which are cryogenic weathering, ice segregation and accumulation, cryoturbation, soli(geli)fluction, frost heave and sorting and frost crack formation (e.g., Bockheim and Tarnocai 1998). Generally, these soil-forming processes are slowed by the low temperatures and the relative high water saturation of the pedon, which are secondary limiting factors besides the time limitation (Ovenden 1990, Everett *et al*. 1981). Moreover, these limiting factors prevent the decomposition and turnover of organic matter resulting in high accumulations of organic matter today (Tarnocai *et al*. 2009). Another mechanism leading to organic matter sequestration is the upward growth of the investigated areas due to continuous fluvial as well as aeolian sedimentation and accumulation of sediments in the topsoil (Zubrzycki *et al*. 2013). The result is an incorporation of the deepest,

partly organic rich, parts of the seasonally thawed layer into the perennially frozen ground (Shur and Ping 1994).

In the investigation area the pedogenic processes occur primarily in the seasonally thawed active layer above the permafrost. However, due to fluctuations of the permafrost table (Gubin and Lupachev 2008) pedogenic processes can also be observed in the upper layer of permafrost (Ping *et al*. 1998).

Repeated freeze thaw cycles result in cryogenic weathering of coarser soil grains (Konishev and Rogov 1993) as well as in cryoturbation of the soil horizons (Bockheim and Tarnocai 1998). Cryoturbation can be driven by physical volume change of water to ice, moisture migration along a thermal gradient in the frozen soil or thermal contraction of the frozen material at low temperatures, or due to continued rapid cooling. Cryoturbation leads to irregular and broken horizon boundaries and sorted rock fragments and organic soil material accumulation (Soil Survey Staff 2010). The same freeze thaw cycles cause at the landscape level the formation of patterned ground (Washburn 1980) with ice wedge polygons dominating wide areas of our investigation area (Zubrzycki *et al*. 2012a, 2012b). Soil formation within these small-scale patterns is variable leading to the genesis of soil complexes of two or three different soil subgroups.

3.2 Investigation area

The presented soil surveys were performed in northeast Siberia between 2008 and 2010. Study-site locations are presented in Figure 14. All sites were chosen as representative of the dominating geomorphic or vegetation units. The study area can be subdivided into the area of the Lena River Delta and the large Siberian masses in the southern hinterland of the Laptev Sea.

The entire study area is located within the continuous permafrost zone (Grigoriev 1960, Yershov *et al*. 1991). It is dominated by an arctic-subarctic climate with continental influence and is characterized by low temperatures and low precipitation. Mean annual air temperatures (MAAT) were lowest in the north in Taimylyr (72° 37’ N, 122° 06’ E) and on Island Dunai

(73° 56’ N, 124° 30’ E) with -13.8 °C and -13.7 °C, respectively (Russia’s Weather Server, 2013). With -11.5 °C highest MAAT for this investigation were measured at the southernmost climate reference station Dzhardzhan (68° 44’ N, 124° 00’ E) (Fig. 15). There was a continuous increase of MAAT with decreasing latitude. The mean annual precipitation was between 227 mm and 379 mm (Russia’s Weather Server, 2013). It was higher at more southern climate reference stations (Fig. 16).

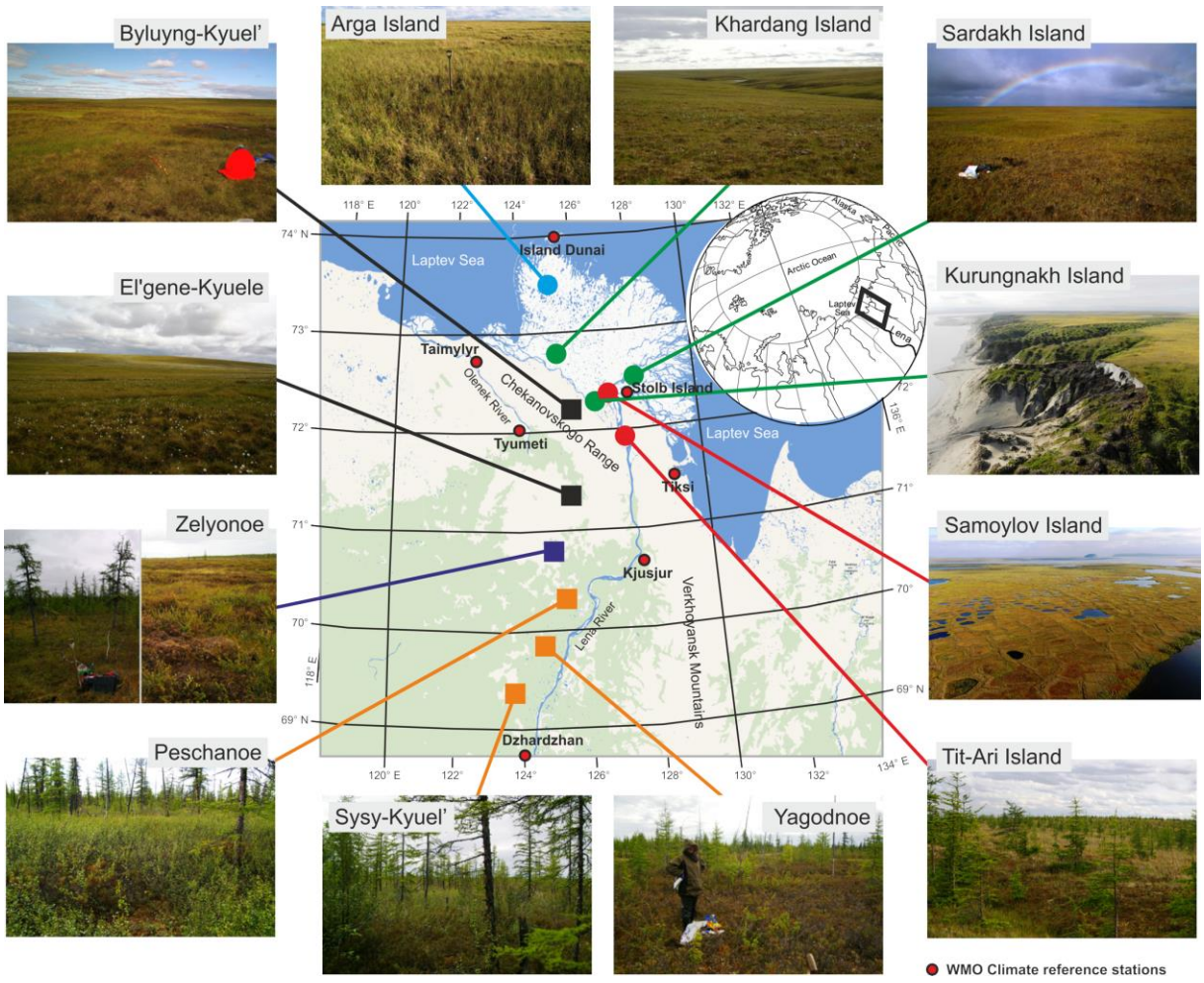

Figure 14: The study area along a latitudinal transect in northeast Siberia with locations of the soil surveys as well as photographs of representative landscapes.

Fig. 14: Das Untersuchungsgebiet entlang eines Nord-Süd-Transekts im Nordosten Sibiriens mit den Lokationen der durchgeführten Bodenstudie sowie Fotos der repräsentativen Landschaften.

The average temperatures of the warmest month July were 7.5 °C to 16.9 °C, whereas the coldest months are January and February with –32.3 °C to -38.5 (Fig. 15) pointing up the extreme temperature amplitude (41.2 °C to 55.3 °C) between polar day and night typical for continental polar regions.

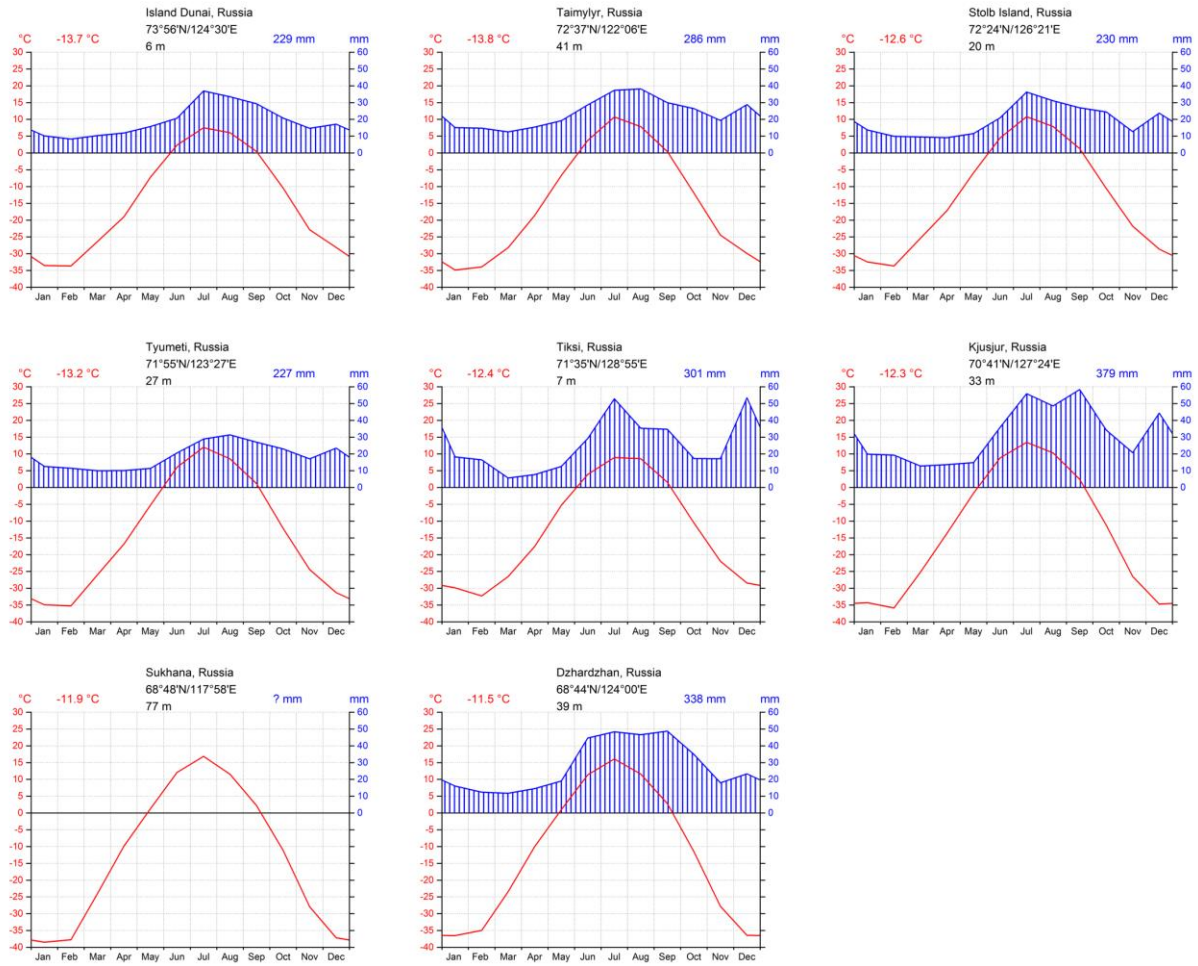

Figure 15: Climate charts for the climate reference sites in Siberian Arctic. Based on data provided by Russia's Weather Server (2013).

Fig. 15: Klimadiagramme der Referenzstationen in der sibirischen Arktis. Basierend auf Daten von Russia's Weather Server (2013).

The highest temperature amplitude was found at the climate station Sukhana (68° 48' N, 117° 58' E). This station is characterised by the highest mean summer temperatures as well as the lowest mean winter temperatures. The generally relatively low temperatures in summer

can be explained by a considerable energy uptake for melting the snow and for thawing the upper parts of the soil. Though the precipitation is low, the climate is anyhow humid due to the low potential evaporation in the area.

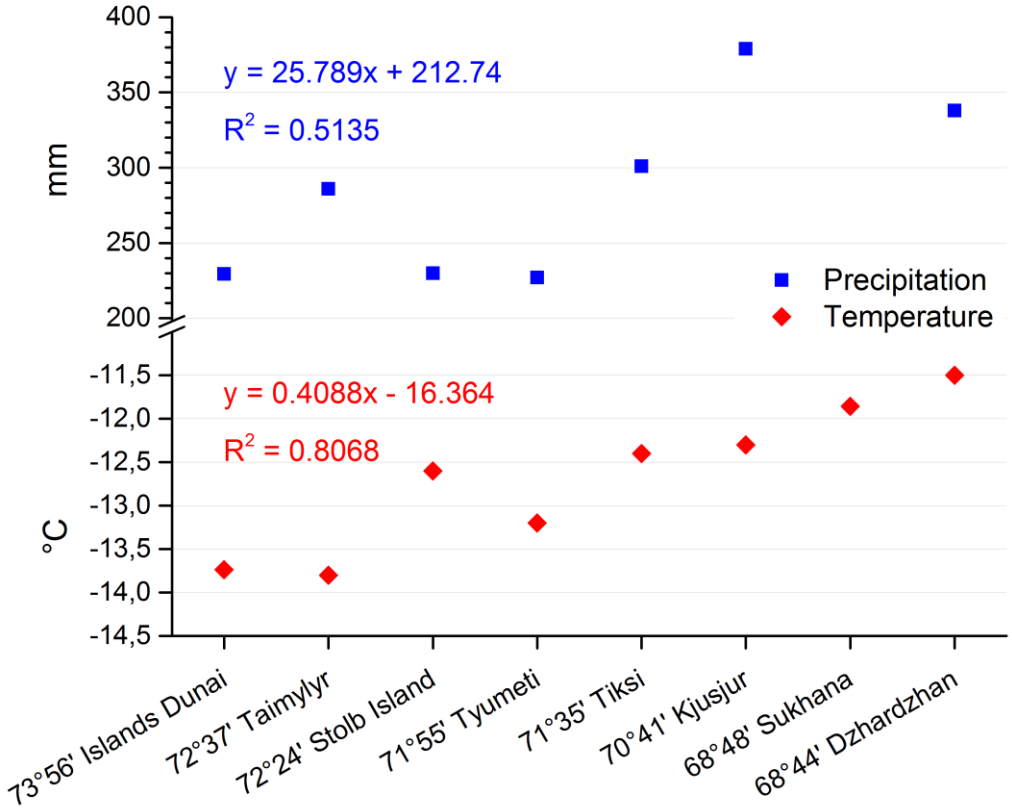

Figure 16: Mean annual air temperatures and mean sum of precipitation at Siberian climate reference stations along a latitudinal transect from North to South. Based on data provided by Russia's Weather Server (2013).

Fig. 16: Die mittlere jährliche Lufttemperatur und die mittlere Niederschalgssumme an Sibirischen Klimareferenzstationen entlang eines Nord-Süd-Transekts. Basierend auf Daten von Russia's Weather Server (2013).

The following is a description of the sampling sites as shown in Figure 14.

All study sites were chosen as representative of the major morphological units of the investigation area, including four different units in the Lena River Delta and three major units in the hinterland.

The Lena River Delta, which is the largest delta in the Arctic (Walker 1998), is generally characterized by flat surfaces with a high number of lakes and scattered thermokarst depressions, in parts with pingos. These features are widespread across the entire area of 32,000 km² with more than 1,500 islands that originate of the annually 15 x 10^6 to 21 x 10^6 tons of suspended sediment load brought by the relatively warm water masses of around 16,400 m^3 s^{-1} (averaged per year) (Solomonov and Larionov 1994, Alabyan *et al.* 1995). Probably only < 30 % of this sediment load reach the Laptev Sea (Korotaev 1991, Alabyan *et al.* 1995) favouring the accumulation of the transported sediment on low elevated parts of the delta such as the active floodplain levels or sand spits and forming new islands.

The three main units of the Lena River Delta are so-called river terraces (Grigoriev 1993). Beyond them, there are actively flooded plains in the delta. These relatively young accumulative floodplains reach up to 5 m a.s.r.l. [above summer river level] and are a fourth unit. The area of the floodplains is characterized by strongly stratified soils and sediment layers (Akhmadeeva *et al.* 1999, Boike *et al.* 2013) caused by frequently flooding events pronouncedly occurring in the spring time. These different layers are dominated by sandy river deposits, organic rich material and pure turf layers. The organic rich and turf layers originate on the one hand from allochthonous material, which was eroded from the coasts within the delta or even in lower reaches of the Lena River and was re-deposited. On the other hand, theses layers developed autochthonous on the floodplain. These autochthonous organic layers probably are a result of the observed recent regular flooding of the sparse vegetation. As a consequence of flooding the vegetation is covered by a fresh sediment layer which hinders the on-going growth. This sediment layers are subsequently populated by a new generation of plants incorporating the covered generation into the top soil horizons (Zubrzycki *et al.* 2013). The vegetation cover reaches from nearly barren sands adjacent the summer river spit to dense vegetation moving more and more away from the river water. These active floodplains were investigated on Samoylov Island (72° 22’ N, 126° 29’ E).

The first river terrace is higher-elevated than the floodplains and varies in sedimentary composition as well as contents of organic matter in the soils. On Samoylov Island, this terrace is around 10 to 16 m a.s.r.l. and of Holocene age (Pavlova and Dorozhkina 1999). This unit is flooded only during extreme flooding events (Schwamborn *et al.* 2002). Fluvial sand

bands visible within the soils are witness for such events. This first river terrace is likely less elevated in the north of the Lena River Delta resulting in various compositions of the parent material for soil genesis. In addition to Samoylov Island, the authors investigated this unit on Tit-Ary Island (71° 59' N, 127° 02' E).

Investigations of the soils, which developed on the so-called second terrace of the Lena River Delta, were carried out at several locations on Arga-Muora-Sise Island (73° 10' N, 124° 34' E) (see Fig. 14). This island dominates the north-western part of the delta. It is 10 to 30 m a.s.r.l high and consists of coarse sediments that are older than 50 kyr (Schirrmeister *et al.* 2011b). This part of the Lena River Delta is dominated by many large lakes with deep hollows. The origin of these large and deep lakes, as well as the entire sandy unit the Arga-Muora-Sise Island belongs to, is still debatable (Are and Reimnitz 2000, Schwamborn *et al.* 2002).

The oldest morphological unit of the Lena River Delta is the so-called third terrace. It was formed in Middle and Late Pleistocene age (Schwamborn *et al.* 2002, Kuzmina *et al.* 2003). This terrace is characterized by island remains along the Olenyokskaya and Bykovskaya Channels embedded in the younger delta. The authors investigated in detail soils on Kurungnakh Island (72° 19' N, 126° 14' E) located in the south of the Lena River Delta. There are several thermokarst depressions on this island and ice-cored pingos. The soils were studied along a morphological transect from a river channel to one of such thermokarst depression crossing the plain covering the underlying ice complex. Other sites on this Pleistocene unit were located on Khardand Island (72° 48' N, 124° 54' E) and Sardakh Island (72° 34' N, 127° 14' E).

The investigated hinterland of the Lena River Delta belongs to the Central Siberian Plateau with elevations up to 700 m. Generally, in the depth crystalline rocks of the stable Siberian Platform underlie this plateau. Younger rocks and sediments cover these rocks (Simkin *et al.* 2006). The area of investigation is dominated by sedimentary deposits of the Anabar-Lena sedimentary basin. The elevations at the study sites were 64 m to 160 m. The main differences among the sites were characterized by the density of forests dominated by *Larix*-species. In the north of the Central Siberian Plateau there were no trees and the area was dominated by a polygonal tundra landscape (Sites: Bylung-Kyuel´ (72° 17' N, 125° 42' E) and El´gene-

Kyuele (71° 17’ N, 125° 33’ E)) whereas the south was densely forested (Sites: Peschanoe (70° 14’ N, 125° 15’ E), Yagodnoe (69° 53’ N, 124° 36’ E) and Sysy-Kyuel´ (69° 24’ N, 123° 49’ E)). Between these two extremes, there was a transition zone of patchy forests and extensive polygonal tundra like areas (Site: Zelyonoe (70° 42’ N, 125° 04’ E)). This transition zone was found around latitude of 70.5° N.

3.3 Material and methods

Prior extensive field investigations of soils, detailed study site inspections were carried out at most of the investigated sites to determine geomorphologic and vegetation patterns, as well as the depth of the seasonally thawed layer. These patterns are an effect of the soil development as well as factors affecting it. With these preliminary results pedologic field base maps were compiled for definition of the settings and construction of prospecting pits for the following soil studies with supplemental vegetation surveys.

The soil descriptions as well as the soil classifications were done according to the US Soil Taxonomy, 11th edition (Soil Survey Staff 2010). This approach allows a broad comparison with other published data on permafrost-affected soils. For additional comparisons with Russian literature, the soils were classified according to the system for permafrost soils of Yakutia by Elovskaya (1987).

For later analyses samples were taken from all investigated soil horizons. These samples were transported to laboratory in plastic bags to avoid moisture loss. In laboratory, all samples were dried at 40 °C to constant weight, sieved (2 mm) and partly grounded. Subsequently, these grounded samples were dried at 105 °C.

At most sites a brief vegetation survey was performed using the Braun-Blanquet method (Braun-Blanquet 1964). The vegetation was classified in three: shrub, herbal and moss layers, and the dominance of species was estimated regarding their coverage of surface area (in %). Subdivision was carried out as follows: the shrub layer was within a height range of 0.5 to 2 m, the herb-layer 0.05 to 0.5 m, and moss layer with heights up to 0.05 m.

The soil texture distribution was analysed according to DIN ISO 11277 with the dry-sieving and pipette-analyses using a Sedimat 4-12, UGT GmbH. Samples with an organic matter content higher than 2 % were pre-treated using H_2O_2 (30 %). Samples with more than 15 % of organic matter were excluded from measurements. There was no need to eliminate carbonates, iron- and manganese-oxides due to low concentrations.

Soil pH was measured according to DIN ISO 10390 with a pH meter Schott, Type CG 820 and the electrical conductivity (EC) was measured using a WTW, LF 90 conductivity meter in the same soil paste.

The gravimetric contents of total carbon and nitrogen were measured with a C-N elemental analyser (Elementar Analyse Systeme GmbH, Vario MAX) according to DIN ISO 10694. Due to the acidic pH value of most of the analysed soil samples, it was assumed that no inorganic carbon (IC) was present in the majority of soil samples; therefore only few samples were analysed for IC using phosphoric acid (H_3PO_4) measured by gas chromatography (SHIMADZU GC-14A, 14B).

The concentrations of exchangeable basic cations were determined according to DIN EN ISO 11260. The measurements were carried out using the atomic absorption spectrometry (AAS) (Perkin-Elmer, 1100B). Titration analyses were used to determine acidic cations (H^+-, Al^{3+}- and Fe^{3+}-Ions). Contents of oxalate-extractable iron (Fe_o) were determined at room temperature, in dark with acid ammonium oxalate at pH 3.25 (Schwertmann 1964, DIN 19684-6). Dithionite-extractable iron (Fe_d) was determined with dithionite-citrate, buffered by bicarbonate at pH 7.3 (Mehra and Jackson 1960). Iron in all extracts was determined using AAS (Perkin-Elmer, 1100B).

Plant-available potassium and phosphate in the soil were extracted with double-lactate according to VDLUFA (1991). Potassium was measured using AAS, whereas phosphate was measured by spectral photometry (Dr Lange, CADAS 100) after complexion with molybdenum.

3.4 Results and discussion

3.4.1 First River Terrace and Floodplains

The detailed study of permafrost-affected soils from Samoylov Island (Fig. 14) shows the high soil diversity on the first river terrace and the active floodplains (compare Zubrzycki *et al.* 2013). We have classified several soil Great Groups under which the soil complex of *Glacic Aquiturbels* and *Typic Historthels* is dominating the main extent of the investigation area. This soil complex develops due to the morphodynamics of ice-wedge polygons and resulting formation of patterned ground with elevated rims and depressed and water-saturated centres. The high water-saturation prevents the organic matter from decomposition resulting in formation of *Typic Historthels (Permafrost Typical Turfness-Gley)* (Fig. 17), whereas lifting of soils by the ice-wedge growth causes cryoturbation of the wet mineral soils resulting in formation of *Glacic Aquiturbels (Permafrost Peat-Gley)* (Fig. 18).

Polygon Centre - *Typic Historthel*

- high water level: 5 cm below surface
- thaw depth: 31 cm (August 8th)
- waterlogged
- predominantly reducing conditions
- peat accumulation
- dense root mat

horizon	depth (cm)	texture	reduc cond.	pH	OC (%)	C/N	roots
Oi	0-11	peat	no	5.0	22.1	43	few
OeBg	11-26	peat+sand	yes	4.8	12.6	35	many
Bg	26-31	sand	yes	4.8	2.1	>100	common
Bf	31-64	sandy loam	yes	5.0	4.2	30	non

Figure 17: *Typic Historthel*, the predominant soil of polygon centres on the first river terrace with a field description as well as soil properties.

Fig. 17: *Typic Historthel*, der Leitboden der Polygonzentren der ersten Flussterrasse mit einer Feldbeschreibung sowie den Bodeneigenschaften.

The pH values of the *Typic Historthel* were strong acidic throughout the soil profile. The contents of OC and N were highest in the topsoil horizon (22.1 % and 0.51 %, respectively). However, the transition from Oe to Bg, where the author found a mixture of organic matter and sand, was rich in OC (12.6 %) and N (0.36 %). These contents were low in the Bg horizon above the permafrost table. This horizon was characterisied by a very low N content of less than 0.02 % resulting in a C/N ratio higher than 100. Within the investigated permafrost horizon, the OC content was higher than within the overlying horizon and the C/N ratio amounted to 30.

Polygon Rim - *Glacic Aquiturbel*

- water level: 45 cm below soil surface
- thaw depth : 47 cm (August 8th)
- distinctly oxic in the top soil, reduced conditions below
- ice wedge at 70 cm
- cryoturbated

horizon	depth (cm)	texture	reduc cond.	pH	OC (%)	C/N	roots
Ajj	0-12	loamy sand	no	5.9	1.8	21	many
Bjjg1	12-15	sandy loam	no	6.2	2.2	21	common
Bjjg2	15-47	loam	yes	5.5	2.9	24	common
Bjjf	47-70	loam	yes	6.0	3.0	20	non

Figure 18: *Glacic Aquiturbel*, the predominant soil of polygon rims on the first river terrace with a field description as well as soil properties.

Fig. 18: *Glacic Aquiturbel*, der Leitboden der Polygonränder der ersten Flussterrasse mit einer Feldbeschreibung sowie den Bodeneigenschaften.

In the organic and nitrogen rich horizons, concentrations of plant available phosphorous (25 mg kg^{-1} ± 12 mg kg^{-1}) and potassium (687 mg kg^{-1} ± 248 mg kg^{-1}) were higher than the B-horizons (6 mg kg^{-1} ± 2 mg kg^{-1} and 98 mg kg^{-1} ± 22 mg kg^{-1}, respectively). The investigated *Aquiturbel* was characterised by a loamy texture within the profile. The upper horizons

contained a higher ratio of coarser grains. The pH values were higher in this soil than the neighboring *Historthel*. The soil above the ice wedge contained only small amouts of OC increasing from 1.8 % in the uppermost horizon to 3.0 % within the frozen ground. The C/N ratios were narrower here indicating higher decomposition of the available organic matter. With 22 mg kg^{-1} ± 9 mg kg^{-1} plant available phosphorous was highest in the A-horizon. Its concentration decreased with depth to less than 1 mg kg^{-1} in the subsoil. The spatial pattern of potassium was similar. The highest concentrations (226 mg kg^{-1} ± 158 mg kg^{-1}) were found in the topsoil, whereas the lowest (38 mg kg^{-1} ± 11 mg kg^{-1}) were detected in the Bjjg2-horizon.

Other soils classified on Samoylov Island, which likely are widespread across the entire first terrace, are *Typic Aquorthels (Permafrost Alluvial Muddy-Peatish-Gley)* and rich in organic *Fluvaquentic Fibristels (Permafrost Alluvial Muddy-Peat-Gley).*

Typically, the polygonal structures are covered by mosses and lichens (nearly 100 % cvg.) as well as by vascular plants. The coverage level of vascular plants is around 35 % and dominated by sedges. *Carex aquatilis* is widespread across both polygonal structures. However, the abundance in the centres is higher. In addition to *C. aquatilis* there are *C. rariflora* and *C. bigelowii* as well as herbs like *Caltha, Cardaminopsis* and *Pedicularis* species in polygonal centres. Dwarf shrubs like *Dryas punctata* and *Salix glauca* dominate the rims. Furthermore, there are *Poaceae* (*Poa arctica* and *Trisetum sibiricum*) and herbs like *Lagotis, Astragalus, Pyrola* and *Saxifraga*.

A substantial part of Samoylov Island belongs to the active floodplain levels and is flooded annually in spring. Theses floodplain levels are dominated by sandy or gleyic subgroups of the *Orthel* suborder as e.g. *Psammentic* and *Typic Aquorthels* (Fig. 19) or *Typic Psammorthels (Permafrost Alluvial Layered Poorly Developed Primitive)* (Fig. 20). The parent material consists of sand, sandy and silty loams with allochthonous and autochthonous organic layers. The autochthonous organic layers originate from the dominant plant species covering substantial parts of the floodplains (*Salix glauca, S. lanata* and *S. reptans, Equiesetum* and *Poaceae*). Other parts are barren. The *Typic Aquorthel* the author investigated was waterlogged and had a pH value close to neutral within the entire profile. The contents of organic carbon varied from one horizon to another. They ranged from 0.8 % to 3.0 %. The nitrogen contents, refered to the carbon contents, were relatively high resulting in C/N ratios

ranging from 10 to 15. Plant available phosphorous was higher concentrated in the topsoil horizons (11 mg kg^{-1}) than deeper within the soil profile (6 mg kg^{-1}). Potassium ranged from 36 mg kg^{-1} to 13 mg kg^{-1}.

Floodplain - *Typic Aquorthel*

- depression close to small brook
- water level: at the soil surface
- thaw depth: 56 cm (July 22th)
- waterlogged
- fluvial silts with alluvial organics (mud)

horizon	depth (cm)	texture	reduc. cond.	pH	OC (%)	C/N	roots
A1	0-5	silt loam	no	6.7	3.0	15	few
A2	5-9	silt loam	no	6.7	1.2	12	common
Bg1	9-20	silt loam	yes	6.7	2.2	13	many
Bg2	20-35	silt loam	yes	6.7	3.0	15	many
Bg3	35-52	silt loam	yes	6.5	2.2	15	few
Bf	52-	silt loam	yes	6.6	0.8	10	none

Figure 19: *Typic Aquorthel*, the predominant soil of parts of the active floodplain with a field description as well as soil properties.

Fig. 19: *Typic Aquorthel*, der Leitboden von Teilen der aktiven Überflutungsebene mit einer Feldbeschreibung sowie den Bodeneigenschaften.

The sand-dominated *Typic Psammorthel* (Fig. 20) was characterised by alternating sandy and sitly layers as well as buried A-horizons. This soil showed the deepest active layer thicknes of the entire study which amounted to 98 cm. The pH values were slightly acidic without any remarkable pattern within the soil profile. The OC contents ranged between 0.1 % and 2.0 %. They were higher in buried A-horizons and lower in the sandy and silty layers. The C/N ratios were narrow indicating an advanced decomposition of the organic matter available within the

soil. The concentrations of of phosphorous and potassium were evenly distributed across the profile and amounted to 9 mg kg^{-1} ± 3 mg kg^{-1} and 36 mg kg^{-1} ± 9 mg kg^{-1}, respectively.

Floodplain - *Typic Psammorthel*

- sandy ridge close to the beach
- fluvial sand and silt layers, buried A-horizons
- water level: 91 cm below surface
- thaw depth: 98 cm (August 13th)

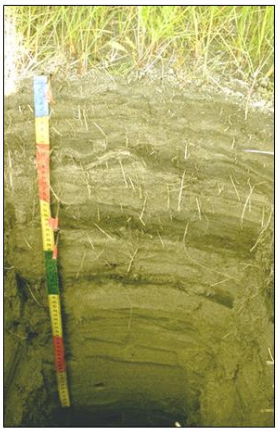

horizon	depth (cm)	texture	reduc cond.	pH	OC (%)	C/N	roots
A	0-11	loamy sand	no	6.7	1.2	13	many
Ab/C	11-21	sand	no	6.5	0.6	15	many
Ab1	21-29	sandy loam	no	6.6	2.0	17	many
C1	29-36	sand	no	6.4	0.2	12	common
Ab2	36-41	loam	no	6.7	1.6	13	few
C2	41-75	sand	no	6.2	0.1	10	non
Cg	75-98	loamy sand	no	6.6	1.0	15	non

Figure 20: *Typic Psammorthel*, the predominant soil of parts of the active floodplain with a field description as well as soil properties.

Fig. 20: *Typic Psammorthel*, der Leitboden von Teilen der aktiven Überflutungsebene mit einer Feldbeschreibung sowie den Bodeneigenschaften.

The Tit-Ary Island is located in the lower reaches of the Lena River at the entry to the delta area (Fig. 14). It is one of the northernmost places of the tree-limit line in the Russian Arctic. The tree coverage (*Larix*) amounted to 5 %. Shrubs, herbs and mosses were estimated to have high coverage of 70 %, 30 % and 80 %, respectively. Dominant vascular species were *Ledum palustre*, *Betula nana* and *Eriophorium spec*.. At the selected predominant site, a cryoturbated soil was found. This soil was classified as a *Typic Aquiturbel (Permafrost Peatish Gley).* The thaw depth on the day of sampling (17.08.2009) reached 30 cm. The pH values increased with depth from strong acidic to moderate acidic whereas the EC did not show any features and

amounted to 62.9 µS cm^{-1} ± 9.0 µS cm^{-1}. The contents of OC and N were highest in the organic Oe-horizon (8.0 % and 0.4 %, respectively; C/N: 21.4) and dropped significantly to 1.7 % ± 0.3 % and 0.11 % ± 0.02 %, respectively in deeper located mineral horizons with C/N ratios of 14.5 and 14.8. The mean sum of basic cations within both mineral horizons was 101.7 $mmol_c$ kg^{-1}. It was slightly higher in the deeper BgjjII-horizon. The amounts of acidic cations decreased with depth and traced the vertical pH pattern. The pedogenic Fe-oxides were double that high in the mineral horizons (around 16 g kg^{-1}) compared to the organic topsoil horizon (8 g kg^{-1}). The parent material of Tit-Ari Island was probably affected by likely Fe-rich minerals from the Kharaulakh Ridge just across the water stream. The degree of activity indicated an advanced pedogenesis. Although this island was affected by comparable factors as the areas of the Lena River Delta, no pronounced polygonal structures were detected in the investigated part of the island. Though these structures were not detected, the investigated soil profile was similar to profiles found at polygonal rims on Kurungnakh Island, especially those that developed on the wide plains covering the ice complex.

3.4.2 Second Terrace

The second terrace of the Lena River Delta consists of the Arga-Muora-Sise Island. This study area is the northernmost investigated area (Fig. 14). The vegetation of this site was dominated by mosses (90 % cvg.) and herbs (30 % cvg.) with two dominant vascular plants: *Carex spec*. and *Cassiope tetragona*. This island provided a sandy parent material for soil genesis. The mean sand content was 93.7 % ± 3.5 %. This sand consisted mainly of the fine sand fraction (55.9 % ± 12.7 %) and the middle sand fraction (37.2 % ± 9.6%), and was comparable in mineralogical and sedimentological patterns with the recent Lena River bed load (Schwamborn *et al.* 2002). The origin of these deposits is still under discussion (Are and Reimnitz 2000). On the one hand, Galabala (1987) and Grigoriev (1993) supposed alluvial plain deposits this area to be composed of. On the other hand, Korotaev (1991) and Mikhailov (1997) believed that the Arga-Muora-Sise Island was composed of marine deposits. A more recent work by Schwamborn *et al.* (2002) supposed a braided river system with highly energetic periglacial channel network with high accumulation rates. The high sand contents

on the one hand and the lack of organic matter in the Arga-Muora-Sise Island sediments on the other hand support the latter idea. These high sand contents characterize the described soils within the patterned ground with vague polygonal structures and elevated rims. Within the two small-scale units of the patterned ground *Typic Psammoturbels (*polygon centre: *Permafrost alluvial primitive sandy*, polygon rim: *Permafrost peatish gleyish)* developed (Fig. 21 and Fig. 22).

Polygon Rim – *Typic Psammoturbel*

- thaw depth : 57 cm (July 31st)
- reduced conditions in the lower part
- sand-dominated
- low water level
- cryoturbated

horizon	depth (cm)	texture	reduc cond.	pH	OC (%)	C/N	roots
A	0-5	silty sand	no	4.8	3.3	18	common
Bgjj1	5-17	sand	yes	5.1	0.8	15	non
Bhjj	17-25	sand	yes	5.2	1.3	16	non
Bgjj2	25-57	sand	yes	5.9	0.2	10	non

Figure 21: *Typic Psammoturbel*, the predominant soil of polygon rims on the second river terrace with a field description as well as soil properties.

Fig. 21: *Typic Psammoturbel*, der Leitboden der Polygonränder der zweiten Flussterrasse mit einer Feldbeschreibung sowie den Bodeneigenschaften.

However, the *Typic Psammoturbels* of both patterned ground units were not identical. The depth of the seasonally active layer was on the day of sampling (August 2009) 20 to 28 cm and 26 to 58 cm of ground at rims and in the polygonal centres, respectively. The rims were covered by a thick (5 to 10 cm) organic horizon insulating well and preserving of thawing. The polygonal centres had organic enriched A-horizons on the top. The pH values of the investigated soils were moderate acidic with a strong acidic topsoil horizon at the rims. The high accumulation of organic matter in the topsoil at the rims had also an influence on the

soluble ions in the soil. The EC was low with 35.1 µS cm^{-1} ± 45.8 µS cm^{-1}. The OC and N contents were high in the organic enriched A- and organic O-horizons and dropped considerably with the depth.

Polygon Centre - *Typic Psammoturbel*

- thaw depth : 25 cm (August 1st)
- reduced conditions in the lower part
- sand-dominated
- water- level: 18 cm below surface
- thick organic enriched top horizon
- cryoturbated

horizon	depth (cm)	texture	reduc cond.	pH	OC (%)	C/N	roots
A	0-9	loamy sand	no	4.3	23.1	22	many
Bgjj1	9-21	sand	yes	5.2	0.9	16	common
Bhjj	21-25	sand	yes	5.0	0.6	13	common

Figure 22: *Typic Psammoturbel*, the predominant soil of polygon centres on the second river terrace with a field description as well as soil properties.

Fig. 22: *Typic Psammoturbel*, der Leitboden der Polygonzentren der zweiten Flussterrasse mit einer Feldbeschreibung sowie den Bodeneigenschaften.

The resulting C/N ratios were narrow in the polygonal centres as well as in the polygonal rims. The determined CEC and the sum of basic cations were low with mean values of 19.1 $mmol_c$ kg^{-1} ± 12.4 $mmol_c$ kg^{-1}, respectively. In contrast the concentrations of the "acidic" cations were high (mean Al^{3+} was 16.5 $mmol_c$ kg^{-1} ± 19.6 $mmol_c$ kg^{-1}; mean H^+ was 2.5 $mmol_c$ kg^{-1} ± 4.6 $mmol_c$ kg^{-1}) with notable 55.0 $mmol_c$ kg^{-1} of Al^{3+}-ions and 10.7 $mmol_c$ kg^{-1} of H^+-ions within the strong acidic topsoil horizon in the *Psammoturbel* of the rim. The pedogenic Fe-oxides of the same horizon were distinctly higher (25.6 g kg^{-1}) than the mean concentration of 6.8 g kg^{-1} ± 10.6 g kg^{-1}. The high degree of activity indicated young soil development in both topsoil horizons. It was more advanced in higher depths, especially at the rims. Here, pronounced gleying properties were detected with oxidized spots

as well as depletions caused by reducing properties. The *Psammoturbel* in the centre was characterized by mostly pedogenic unaffected soil parent material underlying the Ah-horizon

3.4.3 Third Terrace

The investigation area is characterised by extensive plains, crossed by valleys and dominated by large thermokarst depressions. Such depressions are called Alases and cover around 20 % of the area of the third terrace. However, with 38 % this percentage is significantly higher on Kurungnakh Island (Morgenstern *et al.* 2011), where the detailed soil survey was performed (Fig. 14). The soils of the second terrace of the Lena River Delta closely follow the pattern of the geomorphic units found in the investigation area as well as the small-scale site hydro-morphology. The extensive plains of Kurungnakh Island were characterised by large polygonal structures with depressed and water saturated polygonal centres vegetated by *Sphangnum spec.* and wet polygonal rims with *Sphagnum squarrosum*. The vegetation coverage was dominated by mosses with 80 % and 70 % in the polygonal rim and the centre, respectively. Vascular plants dominating were *Betula nana*, *Dryas octopetala* on rims and *Eriophorum scheuchzeri* in the centres. Such polygons were covered by a soil complex of *Glacic Aquiturbel (Permafrost tundra peatish-gley)* (Fig. 23) and *Ruptic Historthel (Permafrost tundra peat)* (Fig. 24). The *Glacic Aquiturbels* at the elevated polygonal rims contained a considerably thick organic layer. The underlying cryoturbated horizons consisted of sandy loams with a huge portion of clay. These sediments of aeolian type originated from the same source as described for the soils of the degraded cliff, namely the surrounded sand banks and the sediments deposited there. Due to longer distance from the place of origin, more silty sediments than sandy sediments were deposited. Within the top 4 cm of the elevated rim there were still small amounts of IC found indicating freshly deposited carbonates not yet depleted by the light acidic soil horizon. The following deeper horizons showed more acidic pH values probably due to lower influence of the deposited likely carbonate containing aeolian silts and fine sands. Due to high OC, texture analyses of the topsoil horizon and the centre profile were not conducted. The depth of the thawed layer on 10.08.2008 was determined at 23 cm and 35 cm below ground in the polygonal rim and

centre, respectively. The EC amounted to 21 µS cm^{-1} ± 10 µS cm^{-1} and 61 µS cm^{-1} ± 77 µS cm^{-1} for the *Aquiturbel* and the *Historthel*, respectively.

Polygon Rim – *Glacic Aquiturbel*

- thaw depth : 23 cm (August 10th)
- ice-wedge in 23 cm depth
- reduced conditions
- water level: 9 cm below surface
- cryoturbated

horizon	depth (cm)	texture	reduc cond.	pH	OC (%)	C/N	roots
Oie	0-4	org. matter	no	6.2	11.6	22	common
Oe	4-9	org. matter	yes	5.9	9.5	18	common
Bgjj1	9-14	sandy loam	yes	5.3	2.5	19	non
Bgjj2	14-23	sandy loam	yes	5.5	2.2	22	non

Figure 23: *Glacic Aquiturbel*, the predominant soil of polygon rims on plains of the third river terrace with a field description as well as soil properties.

Fig. 23: *Glacic Aquiturbel*, der Leitboden der Polygonränder der Ebenen der dritten Flussterrasse mit einer Feldbeschreibung sowie den Bodeneigenschaften.

Within the *Historthel* it dropped from 150 µS cm^{-1} in the topsoil to 16 µS cm^{-1} in the second horizon. The OC in the *Historthel* was high throughout the horizon (mean 15.5 % ± 4.2 %). The OC content of the *Aquiturbel* was high in organic horizons (mean 10.5 %) and distinctly lower in the mineral subsoil with gleying properties (2.4 %). The N contents behaved corresponding to OC, but on a significantly lower level, ranging from 0.10 % to 0.68 %. High water levels and the long periods of prevailing coldness inhibit the litter decomposition resulting in an increasing thickness of the organic layers consisting of *Sphagnum* and the other dominant species. The C/N ratios were 20.2 ± 2.0 and 28.2 ± 6.9 in the *Aquiturbel* and *Historthel*, respectively. The range was distinctly higher in the polygonal centre and the *Historthel*. Although decomposition is low, there were detectable differences within the organic horizons. The uppermost, likely youngest was very little decomposed with a high

fiber content after rubbing. The older horizons were more decomposed. However, they showed still more than 17 % of fiber, supporting the finding of inhibited decomposition. In the deepest horizon of the polygonal centre (Oe2) the author found the same decomposition level as in the horizon above, though the content of mineral soil in this horizon was distinctly higher with a loamy texture, determined in field according to the AG Boden (2005). Presumably, this horizon, a former top soil horizon, was exposed to higher sedimentation loads than the top horizons in recent times. The OC content of this Oe2 horizon is consequently lower than of those above.

Polygon Centre – Ruptic Historthel

- thaw depth : 35 cm (August 10th)
- reduced conditions
- organic matter-dominated
- water-logged
- thick organic enriched top horizon

horizon	depth (cm)	texture	reduc cond.	pH	OC (%)	C/N	roots
Oie	0-5	org. matter	yes	5.6	17.4	36	many
Oe1	5-25	org. matter	yes	5.4	19.1	28	many
Oe2	25-35	org. matter	yes	5.5	11.0	21	common

Figure 24: *Ruptic Historthel*, the predominant soil of polygon centres on plains of the third river terrace with a field description as well as soil properties.

Fig. 24: *Ruptic Historthel*, der Leitboden der Polygonzentren der Ebenen der dritten Flussterrasse mit einer Feldbeschreibung sowie den Bodeneigenschaften.

Within the described soil complex the CEC for one organic rich horizon as well as the mineral horizons could be measured. The observed results were of high interest, demonstrating that considerable amounts of cations were found within the organic horizons (241 $mmol_c\ kg^{-1}$ ± 127 $mmol_c\ kg^{-1}$), especially calcium and magnesium. Up to five times more cations were stored within these horizons, however, the CEC was only 50 % higher there than in the mineral horizons. The acidic cations showed partly a contrary characteristic with remarkably

higher concentrations of Al^{3+} in the mineral soil horizons than the organic-rich - at the same pH value. Hydrons were enriched in the polygon centre where the water level was high. The pedogenic Fe- and Mn-oxides showed high concentrations within the organic horizons with values ranging from 14.9 g kg^{-1} to 25.5 g kg^{-1} and 0.24 g kg^{-1} to 1.8 g kg^{-1}, respectively suggesting an advanced development of these secondary oxides. There were significantly higher concentrations as well as lower degrees of activity of both oxide types in the organic horizons suggesting the presence of Fe-organic matter complexes (Cornell and Schwertmann 2004). The concentrations of plant available nutrients are essential for assuming the environmental factors controlling the microbial and plant life. Within this plain area of Kurungnakh Island the available potassium and phosphorus were bounded in the organic soil layers, especially within the upper horizons of the *Ruptíc Historthel* (770 mg K^{+} kg^{-1} and 21 mg P kg^{-1} within the top 5 cm of ground). These nutrients are important soil properties, responsible for plant growth. However, due to the general strong N limitation of arctic regions the high concentration may stay unused.

Within the investigated thermokarst depression there were two distinctly different levels likely illustrating the retreat of the water body. These levels were covered by two various soil complexes. The soils adjacent a large lake had a higher impact by aquic conditions. Here, the vegetation of rims was composed of *Sphagnum spec.* and *Potentilla palustris*. A soil complex of *Ruptic-Histic Aquiturbel (Permafrost tundra peat slimy-gley)* and *Ruptic Historthel (Permafrost tundra humus-peat)* was dominant here, whereas the higher and likely older terrace was dominated by a soil complex of *Ruptic Histoturbel (Permafrost tundra peat-gleyic)* (Fig. 25) and *Ruptic Historthel (Permafrost tundra peat)* (Fig. 26). The vegetation within the depression followed the morphology of the patterned ground. Mosses covered the rims. *Hylocomium splendens* was dominant. The water saturated soils in the polygon centres were covered by *Carex chordorrhiza, Carex stans* and *Eriophorum scheuchzeri*. The soils of ther higher terrace were thawed down to 26 cm and 38 cm depths in the rim and the centre, respectively. The thaw depth was higher in the water saturated centres due to the heat effect of the water. Additionally, the *Histoturbels* in the rims were drier and had two organic horizons insulating the soils and preserving of thawing. The pH values were strong to moderate acidic varying between 4.9 and 5.8. The lowest and the highest value were found within the Oi- and

Oe-horizon of the *Histoturbel*, respectively. The other horizons were dominated by pH values with a mean of 5.2 ± 0.1. There were no significant differences between organic and mineral horizons. Within the strong acidic Oi-horizon a distinctly higher EC was determined (280 µS cm^{-1}) than in other horizons (24.5 µS cm^{-1} ± 24.2 µS cm^{-1}). Generally, higher EC were found in the *Histoturbels* (90 µS cm^{-1} ± 109 µS cm^{-1}) than the *Historthels* (10 µS cm^{-1} ± 2 µS cm^{-1}). The high OC and N contents decreased with profile depth in both soils. The Oejj-horizon in the *Ruptic Histoturbel* had a higher OC content than the overlying B(h). However, the B(h) was strongly enriched by organic matter and had a OC content of 5.9 %. In the *Historthel* in the polygonal centre OC contents varied between 8.5 % and 22.5 % (mean 14.5 % ± 6.0 %) and the N contents varied between 0.48 % and 0.79 % (mean 0.62 % ± 0.13 %). The mean C/N ratio in the polygonal centre was 22.6 ± 4.9. In the polygonal rim the OC content varied between 2.2 % and 15.9 % and N content varied between 0.1 % and 0.8 % resulting in C/N ratios from 14.3 to 19.4.

Polygon Rim – *Ruptic Histoturbel*

- thaw depth : 26 cm (August 11th)
- red-ox conditions
- water level: 8 cm below surface
- cryoturbated
- mineral and organic horizons alternating

horizon	depth (cm)	texture	reduc cond.	pH	OC (%)	C/N	roots
Oi	0-4	org. matter	no	4.9	15.9	19	many
Oe	4-7	silty sand	no	5.8	6.6	14	common
B(h)	7-11	loamy sand	yes	5.1	5.9	15	common
Oejj	11-16	org. matter	yes	5.1	9.2	14	common
Bgjj	16-26	silty sand	yes	5.2	2.2	18	non

Figure 25: *Ruptic Histoturbel*, the predominant soil of polygon rims in thermokarst depressions of the third river terrace with a field description as well as soil properties.

Fig. 25: *Ruptic Histoturbel*, der Leitboden der Polygonränder in Thermokarstsenken der dritten Flussterrasse mit einer Feldbeschreibung sowie den Bodeneigenschaften.

The polygonal rim investigated here likely suggested changes in the environment of the higher terrace in the past. Probably the thermokarst depression was flooded by water several times with periodical retreat of the water and therefore periodical soil and vegetation development resulted in growing organic soil layers. These vegetated soils were flooded by advancing water and subsequent covered by a sediment layer.

Polygon Centre – *Ruptic Historthel*

- thaw depth : 28 cm (August 11th)
- reduced conditions
- water level: 2 cm below surface
- organic horizons underlain by mineral layers (in a depth of ca. 30 cm)

horizon	depth (cm)	texture	reduc cond.	pH	OC (%)	C/N	roots
Oi	0-9	org. matter	no	5.4	22.5	28	many
Oe1	9-14	org. matter	yes	5.3	13.1	20	common
Oe2	14-24	org. matter	yes	5.1	18.9	27	common
Oe3	24-30	org. matter	yes	5.4	9.8	19	common
Bg(O)	30-38	silty loam	yes	5.2	8.5	18	common

Figure 26: *Ruptic Historthel*, the predominant soil of polygon centres in thermokarst depressions of the third river terrace with a field description as well as soil properties.

Fig. 26: *Ruptic Historthel*, der Leitboden der Polygonzentren in Thermokarstsenken der dritten Flussterrasse mit einer Feldbeschreibung sowie den Bodeneigenschaften.

The distribution of the basic cations was similar in both soils with a mean sum for these cations of 132 $mmol_c\ kg^{-1}$ ± 84 $mmol_c\ kg^{-1}$ and 125 $mmol_c\ kg^{-1}$ ± 25 $mmol_c\ kg^{-1}$ for the *Histoturbel* and *Historthel*, respectively. The distribution within the *Ruptic Histoturbel* traced the changes between mineral (lower sum of basic cations) and organic soil horizons (higher sum of basic cations). The concentrations of the "acidic" cations were distinctly higher in the polygonal centre in the *Historthel*. The mean Al^{3+} concentrations were 11.1 $mmol_c\ kg^{-1}$ ± 8.3 $mmol_c\ kg^{-1}$ and 26.5 $mmol_c\ kg^{-1}$ ± 10.0 $mmol_c\ kg^{-1}$ in the *Histoturbel* and *Historthel*, respectively. In the *Histoturbel* at the rim, these concentrations increased with depth, whereas

in the *Historthels* in the centre these concentrations decreased. The H^+-ions showed no recognizable vertical pattern. They were higher concentrated in the polygonal centre as well. Concentrations of potassium and phosphorous were highest in the topsoil horizons of both soils and amounted in the *Histoturbel* to 135 mg kg^{-1} and 20 mg kg^{-1}, respectively and in the *Historthel* to 107 mg kg^{-1} and 7 mg kg^{-1}, respectively. They decreased with increasing depth. Besides these horizons, the concentrations were distinctly lower than the averaged concentrations for the study. The concentrations of pedogenic Fe- and Mn-oxides were high within both soils. Fe_d varied from 6.9 g kg^{-1} to 27.8 g kg^{-1} and from 14.5 g kg^{-1} to 31.1 g kg^{-1} in the *Histoturbel* and *Historthel*, respectively. Mn-oxides had an averaged content of 0.59 % ± 0.87 % with a distinctly higher content in the topsoil of the *Histoturbel* of 3.01 %. The degree of activity indicated more well-crystallized oxides in the polygonal centre than the rim. Generally, there was a varying pattern of the Fe-oxide A_f. The manifold changes from higher to lower A_f of the Fe-oxides suggested varying stages and environments for pedogenic development. These findings support the assumption of repeated flooding of the higher terrace within the thermokarst depression.

The soils adjacent a large lake were characterised by moderate to light acidic pH values. The EC was low in both soils. Only the topsoil horizons of both soils were different. While the EC was 31.5 µS cm^{-1} in the topmost horizon of the *Aquiturbel*, it was 8.5 µS cm^{-1} in the correspondent horizon of the *Historthel*. Both topmost horizons were followed by horizons with similar EC values of 12.6 µS cm^{-1} ± 0.8 µS cm^{-1}. The OC and N contents were high throughout the *Historthel* (mean OC 20.0 % ± 8.7 %, mean N 0.70 % ± 0.13 %). In the *Aquiturbel* both, OC and N, were high (16.2 %) with exception of the deepest mineral horizon, where the OC and N were 1.2 % and 0.07 %, respectively. The *Historthel* had distinctly higher C/N ratios (27.6 ± 8.0) than the *Aquiturbel* (17.9 ± 3.8). The profile of the *Ruptic-Histic Aquiturbel* suggested that this part of the thermokarst depression was a part of the lake bottom when this expanded in the past. Due to its lower relative elevation above the present lake water lever than the elevation of the higher terrace, the flooding events were likely more often and probably for a longer period of time. The mineral horizons here composed of medium and fine sand (46 % and 41 %, respectively) and small portions of clay (5 %) and silt (6 %). The concentrations of both, basic and acidic cations were higher in the

polygon centre in the *Historthel*. The mean sums of basic cations were 102 $mmol_c\ kg^{-1}$ ± 93 $mmol_c\ kg^{-1}$ and 242 $mmol_c\ kg^{-1}$ ± 99 $mmol_c\ kg^{-1}$ in the *Aquiturbel* and *Historthel*, respectively. Al^{3+} showed values of 4.1 $mmol_c\ kg^{-1}$ ± 3.3 $mmol_c\ kg^{-1}$ and 9.2 $mmol_c\ kg^{-1}$ ± 4.0 $mmol_c\ kg^{-1}$; H^+ 1.5 $mmol_c\ kg^{-1}$ ± 0.8 $mmol_c\ kg^{-1}$ and 4.2 $mmol_c\ kg^{-1}$ ± 2.1 $mmol_c\ kg^{-1}$ in the *Aquorthel* and *Historthel*, respectively. The sandy horizon was characterized by low concentrations of all cations as well as the nutrients potassium and phosphorous. Within the depressed terrace, the highest concentrations of pedogenic Fe-oxides were found in organic soil horizons of both soils. In the *Aquiturbel* there were 41 $g\ kg^{-1}$ of the dithionite soluble iron-oxides (Fe_d) in the uppermost horizon. This concentration dropped to 4.8 $g\ kg^{-1}$ in the second and to 1.0 $g\ kg^{-1}$ in the lowest, the sandy mineral soil horizon. The vertical distribution in the *Historthel* was different from in the *Aquiturbel* with comparably high concentrations throughout the entire profile and a maximum in the second, Oe-horizon and 41.5 $g\ kg^{-1}$. The pedogenic Mn-oxides followed a similar vertical pattern in the *Aquiturbel* as the Fe-oxides with values between 0.02 $g\ kg^{-1}$ and 3.5 $g\ kg^{-1}$. In the *Historthel* the distribution was different to the distribution of Fe-oxides with both upper horizons containing 0.58 $g\ kg^{-1}$ and the deepest with 0.18 $g\ kg^{-1}$.

The slopes showed pronounced solifluction phenomena as hummocky lobes of different intensity due to varying inclinations. *Peltigera aphtosa* lichen and *Hylocomium splendens* mosses dominated the vegetation. Dominating vascular plants were *Betula nana, Cassiope tetragona* and *Dryas octopetala*.

The lower slope (foot slope) was covered by *Ruptic-Histic Aquiturbels (Permafrost tundra peatish-gleyic)* (Fig. 27) and *Ruptic-Histic Aquorthels (Permafrost tundra peat-silty-gleyic)* (Fig. 28), whereas a soil complex of *Typic Aquiturbel (Permafrost tundra peatish-silty-gley)* and *Fluvaquentic Historthel (Permafrost tundra peat slimy-gleyic)* dominated the middle slope. The slope shoulder was characterised by low centre polygons. *Glacic Aquiturbels* (*Permafrost tundra peatish-gley*) covered the wet polygon rims and *Fluvaquentic Historthels* (*Permafrost tundra peatish slimy-gley*) the water-saturated polygon centres. The vegetation cover was dominated by mosses (*Sphangnum spec.*, *Hylocomium splendens* and *Pogonatum alpinum*), *Carex stans*. and *Salix glauca*. The soils of the slope shoulder were characterised by moderately to light acidic pH values. The Oa-horizon of the *Historthel* had the highest pH and

a distinctly higher EC (155 µS cm^{-1}) than the other horizon of the two profiles (16 µS cm^{-1} ± 4 µS cm^{-1}). The mineral soil horizons of the *Glacic Aquiturbel* and the subsoil horizon of the *Fluvaquentic Historthel* were similar in their chemical composition as well as the physical properties indicating the same source of parent material and only a small accumulation of organic matter in the polygonal centre. The clay rich soil horizon did not act as a barrier in this part of the plain, since there were no accumulations of any chemical element above. However, the water content in this waterlogged environment was distinctly lower in the subsoil horizon than the overlying one suggesting a lower pore volume there.

Mound – *Ruptic-Histic Aquiturbel*

- thaw depth : 41 cm (August 13th)
- reduced conditions
- silt dominated
- water level: 10 cm below surface
- hummocky surface

horizon	depth (cm)	texture	reduc cond.	pH	OC (%)	C/N	roots
Ah	0-11	loamy silt	yes	5.9	4.6	14	many
Bgjj1	11-32	sandy loam	yes	5.6	2.3	13	common
Bgjj2	32-41	silty sand	yes	5.3	3.5	16	common

Figure 27: *Ruptic-Histic Aquiturbel*, the predominant soil of mounds on slopes of the third river terrace with a field description as well as soil properties.

Fig. 27: *Ruptic-Histic Aquiturbel*, der Leitboden der Hügel an Hängen der dritten Flussterrasse mit einer Feldbeschreibung sowie den Bodeneigenschaften.

The OC and N contents were highest in Oa-horizon followed by the Oe-horizon with 22.5 % and 1.1 %; 14.0 % and 0.8 %, respectively. The C/N ratios were even throughout the horizons (19.9 ± 1.8). The sum of basic cations in the mineral horizons was on average 79 $mmol_c$ kg^{-1} ± 7.6 $mmol_c$ kg^{-1} and lower than the mean of the study. It was higher (262 $mmol_c$ kg^{-1}) in the organic horizons of the *Historthel* due to higher Ca-cation and Mg-cation concentrations hold by the organic material. "Acidic" cations (Al^{3+} and H^{+}) were found within horizons of

moderately acidic pH. Their concentrations were in the range of the averaged values of this study and amounted to 17 $mmol_c$ kg^{-1} and 1.5 $mmol_c$ kg^{-1} for Al^{3+} and H^+, respectively. Although these cations were present in the topsoil horizon of the polygonal centre, there were still remains of IC reaching 0.1 %. However, this accounts to only 0.5 % of the total C and therefore is negligible.

Vale – *Ruptic-Histic Aquorthel*

- thaw depth : 27 cm (August 13th)
- red-ox conditions
- water level: 4 cm below surface
- cryoturbated below 20 cm depth
- in vale amoung hummocks

horizon	depth (cm)	texture	reduc cond.	pH	OC (%)	C/N	roots
Ah	0-7	loamy silt	no	6.6	12.3	26	common
Bg	7-20	loamy silt	yes	6.6	4.2	16	common
Bg(Fe)	20-25	loamy sand	yes	5.9	1.8	15	non
Bgjj	25-27	loamy sand	yes	5.4	2.5	16	non

Figure 28: *Ruptic-Histic Aquorthel*, the predominant soil of vales on slopes of the third river terrace with a field description as well as soil properties.

Fig. 28: *Ruptic-Histic Aquorthel*, der Leitboden der Mulden an Hängen der dritten Flussterrasse mit einer Feldbeschreibung sowie den Bodeneigenschaften.

The pedogenic Fe-oxides showed high contents in the organic horizons as well as the topsoil of the *Aquiturbel*. The degree of activity increased with depth. The Mn-oxides were extremely high concentrated in the topsoil of the *Historthel* with 2.3 g kg^{-1} compared to other horizons of the *Aquiturbel* (0.06 g kg^{-1} ± 0.04 g kg^{-1}). The deepest horizons of both, the *Historthel* and the *Aquiturbel* had a similar Fe- and Mn-oxides composition with high portions of amorphous forms. The horizons located above had distinctly more pedogenic oxides, and there were further developed and crystallized forms present assuming more pronounced pedogenesis.

The high Mn-oxide content in the topsoil of the *Historthel* favoured the remarkable dark colour of this horizon.

Both investigated soils of the middle slope were water logged in the lower part of their soil profiles with moderate acidic pH values. The thaw depths on 13.08.2008 were 39 cm and 21 cm in the hillock and the vale, respectively. Although the thaw depth was so different in both soils, the surface of the frozen layers was even. However, it was sloped allowing the water to flow downwards washing out nutrients and other soluble elements. The EC was highest in both topsoil horizons (41 µS cm^{-1} and 59 µS cm^{-1} for the *Aquiturbel* and *Historthel*) where the water flow and wash out had a low affect. The mean EC in the subsoil was low and amounted to 17 µS cm^{-1} ± 7 µS cm^{-1}. The mean CEC was 111 $mmol_c$ kg^{-1} ± 18 $mmol_c$ kg^{-1}. Among all cations there was a distinct enrichment of Ca^{2+} in the *Historthel* in the vale that lead to a general higher sum of basic cations within the *Historthel* (261 $mmol_c$ kg^{-1} ± 163 $mmol_c$ kg^{-1}) compared to the *Aquiturbel* (104 $mmol_c$ kg^{-1} ± 33 $mmol_c$ kg^{-1}). The OC and N contents were high in the topsoils as well. The topsoil horizon thickness of the *Aquiturbel* was little. Though organic rich it consisted of considerable amounts of mineral soil of sandy loam texture. The BgjjI-horizon was of the same texture composition but with distinctly lower OC and N contents. Within these two upper horizons, advanced pedogenesis could be assumed due to the clay enriched and Fe-oxide rich soils. In contrary to those horizons, the second BgjjII-horizon with the pronounced water saturation had a coarser texture with a higher silt portion and a lower clay portion. Additionally, the high degree of activity (Fe-oxides) indicated a slow or only initial pedogenesis. Within the entire profiles of both soils the C/N ratios were even, amounted to 17.9 ±1.3, and gave no additional information about differences among the soil profiles and their OM decomposition. The averaged C/N ratio for this site was lower than the averaged ratio for the entire study. Within both soils the concentrations of pedogenicly formed Fe-oxides were high and decreased with depth. The portion of the active amorphous oxides (Fe_o) increased with depth leading to an increasing A_f for these oxides. The value of Mn-oxides was distinctly higher in the *Historthel* than the *Aquiturbel*. The degree of activity was lower in the *Historthel* and decreased with depth.

The soil profile on the foot slope had a low stability and collapsed rapidly after digging. The depth of the seasonally thawed layer was in the hillocks 41 cm and in the vales 27 cm of

ground and corresponding to the situation in the upper slope there was a visible water flow down slope on the surface of the frozen ground. The pH values were moderately to light acidic and varied between 5.3 and 6.6. They were distinctly higher in the upper soil horizons. However, the pH did not show any differences to the upper slope soils. The low EC (mean 25.4 µS cm^{-1} ± 15.3 µS cm^{-1}) decreased with increasing depth in both soil horizons, probably because of outwash of soluble ions. The contents of OC and N were highest in the topsoil with a maximum of 12.3 % (OC) and 0.47 % (N) in the Ah/Oe-horizon of the *Aquorthel*. The organic topsoil horizon in the vale of the upper slope could accumulate a thicker layer of organic matter with a higher OC content than that one of the lower slope. Nevertheless, this *Aquorthel* was characterized by more different mineral horizons with a varying grain size distribution. The *Aquiturbel* had narrow C/N ratios ranging from 13.4 to 16.0. They were wide in the *Aquorthel* (18.2 ± 5.2). The CEC was in mean 113 $mmol_c$ kg^{-1} ± 40 $mmol_c$ kg^{-1}. It was higher in the organic topsoil than the mineral subsoils. The sum of basic cations was highest in the Ah/Oe and BgI-horizons of the *Aquorthel* with 367 $mmol_c$ kg^{-1} and 215 $mmol_c$ kg^{-1}, respectively. These values decreased with depth as well. In the deep Bgjj-horizon of the *Aquiturbel* a high concentration of Al^{3+}-ions was detected (21 $mmol_c$ kg^{-1}) whereas all other horizons had lower concentrations (mean 1.7 $mmol_c$ kg^{-1} ± 1.8 $mmol_c$ kg^{-1}). Both soils had noticeable concentrations of K^+ and P. Especially in the subsoil where the water was likely to flow down slope these nutrients were significantly enriched. The BgFe-horizon had an exceptional high sand content of 62.5 % and was underlain by a horizon with 15 % lower sand content but instead higher portions of silt (+ 13 %) and clay (+ 2.5 %). The sand rich horizon was depleted in K^+, P, Al^{3+}, K^+, Na^+ likely demonstration the aquifer where the outwash take place. The underlying horizon did not show any affection caused by a down slope water flow and outwash. The Fe_d concentration in the *Aquiturbel* was highest in the BgjjI-horizon where the redox depletions were highly visible. Within the *Aquorthel* these oxides concentrated more within the upper 20 cm (16 g kg^{-1}) and were lower in the subsoil (8 g kg^{-1}). These low concentrations in the subsoil of the *Aquorthel* were surprising due to the visible redox depletions. The concentrations of the pedogenic Mn-oxides varied between 0.06 g kg^{-1} and 0.41 g kg^{-1} and decreased with profile depth in both soils. They were lower than the mean Mn_d concentrations determined for the entire soil transect of this island.

The cliff showing progressive degradation, as well as a depression caused by the drainage of a lake within the last 50 years, were particular sites and obviously different from the other sites of this geomorphic unit. The cliff site had a hilly structure due to thawing of the ancient ice wedges the Ice Complex is composed of. Herbs dominated the vegetation of this site (80 % cvg.). The coverage of mosses was up to 15 %. It was lower on the around 1 m high mounds than in the vales among them. Dominant vascular plants were *Arctagrostis latifolia* on the mounds. In the vales, additionally *Equisetum palustre* was found. The soils on the upper part of the cliff were sand-dominated. The mounds were covered by *Typic Psammorthels (Permafrost tundra (alluvial) turfness-gleyic)*, whereas the soils among these mounds were moister and cryoturbated (*Ruptic-Histic Aquiturbels, Permafrost tundra peatish-gleyic*). The soil profiles were located about 1.5 meters away from the cliff. Therefore, they were affected by the lateral heat flow from the side. The soils were characterized by loamy substrates. Despite the topsoil-horizons in vales that were dominated by aeolian fine sands, the distribution of the different grain size fractions was similar in all horizons. This soil parent material was wind transported and was likely to originate from the surrounding bare sand banks occurring during the summer time when the water level in the river channel reached its minimum. The windblown sandy and silty materials were re-deposited at the investigation site, mainly in the vales. These vales served as traps for the transported sediments as the upper soil horizons indicated. Generally, the sand content decreased with depth, and as a product of physical weathering the content of silt increased. In soil profiles of the exposed mounds this effect was more pronounced indicating an advanced development and pedogenesis. The degree of activity calculated for the pedogenic iron oxides supported this finding. The author suggests that high loads of windblown sediments characterize this site on the one hand, whereas on the other hand the loss of soil substrates due to high erosion rates of the coast is notably. High loss rates of soils were observed during the fieldwork season and were reported by Lantuit *et al.* (2011) in the Arctic Coastal Dynamics Database. Though the loamy parent material was similar, the small scale patterned ground with the mounds and the vales caused the development of two different soil subgroups. The vales were likely to accumulate water in autumn, which subsequently freezes and causes heave and cryoturbation. Therefore, the soils formed there are *Turbels*. These cryoturbated soils had redox depletions and aquic conditions. Their soil surfaces were dominated by discontinuous organic soil material (Soil Survey Staff

2010). On 10.08.2008 the higher elevated *Psammoturbels* and the *Ruptic-Histic Aquiturbels* were thawed to a depth of 96 cm and 50 cm below ground, respectively. Although the results of the soil acidity measurements in soil solution scattered only little the differences between the two described soils were remarkable when additional the sum of base cations and the base saturation were regarded. The latter exceeded 100 % in all horizons. Probably not only the exchangeable ions were detected in the soil solution. However, the base saturation was higher in the *Typic Psammorthel* of the mound, where also the sum of base cations was higher, than in the *Aquiturbel* in the vales corresponding with a contrary pH value distribution. The average CEC of the *Psammorthel* amounted to 212 $mmol_c\ kg^{-1}$, Na, K, Ca and Mg to 2.16 $mmol_c\ kg^{-1}$, 3.07 $mmol_c\ kg^{-1}$, 264.47 $mmol_c\ kg^{-1}$ and 72.43 $mmol_c\ kg^{-1}$, respectively, and where higher in the subsoil horizon. The average CEC of the *Aquiturbel* was 150 $mmol_c\ kg^{-1}$. Due to neutral pH there were no "acidic cations" in the soil solution. The electrical conductivity (EC) was significantly higher in the elevated *Typic Psammoturbel* (around 180 $\mu S\ cm^{-1}$) than it was in the vales (around 60 $\mu S\ cm^{-1}$). The high CEC and EC in the soil of the mound suggested a contrary sedimentation history than it was discussed regarding the soil grain size distribution. Here, the probable import of windblown sediments resulted in an increase of the ion concentrations. This increase was observed in the *Psammorthel* in the mound. The redeposited sediments may have contained small amounts of carbonates resulting in gravimetric inorganic carbon concentrations of 0.07 % as well as the very high base saturation of more than 150 %. Beside the mentioned content of IC the *Typic Psammorthel* had a higher OC content than the *Ruptic-Histic Aquiturbel* in the vale, although the first field inspection led to the opposite assumption. The *Ruptic-Histic Aquiturbel* showed organic carbon (OC) contents of 2.5 % throughout the entire profile. The total nitrogen content (N) increased from 0.11 % in the top soil to 0.20 % in the depth of 50 cm. The generally higher contents of OC and N of the *Psammorthels* increased with depth. The mean C/N ratio amounted to 15.0 ± 4.2. It was wider in the *Aquiturbel* (16.8 ± 4.9) than in the *Psammoturbel* (12.3 ± 0.7). The concentrations of pedogenicly formed iron and manganese oxides varied within the soil profiles with increased concentrations in subsoil horizons. The values of the degree of activity A_f for iron and manganese oxides were lower in the *Psammorthels* than the *Aquiturbels* with averaged values of 0.30 and 0.75 for iron and 0.86 and 1.00 for manganese, respectively.

The new findings about the chemical properties of this vulnerable to erosion cliff area are important for the wider surroundings due to the export of these soil compounds into the river channels and transport into the Laptev Sea. These compounds are likely to be re-deposited on the floodplains of the Lena River Delta and to change their soil properties.

The particular depression caused by lake drainage lake was about 125,500 m² and characterised by mounds surrounded by wet vales with *Typic Aquorthels (Permafrost alas peat-gley)*. The mounds had *mollic* epipedons and were cryoturbated - forming *Typic Molliturbels (Permafrost alas turfness-gleyic).* The plants of the aerated mounds were dominated by *Arctagrostis latifolia* covering 50 % to 75 % of the investigated area. The vales were covered by *Arctophila fulva* and *Carex stans*.. The general herbs coverage amounted to 70 % and 80 % for mounds and vales, respectively. The coverage level of mosses was low. The parent material for soil genesis at those hilly structures was sandy loam in the topsoil followed by loamy silt in deeper horizons. These sandy loams had a considerable portion of clay amounting to 22 %. The clay content was a result of pedogenic processes in the topsoil. This soil development resulted from the long-term addition of organic materials derived from plant roots or plant remains incorporated into the pedon resulting in the dark colours and development of secondary clay minerals and Fe-oxides. The *Typic Molliturbel* was cryoturbated and the depth of the seasonally thawed layer on 11.08.2012 was 65 cm below ground. The *Typic Aquorthel* of the vale was not cryoturbated. It was dominated by aquic conditions and redox depletions. The thaw depth was 42 cm of ground. The pH was light basic in the subsoil of the *Molliturbel*. In its topsoil as well as the entire profile of the *Aquorthel* pH values were moderately and light acidic. The acidic pH values in the topsoils of both, the *Aquorthel* and the *Molliturbel* indicated that the influence of the likely carbonate containing aeolian sediments within the basin of the drained lake was low or not existent in the past. However, measurements of IC demonstrate that the subsoil horizons of the hillock were affected by these sediments when these horizons were the topsoil horizons in past. The portion of IC was high and amounted 3 to 10 % of the total carbon (TC). The OC was high in the *Aquorthel* (10.3 %). Within the *Molliturbel*, the OC content decreased from the organic enriched topsoil horizon (7.1 %) to 2.3 % in the deepest horizon. The N contents varied from 0.4 to 0.2 % in the *Molliturbel*. The *Aquorthel* had 0.6 % of N and a C/N of 18 within the

profile. The C/N ratio in the *Molliturbel* was 18.6 in the topsoil horizon and decreased notably with depth to narrow ratios of around 11 in the B-horizons. The deepest horizon was particular and seemed different from the overlying soil horizons due to its light basic pH, high EC and base saturation as well as higher clay content. The author assumed this horizon to have still the former properties of the lake bottom. It was likely the top soil horizon or at least it was well aeriated with the resulting high amounts of well-crystallized Fe-oxides developed during this time. The degree of activity in this particular horizon was 0.3 and the lowest determined on the third river terrace of the Lena River Delta. However, the highest concentrations of pedogenic Fe- and Mn-oxides were measured in the water saturated *Aquorthel* (24 g kg^{-1} and 0.4 g kg^{-1}, respectively). Also here, the author found the highest values for the degree of activity indicating high portions of amourphous Fe and young oxide synthesis. The mean concentration for Fe- and Mn-oxides in the *Molliturbel* were 11 g kg^{-1} ± 2.6 g kg^{-1} and for Mn-oxides 0.23 g kg^{-1} ± 0.14 g kg^{-1}. The EC was higher in the *Molliturbel* than the *Aquorthel* and amounted to 223 µS cm^{-1} ± 100 µS cm^{-1} and 27 µS cm^{-1}, respectively. The high EC, which increased with increasing depth, corresponded to the sum of basic cations, especially the increasing concentrations of Ca^{2+}-ions. The CEC was highest in the soil profile of the *Aquorthel* in the vale due to the high OC content. However, high CEC were found in all soil horizons ranging from 147 to 223 $mmol_c$ kg^{-1}.

The investigated site on Sardakh Island showed no distinct patterned ground. The soil we described had gleying properties and was classified as *Typic Aquiturbel (Permafrost silty-peat-gley).* The vegetation of the investigated western part was dominated by *Dryas punctata* and *Poaceae*-species. The coverage of herbs and mosses amounted to 60 % and 90 %, respectively. The topsoil horizon consisted of organic substrates with an OC and a N content of 8.3 % and 0.5 %, respectively. The pH value was strong acidic and the EC amounted to 98.5 µS cm^{-1} and was close to the mean EC of the study. The subsoil horizon consisted of silty loam and had gleying properties. Its OC and N contents were 2.5 % and 0.2 %, respectively; the pH value was 5 and the EC 42.8 µS cm^{-1}. Summarizing the properties, their strong relation to the quality of the substrate was pointed up. The organic topsoil horizon as well as the mineral subsoil horizoan had a C/N ratio of 16.7. The thaw depth of the investigated soil was 24 cm on 18.08.2009. The CEC was higher in the organic horizon

(145 $mmol_c$ kg^{-1}) than the mineral one (87 $mmol_c$ kg^{-1}).The sum of basic cations K^+, Ca^{2+} and Mg^{2+} was higher in the organic topsoil, as well as the concentrations of plant available nutrients potassium and phosphorous. The mean contents of Al^{3+}- and H^+-cations were 14.8 $mmol_c$ kg^{-1} ± 1.8 $mmol_c$ kg^{-1} and 2 $mmol_c$ kg^{-1} ± 1.4 $mmol_c$ kg^{-1}, respectively. The Al^{3+}-ions did not trace the pH values as observed at other sitey, while the H^+-ions did. The concentrations of pedogenic Fe- and Mn-oxides were 8.9 g kg^{-1} ± 0.2 g kg^{-1} and 0.3 g kg^{-1} ± 0.3 g kg^{-1}, respectively. There were not only amorphous Fe-oxides determined, but also well developed oxides suggesting initial pedogenic changes in the Fe-oxide fractions.

The area of the so-called Mutnoe Lake on Khardang Island, which also belongs to the third river terrace of the Lena River Delta, was characterised by plains without any patterned ground. We found high moss coverage of 90 % and herbs (50 % cvg) with *Poaceae*-species and *Dryas punctata* as dominant higher plants. Due to the monotonous geomorphic characteristics, only one predominant soil was determined. It had a *folistic* epipedon and was classified as *Folistic Haplorthel (Permafrost turfness-gley)*. The pH values within the thawed layer of 39 cm on 05.08.2009 varied between 6.5 and 7.4. The EC was low (22.3 µS cm^{-1}) in the organic and N rich topsoil (OC: 8.4 %; N: 0.57 %). It amounted to 116.4 µS cm^{-1} in the B-horizon with gleying properties. This horizon was characterized by a silty texture (75 %) with additional considerable contents of clay (20 %). The C/N ratio in the Ah-horizon amounted to 14.8 and in the Bg-horizon to 12.6. The CEC in the topsoil horizon was the highest determined within the latitudinal transect (408 $mmol_c$ kg^{-1}). The CEC in the Bg horizon was only half that high, however it was considerably higher than the averaged CEC of this study. The sum of basic cations was quite different in these two horizons. The differences were caused mainly by strongly differing Ca^{2+}- and Mg^{2+}-ions. Concentrations of plant available potassium and phosphorous reached values in the range of averaged determined concentrations for this study. Interesting was that the distribution pattern was contrary due to the nutrient regarded. While more potassium (123 mg kg^{-1}) was found in the topsoil and lower concentrations (65 mg kg^{-1}) were determined in the subsoil horizon, phosphorous was enriched in the subsoil (11 mg kg^{-1}) and showed a lower concentration in the topsoil horizon (8 mg kg^{-1}). The concentrations of pedogenic Fe-oxides corresponded to the mean concentration measured in *Turbels*. Mn-oxides were low concentrated and consisted mainly of

amorphous forms. The degree of activity of the Fe-oxide fraction indicated an advanced pedogenesis with high amount of well-crystallized oxides. The brownish colours of the profile assumed brunification processes. The high silt and low sand contents, different from those at comparable sites, likely illustrated the effects of physical weathering with thermal stress and frost weathering. This location offered good conditions for pedogenesis as well as a good habitat for vegetation.

Although all three islands (Kurungnakh, Sardakh and Khardang) belong to the third river terrace of the Lena River Delta the grain size distribution in the mineral soils of Sardakh Island was noticeable different to those of Kurungnakh Island but similar to this of Khardang Island. While the clay content was high at 20 % and similar in all horizons, the silt and sand contents varied strongly on both islands. On Kurungnakh Island, the predominant loam had high sand contents of 29 % to 41 % classifying the texture to sandy loams. The loam on Sardakh Island was silt rich (65 %) while the sand content was low at 14 %. The texture on Khardang Island was classified to clay rich silt due to the very high silt content of 75 %. The sand content on this island amounted to 5 %. These differences assume a higher aeolian sediment load on Sardakh Island and Khardand Island than on Kurungnakh Island and probably different stages of physical weathering caused by thermal stress and frost weathering resulting in a reduction of grains size. Generally, an inspection of the grain size distribution should be conducted on Kurungnakh Island at several sites between the degraded cliff and the slope shoulder described above (about 700 m). The author believed to find a decreasing content of the sand fraction to the benefit of the silt and clay fraction. With decreasing speed and longer distance from the source area, the coarser and heavier fine sand grains are likely to be redeposited adjacent to the cliff whereas the fine fraction can be transported over longer distances over the island.

3.4.4 Hinterland: Polygonal Tundra

The polygonal tundra landscape investigations in the hinterland of the Lena River Delta were performed at two sites. Byluyng-Kyuel´ lies between the Chekanovskogo Range and the delta, the more southern site, El´gene-Kyuele, is located south-west to the Chekanovskogo Range.

The vegetation of Byluyng-Kyuel´ is dominated by mosses (100 % cvg.). Herbs and shrubs (30 % and 20 %) are less abundant. *Betula nana* and *Eriophorium spec.* dominate as vascular plants. *Betula nana* dominates also the southern site El´gene-Kyuele (with *Ledum palustre*). Here the mosses are characterised by a lower coverage level of 50 %. The soils, which developed on the polygonal patterned ground, are comparable on both sites. The *Typic Historthels (Permafrost peat lowland)* (Fig. 29) in the polygon centres of both sites were characterised by shallow active layer depths of 18 cm and 24 cm at Byluyng-Kyuel´ and at El´gene-Kyuele sites, respectively. The active layer on the rims was 25 cm and 29 cm, respectively. The soils, which developed on both rims, were classified as *Ruptic Historthels (Podbur over permafrost with poor gleying)* (Fig. 30). At the site El´gene-Kyuele the organic carbon content increased with depth from 35 % to 41 % and from 37 % to 48 % in the polygonal centre and polygonal rim, respectively. Besides the high OC contents also the N was high (1.9 % ± 0.3 %) showing increased concentrations with increasing depth. They were distinctly higher at this site than the determined mean N concentration for this study of 1.0 %. The resulting mean C/N ratio amounted to 21.7 ± 3.5 and was wider in the polygonal rim with 25.5 ± 1.1 than the polygonal centre (19.1 ± 0.2). The strong acidic pH (4.2 ± 0.4) allowed a high leaching of the acidic cations. Al^{3+} reached values of 78.3 $mmol_c\ kg^{-1}$ ± 51.3 $mmol_c\ kg^{-1}$ with a maxiumum of 166.8 $mmol_c\ kg^{-1}$ in the topsoil horizon of the *Ruptic Historthel* having a pH of 3.6. It was the highest Al^{3+}-ion concentration of the performed study found in the horizon with the most acidic pH valued measured. The highest H^{+}-ion concentration was determined in the topsoil of the *Typic Historthel* in the polygonal centre. It amounted to remarkable 12.3 $mmol_c\ kg^{-1}$ whereas the mean value was 5.5 $mmol_c\ kg^{-1}$ ± 4.0 $mmol_c\ kg^{-1}$. The sums of basic cations varied between 74.0 $mmol_c\ kg^{-1}$ and 315.6 $mmol_c\ kg^{-1}$. They were lower in the topsoils and increased in depth. The observed increase was distinctly high in the *Historthel* at the rim. In the soil developed in the polygon centre there was an increase of the cation sum up to 180 $mmol_c\ kg^{-1}$ and subsequent a decrease (165 $mmol_c\ kg^{-1}$). There was a pronounced decrease of plant available potassium with increasing depth. Phosphorous' distribution was different and varied in the different investigated horizons. The concentrations of pedogenic Fe-oxides were higher in topsoil horizons than in higher depths. Mainly amorphous and not crystallized forms were determined suggesting a young pedogenesis. The average concentration of dithionite soluble Fe-oxide amounted to 7.4 g kg^{-1} ± 3.0 g kg^{-1}.

There were no considerable concentrations of pedogenic Mn-oxides within the investigated area.

El´gene-Kyuele – *Typic Historthel*

- thaw depth : 24 cm (August 5th)
- red-ox conditions
- low water level, high moisture
- dark, more decomposed subsoil horizons

horizon	depth (cm)	texture	reduc cond.	pH	OC (%)	C/N	roots
Oi	0-2	org. matter	no	4.3	35.0	19	common
Oie	2-11	org. matter	no	4.4	40.0	19	common
Oe	11-24	org. matter	yes	4.6	40.7	19	few

Figure 29: *Typic Historthel*, the predominant soil of the El´gene-Kyuele site with a field description as well as soil properties.

Fig. 29: *Typic Historthel*, der Leitboden des Standortes El´gene-Kyuele mit einer Feldbeschreibung sowie den Bodeneigenschaften.

The soils of Byluyng-Kyuel´ had a moderate acidic to strong acidic pH (5.1 ± 0.3) and an EC of 70.1 µS cm^{-1} ± 35.3 µS cm^{-1} decreasing with increasing depth. The EC was in the range of mean values determined for the latitudinal transect, whereas the pH was less acidic than its mean value. The mean sum of basic cations in the *Typic Historthel* in the polygonal centre was 167.3 $mmol_c$ kg^{-1} ± 122.5 $mmol_c$ kg^{-1} and decreased with depth. In the *Ruptic Historthel* of the rim, the determined mean sum of basic cations amounted to 187.4 $mmol_c$ kg^{-1} ± 116.3 $mmol_c$ kg^{-1}. The decrease of the value was affected by notably lower contents of Ca^{2+} as well as Mg^{2+} in deeper horizons. The acidic cations were present within the pH milieu of this site and amounted to 16.5 $mmol_c$ kg^{-1} ± 13.4 $mmol_c$ kg^{-1} and to 1.4 $mmol_c$ kg^{-1} ± 0.9 $mmol_c$ kg^{-1} for Al^{3+}-ions and H^{+}-ions, respectively. The OC contents in the polygonal centre were high to a depth of 16 cm and amounted to 19.7 % followed by a thin mineral horizon with only 3.9 % OC. The topsoil of the *Ruptic Historthel* at the rim had 11 % OC, in

contrast to the following mineral horizon with 3.6 %. The N contents varied between 0.20 % and 1.21 % and were high in OC rich horizons and lower in horizons with low OC contents. The determined C/N ratios were even within both soils and amounted to 18.3 ± 1.1.

Byluyung-Kyuel´ – *Ruptic Historthel*

- thaw depth : 25 cm (August 6th)
- red-ox conditions
- water level: 20 cm below surface
- brunified Bg-horizon
- sandy loams coverd by organic-rich horizon

horizon	depth (cm)	texture	reduc cond.	pH	OC (%)	C/N	roots
Oe	0-7	org. matter	no	5.5	11.0	19	many
Bg	7-25	sandy loam	yes	5.2	3.6	17	common

Figure 30: *Ruptic Historthel*, the predominant soil of the Byluyng-Kyuel´ site with a field description as well as soil properties.

Fig. 30: *Ruptic Historthel*, der Leitboden des Standortes Byluyng-Kyuel´ mit einer Feldbeschreibung sowie den Bodeneigenschaften.

The determined concentrations of plant available nutrients were distinctly lower than their mean values for the entire study. Only the *Typic Historthel* in the polygonal centre held a huge portion of potassium in topsoil horizon. Roots strongly penetrated this horizon. The concentrations of pegogenic Fe-oxides were relatively high (24.1 g kg^{-1} ± 18.6 g kg^{-1}) including the maximum concentration measured in this study (52.5 g kg^{-1}). It was determined within the O(g)-horizon of the *Typic Hitorthel* with visible redox depletions. A notable concentration of 7.5 g kg^{-1} pedogenic Mn-oxides was measured in the topsoil in the polygonal centre. This concentration is as well the highest measured in this study. The mean Mn-oxide concentration of the other soil horizons was 0.51 g kg^{-1} ± 0.49 g kg^{-1}. The degree of activity of both, the Mn- as well as the Fe-oxides suggested a relatively young pedogenesis. It was more advanced in the *Ruptic Historthel* at the rim. The pedogenesis was likely influenced by iron and manganese containing deposits eroded in the mountain range and transported to the

investigation site by the small water stream system at the northeast slope of the ridge draining into the Olenekskaya Channel.

3.4.5 Hinterland: Tundra-Taiga-Transition Zone

The study site around the Zelyonoe Lake belongs to the transition zone of tundra and taiga. This site was characterized by patchy forested places and widespread plains with dwarf tundra shrubs. Furthermore, there were herbs and mosses (30 % and 5 % cvg., respectively). *Ledum palustre* and *Betula nana* were the dominant vascular plants on plains. In the forested places *Ledum palustre* and *Larix*-species dominated. The authors investigated both, a forested patch as well as the tundra plain to compare the soils developing in this area. In the forest we described a shallow (25 cm on 07.08.2009) *Ruptic-Histic Aquiturbel (Permafrost peat-gley)* (Fig. 31). The non-forested plains were covered by *Ruptic Historthels (Permafrost peatish with gleying)* (Fig. 32) sampled in a very shallow active layer of 20 cm. In the forest the shallow strong acidic (4.5 ± 0.1) *Ruptic-Histic Aquiturbel* developed with an extreme high OC content of 46 % in the topsoil over a cryoturbated Bgjj-horizon with 4.8 % OC. The N contents varied between 0.15 % and 1.90 %. The mean C/N ratio of the forested patch was 35.8 ± 14.1. In the organic topsoil horizon, an extreme wide C/N ratio of 51 was determined. This extreme difference in OC content of the organic and mineral soil horizons illustrated that the translocation from the topsoil and incorporation of organic compounds into the subsoil was inhibited. The non-forested dwarf shrub tundra was characterized by a mean C/N ratio of 23.6 ± 4.5. The plains were covered by *Ruptic Historthel* soils with strong and very strong acidic horizons, high OC contents of 17 % to 50 %, decreasing with depth, and a relative high N content of 1.5 % ± 0.6 %. The lower most soil horizon was enriched in organic indicating a likely different situation in the non-forested plain compared to the forested patch. Here the OC was translocated from the organic rich topsoil downwards and accumulated in the mineral horizon to a high extent of 17 % OC. The sum of the basic cations in the forested patch was 164.8 $mmol_c\ kg^{-1}$ ± 74.3 $mmol_c\ kg^{-1}$ and in the tundra plain 178.2 $mmol_c\ kg^{-1}$ ± 131.2 $mmol_c\ kg^{-1}$. In the forested area remarkable Al^{3+} values of up to 152.4 $mmol_c\ kg^{-1}$ with

an allover mean of 84.7 $mmol_c\ kg^{-1}$ ± 50.2 $mmol_c\ kg^{-1}$ were determined. H^+-ion values ranged between 0.6 $mmol_c\ kg^{-1}$ and 10.3 $mmol_c\ kg^{-1}$ with higher values in the topsoils.

Forested – *Ruptic-Histic Aquiturbel*

- thaw depth : 26 cm (August 6th)
- red-ox conditions in lower part
- water level: 14 cm below surface
- organic horizons underlain by mineral layers (in a depth of ca. 20 cm)

horizon	depth (cm)	texture	reduc cond.	pH	OC (%)	C/N	roots
Oi	0-5	org. matter	no	4.4	46.8	51	common
Oe	5-20	org. matter	no	4.7	45.5	24	common
Bgjj	20-25	sandy loam	yes	4.6	4.8	32	non

Figure 31: *Ruptic-Histic Aquiturbel*, the predominant soil of forested areas of the tundra-taiga-transition zone with a field description as well as soil properties.

Fig. 31: *Ruptic-Histic Aquiturbel*, der Leitboden der bewaldeten Bereiche der Tundra-Taiga-Übergangszone mit einer Feldbeschreibung sowie den Bodeneigenschaften.

The concentrations of pedogenic Fe-oxides were high throughout the *Aquiturbel* profile with a maximum of 29.3 g kg^{-1} in the Oc-horizon in a depth of 5 cm to 20 cm. The highest concentrations of these oxides were determined in the depth of 4 cm to 14 cm within the non-forested places. The concentrations of plant available potassium were extremely high in both topsoil horizons of this site. The highest measured concentration of this study (653 mg kg^{-1}) was found in the non-forested plain. It was five times higher than the mean potassium concentration of the study. However, the underlying horizon was in the range of the mean and amounted to 167 mg kg^{-1} and the deepest, mineral horizon had only 8 mg kg^{-1}. The same pattern was found in the soil of the forested patch. Phosphorous was enriched in the topsoil of the non forested plain only. Generally, these two sites were similar in their soil properties and there was no distinct indication for the patchy distribution of the trees. The author assumed

that at the investigated site the soil was not the driving force for the *Larix* trees development on the one and dwarf *Betula nana* development on the other side.

Non-Forested – *Ruptic Historthel*

- thaw depth : 20 cm (August 7th)
- water level: 14 cm below surface
- organic horizons underlain by mineral layers (in a depth of ca. 14 cm)

horizon	depth (cm)	texture	reduc cond.	pH	OC (%)	C/N	roots
Oi	0-4	org. matter	no	4.0	50.0	29	many
Oe	4-14	org. matter	no	3.9	39.8	21	common
Bg	14-20	sandy loam	yes	4.4	16.9	21	non

Figure 32: *Ruptic Historthel*, the predominant soil of non-forested areas of the tundra-taiga-transition zone with a field description as well as soil properties.

Fig. 32: *Ruptic Historthel*, der Leitboden der unbewaldeten Bereiche der Tundra-Taiga-Übergangszone mit einer Feldbeschreibung sowie den Bodeneigenschaften.

3.4.6 Hinterland: Northern Taiga

The soils of the Northern Taiga were investigated at three sites within a latitudinal transect (70.22° N - 69.40° N). From north to south, the active layer thickness increased from 19 cm to 49 cm and the height of *Larix* trees increased from around 2-3 m to 5-7 m at the southern site Sysy-Kyuel´. The soils of these three sites were different due to varying parent material. At the site Peschanoe the soil classified as *Typic Histoturbel (Permafrost peatish-gleyic)* (Fig. 33) consisted of a 14 cm thick organic layer underlain by a cryoturbated mineral horizon with gleying properties. Besides *Larix* (10 % cvg.) this soil was vegetated by *Betula nana* shrubs (height around 1 m, 90 % cvg.) herbs (10 %) and mosses (5 %). The thaw depth on 06.08.2009 at the site Peschanoe was 19 cm. The thick organic layer was insulating and kept the ground frozen. The pH values varied from 3.9 in the topsoil to 5.0 in the mineral horizon

in the depth of 14 cm to 19 cm. The EC decreased with depth from 139.1 µS cm^{-1} to 78.1 µS cm^{-1}. The highest OC content was determined in the Oi-horizon on the top (49.2 %). Though mineral, the Bgjj-horizon contained 13.3 % OC. The highest N-content of 2.2 % was measured in the second horizon while the mean N content amounted to 1.5 % ± 0.7 %. The resulting C/N ratios were wide in the top (33) and decreased with depth to 18 in the Bgjj-horizon. The sum of basic cations was 284.0 $mmol_c$ kg^{-1} ± 58.1 $mmol_c$ kg^{-1}. Plant available potassium was highly concentrated in the topsoil (644 mg kg^{-1}).

Peschanoe – *Typic Histoturbel*

- thaw depth : 19 cm (August 6th)
- water level: 12 cm below surface
- reduced black band in 13 cm depth
- subsoil mineral horizon rich in organic matter

horizon	depth (cm)	texture	reduc cond.	pH	OC (%)	C/N	roots
Oi	0-9	org. matter	no	3.9	49.2	33	many
Oe	9-14	org. matter	yes	4.4	40.4	19	common
Bgjj	14-19	silty loam	yes	5.0	13.3	18	non

Figure 33: *Typic Histoturbel*, the predominant soil of the Peschanoe site with a field description as well as soil properties.

Fig. 33: *Typic Histoturbel*, der Leitboden des Standortes Peschanoe mit einer Feldbeschreibung sowie den Bodeneigenschaften.

Phosphorous reached in the investigated soil the maximum concentration measured within this study. It amounted to 88 mg kg^{-1}. The pegogenic Fe-oxides were enriched in the second organic horizon. In this horizon, there was a dark band visible during the profile description. The high degree of activity suggested a young pedogenesis within the entire soil profile. Mn-oxide contents were negligible in the investigated soil. This soil is alike the soils described at the Zelyonoe Lake site. The only significant difference was observed in the concentrations of Al^{3+} cations. The concentrations at the current site were lower and amounted to

26.0 $mmol_c$ kg^{-1} ± 20.4 $mmol_c$ kg^{-1}, whereas in the soils of the transition zone at the Zelyonoe Lake they amounted to 84.7 $mmol_c$ kg^{-1} ± 50.2 $mmol_c$ kg^{-1}. Both sites had similar pH values.

The Yagodnoe site was also characterised by a dense cover of *Betula nana* shrubs (70 % cvg.). However, this site was dominated by a moss-cover of 100 % with *Ledum palustre* (5 % cvg.). The soil at this peaty site was characterised by thick organic horizons of different decomposition stages. Although probably *Histels*, due to the shallow active layer (29 cm) and no access to deeper and likely organic rich horizons the soils of this site were classified as *Fluvaquentic Historthel (Permafrost peat)* (Fig. 34).

Yagodnoe – *Fluvaquentic Historthel*

- thaw depth : 29 cm (August 8th)
- water level: 5 cm below surface
- reduced black bands in 10 cm and 19 cm depths
- organic matter-dominated
- presumable a *Histel*

horizon	depth (cm)	texture	reduc cond.	pH	OC (%)	C/N	roots
Oi	0-8	org. matter	no	3.6	42.2	33	many
Oi (b*)	8-9	org. matter	yes	3.6	45.2	27	few
Oe	9-19	org. matter	yes	3.7	43.7	22	few
Oe (b*)	19-20	org. matter	yes	3.9	39.5	22	few
OeII	20-29	org. matter	yes	4.2	41.5	24	few

b* = band

Figure 34: *Fluvaquentic Historthel*, the predominant soil of the Yagodnoe site with a field description as well as soil properties.

Fig. 34: *Fluvaquentic Historthel*, der Leitboden des Standortes Yagodnoe mit einer Feldbeschreibung sowie den Bodeneigenschaften.

The seasonally thawed active layer was 29 cm deep in the investigate soil profile on the day of sampling. The investigated soil consisted of moist organic rich horizons (OC: 42.4 % ± 2.2 %) and two darker bands. The N content was high and amounted to 1.7 % ± 0.2 %. The mean C/N ratio was 25.6 ± 4.4 and varied from 32.6 in the topsoil to ratios of around 23 in the

deeper horizons. The pH values were very strong acidic, in the deepest horizon (OeII) strong acidic. The EC of this soil was determined and had values between 51.6 µS cm^{-1} and 148.7 µS cm^{-1}. It decreased with depth. The sum of basic cations was 143.7 $mmol_c$ kg^{-1} ± 20.2 $mmol_c$ kg^{-1} and corresponded with the mean determined for the entire study. Remarkable was, that sum of cations scattered only little with the profile, whereas soil profiles from other investigated sites were characterized by a decreasing value with profile depth. There were high amounts of acidic cations present in the soil and distributed across the profile. The Al^{3+}-cations had an average value of 92.6 $mmol_c$ kg^{-1} ± 38.0 $mmol_c$ kg^{-1}, the H^{+}-cations had on average 7.6 $mmol_c$ kg^{-1} ± 5.0 $mmol_c$ kg^{-1}. The mean values for this soil were distinctly higher than the mean values of the entire study. While the Al^{3+}-ion concentrations stayed high even in deeper soil horizons, the H^{+}-ions were depleted in depth. Pedogenic Fe-oxides were enriched in the upper dark band (18 g kg^{-1}), while the above all mean concentration was 7.9 g kg^{-1} ± 6.0 g kg^{-1}. The degree of activity was high throughout the horizon indicating young pedogenesis with only few well crystallized Fe-oxides. There were no Mn-oxides in the investigated area.

The southernmost site Sysy-Kyuel´ was characterised by dense vegetation. The coverage level of *Larix* trees amounted to around 50 %, this of *Betula nana* and *Alnus crispa* shrubs to 70 % and mosses to 90 %. There were no remarkable geomorphic features at this site. The investigated soil was classified as *Typic Haploturbel (Cryogenic soil)* (Fig. 35). The investigated soil profile consisted of an organic enriched A-horizon overlying unremarkable B-horizons of silty loam texture. The predominant soil of this area was classified as *Typic Haploturbel*. The thaw depth on the day of sampling (08.08.2009) was 49 cm of ground. The pH values varied from strong acidic to light acidic values (4.0 to 6.2). The pH value differences of horizons lying upon another were significant with a general increase with increasing depth. The EC was highest in the Ah-horizon, which was characterized by high OC and N contents of 17.7 % and 0.59 %, respectively. The contents of OC and N of the mineral subsoil horizons were lower and amounted to 2.2 % and 0.1 %, respectively. No significant translocation of OC (humic material) could be assumed. Besides the OC and N amounts, also the C/N ratio was lower in the mineral subsoil. It amounted to 20, whereas the C/N ratio of the Ah-horizon was 30 suggesting low decomposition of the organic compounds. The mean

sum of basic cations was high and amounted to 255.6 $mmol_c\ kg^{-1}$ ± 12.5 $mmol_c\ kg^{-1}$. These cations were smoothly distributed within the depth. There was no difference between the organic enriched Ah-horizon and the B-horizons. However, K^+-cations were enriched in the topsoil (10 $mmol_c\ kg^{-1}$) and were double that high as the mean concentration of this study. Its concentration dropped significantly to 1.55 $mmol_c\ kg^{-1}$ in both B-horizons. The vertical distribution of the other basic cations did not show any patterns. The amounts of acidic cations were highest in the strong acidic Ah-horizon and decreased dramatically with depth due to the changing pH value in depth. The concentration of Al^{3+}-ions in the Ah-horizon corresponded to the mean concentrations determined during the study, whereas the H^+-ions were higher than their mean values of the study.

Sysy-Kyuel´ – *Typic Haplorthel*

- thaw depth : 49 cm (August 8th)
- water level: 34 cm below surface
- organic enriched topsoil horizon underlain by mineral horizons

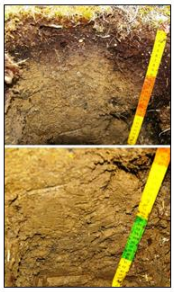

horizon	depth (cm)	texture	reduc cond.	pH	OC (%)	C/N	roots
Ah	0-7	org. matter	no	4.0	17.7	30	many
B	7-23	silty loam	no	5.7	2.2	22	common
BII	23-49	silty loam	yes	6.2	2.2	18	few

Figure 35: *Typic Haplorthel*, the predominant soil of the Sysy-Kyuel´ site with a field description as well as soil properties.

Fig. 35: *Typic Haplorthel*, der Leitboden des Standortes Sysy-Kyuel´ mit einer Feldbeschreibung sowie den Bodeneigenschaften.

Plant available potassium and phosphorous were enriched in the Ah-horizon and served the vegetations as a nutrient storage. The underlying B-horizons contained only low portions of these plant nutrients. The concentrations of Fe- and Mn-oxides amounted to 11.2 $g\ kg^{-1}$ ± 1.2 $g\ kg^{-1}$ and 0.08 $g\ kg^{-1}$ ± 0.03 $g\ kg^{-1}$, respectively. The pedogenic Fe- and Mn-oxides suggested an advanced pedogenesis at the Sysy-Kyuel' site. Probably the B-horizons were

affected by brunification processes caused by chemical weathering and subsequent coatings of the minerals with Fe-oxides.

3.4.7 Discussion of soil properties

Due to the high diversity and variability of the soils that develop within the severe climate of the Lena River Delta and along the latitudinal transect a comparison on the soil great group level according to the US Soil Taxonomy (Soil Survey Staff 2010) is not readily practicable. Nevertheless, a discussion of the determined soil properties with values from other reported studies is needed. Hence, the author decided to compare means or ranges of several soil properties with selected published studies from Siberia as well as other permafrost regions.

The pH value is one of the most important soil chemical parameter affecting many of soil properties. It controls the availability of plant nutrients by affecting the cation exchange. pH plays also a huge role for the availability of heavy metals. The species assemblage of vegetations units and corresponding quality of organic matter produced and stored with the investigated soils as well as its decomposition is controlled by pH value.

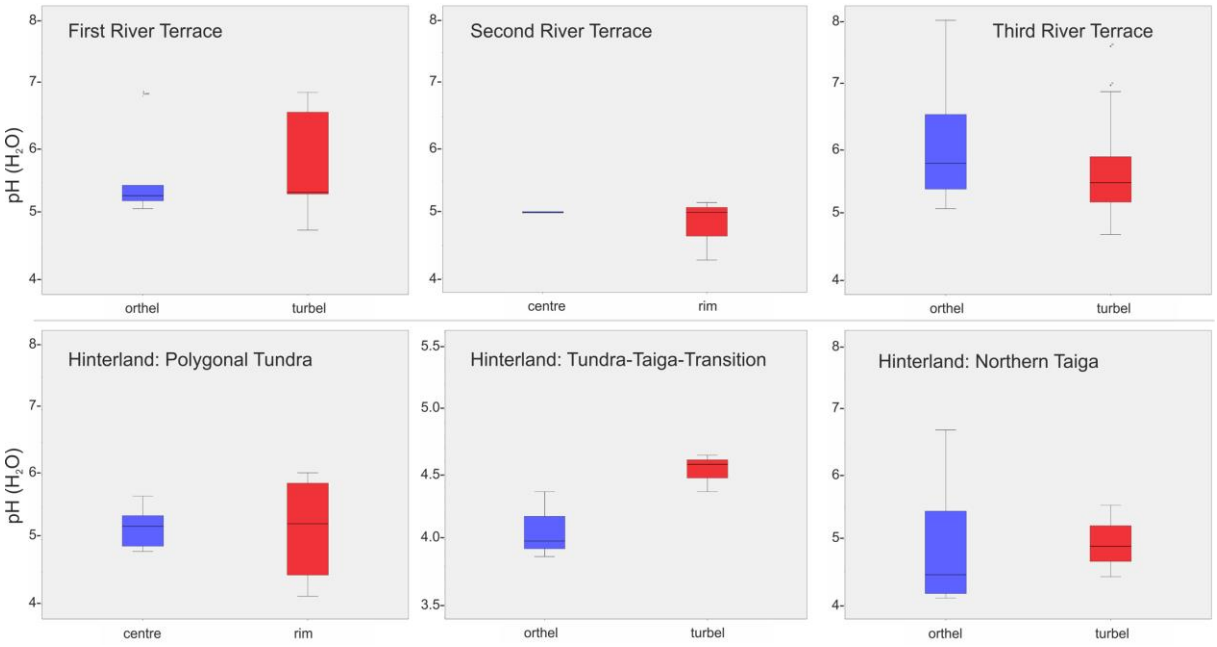

Figure 36: The pH values of soils investigated at all geomorphic units.

Fig. 36: Die pH-Werte der Böden, die innerhalb aller geomorphologischen Einheiten untersucht wurden.

The pH values across the investigated geomorphic units varied strong. However, generally the values were moderate acidic to acidic (Fig. 36). The hinterland of the delta was characterised by stronger acidic soil reaction than the three units of the delta.

All values are in the range of studies from former soil investigations conducted within this region. Sanders (2011) determined pH values for various units of Samoylov Island ranging from 6.0 to 7.2. Kutzbach (2000) described for the same island and within a transect through an ice wedge polygon pH values of 4.5 to 6.5 measured in a $CaCl_2$ solution. In the north of the Lena River Delta in Sagastyr Mueller (1997) reported pH values measured in a H_2O solution of 5.4 to 6.7 in soils of different polygons. Gundelwein (1998) investigated several soil profiles on Taymyr peninsula as well as on Severnaya Zemlya Island with pH values measured in a $CaCl_2$ solution of 3.2 to 7.6. The high range of soil acidity presented by Gundelwein (1998) confirms the high hererogeneity, which was found within the presented soil surveys (Fig. 36). Ping *et al.* (2005) determined comparable pH values within a soil catena in Caribou Poker Creek in Alaska ranging from 3.7 to 6.1 suggesting the mentioned heterogeneity. For soils in Arctic Alaska Ping *et al.* (1998) reported more basic pH values for the coastal plains (measured in a saturated paste in field) ranging from 6.5 to 8.1.

The electrical conductivity of the soil solution gives an indication about the content of water-soluble ions in the soil. As a bulk parameter, it summarizes the conductivities of all present ions and therefore it cannot be used for the calculation of concentrations of single ions. This bulk electrical conductivity varied strongly among the investigated soil and their horizons. The mean EC of soils investigated on the third river terrace was higher, especially within the *Orthels* (Fig. 37) indicating more ions within this area. In general, there was no clear pattern for EC within the investigated soils. Using the results of the concentrations of the basic and acidic cations supported the observation of the varying mean values for EC within the two soil groups.

Concentrations of Na^+- K^+- Ca^{2+}- Mg^{2+}- Al^{3+}- and H^+-ions were slightly higher in *Orthels* (centres) than in *Turbels* (rims) (Fig. 38). The cation-exchange capacity, the maximum concentration of cations available for exchange a soil can hold at a given pH value was on average 132 $mmol_c\ kg^{-1}$ ± 75 $mmol_c\ kg^{-1}$. The cation-exchange capacity determined within this study was distinctly higher than reported by Ping *et al.* (1998) for arctic coastal plains in

Alaska as well as Ping *et al.* (2005) for the research area of Caribou Poker Creek in Alaska. The averaged value was comparable with results of Kutzbach (2000) whereas Mueller (1997) reported higher mean cation-exchange capacity of around 160 $mmol_c\ kg^{-1}$ ± 71 $mmol_c\ kg^{-1}$ for the northern part of the Lena River Delta.

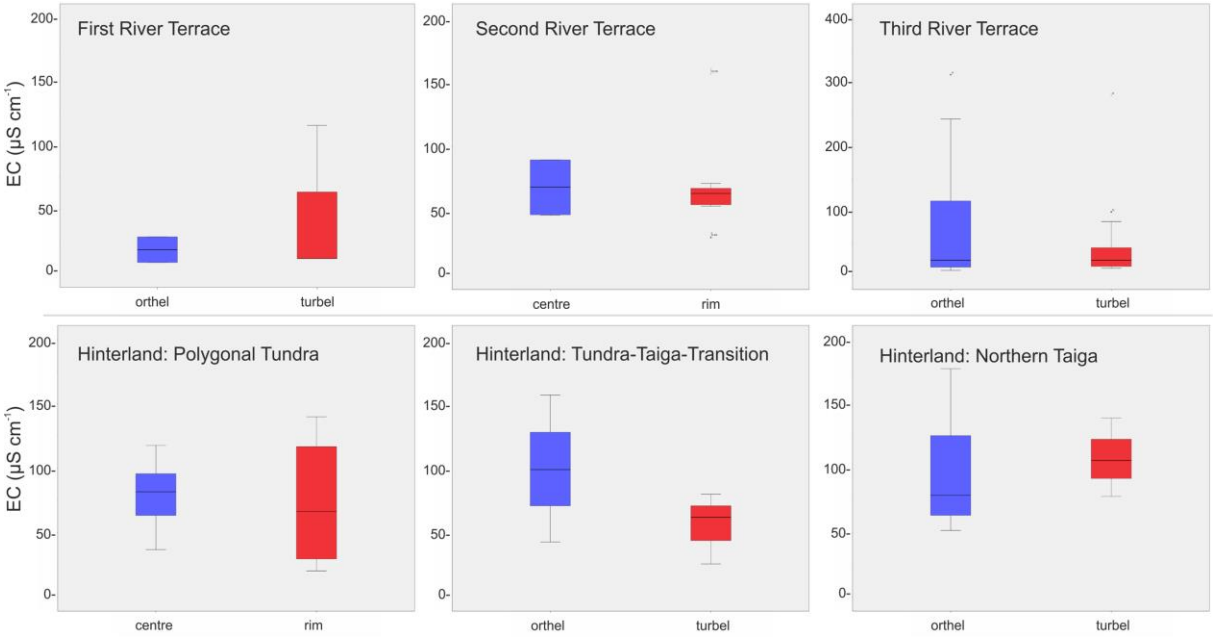

Figure 37: The electrical conductivity (EC) of soils investigated at all geomorphic units.

Fig. 37: Die elektrische Leitfähigkeit der Böden, die innerhalb aller geomorphologischen Einheiten untersucht wurden.

The total carbon TC content is the sum of the contents of organic carbon (OC) and inorganic carbon (IC). The majority of the samples contained only OC. The mean OC content was high and amounted to 15 % with a high SD of 15 %. The mean OC content in the soils of the Lena River Delta was distinctly lower than in the soils investigated along the latitudinal transect in the hinterland (8.73 % ± 6.90 % and 22.15 % ± 17.46 %, respectively). The latitudinal transect through Northeast Siberia was characterized by few sites with very high OC contents comparable to bogs. The OC contents of *Orthels* were slightly higher than the contents of *Turbels* (18.40 % ± 15.14 % and 10.00 % ± 13.26 %). The mean and median OC contents (Fig. 39) were in the range of previously published studies. However, the OC contents scattered strongly (Ping *et al.* 1998: 0.3 % to 26 %, Ping *et al.* 2005: 0.2 % to 51. 4 %;

Sanders 2011: 0.2 % to 19 %, Kutzbach 2000: 0.5 % to 24 %, Gundelwein 1998: 0.1 % to 45.8 %, Mueller 1997: 1.6 % to 8.9 %). When the soil group was indicated by the authors, generally *Turbels* contained less OC than the *Orthels* and *Histels*.

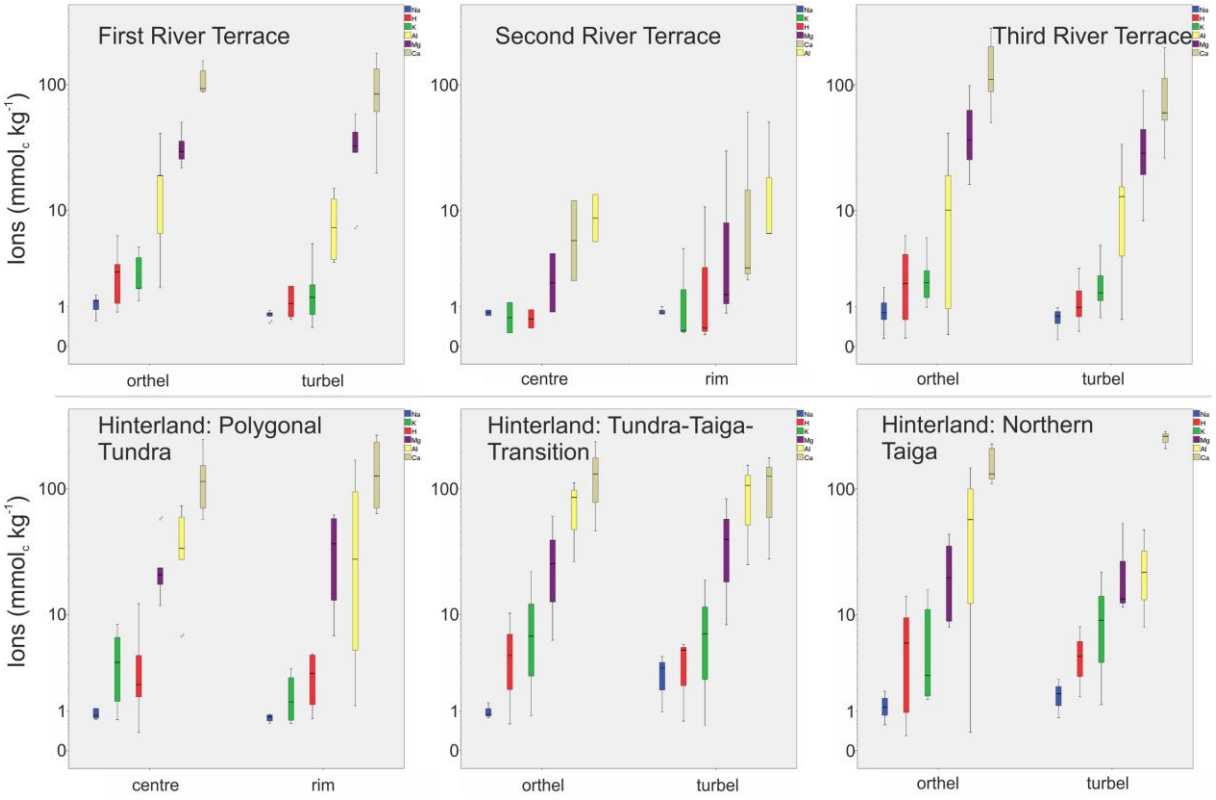

Figure 38: Concentrations of ions in soils investigated at all geomorphic units. In blue – Sodium (Na^+), green – Potassium (K^+), red – Hydrogen (H^+), yellow – Aluminium (Al^{3+}), purple – Magnesium (Mg^{2+}), brown – Calcium (Ca^{2+}).

Fig. 38: Die Konzentrationen von Ionen in Böden, die innerhalb aller geomorphologischen Einheiten untersucht wurden. In blau – Natrium (Na^+), grün – Kalium (K^+), rot – Wasserstoff (H^+), gelb – Aluminium (Al^{3+}), violett – Magnesium (Mg^{2+}), braun – Calcium (Ca^{2+}).

The distribution of nitrogen contents followed strongly the distribution of OC likely due to high N contents in not decomposed plant remains. Therefore, the N content of *Orthels* was higher than the N content of *Turbels* (Fig. 40). The all over mean N content amounted to 0.66 % ± 0.59 % and was of the same range of previously published studies.

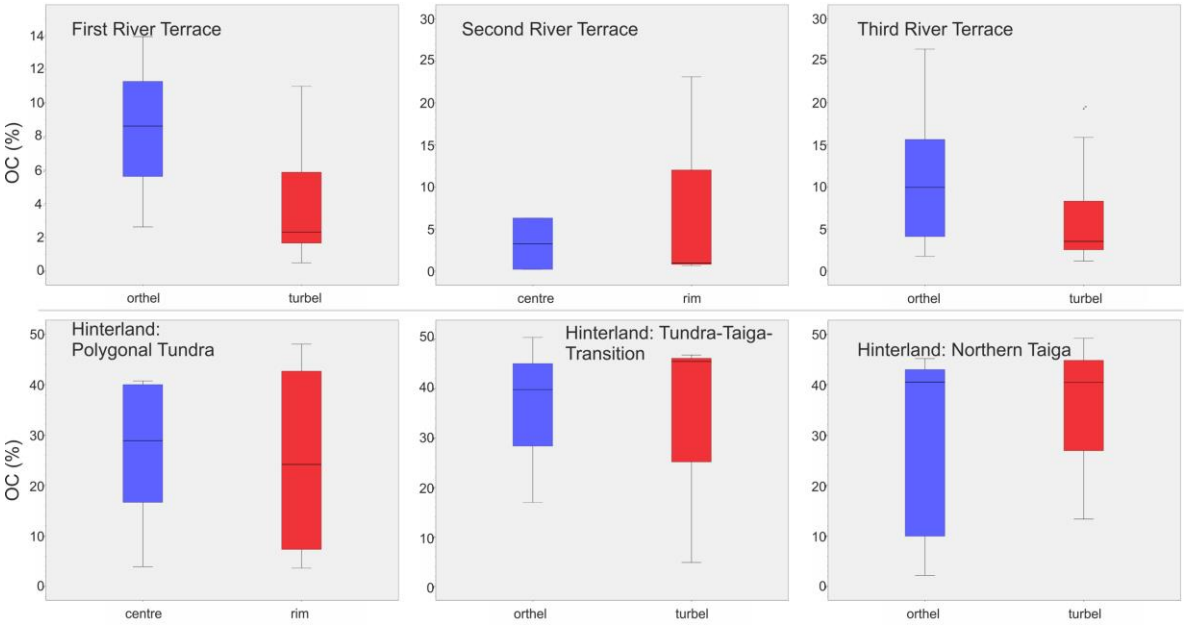

Figure 39: Gravimetric contents of organic carbon (OC) in soils investigated at all geomorphic units.

Fig. 39: Gravimetrische Gehalte an orgenischem Kohlenstoff in Böden, die innerhalb aller geomorphologischen Einheiten untersucht wurden.

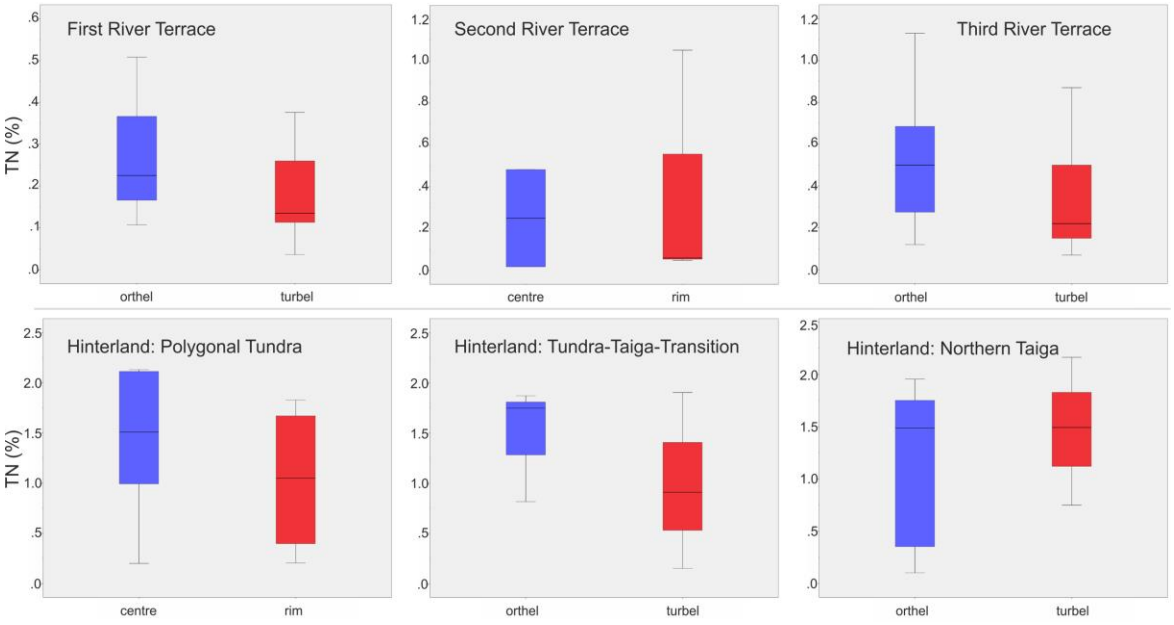

Figure 40: Gravimetric contents of total nitrogen (TN) in soils investigated at all geomorphic units.

Fig. 40: Gravimetrische Gehalte am Gesamtstickstoff in Böden, die innerhalb aller geomorphologischen Einheiten untersucht wurden.

The pedogenic Fe- and Mn-oxides are secondary minerals mainly results of synthesis of weathered materials. These oxides with their strong colors are important soil features indicating pedogenic processes such as gleying or brunification. The genesis of Fe- and Mn-oxides depends of several properties.

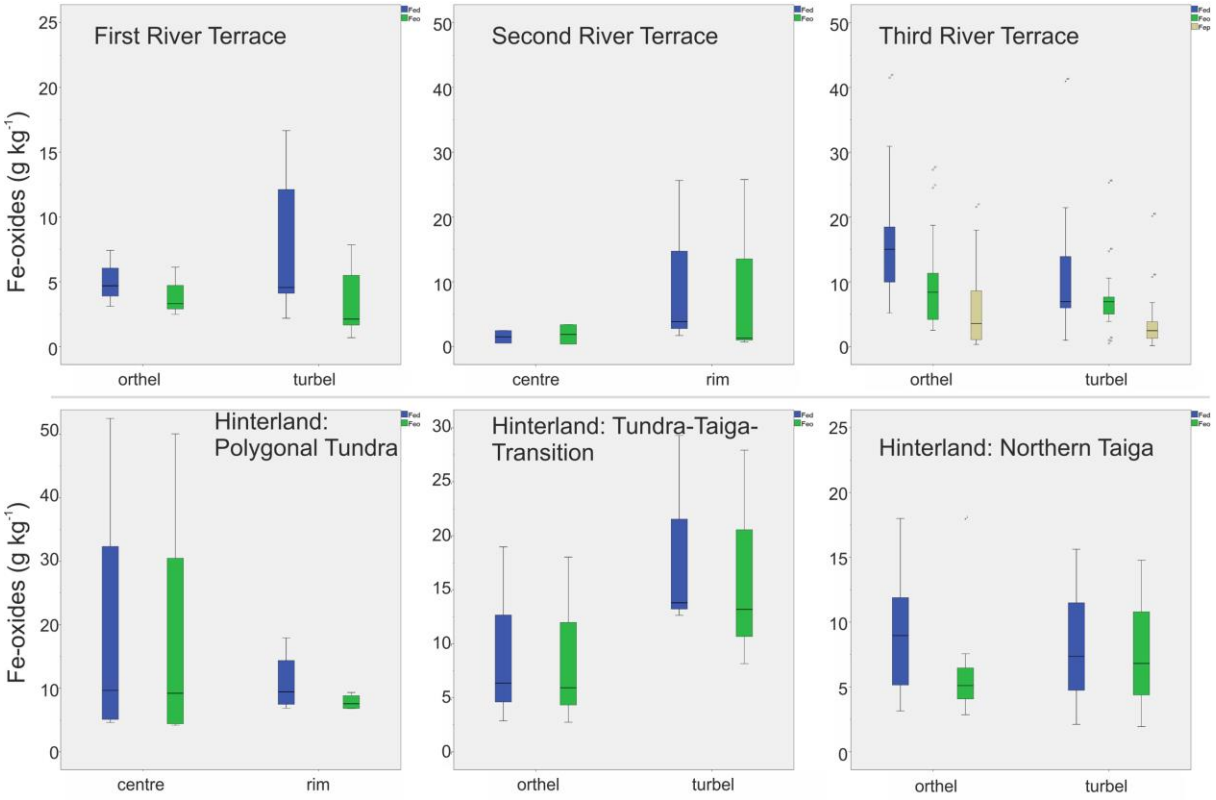

Figure 41: Concentrations of pedogenetically formed forms of iron oxides in soils investigated at all geomorphic units. In blue = Fe_d, green = Fe_o, brawn = Fe_p.

Fig. 41: Konzentrationen pedogen gebildeter Eisenoxide in Böden, die innerhalb aller geomorphologischen Einheiten untersucht wurden. In blau = Fe_d, grün = Fe_o, braun = Fe_p.

The combination of temperature, water content and redox properties result in development of a special oxide. Within the investigation area, mainly amorphous, not well-crystallized oxides were present (Fig. 41 and Fig. 42) indicated by high degrees of activity (0.78 ± 0.27 and 0.92 ± 0.33 for Fe-oxides and Mn-oxides, respectively). Assailable results were presented for recent soils of Sagastyr (Mueller 1997) and Samoylov Island (Kutzbach 2000, Zubrzycki 2009) in the Lena River Delta. They were distinctly lower in paleosoils determined by

Zubrzycki (2009) for the Bol'shoy Lyakhovsky Island (A_f Fe: 0.29 to 0.47) and for soils from the Cape Mamontovy Klyk (A_f Fe: 0.29 to 0.45).

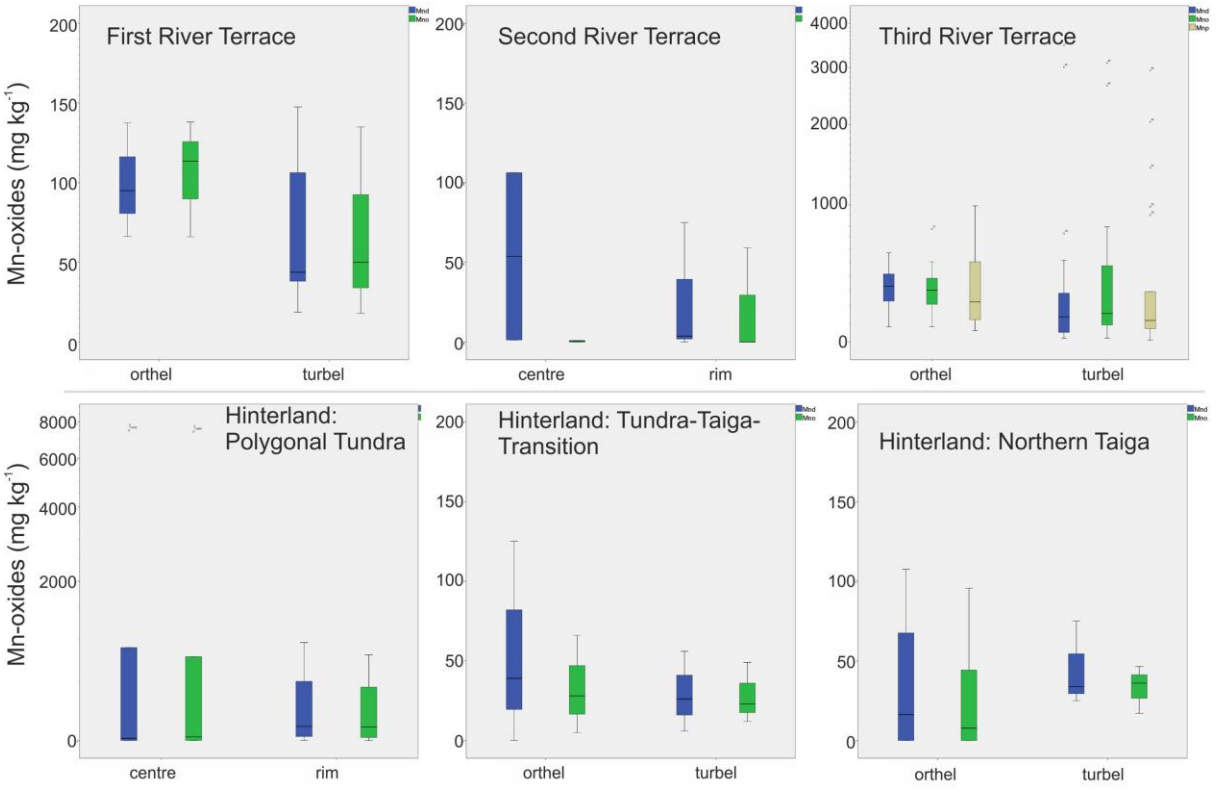

Figure 42: Concentrations of pedogenetically formed forms of manganese oxides in soils investigated at all geomorphic units. In blue = Mn_d, green = Mn_o, brawn = Mn_p.

Fig. 42: Konzentrationen pedogen gebildeter Manganoxide in Böden, die innerhalb aller geomorphologischen Einheiten untersucht wurden. In blau = Mn_d, grün = Mn_o, braun = Mn_p.

3.4.8 Soil assessment and conclusions

There is no defined approach to assess permafrost-affected soils so far because huge parts of these soils are not used as arable land today. To demonstrate how low the general pressure or will to assess these soils was in the past, one just needs to consider the official soil classification system of the Soviet Union published in 1977 (Anon 1986). The largest country in the world simply ignored 70 % of its extent in terms of soil coverage and even did not try to describe and classify these soils due to the lack of usage.

In this work, the author showed that permafrost-affected soils are characterized by high diversity. Sometimes, this diversity is higher than the number of qualifiers provided by the up to date classification systems.

The permafrost-affected soils started to attract broader, especially scientific attention, since the increasing knowledge about the carbon pool stored within these soil was coupled with the climate change and temperature trend projections leading to the assumption of a positive feedback loop of warming when released "permafrost carbon" will increase the greenhouse effect (compare Beer 2009).

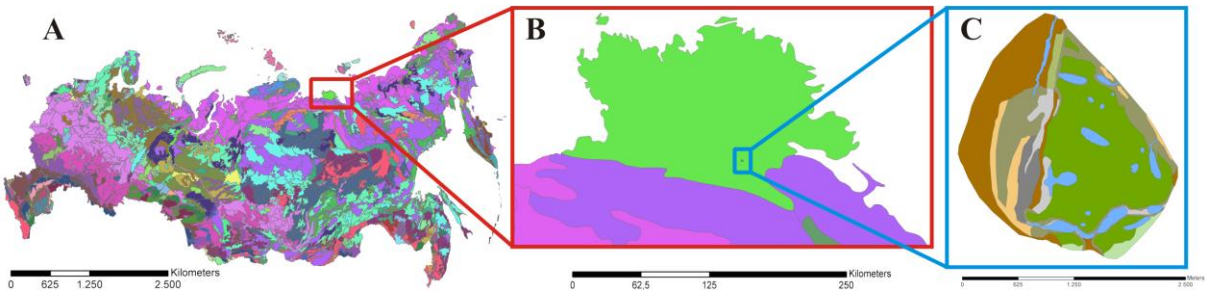

Figure 43: A comparison of soil maps of different scale. A: the up-to-date soil map of Russia compiled from data provided by Stolbovoi and McCallum (2002) in Land Resources of Russia database. B: overview of the soils of the Lena River Delta, excerpt of Figure 43A. C: overview of the soil diversity on Samoylov Island. For a detailed description, see Figure 54.

Fig. 43: Ein Vergleich von Bodenkarten unterschiedlicher Maßstäbe. A: die aktuelle Bodenkarte Russlands. Erstellt aus Daten der Land Resources of Russia database von Stolbovoi and McCallum (2002). B: Übersicht der Böden des Lenadeltas, Auszug au der Figure 43A. C: Übersicht der Böden der Insel Samoylov. Für eine detailierte Beschreibung siehe Figure 54.

In this study, a great number of predominant soil profiles was described in detail pointing out the enormous soil diversity which developed essentially in the shallow active layer and mainly during the short summer period. Maps illustrating the soil diversity in these regions are rare and at too large scale to point out the diversity as compared in Figure 43. In chapter 2.3 on page 22 one of the first maps compiled for Samoylov Island is presented. This map was developed further (see Fig. 54) and more areas were investigated resulting in small-scale maps (see also Ulrich *et al*. 2009, Ivanova *et al*. 2012).

Although only few decimetres in thickness these soils played a major role in carbon sequestration for long time periods (chapter 2.2, page 14) and the question if they still are, is highly controversial and probably region dependent (chapter 2.2, page 20). However, taking into account the projected increases of temperatures (IPCC 2007) these soils with their storages of carbon (see chapter 4) might play an important role in affecting the future climate.

Therefore, it is highly important to continue investigations of these unique and manifold soils in future and take into account detailed investigations of the carbon storage (see chapters 4 and 5) and the storages of nutrients as well as to try to understand the decomposition processes of the organic matter. Thus, besides descriptions of the soil properties and their mapping, collection of high quality samples and implementation of laboratory experiments is necessary to gain knowledge about what is likely to happen, when these permafrost-affected soils will get warmer and their properties will change.

4. Soil Organic Carbon and Nitrogen Stocks in the Lena River Delta

4.1 Introduction

Since the degradation of permafrost both is affected by climate change and results in important feedbacks to climate change, the characterisation of permafrost-underlain areas, permafrost-affected soils, and their stocks of soil organic carbon and nitrogen is an important issue for understanding biogeochemical cycle interactions with the global climate. The area occupied by permafrost-affected soils amounts to more than 8.6 million km², which is about 27 % of all land areas north 50 °N (Jones *et al.* 2010). Enormous amounts of organic matter have accumulated in permafrost-affected soils during the Quaternary period (Harden *et al.* 1992, Smith *et al.* 2004, Zimov *et al.* 2006, Gorham *et al.* 2007, Schirrmeister *et al.* 2011). Recent estimates show that today there might be up to 496 Pg (1 Pg = 10^{15} g) of soil organic carbon stored within the uppermost one meter of the permafrost-affected soils (Tarnocai *et al.* 2009). Although the area occupied by the main arctic deltas as mentioned by Walker (1998) amounts only to 77,000 km² (total area of arctic and alpine tundra: 7.4 10^6 km^2 according to Loveland *et al.* (2000)), their contribution to the total soil organic carbon pool within the permafrost-underlain areas is high (Tarnocai *et al.* 2009) due to the large thickness of their deposits resulting from typical river deltaic sedimentation and accumulation processes (e.g., Schwamborn *et al.* 2002). Permafrost-affected soils are expected to undergo fundamental property changes due to the observed and projected progressive climate changes (Koven *et al.* 2011), including higher turn-over and mineralization rates of organic matter and increased climate-relevant methane and carbon dioxide release to the atmosphere (Dutta *et al.* 2006, Wagner *et al.* 2007, Khvorostyanov *et al.* 2008, Schuur *et al.* 2009). Thus, permafrost-affected soils have to be considered as a globally important element of the cryosphere within the global climate system. The majority of published articles on element stocks in permafrost-affected soils focuses on the North American region (see chapter 2.3, page 21 and Fig. 9). In recent years, however, some areas of the Eurasian permafrost - especially in the Russian region - have also been increasingly studied (Kolchugina *et al.* 1995, Matsuura and Yefremov 1995, Chestnyck *et al.* 1999, Stolbovoi *et al.* 2006, Gundelwein *et al.* 2007, Hugelius and Kuhry 2009).

Most previous studies analyzed carbon pools of specific regions or components of permafrost-affected soil carbon pools (e.g. Stolbovoi 2002, Tarnocai *et al.* 2003, Zimov *et al.* 2006, Ping *et al.* 2008, Bliss and Maursetter 2010, Schirrmeister *et al.* 2011), resulting in the overall challenge to compare and combine the different regional assessments, including soil-type / -order specific soil organic carbon pools and pools calculated over various depths. First important steps towards unification in mapping the distribution of soil types and soil carbon stocks were achieved by assembling the Soil Atlas of the Arctic (Jones *et al.* 2010) and a new pan-arctic estimate of soil organic carbon pools in permafrost (Tarnocai *et al.* 2009). These studies suggest that the total soil organic carbon pool of the permafrost-affected soils to 3 m depth is very high at 1024 Pg (Tarnocai *et al.* 2009), exceeding the carbon pools within the entire global vegetation biomass (650 Pg) or the atmosphere (750 Pg), respectively (IPCC 2007). However, despite this improved quantification, soil organic carbon data for the huge areas of Siberia are still scarce, uncertainties are high, and more detailed landscape-scale assessments are necessary (Tarnocai *et al.* 2009, see chapter 2.2, page 14 and Tab. 2).

Here, the author focuses on the assessment of soil organic carbon and total nitrogen pools in the Northeast-Siberian Lena River Delta. The area that the Lena River Delta occupies amounts to 42 % of the total area of all arctic deltas. The soil organic carbon pool for the Lena River Delta was estimated at 131 Pg (Tarnocai *et al.* 2009). While this river delta consists of various geomorphic units, including some of non-deltaic origin (Schwamborn *et al.* 2002), this study concentrates on the element stocks of soils in areas of Holocene deltaic sedimentation, in particular the Holocene river terrace and the active floodplains. The first goal of the study was a detailed quantification of the soil organic carbon as well as the total nitrogen stocks of the different soil units on Samoylov Island, located in the southern-central Lena River Delta. Of special interest were the rarely investigated currently permanently frozen layers from 50 cm up to 100 cm depth. Samoylov Island is composed of two geomorphic parts that are regarded to be representative for the Holocene river terrace and the active floodplains within the Lena River Delta, respectively. The second goal was to upscale the results from Samoylov Island across the correspondent soil-covered areas of the Holocene river terrace and the floodplains within the Lena River Delta using remote sensing data

(Landsat-7 ETM+ and WorldView-1) and to estimate the soil organic carbon and the total nitrogen pools for these areas.

4.2 Study area

The study site is located on Samoylov Island (72° 22’ N, 126° 30’ E), situated at one of the main Lena River channels, the Olenyokskaya Channel in the southern central part of the Lena River Delta, about 180 km south of the coast of the Arctic Ocean (Fig. 44). At around 32,000 km² (Are *et al.* 2000), the Lena River Delta is the largest arctic delta. It is located in northeastern Siberia, where the Lena River cuts through the Verkhoyansk Mountains and discharges into the Laptev Sea, a part of the Arctic Ocean.

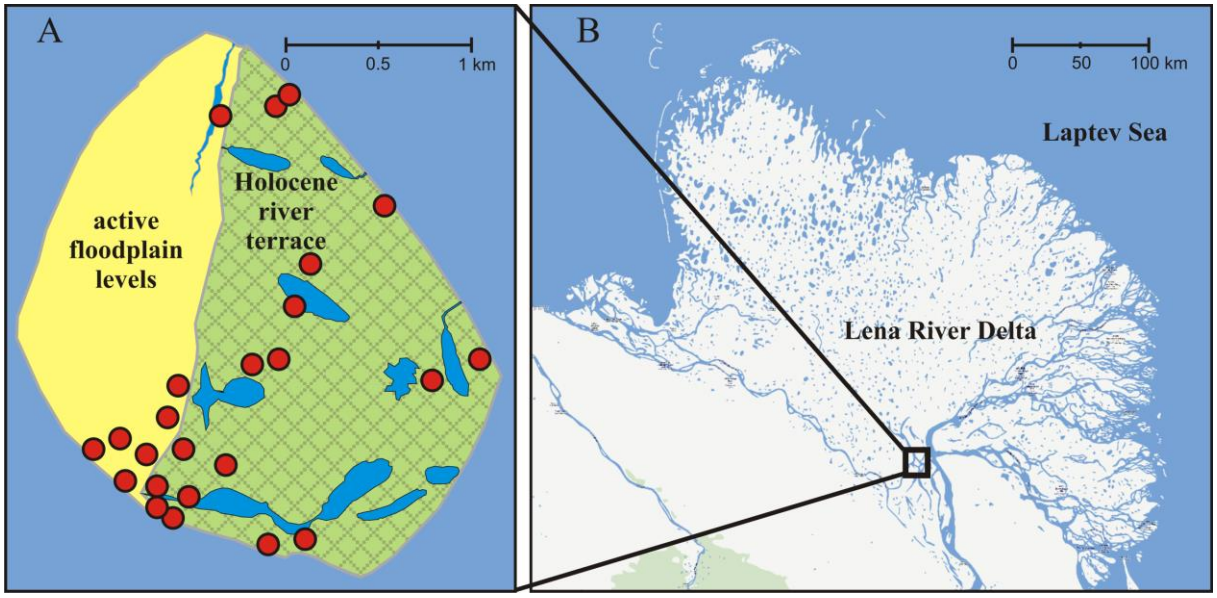

Figure 44: A: Map of Samoylov Island with locations of study sites. B: The investigation area in the Lena River Delta in north-east Siberia with the location of Samoylov Island (Map B based on Google & Geocentre Consulting 2011).

Fig. 44: A: Eine Karte der Insel Samoylov mit den Beprobungslokationen. B: Das Untersuchungsgebiet im Lenadelta in Nordost-Sibirien mit der Lage der Insel Samoylov (Die Karte B basiert auf Google & Geocentre Consulting 2011).

The Lena River Delta consists of three main geomorphic terrace-like units and the modern floodplain levels (Grigoriev 1993, Schwamborn *et al.* 2002). Only the youngest Holocene river terrace and the modern floodplains are of Holocene deltaic origin, while the second and third terrace-like units are largely of pre-Holocene age and have a different composition and genesis (Schwamborn *et al.* 2002).

Samoylov Island is part of this Holocene delta and consists of two major geomorphic parts (Akhmadeeva *et al.* 1999) (Fig. 44), which vary in sedimentary composition as well as contents of organic matter in the soils. The western part of Samoylov Island is represented by a modern floodplain up to 5 m above sea level (a.s.l.) which is flooded annually in spring. The eastern part of the island consists of an elevated (10...16 m a.s.l.) river terrace of Late Holocene age (Pavlova and Dorozhkina 1999). Between these two units, there is a distinct and sharp step of about 5 m (Kutzbach 2006). The river terrace is flooded only during extreme flooding events (Schwamborn *et al.* 2002). This Holocene river terrace is characterized by ice wedge polygons with wet sedge tundra vegetation. Polygonal structures imply micro-scale variability in the landscape with polygonal centres and polygonal rims. The rims generally are elevated and characterized by pronounced cryoturbation. The centres can be of different quality depending of the development stage (French 2007). Low-centred polygons have depressed centres with high water saturation during the summer months. High-centred polygons are characterized by elevated centres and drier compared to the centres of low-centred polygons. The soils of Samoylov Island are *Orthels* and *Turbels* (Pfeiffer *et al.* 2000, Pfeiffer *et al.* 2002, Boike *et al.* 2012) according to the US Soil Taxonomy (Soil Survey Staff 2010). The Soil Complex *Glacic Aquiturbel* / *Typic Historthel* dominates the Holocene river terrace (Fiedler *et al.* 2004, Kutzbach *et al.* 2004) and is characterized by ice wedge polygons. The sandy active floodplain is dominated by *Psammentic Aquorthels* (Pfeiffer *et al.* 2002). Furthermore, there are *Psammorthels* and *Fibristels* with different subgroups widespread over the island (Sanders *et al.* 2010). Average observed maximum depth of the seasonally thawed active layer at the river terrace range was about 50 cm in summer (Boike *et al.* 2012). Thaw depths are larger on the floodplain.

These two geomorphic units found on Samoylov Island are also widespread in the Lena River Delta and dominate the northern, eastern and central delta. In the western delta, Ulrich *et al.*

(2009) studied the surface spectral and soil characteristics of geomorphic units and also separated a Holocene river terrace and the active floodplains from the second and third main geomorphic terrace. Soil characteristics and active layer depths in their study are similar to those found on Samoylov Island. Morgenstern *et al.* (2008) estimated the combined area of the Holocene river terrace and the active floodplain levels at 55 % of the Lena River Delta area.

The investigation area is dominated by an arctic-subarctic climate with continental influence and is characterized by low temperatures and low precipitation (Fig. 45).

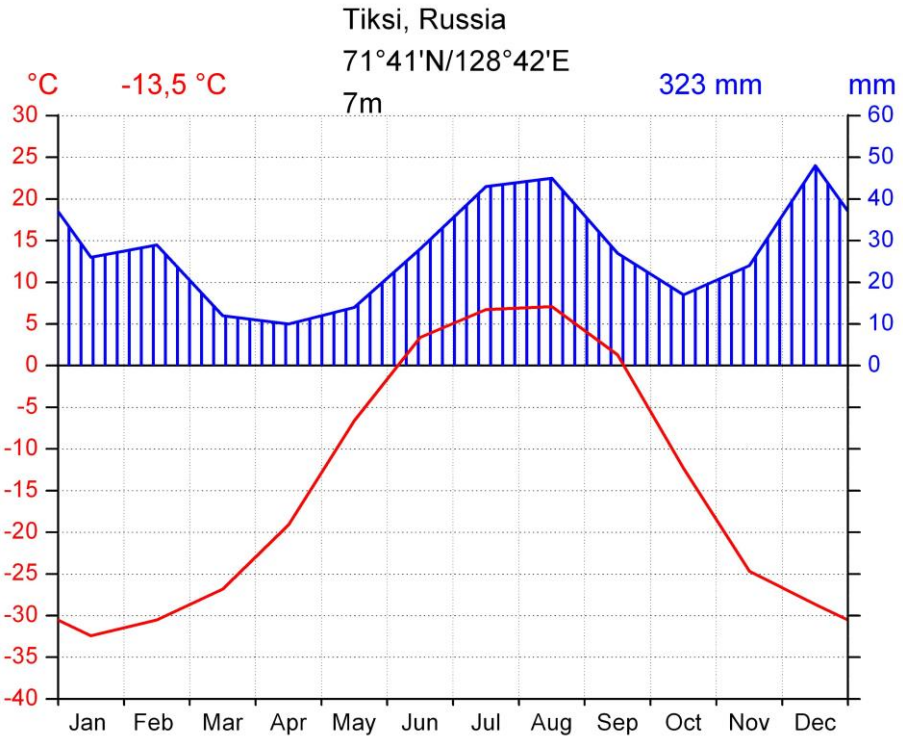

Figure 45: Climate chart for the climate reference site Tiksi. Based on data for the years 1961...1990 provided by Roshydromet (2011).

Fig. 45: Ein Klimadiagramm der Referenzstation in Tiksi. Basierend auf Daten von Roshydromet (2011) für die Jahre 1961...1990.

The mean annual air temperature, measured at the climate reference site in Tiksi (71°41' N, 128°42' E), which is located about 110 km south-east from Samoylov Island, was -13.5 °C, and the mean annual precipitation was 323 mm during the 30-year period 1961...1990

(Roshydromet 2011). The average temperature of the warmest month August was 7.1 °C, whereas the coldest month is January with –32.4 °C (Roshydromet 2011) indicating an extreme seasonal temperature amplitude typical for continental polar regions. Data derived from the meteorological station on Samoylov Island indicated a mean annual air temperature of -12.5 °C and a distinctly lower mean annual precipitation of around 190 mm for the years 1998...2011 and 1999...2011, respectively (Boike *et al.* 2012).

The region is underlain by deep continuous permafrost of 400...600 m thickness (Grigoriev 1960, Yershov *et al*. 1991).

4.3 Methods

4.3.1 Drilling frozen soils

4.3.1.1 General information

For this study a portable permafrost auger set was used to obtain a large number of shallow cores. The set consisted of an engine power head STIHL BT 121 (Andreas Stihl AG & Co. KG) and a Snow-Ice-Permafrost-Research-Establishment (SIPRE) coring auger (Jon's Machine Shop, Fairbanks, Alaska) (Fig. 46 and Fig. 47A). The author collected 37 frozen cores of 1 m length in April and May 2011. Four cores were excluded from further analysis because they did not match the quality requirements. These requirements were that the length of the undisturbed sample should be ≥ 1 m and that the sample site was not a water-filled polygon. For further detailed investigations on mineralization rates, nutrient availabilities and dating, the author stored another four cores from the collection in full length undisturbed and unsampled. The remaining 29 frozen cores were subsampled immediately in the field laboratory by slicing six (i = 1,2,…,6) cylindrical samples (each with a volume of approximately 92 cm³) of each of the cores from the following depths: 0…2 cm (i = 1), 8…10 cm (i = 2), 28…30 cm (i = 3), 48…50 cm (i = 4), 73…75 cm (i = 5), and 98…100 cm (i = 6) (Fig. 47B).

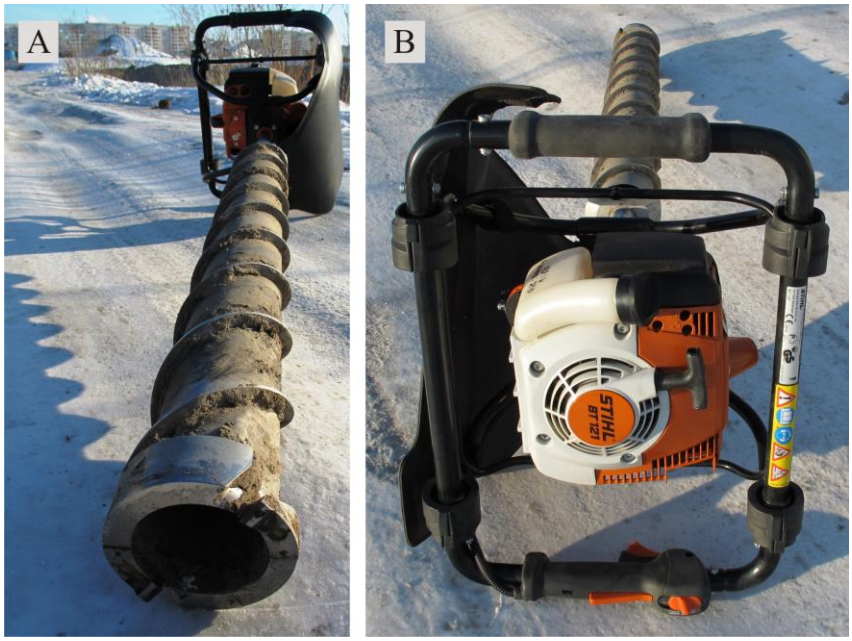

Figure 46: The auger set used for sampling during the spring field campaign. A = SIPRE coring auger by Jon's Machine Shop, Fairbanks, Alaska. B = STIHL BT 121 engine power head (Photo: Alexey R. Desyatkin).

Fig. 46: Das während der Feldarbeiten eingesetzte großkalibrige Erdbohrer-System. A = Kernrohr des SIPRE-Systems von Jon's Machine Shop in Fairbanks, Alaska. B = STIHL BT 121 Motorkopf. (Foto: Alexey R. Desyatkin).

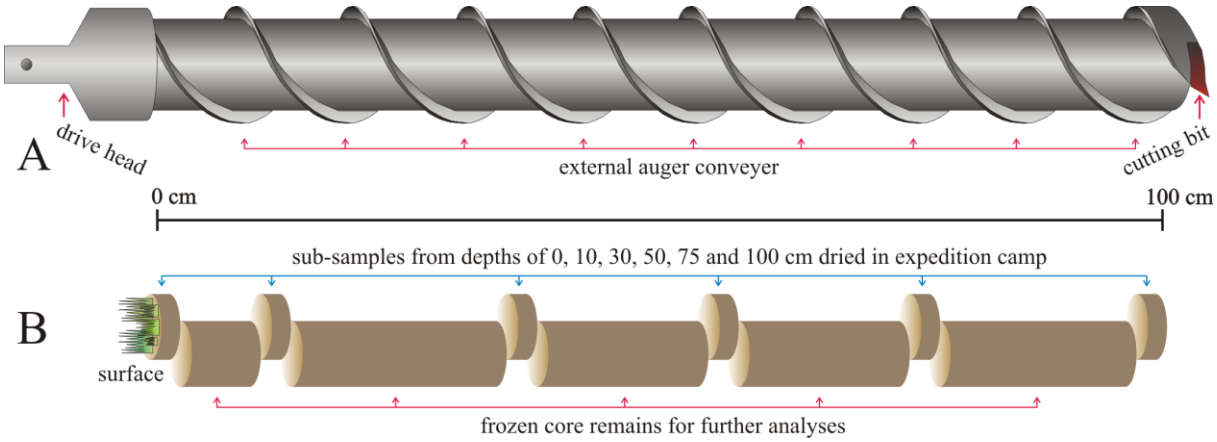

Figure 47: Schematic view of the SIPRE coring auger barrel (A), and the core sampling set up used during field work in spring 2011 (B).

Fig. 47: Schematische Ansicht des SIPRE Kernrohrs (A) und die Beprobungsanordnung, welche währrend der Feldarbeit im Frühjahr 2011 angewandt wurde (B).

4.3.1.2 SIPRE coring auger

The equipment set used was designed to retrieve sediment cores of up to 3 m in length. It was packed in a plastic Pelican 1750 shipping case and consisted of a 1 m coring barrel with an external auger conveyer, a quick change drive head, two one meter and one half meter drive extensions, a T-handle, six carbide tipped cutting bits, fife extension ball detent pins, an adapter to drive motor output shaft, a core retriever with drive head and two connector pins, a core pusher and a frost probe. The total weight incl. the Pelican box was 29.4 kg. The price in fall 2010 was about USD 10,000 including shipping from Alaska to Europe, customs and import turnover tax. Due to the augur's scientific purpose, it is possible to get the shipment exempt from customs fees, though because of its "commercial" appearance the process is unnerving and protracted. The user choosing this procedure has to complete the declaration for scientific instruments ("*Erklärung für wissenschaftliche Instrumente oder Apparate"*) and to satisfactorily demonstrate the scientific purpose of its operation.

Another problem can occur when the SIPRE auger has to be transported abroad to the county of its ultimate use. The usage of the international custom document ATA carnet (probably) will be refused by the Chamber of Commerce of the country where your field work is planned because of the auger's role as a tool for exploration of soils. So all key benefits the ATA carnet provides are unattainable. One should therefore be prepared to purchase temporary import bonds and to pay applicable duties and taxes once more.

In order to avoid custom problems when coming back home from field work abroad (without the ATA carnet), the home custom office should be visited before leaving to the field to complete the form for returned goods (INF 3) (*Auskunftsblatt "Rückwarenregelung"*). A pro forma invoice is needed with a detailed list of the equipment and prices. Pictures of all equipment pieces should be included. The custom office will keep one original form for its record, and a second original will be handed out. It should be shown to the custom officers when crossing the border back to Europe.

4.3.1.3 Auger engine

The STIHL BT 121 engine, the author used, is available worldwide. For this field study, the engine was bought from an official STIHL dealer in Yakutsk, Russia. Besides the specific details of the engine (Tab. 4), it is important to know that the STIHL BT 121 is a two-stroke engine; hence, a 1:50 gasoline oil ratio is required for operation. The fuel tank capacity is about 0.6 L. The gasoline consumption during the spring field trip was low and amounted to an average of 0.5 L per 1 m sediment core from deeply frozen ground.

The STIHL BT 121 engine has a "QuickStop drill brake" including a release lever. This mechanism will interrupt the power flow from the engine to the spindle in case the drill jammed in the ground by turning the release lever towards the operator's thigh. The connected SIPRE coring auger will stop rotate immediately. Because air transportation of gasoline driven engines is strongly restricted, it is a big advantage buying the STIHL BT 121 at the place of work. Above all, it should be taken into account that two stroke engine oil and the required unleaded gasoline with a minimum of 89 octane rating could not be available everywhere. In its instruction manual, STIHL does not recommend using fuel additives to increase octane rating because doing so can create running problems or even damage of the engine.

Table 4: Important specific details of the engine.

Tab. 4: Wichtige Spezifikationen des Motors.

Displacement:	30.8 cm3
Power:	1.3 kW/1.8 bhp
Spindle speed:	190 rpm
Vibration level (left/right):	2.2/2.5 m s-2
Sound power level:	109.0 dB(A)
Sound pressure level:	103.0 dB(A)
Weight:	9.4 kg
Price in fall 2010:	approx. 1,000 EUR

4.3.1.4 Working with the auger set

In the field, work with the auger set is satisfactory and productive. During my field campaign, the STIHL engine worked well without any problems. Starting the engine at temperatures of minus 10 °C caused no big effort. To start the engine during cold mornings, cranking up to 15 times was enough.

Since the weight of the whole set is about 40 kg, the equipment for a day trip should be limited to the essential pieces if no vehicle is available. It proved successful to pack among the engine, the coring barrel and the adapter connecting both, the core catcher with one 1 m extension and the T-handle. The core pusher was needed to avoid core destruction when weakly cemented ground was expected. A toolbox and approx. 2 L of gasoline oil mix were very helpful. Constructed as a one-man auger, the set really fulfilled expectations (Fig. 48A-C) although working in a two-men team was more helpful. Working as a team is especially important after the work day when additionally to the equipment of around 25 kg the sample's weight was added and all had to be transported to the base camp. The weight of a 1 m core was about 5 to 6 kg (Fig. 48D).

A further advantage of working in a pair was the easier handling of the coring barrel and engine set for coring. The total weight of this set was about 18 kg, and this weight had to be lifted up regularly while coring to avoid jamming in the frozen ground. Furthermore, the weight of two operators was of additional benefit, especially when initiating the drill into the frozen surface with the auger not yet stabilized in the borehole.

The external auger conveyer has performed excellently (Fig. 47A). The borehole debris was easily transported upward and usually preserved the auger from jamming. To avoid jamming, lifting up the auger was required while coring to help the conveyer transporting upward the debris, especially when fine-grained ground was drilled. The few times it jammed in the ground, the "Quick stop drill brake" mechanism worked well and stopped the auger immediately. Once the auger jammed in the ground and stopped, the brake should be disengaged and the auger run slowly when trying to lift it up. Acting quickly can prevent the debris from freezing to the auger barrel. Recovery from such an event will be time-consuming and power-intensive.

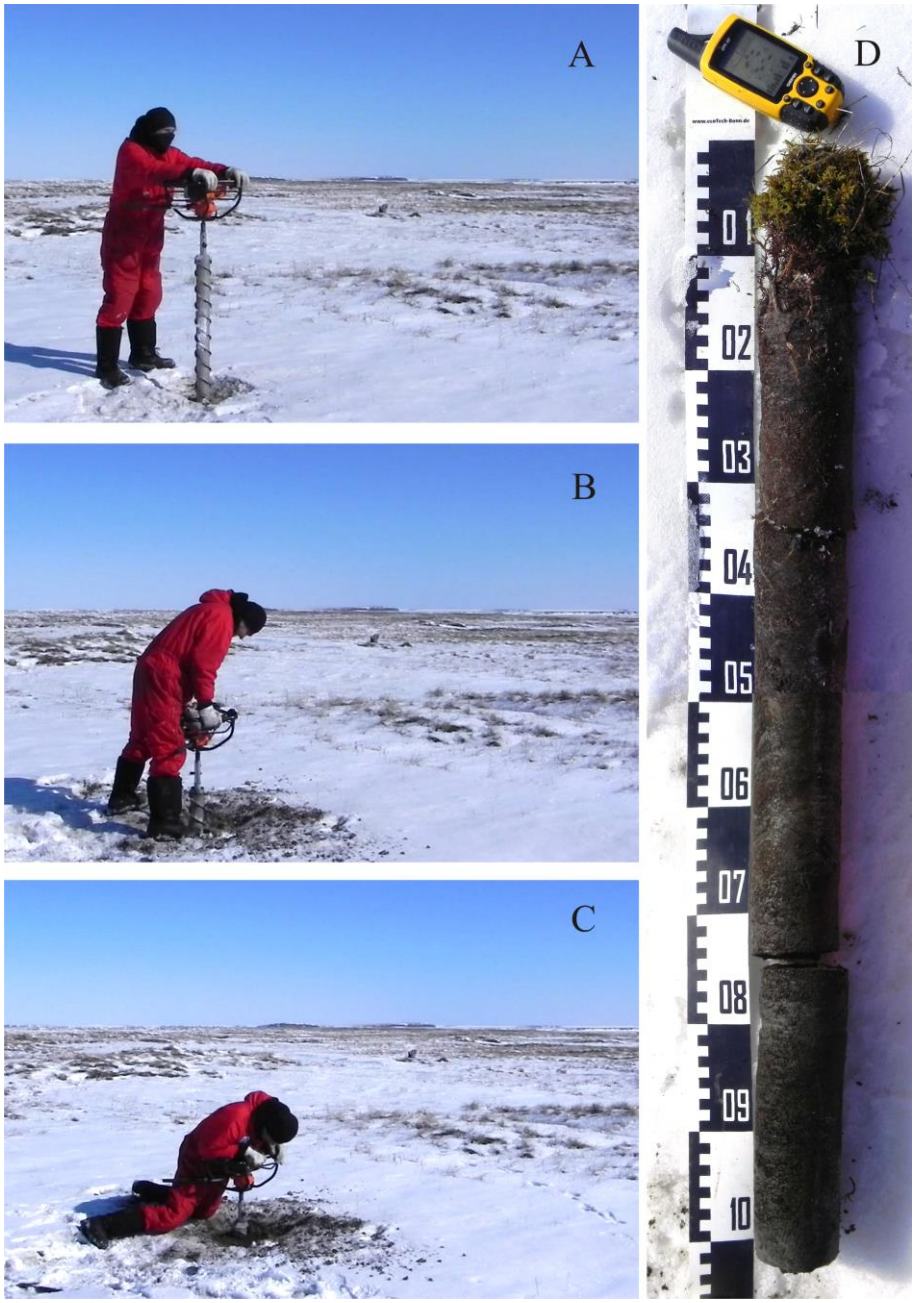

Figure 48: Fieldwork with the SIPRE auger on Samoylov Island, Lena River Delta, North-East Siberia in April 2011. A, B and C = different stages of drilling progress. D: The result of the hard work – 1 m long core of organic rich permafrost-affected soil.

Fig. 48: Feldarbeit mit dem SIPRE Bohrer auf der Insel Samoylov im Lena-Delta in Nordost-Sibirien im April 2011. A, B und C: Die unterschiedlichen Arbeitsabschnitte beim Bohren. D = Das Ergebnis harter Arbeit – ein ca. 1 m langer Bohrkern eines von Permafrost beeinflussten Bodens mit hohem Anteil an organischem Material.

Additionally, the total height of the set used should be mentioned. It was around 150 cm which resulted in a disadvantageous angle between the equipment and the arms of operator (Fig. 48A) limiting handling and transmission of manpower. The initiation of a new borehole arose as the most crucial moment when full power was needed. A great enhancement could be the addition of a coring barrel of around 50 cm for starting a new borehole. This short barrel could be replaced by the longer one once coring depth increases.

Usually, the cores were retrieved without stress, but in a few cases hard work was needed to retrieve them from the barrel. The heat generated during the coring process can melt frozen water at outer face of the core. When drilling was interrupted or completed, this water sometimes refroze rapidly, and the core jammed in the barrel. In that case a small gas-driven laboratory burner was beneficial to heat up the barrel and then the core pusher was used to remove the core from it.

Despite the few resolvable problems described, the equipment is worth a recommendation and the samples recovered were of high quality (Fig. 48D). For analyses in the field, the cores were sawed into pieces collecting six small samples from each core while the frozen major remains were kept for future analyses.

Coring should be performed while the entire ground is frozen to get good quality samples throughout the entire core from surface to bottom. Additionally, the impact to the natural environment is lower when the ground is frozen, especially when a vehicle is used for transportation.

4.3.2 Soil-chemical analyses

The gravimetric contents of organic carbon c_{OC} and total nitrogen c_N were analyzed with a element analyzer based on high temperature combustion and subsequent gas analysis (Vario MAX CNS, Elementar Analysesysteme GmbH, Germany) using oven-dried (12 h at 105 °C) and ground samples. The bulk density (ρ_d) was calculated as the ratio of the dry mass of an undisturbed soil sample and the volume of a cylindrical sample of a core with a height of 20 mm and the diameter of 76 mm. There were no coarse fragments > 2 mm in any of the undisturbed soil samples. The gravimetric ice contents were determined by drying soils at

65 °C for 2 days and measuring the frozen-fresh sample mass before and the dry sample mass after drying. The frozen water mass was related to the fresh soil mass.

4.3.3 Soil organic carbon and nitrogen stock calculations

The volumetric contents of soil organic carbon ρ_{OC} and total nitrogen ρ_N (both in kg m^{-3}) of the 2-cm soil layers were calculated as:

$$\rho_{OC} = c_{OC} \cdot \rho_d \quad (1) \qquad \text{and} \qquad \rho_N = c_N \cdot \rho_d \quad (2)$$

where c_{OC} and c_N are the gravimetric contents of organic carbon and total nitrogen, and ρ_d is the bulk density. For the estimation of the soil organic carbon and total nitrogen stocks over specific soil depths, volumetric contents of soil organic carbon and total nitrogen of the non-sampled soil layers between the 2-cm soil layers that were sampled and analysed were estimated by linear interpolation in 1-cm intervals. Stocks of soil organic carbon $S_{OC}(h_r)$ and total nitrogen $S_N(h_r)$ over different reference depths h_r were then calculated by integrating the volumetric contents of organic carbon and total nitrogen over soil depth h from the soil surface (0 cm) to the respective reference depths h_r as:

$$S_{OC}(d) = \int_{0cm}^{d} \rho_{OC} \quad (3) \qquad \text{and} \qquad S_N(d) = \int_{0cm}^{d} \rho_N \quad (4)$$

where the following reference depths h_r were chosen: 2 cm, 10 cm, 30 cm, 50 cm, 75 cm, 100 cm.

4.3.4 Synthesis of existing soil information

In addition to investigating the general soil organic carbon stocks of Samoylov Island based on the new core data and a characterization of morphological units on this island, the author also synthesized existing soil data from Samoylov Island mapped during previous expeditions (Pfeiffer *et al.* 2000, Pfeiffer *et al.* 2002). Prior reanalyzing the Samoylov soil data he updated

the existing soil map (Pfeiffer *et al.* 2000, Sanders *et al.* 2010; see chapter 2.3) for Samoylov Island with the extent of the island shape in August 2010 (Fig. 1). This was necessary due to the high riverbank dynamics within the central Lena River Delta. For example, high erosion rates in the southeastern and pronounced accumulations rates in the western part of the island were observed.

4.3.5 Organic carbon and total nitrogen pool calculations

For the calculation of the soil organic carbon and nitrogen pools for the two geomorphologic units investigated on Samoylov Island, upscaling of the S_{OC}(100 cm) and S_N(100 cm) stocks was performed by multiplying the means of S_{OC}(100 cm) and S_N(100 cm) by the estimated areas of the two geomorphologic units, the Holocene river terrace and the active floodplain levels, respectively.

4.3.6 Satellite data and image processing

A Landsat image mosaic covering more than 98% of the delta was used to determine the extent of the Holocene river terrace and the active floodplains. The mosaic was generated from three Landsat-7 ETM+ satellite images taken during the summer on 27 July 2000 (path 131, row 8 and 9) and on 26 July 2001 (path 135, row 8). A detailed description of the image processing, atmospheric corrections, image co-referencing, and mosaicking is provided by Schneider *et al.* (2009). The final mosaic has a spatial resolution of 30 m, encompasses the multispectral Landsat-7 bands 1...5 and 7, and has a horizontal accuracy of about 50 m.

The areas of the sand-rich Arga Complex belonging to the 2nd main geomorphic unit in the Lena River Delta, and the Yedoma islands of the 3rd main geomorphic unit were not considered in this study of the Holocene and active delta portions. Therefore, the author removed these areas by clipping with a mask based on geographic information system layers of those two geomorphic units provided by Morgenstern *et al.* (2011), who delineated the extent of these two terraces manually from the same Landsat image mosaic under inclusion of cryostratigraphic and geologic field knowledge. In addition, the sandy barrier islands offshore

the western delta and the mountainous mainland areas along the southern delta boundary were masked.

For accuracy assessment of the classification of the Holocene river terrace and the active floodplains, multiple WorldView-1 images (panchromatic band, 0.5 m ground resolution) from three different delta portions as independent high-resolution dataset were used from which visually land unit type interpretations were done. The images were acquired during the snow-free seasons of 2009 (26 September and 7 August) and 2011 (11 June). The images have a geolocation accuracy better than the Landsat pixel size. For all processing steps ArcGIS 10 (ESRI) was used.

4.3.6.1 Supervised classification

For the supervised classification, the author created ten training sample areas per target geomorphic unit in the Lena River Delta displayed in the satellite image. Based on general geomorphic classifications of the Lena River Delta by Grigoriev (1993), the target units for the image classification were (1) the Holocene river terrace, (2) the active floodplains, and (3) the water bodies. He performed a supervised "Maximum Likelihood Classification" with the created training sample areas.

4.3.6.2 Post-classification imagery processing

A post-classification generalization of the results was performed in ArcGIS. The author first grouped connected pixels of the same class into regions (function: Region Group), then merged isolated pixels surrounded entirely by pixels of a different class with that class (function: Nibble), and lastly re-assigned class identity for pixels in regions consisting of less than four pixels by applying an Euclidean distance approach to identify and assign the most appropriate class for such pixels from its nearest neighbours (ArcGIS Resource Center 2012). He next excluded all water bodies > 3,600 m² (4 Landsat pixels) from the satellite imagery of the Lena River Delta for later upscaling over soil-covered areas only. Additionally, the author corrected the extent of the Holocene river terrace's soil-covered area reducing it by the

percentage of small water ponds and troughs (14 %) detected by high-resolution aerial photography for Samoylov Island (Sachs *et al.* 2010).

4.3.6.3 Accuracy assessment of the classification

Within the footprint of the WorldView-1 images that overlapped with delta portions, 150 points in the delta regions covered by the three main classes (water, Holocene terrace, active floodplain) were randomly selected (Fig. 49). Both Holocene terrace and active floodplains are clearly differentiated in their characteristics in these high-resolution images. While the active floodplain areas do not have any relief and any ice wedge polygonal structures, the Holocene river terrace shows well developed ice wedge polygons. For all points the author first visually interpreted the dominant land unit within a 10 m circular buffer from WorldView-1 data and then extracted the class from the Landsat classification for direct comparison. Data points were then cross-tabulated and various classification accuracy parameters calculated.

4.3.7 Statistics

Descriptive statistics as well as correlation analyses for soil data were performed using the SPSS package version 16.0.1.

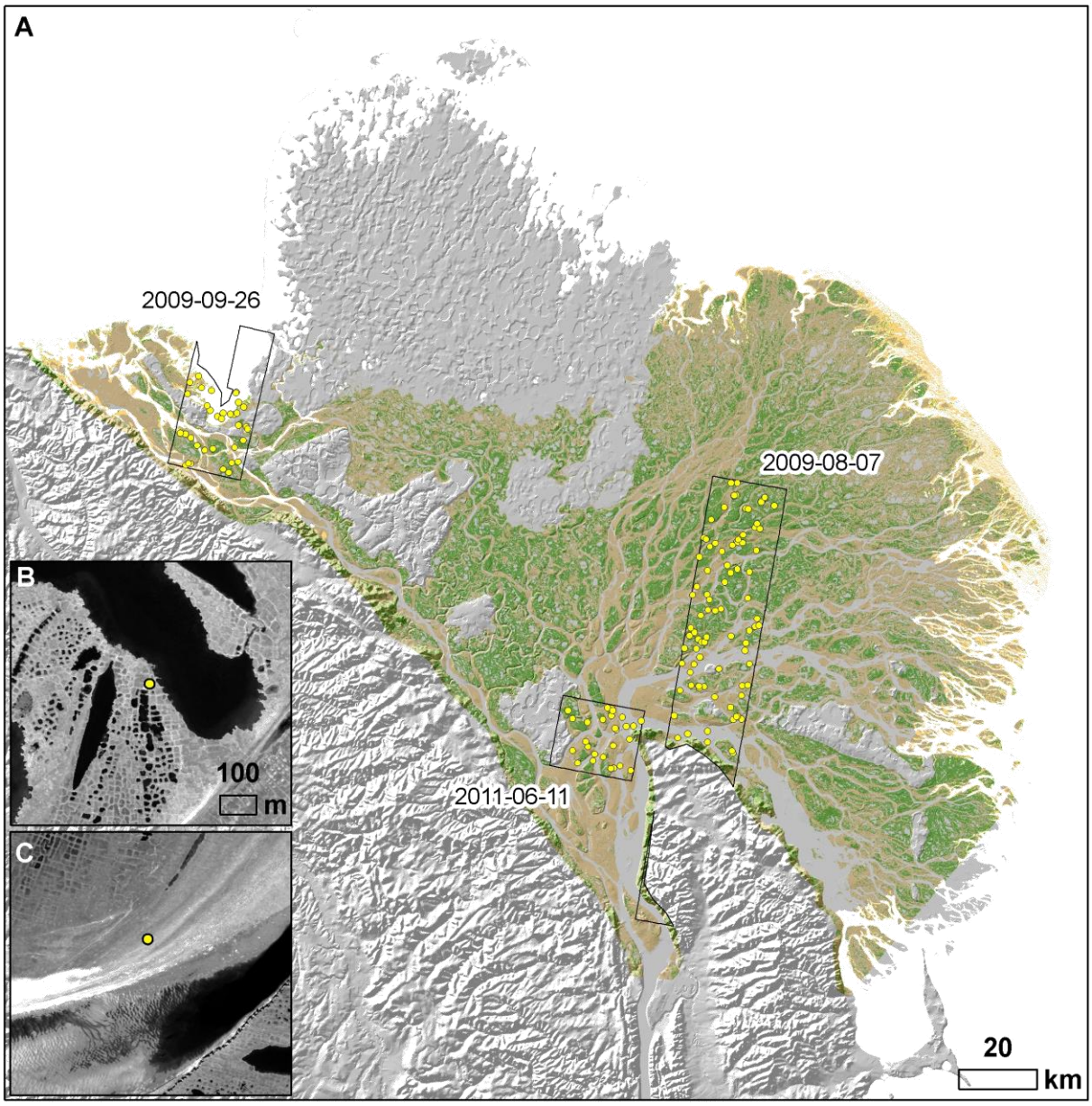

Figure 49: A: Delta classification overview showing areas covered with very high resolution WorldView-1 data (©DigitalGlobe) (black frames, including acquisition date) used for ground truth of the classification (150 yellow dots). B: Example of ground truth point on Holocene terrace. C: Example of ground truth point on active floodplain.

Fig. 49: A: Übersicht der Deltaklassifizierung mit der Abdeckung mit sehr hoch aufgelösten Daten von WorldView-1 (©DigitalGlobe) (schwarze Rahmen, mit dem Aufnahmedatum), die zur Überprüfung der Klassifikation genutzt wurden (150 gelbe Punkte). B: Ein Beispiel der Überprüfung auf der Holozänen Terrasse. C: Ein Beispiel der Überprüfung auf der Überflutungsebene.

4.4 Results

4.4.1 Soil properties

The mean bulk densities ρ_d within the floodplain soils varied among the different six investigated soil layers from 1.0 g cm^{-3} to 1.5 g cm^{-3} whereas the mean ρ_d of the soils sampled on the higher elevated river terrace varied between 0.2 g cm^{-3} and 0.9 g cm^{-3} (Tab. 5). The results generally showed a high scatter ranging from 0.08 g cm^{-3} to 2.37 g cm^{-3} at the floodplains and 0.02 g cm^{-3} to 2.0 g cm^{-3} at the river terrace, respectively.

Table 5: Results of the bulk density determination for all six investigated soil depths and the both morphological units, the Holocene river terrace and the active floodplain levels expressed in g cm^{-3} with the mean values and the respective standard deviations (SD) as well as the minima (Min.) and maxima (Max.).

Tab. 5: Ergebnisse der Bodendichtebestimmung für alle sechs untersuchten Bodentiefen und die beiden morphologischen Einheiten, die Holozäne Flussterrasse und die aktive Überflutungsebene, ausgedrückt in g cm^{-3} mit den Mittelwerten und den entsprechenden Standardabweichungen (SD) sowie den Minima (Min.) und Maxima (Max.).

	Holovene River Terrace				Active Floodplain			
Soil depth [cm]	**Mean** [g cm^{-3}]	**SD**	**Min.** [g cm^{-3}]	**Max.** [g cm^{-3}]	**Mean** [g cm^{-3}]	**SD**	**Min.** [g cm^{-3}]	**Max.** [g cm^{-3}]
0…2	0.227	0.245	0.016	1.018	1.010	0.668	0.080	2.000
8…10	0.485	0.493	0.022	1.467	1.327	0.224	1.015	1.609
28…30	0.721	0.476	0.075	1.601	1.461	0.271	1.175	1.986
48…50	0.905	0.536	0.105	1.997	1.545	0.175	1.175	1.704
73…75	0.916	0.545	0.292	1.971	1.455	0.480	0.922	2.374
98…100	0.918	0.445	0.278	1.980	1.490	0.308	0.922	1.830

Within the soil profiles there was a clear increase of the mean ρ_d with depth to a point where the ρ_d reached a relatively stable value with depth. For the soils of the river terrace, this point

was around 30 cm below the soil surface for an ρ_d of about 0.9 g cm^{-3}. For the active floodplain levels, it was around 10 cm below the soil surface for an ρ_d of 1.5 g cm^{-3} (Tab. 5).

The gravimetric ice contents were higher in soils of the Holocene river terrace with mean values of more than 75 % than in soils of the active floodplain levels with mean values of around 35 %, respectively. Within both morphological units, the mean ice contents decreased from the surface to the deeper soil layers to 45 % in the soils of the river terrace and to 16 % in the soils of the active floodplains, respectively (Tab. 6).

Table 6: Results of the gravimetric ice content determination for all six investigated soil depths and the both morphological units, the Holocene river terrace and the active floodplain levels expressed in percent related to fresh weight with the mean values and the respective standard deviations as well as the minima and maxima.

Tab. 6: Ergebnisse der Bestimmung des gravimetrischen Eisgehaltes für alle sechs untersuchten Bodentiefen und die beiden morphologischen Einheiten, die Holozäne Flussterrasse und die aktive Überflutungsebene, ausgedrückt in Prozent bezogen auf des feldfirsche Gewicht mit den Mittelwerten und den entsprechenden Standardabweichungen (SD) sowie den Minima (Min.) und Maxima (Max.).

	Holocene River Terrace				Active Floodplain			
Soil depth	**Mean**	**SD**	**Min.**	**Max.**	**Mean**	**SD**	**Min.**	**Max.**
[cm]	[%]		[%]	[%]	[%]		[%]	[%]
0…2	76.9	16.6	39.1	98.1	34.9	29.0	8.7	91.1
8…10	67.4	25.4	21.3	97.6	23.6	9.5	11.3	36.0
28…30	53.0	22.7	20.2	93.7	15.3	9.3	3.6	26.1
48…50	46.9	20.7	18.5	89.2	12.9	7.5	3.5	21.6
73…75	45.8	19.7	13.1	73.9	15.5	9.1	7.9	34.2
98…100	44.6	17.3	16.0	77.8	15.9	8.2	7.9	28.5

The mean results of the ice content were strongly negatively correlated with the mean bulk density results. The Pearson product-moment correlation coefficients were R = -0.996 for the river terrace and R = -0.992 for the active floodplains, respectively.

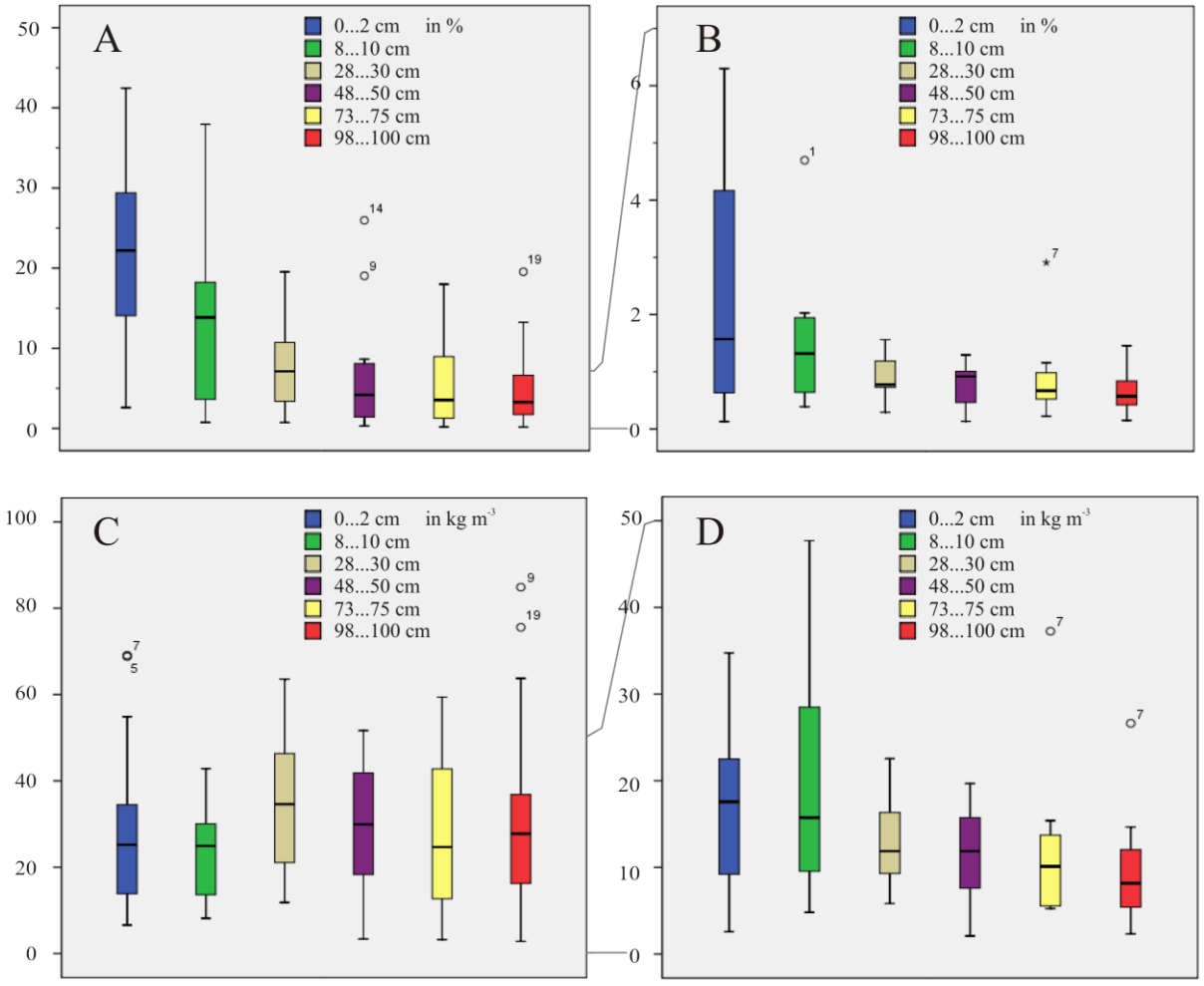

Figure 50: A and B: gravimetric contents of organic carbon (%) in the investigated soils layers (*i* = 1…6) of the Holocene river terrace (A) and the active floodplain levels (B). In B and the depth of 0…2 (*i* = 1) an extreme value of 27 % was removed prior plotting. C and D: volumetric contents of organic carbon for all six investigated horizons (*i* = 1…6) (kg m^{-3}) of the Holocene river terrace (C) and the active floodplain levels (D). Note different scale for y-axis on the graphs.

Central black line: median, lower/upper box end: lower/upper quartile, lower/upper horizontal bar: minimum, maximum. Outliers (values between 1.5 and 3 times the interquartile range from a quartile) are marked by circles, extreme values (values more than 3 times the interquartile range) by asterisks.

Fig. 50: A und B: gravimetrische Gehalte an organischem Kohlenstoff (%) in den untersuchten Bodenhorizonten (*i* = 1…6) der Holozänen Flussterrasse (A) und der aktiven Überflutungsebenen (B). In B und der Tiefe von 0...2 (*i* = 1) wurde ein Extremwert von 27 % vor dem Plotten entfernt. C und D: volumetrische Gehalte an organischem Kohlenstoff für alle untersuchten Bodenhorizonte (*i* = 1…6) (kg m^{-3}) auf der Holozänen Flussterasse (C) und den aktiven Überflutungsebenen (D). Bitte die unterschiedliche Skalierung der y-Achse beachten.

Die zentrale schwarze Line: Median, unteres/oberes Boxende: unteres/oberes Quartil, unterer/oberer horizontaler Strich: Minimum, Maximum. Ausreisser (Werte zwischen 1,5 und 3-fachem Interquartilbereichs vom Quartil) sind mit einem Kreis markiert, Extremwerte (Werte mit mehr als den 3-fachen Bereich des Interquartils) mit einem Sternchen.

The gravimetric contents of organic carbon c_{OC} showed a high scatter ranging from 0.17 % to 42.46 % in the soils of the Holocene river terrace and ranging from 0.13 % to 27.71 % in the soils of the active floodplain levels (Fig. 50). The highest mean c_{OC} were measured in the soil surface layers (0…2 cm) (river terrace: 21.85 % ± 10.86 %, active floodplains: 5.89 % ± 9.88 %), followed by the soil layers in the depth from 8...10 cm (Holocene river terrace: 12.77 % ± 9.60 %, active floodplains: 1.65 % ± 1.49 %). The soils of the river terrace had significantly higher cOC than the soils of the active floodplains (One-way ANOVA: p = 0.002...0.047).

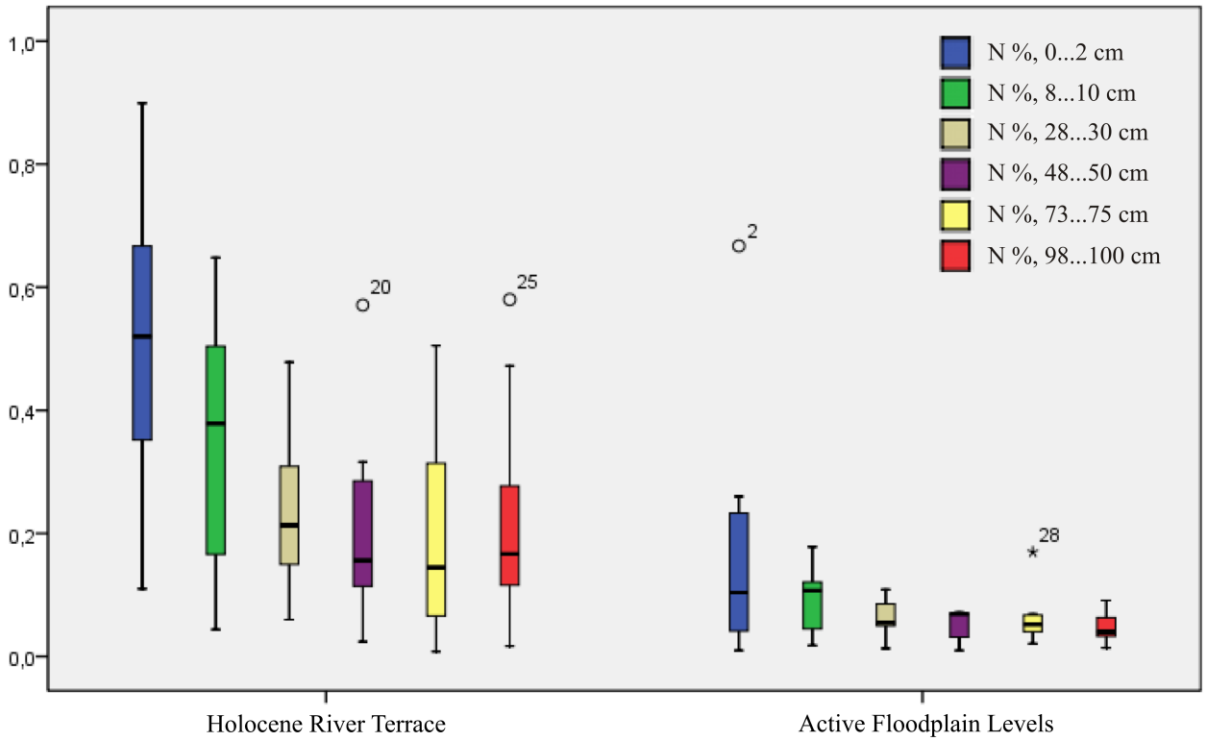

Figure 51: Contents of Nitrogen (%) in the investigated soils layers (*i* = 1…6) and geomorphic units. Central black line: median, lower/upper box end: lower/upper quartile, lower/upper horizontal bar: minimum, maximum. Outliers (values between 1.5 and 3 times the interquartile range from a quartile) are marked by circles, extreme values (values more than 3 times the interquartile range) by asterisks.

Fig. 51: Gehalte an Gesamtstickstoff (%) in den untersuchten Bodenhorizonten (*i* = 1…6) und geomorphologischen Einheiten. Die zentrale schwarze Line: Median, unteres/oberes Boxende: unteres/oberes Quartil, unterer/oberer horizontaler Strich: Minimum, Maximum. Ausreisser (Werte zwischen 1,5 und 3-fachem Interquartilbereichs vom Quartil) sind mit einem Kreis markiert, Extremwerte (Werte mit mehr als den 3-fachen Bereich des Interquartils) mit einem Sternchen.

The gravimetric contents of total nitrogen c_N were significantly higher (One-way ANOVA: p = 0.001...0.049) in the soils of the river terrace than in the soils of the active floodplains (Fig. 51). There was a significant decrease of the contents with increasing depth of the soil profile within both morphological units: from 0.51 % in the surface horizons to 0.21 % at a depth of 98…100 cm in the soils of the river terrace and from 0.19 % in the surface horizons and 0.05 % at a depth of 100 cm in the soils of the active floodplain levels. The c_N ranged between 0.01 % and 0.90 % in the soils of the river terrace and between 0.01 % and 0.67 % in the soils of the active floodplains, respectively.

The C/N ratios ranged between 9 and 70 and were distinctly different in the soils of the river terrace and the soils of the active floodplains and additionally varied with depth (Tab. 7). The mean C/N ratios in the uppermost horizons were 41 ± 14 at the river terrace and 21 ± 11 at the floodplains, respectively. In the deepest investigated soil layers (98…100 cm), the C/N ratios were 21 ± 8 at the river terrace and 13 ± 2 at the floodplains, respectively.

Table 7: Results of the C/N ratio determination for all six investigated soil depths and the both morphological units, the Holocene river terrace and the active floodplain with the mean values and the respective standard deviations as well as the minima and maxima.

Tab. 7: Ergebnisse der Bestimmung des C/N-Verhältnisses für alles sechs untersuchten Bodentiefen und die beiden morphologischen Einheiten, die junge Flussterrasse und die active Überflutungsebene mit den Mittelwerten und den entsprechenden Standarabweichungen so wie den Minima und den Maxima.

	Holocene River Terrace				Active Floodplain			
Soil depth [cm]	**Mean**	**SD**	**Min.**	**Max.**	**Mean**	**SD**	**Min.**	**Max.**
0…2	41.39	13.64	16.19	67.08	20.93	10.89	12.90	41.54
8…10	32.88	13.21	15.00	69.65	17.18	5.134	12.34	26.39
28…30	28.49	11.73	12.32	51.05	15.50	3.438	12.52	22.54

48…50	24.19	12.22	8.60	60.25	14.81	2.183	12.75	18.49
73…75	23.75	8.53	11.04	39.55	13.68	2.50	10.52	17.11
98…100	20.73	7.75	10.24	40.09	13.32	1.86	10.79	15.99

4.4.2 Soil organic carbon stocks

The overall mean soil organic carbon stock estimated for a reference depth of 1 m S_{OC}(100 cm) using all selected cores (N = 29) was 25.7 kg m^{-2} ± 12.0 kg m^{-2}, with a median of 24.9 kg m^{-2}. The range of the estimated S_{OC}(100 cm) was 42.0 kg m^{-2} with a minimum of 6.5 kg m^{-2} and a maximum of 48.6 kg m^{-2}.

The soil organic carbon stock within the seasonally thawed active layer (0…50 cm) S_{OC}(50 cm) reached 13.0 kg m^{-2} ± 5.3 kg m^{-2}. The perennially frozen soil layers (50…100 cm) store 49 % of the entire estimated S_{OC}(100 cm). The summed total stocks for the depths of 0…30 cm, 0…75 cm were: 7.7 kg m^{-2} ± 3.2 kg m^{-2} and 19.2 kg m^{-2} ± 8.5 kg m^{-2}, respectively. The author proved the evident smooth increase of the SOC stock with depth using correlation analysis for the relationship between core depth and mean SOC stock. The Pearson product-moment correlation coefficient was R = 1.00. A regression analysis with the mean SOC stock as dependent variable and the core depth as independent variable (standard error of the estimate (SEE) = 0.2281) indicates that with every additional centimetre of depth the mean SOC stock increases by 0.254 kg m^{-2} with a standard error (SE) of 0.003 kg m^{-2}.

4.4.3 Holocene river terrace and the active floodplain

The S_{OC}(100 cm) for the soils across the investigated island showed a broad range of 42.0 kg m^{-2}, indicating a high heterogeneity among the sampled cores. To get a more differentiated picture of the soil organic carbon stocks of the two geomorphic units, the samples of the Holocene river terrace (N = 22) and the floodplain (N = 7), respectively, were separated. Pronounced differences between the soils in these two units were found. Generally, distinctly higher $S_{OC}(h_r)$ were found in the soils of the Holocene river terrace (Fig. 52). This characteristic increased with increasing reference depth h_r. The mean S_{OC}(100 cm) in soils of

the river terrace was estimated at 29.5 kg m^{-2} ± 10.5 kg m^{-2} with a median of 27.0 kg m^{-2} (minimum 12.7 kg m^{-2}, maximum 48.5 kg m^{-2}). The S_{OC}(100 cm) in soils of the active floodplains were lower with a mean of 13.6 kg m^{-2} ± 7.4 kg m^{-2} and a median of 11.6 kg m^{-2} (minimum 6.5 kg m^{-2}, maximum 26.6 kg m^{-2}).

With these estimated results a SOC stock map for Samolyov Island was plotted (Fig. 53).

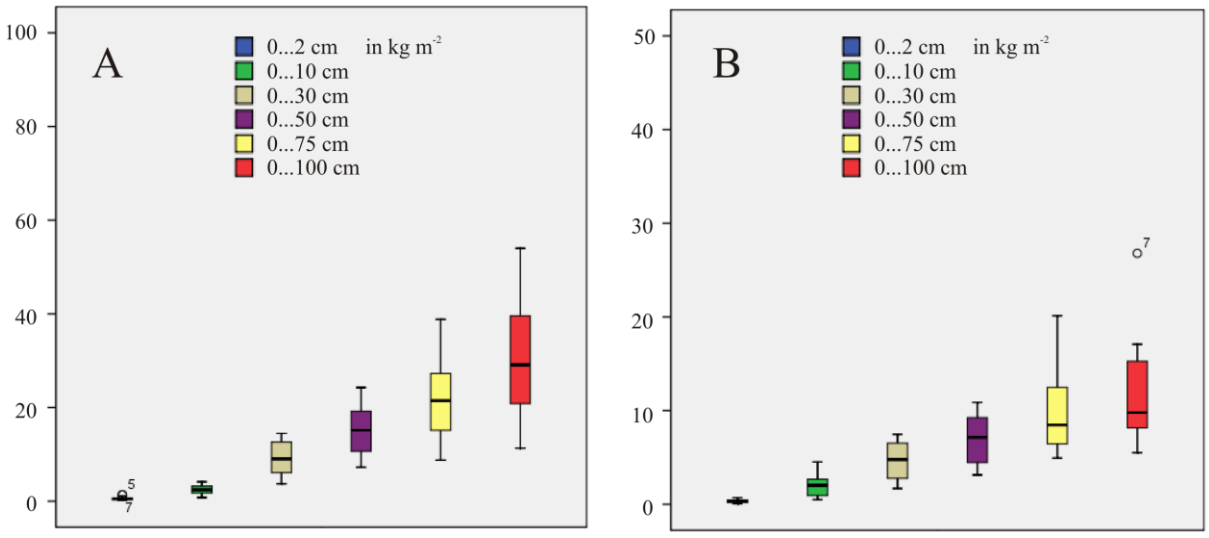

Figure 52: The cumulative carbon stock for all six investigated depths of the Holocene river terrace (A) and of the active floodplains (B) on Samoylov Island (kg m^{-2}). Note different scale for y-axis on the graphs.

Fig. 52: Die kumulierten Kohlenstoffpools für alle untersuchten Bodentiefen der Holozänen Flussterasse (A) und der aktiven Überflutungsebene (B) auf Samoylov der Holozänen Flussterrasse (A, B) und der aktiven Überflutungsebene (C, D) auf der Insel Samoylov (kg m^{-2}). Bitte die unterschiedliche Skalierung der y-Achse beachten.

For the relationship between soil depth and mean SOC stock in the river terrace the Pearson product-moment correlation coefficient was R = 1.00. The regression analysis with the mean SOC stock in the unit as dependent variable and the soil depth as independent variable (SEE = 0.3764) indicated that with every additional centimetre of depth the mean SOC stock increases by 0.293 kg m^{-2} with a SE of 0.004 kg m^{-2}. The same statistical analyses for the soils of the active floodplain levels resulted in R = 0.998 and the corresponding regression analysis (SEE = 0.3936) indicated an increase of the SOC stock by 0.132 kg m^{-2} with a SE of 0.005 kg m^{-2} with increasing soil depth of 1 cm.

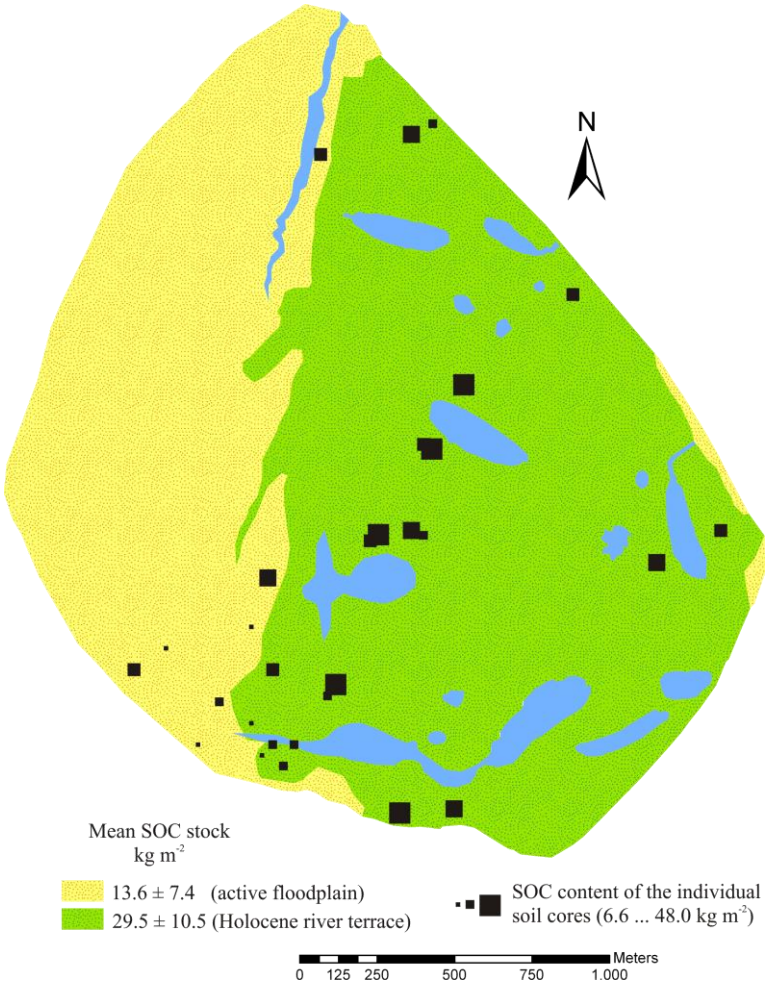

Figure 53: A map of Samoylov Island indicating the distribution of the SOC stock within the two morphological units with the soil organic carbon content of all individual soil cores.

Fig. 53: Eine Karte der Insel Samoylov mit der Verteilung des Pools an bodeneigenem organischen Kohlenstoff innerhalb der beiden morphologischen Einheiten mit den Gehalten des organischen Kohlenstoffs in allen Bodenkernen.

4.4.4 Polygon centres, polygon rims, and soil units

To account for pronounced small-scale spatial soil variability within the polygonal tundra of the Holocene river terrace the author analyzed and compared the characteristics of cores from the polygon rims (N = 6) and from the polygon centres (N = 16). Additionally, separate core analyses were done on the soil subgroup level.

The estimated mean soil organic carbon stock within the surface layers S_{OC}(2 cm) was substantially higher in the polygon rims (0.9 kg m^{-2} ± 0.5 kg m^{-2}) than for the corresponding layers in the polygon centres (0.5 kg m^{-2} ± 0.3 kg m^{-2}). Including the soil layers down to 10 cm depth, this difference decreased (S_{OC}(10 cm) was 3.2 kg m^{-2} ± 1.5 kg m^{-2} for the rims and 2.5 kg m^{-2} ± 0.9 kg m^{-2} for the centres). The estimated mean soil organic carbon stock within 30 cm depth S_{OC}(30 cm) was slightly higher in the centres (8.8 kg m^{-2} ± 2.8 kg m^{-2}) than at the rims (7.5 kg m^{-2} ± 3.1 kg m^{-2}). The mean soil organic carbon stock over 1 m deep soil profiles S_{OC}(100 cm) was 33.3 kg m^{-2} ± 9.7 kg m^{-2} in the centres with a median of 34.5 kg m^{-2}, whereas at the polygonal rims the mean S_{OC}(100 cm) was 19.4 kg m^{-2} ± 3.7 kg m^{-2} with a median of 19.5 kg m^{-2}.

For these two sub stocks, the Pearson product-moment correlation coefficients were determined. For the mean SOC stocks and the soil profile depth for both, the polygonal centre and the polygonal rim, the coefficients were R = 0.999 and R = 0.997, respectively. The results of the corresponding regression analyses indicate that the SOC stock in polygonal centres (SEE = 0.6919) increases with each centimetre depth by 0.333 kg m^{-2} with a SE of 0.008 kg m^{-2} whereas in polygonal rims (SEE = 0.6347) this stock increases by only 0.184 kg m^{-2} with a SE of 0.007 kg m^{-2}.

Prior analyses of separate cores on the soil subgroup level the author updated the existing soil map (Pfeiffer *et al.* 2000, Sanders *et al.* 2010, Fig. 10) for Samoylov Island with the extent of the island shape in August 2010 (Fig. 54). This was necessary due to the high river bank dynamics within the central Lena River Delta. For example, high erosion rates in the southeastern and pronounced accumulations rates in the western part of the island were observed.

The results of the analyses on soil subgroup level indicated a large variability among the eight known soil subgroups of Samoylov Island (Fig. 54). The S_{OC}(100 cm) estimates based on the one sampled core were 31.1 kg m^{-2} for the *Typic Aquorthel* (Silty) and 45.3 kg m^{-2} for the *Typic Aquiturbel*/ *Typic Aquorthel* soil complex, respectively. The results of the mean S_{OC}(100 cm) estimations for the other soil units of Samoylov Island with a higher number of sampled cores showed a high scatter (Fig. 54). Minima ranged from 6.5 kg m^{-2} to 19.5 kg m^{-2},

maxima ranged from 20.4 kg m^{-2} to 48.5 kg m^{-2}. The mean carbon stocks of the different soils varied strongly within the soil units as well as across the depth profiles (Fig. 55).

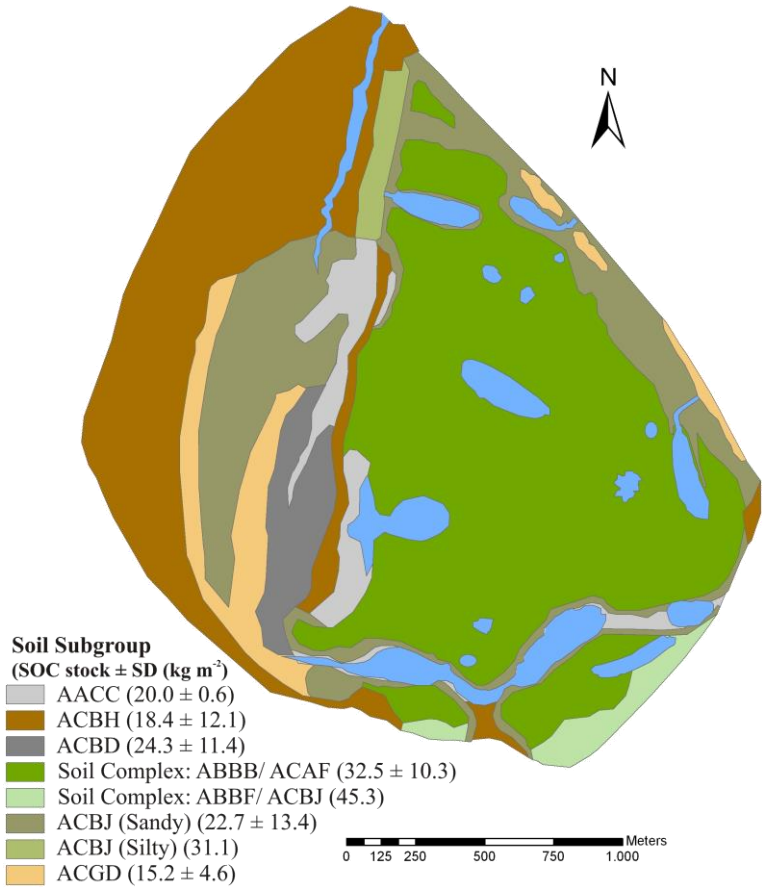

Figure 54: A soil map of Samoylov Island as a result of long-term soil research within this area. Generated from data by Pfeiffer *et al.* 2000 and Pfeiffer *et al.* 2002 (compare Sanders *et al.* 2010). Soil classification according to the US Soil Taxonomy (Soil Survey Staff 2010). Soil organic carbon stocks for the soil units down to 100 cm depth is provided in parentheses after each soil subgroup. AACC - *Fluvaquentic Fibristel*, ACBH - *Psammentic Aquorthel*, ACBD - *Ruptic-Histic Aquorthel*, Soil Complex: ABBB/ ACAF - *Glacic Aquiturbel/ Typic Historthel*, Soil Complex: ABBF/ ACBJ - *Typic Aquiturbel/ Typic Aquorthel*, ACBJ - *Typic Aquorthel*, ACGD - *Typic Psammorthel*.

Fig. 54: Die Bodenkarte der Insel Samoylov als Ergebnis langjähriger Bodenforschung innerhalb dieser Region. Erzeugt aus Daten von Pfeiffer *et al.* 2000 and Pfeiffer *et al.* 2002 (vergleiche Sanders *et al.* 2010). Die Bodenklassifizierung gemäß der US Soil Taxonomy (Soil Survey Staff 2010). Die Pools an bodeneigenem organischen Kohlenstoff der Bodeneinheiten bis in die Tiefe von 100 cm sind in Klammern angegeben. AACC - *Fluvaquentic Fibristel*, ACBH - *Psammentic Aquorthel*, ACBD - *Ruptic-Histic Aquorthel*, Soil Complex: ABBB/ ACAF - *Glacic Aquiturbel/ Typic Historthel*, Soil Complex: ABBF/ ACBJ - *Typic Aquiturbel/ Typic Aquorthel*, ACBJ - *Typic Aquorthel*, ACGD - *Typic Psammorthel*.

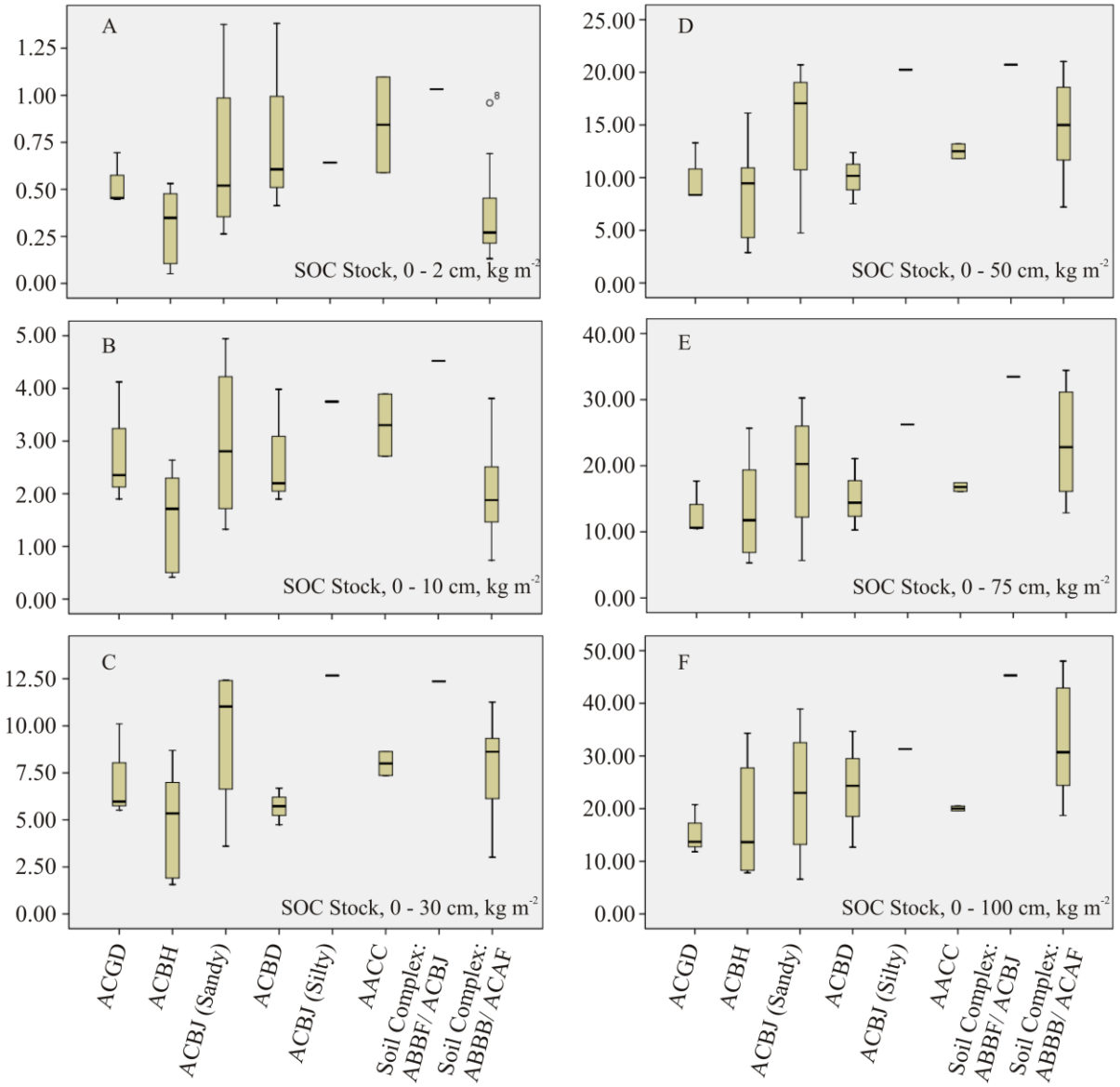

Figure 55: SOC stocks (kg m^{-2}) of the soil subgroups identified on Samoylov Island according to the US Soil Taxonomy (Soil Survey Staff 2010). A: 0...2 cm; B: 0...10 cm; C: 0...30 cm; D: 0...50 cm; E: 0...75 cm; F: 0...100 cm. Note different scale for y-axis on all graphs.

Fig. 55: Der Pool an SOC (kg m^{-2}) der auf der Insel Samoylov identifizierten Bodeneinheiten gemäß der US Soil Taxonomy (Soil Survey Staff 2010). A: 0...2 cm; B: 0...10 cm; C: 0...30 cm; D: 0...50 cm; E: 0...75 cm; F: 0...100 cm. Bitte die unterschiedliche Skalierung der y-Achse beachten.

4.4.5 Nitrogen stocks

For the description of the nitrogen (N) stocks the author used the same set up as it is mentioned in the SOC stock result section (4.4.2). The N stock of the investigation area and the depth of 100 cm varied between 0.41 kg m^{-2} and 1.94 kg m^{-2}. The mean N stock amounted to 1.10 kg m^{-2} ± 0.39 kg m^{-2} (Tab. 8A). Regarding the two different investigated geomorphic units, the Holocene river terrace and the active floodplain levels, the mean N stocks were 1.18 kg m^{-2} ± 0.36 kg m^{-2} and 0.88 kg m^{-2} ± 0.40 kg m^{-2}, respectively. The distinctly higher total N stock of the Holocene river terrace had a different vertical distribution. While the active floodplain stored about 35 % of the entire estimated N stock within the seasonally thawed active layer (depth 0...30 cm), only 25 % of the N stock of the Holocene river terrace was determined in the seasonally thawed active layer (Tab. 8B, C). The polygon centres had higher S_N(100 cm) (1.26 kg m^{-2} ± 0.35 kg m^{-2}) than the rims (0.96 kg m^{-2} ± 0.31 kg m^{-2}). The rim soils stored about 33 % of their S_N(100 cm) within the seasonally thawed active layer, whereas only 24 % were stored in this layer at the polygon centre soils (Tab. 8D, E).

Table 8: The nitrogen stocks of (A) the entire investigation area, (B) the Holocene river terrace, (C) the active floodplain, (D) the polygonal centres, and (E) the polygonal rims. The results are expressed in kg m^{-2} with the mean values and the respective standard deviations as well as the minima and maxima.

Tab. 8: Die Stickstoffpools (A) im gesamten Untersuchungsgebiet, (B) in der Holozänen Flussterrasse, (C) in der aktiven Überflutungsebene, (D) in den Polgonzentren und (E) in den Polygonwällen. Die Ergebnisse sind in kg m^{-2} als Mittelwerte dargestellt mit den entsprechenden Standardabweichungen so wie den Minima und den Maxima.

	A				B				C			
Soil depth [cm]	**Mean** [kg m^{-2}]	**SD**	**Min.** [kg m^{-2}]	**Max.** [kg m^{-2}]	**Mean** [kg m^{-2}]	**SD**	**Min.** [kg m^{-2}]	**Max.** [kg m^{-2}]	**Mean** [kg m^{-2}]	**SD**	**Min.** [kg m^{-2}]	**Max.** [kg m^{-2}]
0…2	0.02	0.01	0.00	0.05	0.02	0.01	0.00	0.05	0.02	0.01	0.00	0.03
0…10	0.09	0.05	0.01	0.23	0.09	0.05	0.01	0.23	0.10	0.05	0.02	0.15
0…30	0.31	0.15	0.06	0.76	0.31	0.16	0.06	0.76	0.30	0.15	0.08	0.49
0…50	0.54	0.23	0.15	1.23	0.57	0.23	0.16	1.23	0.47	0.21	0.15	0.74
0…75	0.81	0.30	0.24	1.62	0.86	0.30	0.24	1.62	0.68	0.29	0.32	1.17
0…100	1.10	0.39	0.41	1.94	1.18	0.36	0.41	1.94	0.88	0.40	0.49	1.65

	D				E			
Soil depth [cm]	**Mean** [kg m^{-2}]	**SD**	**Min.** [kg m^{-2}]	**Max.** [kg m^{-2}]	**Mean** [kg m^{-2}]	**SD**	**Min.** [kg m^{-2}]	**Max.** [kg m^{-2}]
0…2	0.02	0.01	0.00	0.05	0.02	0.01	0.00	0.03
0…10	0.08	0.06	0.03	0.23	0.09	0.04	0.01	0.13
0…30	0.30	0.16	0.10	0.76	0.33	0.17	0.06	0.57
0…50	0.57	0.24	0.24	1.23	0.55	0.24	0.16	0.87
0…75	0.90	0.30	0.45	1.62	0.74	0.28	0.24	0.99
0…100	1.26	0.35	0.78	1.94	0.96	0.31	0.41	1.26

The S_N(100 cm) for the soil subgroup-related analyses showed means between 0.85 kg m^{-2} ± 0.31 kg m^{-2} and 1.94 kg m^{-2} for the specific soil subgroups. High S_N(100 cm) was found in the two soil complexes of *Aquiturbels* and *Historthels* that dominated Samoylov Island (Tab. 9).

Table 9: The nitrogen stocks of the soil subgroups of Samoylov Island. (A) *Typic Psammorthel*, (B) *Psammentic Aquorthel*, (C) *Typic Aquorthel* Sandy, (D) *Ruptic-Histic Aquorthel*, (E) Soil Complex: *Glacic Aquiturbel*/*Typic Historthel*, (F) *Fluvaquentic Fibristel*, (G) *Typic Aquorthel* Silty, and (H) Soil Complex: *Typic Aquiturbel*/*Typic Historthel*. The results are expressed in kg m^{-2} with the mean values and the respective standard deviations as well as the minima and maxima.

Tab. 9: Die Stickstoffpools in den Bodenuntergruppen der Insel Samoylov. (A) *Typic Psammorthel*, (B) *Psammentic Aquorthel*, (C) *Typic Aquorthel* Sandy, (D) *Ruptic-Histic Aquorthel*, (E) Soil Complex: *Glacic Aquiturbel*/*Typic Historthel*, (F) *Fluvaquentic Fibristel*, (G) *Typic Aquorthel* Silty, and (H) Soil Complex: *Typic Aquiturbel*/*Typic Historthel*. Die Ergebnisse sind in kg m^{-2} als Mittelwerte dargestellt mit den entsprechenden Standardabweichungen so wie den Minima und den Maxima.

	A				B				C			
Soil depth [cm]	**Mean** [kg m^{-2}]	**SD**	**Min.** [kg m^{-2}]	**Max.** [kg m^{-2}]	**Mean** [kg m^{-2}]	**SD**	**Min.** [kg m^{-2}]	**Max.** [kg m^{-2}]	**Mean** [kg m^{-2}]	**SD**	**Min.** [kg m^{-2}]	**Max.** [kg m^{-2}]
0…2	0.02	0.01	0.01	0.03	0.01	0.01	0.00	0.02	0.02	0.01	0.01	0.02
0…10	0.13	0.03	0.09	0.15	0.06	0.04	0.02	0.12	0.09	0.03	0.05	0.13
0…30	0.39	0.00	0.38	0.39	0.21	0.13	0.08	0.35	0.37	0.14	0.24	0.57
0…50	0.57	0.02	0.55	0.60	0.39	0.20	0.15	0.65	0.60	0.23	0.32	0.87
0…75	0.77	0.06	0.71	0.82	0.63	0.30	0.32	1.11	0.80	0.27	0.41	0.98
0…100	0.95	0.11	0.82	1.02	0.86	0.40	0.51	1.53	0.99	0.34	0.49	1.25

	D				E				F		
Soil depth [cm]	**Mean** [kg m^{-2}]	**SD**	**Min.** [kg m^{-2}]	**Max.** [kg m^{-2}]	**Mean** [kg m^{-2}]	**SD**	**Min.** [kg m^{-2}]	**Max.** [kg m^{-2}]	**Mean** [kg m^{-2}]	**Min.** [kg m^{-2}]	**Max.** [kg m^{-2}]
0…2	0.01	0.01	0.01	0.03	0.01	0.01	0.00	0.04	0.02	0.02	0.02
0…10	0.08	0.03	0.04	0.10	0.10	0.05	0.01	0.15	0.10	0.09	0.12
0…30	0.22	0.09	0.12	0.28	0.26	0.13	0.06	0.49	0.35	0.32	0.39
0…50	0.40	0.14	0.24	0.50	0.52	0.20	0.16	0.74	0.65	0.61	0.68
0…75	0.61	0.15	0.44	0.70	0.85	0.31	0.24	1.17	0.93	0.88	0.99
0…100	0.94	0.17	0.83	1.14	1.23	0.42	0.41	1.68	1.18	1.09	1.26

G		H	
Soil depth [cm]	**N pool** [kg m^{-2}]	**Soil depth** [cm]	**N pool** [kg m^{-2}]
0…2	0.04	0…2	0.05
0…10	0.23	0…10	0.18
0…30	0.76	0…30	0.44
0…50	1.23	0…50	0.72
0…75	1.62	0…75	1.11
0…100	1.94	0…100	1.47

Regarding the vertical distribution of the nitrogen contents, high differences emerged among the various soil subgroups. On average, 50 % of the S_N(100 cm) was stored within the upper 50 cm of soil indicating a homogenous distribution over soil depth. In the soil complex of *Glacic Aquiturbels* and *Typic Historthels*, only 42 % was stored within this layer, whereas 63 % of the S_N(100 cm) was found in the upper 50 cm of the *Typic Aquorthel* silty (Tab. 9A, E).

4.4.6 Classifications and upscaling

Based on the Landsat-7 ETM+ satellite image mosaic (Fig. 56A), the results of the supervised classification confirmed previously reported ratios of the water- and land-covered areas in the Lena River Delta (Fig. 56B) of approximately 31 % and 69 %, respectively (Schneider *et al.* 2009). The area covered by water bodies amounted to around 10,000 km^2. Furthermore, the results indicated that the geomorphic unit dominating the Lena River Delta are the active

floodplain levels occupying about 8,830 km² (Fig. 56C). This area represents approximately 40 % of the soil-covered area of the Lena River Delta. The investigated Holocene river terrace (1st terrace) (Fig. 56C) occupies 4,760 km² which represents around 22 % of the soil-covered area of the Lena River Delta. According to Morgenstern *et al*. (2008) the other geomorphic parts of the Lena River Delta account to 6,099 km² (2nd terrace) and 1,712 km² (3rd terrace). The overall accuracy of the performed classification aiming at separating the Holocene river terrace and the active floodplain was 77 %, with a producer accuracy of 78 % and a user accuracy of 78 % (Tab. 10). This accuracy is on the same level as a previous Landsat-based land cover classification in the Lena Delta using the same image mosaic that focused on classes useful for methane emission assessment (Schneider *et al*. 2009; overall accuracy of 78 %). In this classification, part of the mix-up between water and non-water classes may be related to the different acquisition dates of the imagery that may result in somewhat different water levels and hence exposure or inundation of surfaces especially for the active floodplain.

Table 10: Accuracy assessment of Landsat-based geomorphic land unit classification for the Holocene terrace, the active floodplain, and water, using high-resolution WorldView-1 data.

Tab. 10: Präzisionsprüfung der Landsat-basierten Klassifikation der geomorphologischen Einheiten: Holozäne Flussterrasse, active Überflutungsebenen und Wasser unter Zuhilfenahme von hoch aufgelösten WorldView-1 Daten.

Landsat-7 / WorldView-1	Active floodplains	Holocene terrace	Water	Other*	Total	User's accuracy
Active floodplains	42	8	5	0	55	76.4
Holocene terrace	10	33	2	0	45	73.3
Water	6	1	41	0	48	85.4
Other*	2	0	0	0	2	0
Total	60	42	48	0	150	
Producer's accuracy	70.0	78.6	85.4	0		77.3

*Other includes coastal beach and a drained lake basin on the 2nd geomorphic delta terrace.

After correcting for the spatial coverage of small ponds in the polygonal tundra of the Holocene river terrace, the soil covered land area of the river terrace, which was used for later calculations and upscaling, amounted to 4,090 km².

The results of the upscaling (Fig. 56D) indicate a continuous increase of the soil organic carbon pool estimates with increasing reference soil depths. The surface soil layers ranging from 0…2 cm store a total soil organic carbon mass of 2.4 Tg ± 1.5 Tg on the Holocene river terrace and 3.0 Tg ± 2.0 Tg on the active floodplain, respectively. The author estimated for the reference depth of 50 cm a soil organic carbon pool of 59.9 Tg ± 18.5 Tg for the river terrace and 67.2 Tg ± 34.0 Tg for the floodplains (Tab. 11). This depth is approximately the average depth of the seasonally thawed active layer in the summer.

Table 11: The depth distributions of the total soil organic carbon mass within the seasonally thawed and perennially frozen soil for the Holocene river terrace and the active floodplain levels in the Lena River Delta. Represented are the mean calculated soil organic carbon stocks (kg m^{-2}) and the estimated mean soil organic carbon mass (Tg) for all investigated soil horizons with the respective standard deviations.

Tab. 11: Die Tiefenverteilung der Gesamtmasse des bodeneigenen organischen Kohlenstoffs im Auftauboden und innerhalb des Permafrostes der Holozänen Flussterrasse und der aktiven Überflutungsebene im Lenadelta. Dargestellt sind die kalkulierten Gehalte des organischen Kohlenstoffs (kg m^{-2}) und geschätzten Mittelwerte der Masse an SOC (Tg) für alle untersuchten Bodenhorizonte mit ihren Standardabweichungen.

		Holocene River Terrace area: 4,090 km^2			**Active Floodplain Levels** area: 8,830 km^2		
Soil depth (cm)		**Stock** (kg m^{-2}) ± **SD**	**Mass** (Tg)	**SD**	**Stock** (kg m^{-2}) ± **SD**	**Mass** (Tg)	**SD**
0...2	seasonally thawed soil	0.6 ± 0.4	2.41	1.50	0.3 ± 0.2	2.99	1.96
0...10		2.7 ± 1.1	10.93	4.61	1.9 ± 1.3	16.57	11.39
0...30		8.4 ± 2.8	34.56	11.59	5.2 ± 3.0	45.64	26.76
0...50		14.6 ± 4.5	59.91	18.50	7.6 ± 3.8	67.17	33.99
0...75	perma-frost	21.9 ± 7.4	89.76	30.33	10.7 ± 5.5	94.34	48.17
0...100		29.5 ± 10.5	120.66	42.96	13.6 ± 7.4	119.83	65.63

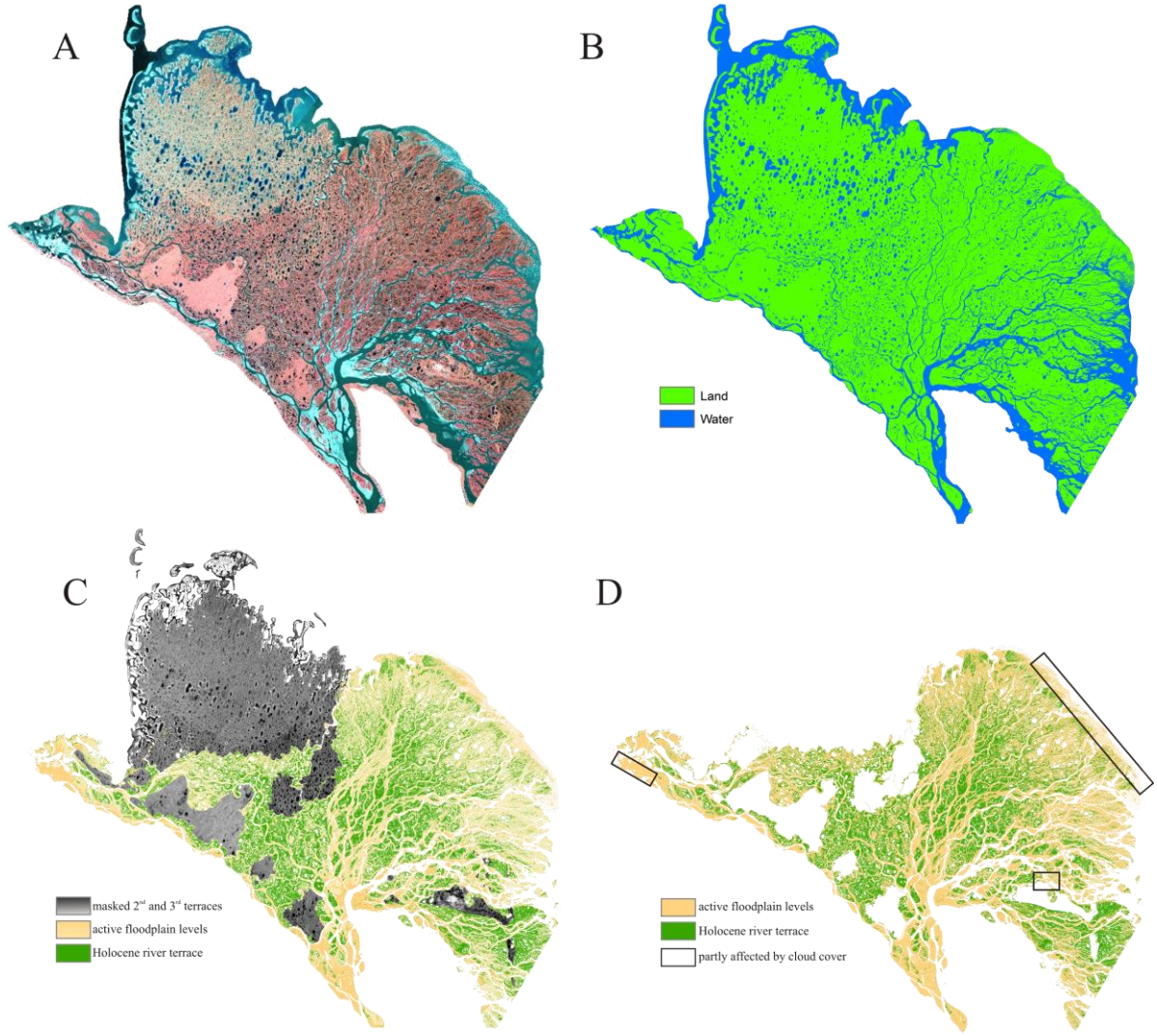

Figure 56: Landsat-7 ETM+ remote sensing image mosaic of the Lena River Delta from 27 July 2000 and 26 July 2001 (A), results of land-water classification (B), results of classification into main geomorphic terraces (C), and upscaling of SOC stocks to Holocene river terrace and active floodplain levels (D).

Fig. 56: Landsat-7 ETM+ Fernerkundungsbildmosaik des Lenadeltas vom 27. Juli 2000 und 26. Juli 2001 (A), das Ergebnis der Land-Wasser-Klassifikation (B), das Ergebnis der Klassifikation nach den geomorphologischen Hauptterrassen (C) und die Hochskalierung des SOC Pools auf die Holozäne Flussterrasse und die aktive Überflutungsebene (D).

The total pools of the soil organic carbon stored within a depth of 100 cm were estimated at 120.7 Tg ± 43.0 Tg on the Holocene river terrace and at 119.8 Tg ± 65.6 Tg on the active floodplains of the Lena River Delta. Roughly 47 % of the soil organic carbon mass stored

within the top 100 cm of soils in the investigation area, specifically about 61 Tg at the Holocene river terrace and 53 Tg at the floodplains, are located within the currently perennially frozen layers deeper than 50 cm.

The nitrogen stored within the top 100 cm of soils was estimated at 4.8 Tg ± 1.5 Tg for the Holocene river terrace and at 7.7 Tg ± 3.6 Tg on the active floodplains of the Lena River Delta. About 49 % of this nitrogen pool within the top 100 cm of soils was found within the currently perennially frozen layers. This proportion was 52 % on the Holocene river terrace, and 47 % on the active floodplains (Tab. 12).

Table 12: The depth distributions of the total nitrogen mass within the seasonally thawed and perennially frozen soil for the Holocene river terrace and the active floodplain levels in the Lena River Delta. Represented are the mean calculated nitrogen stocks (kg m^{-2}) and estimated mean nitrogen mass (Tg) for all investigated soil horizons with the respective standard deviations.

Tab. 12: Die Tiefenverteilung der Gesamtmasse des Gesamtstickstoffs im Auftauboden und innerhalb des Permafrostes der Holozänen Flussterrasse und der aktiven Überflutungsebene im Lenadelta. Dargestellt sind die kalkulierten Gehalte des organischen Kohlenstoffs (kg m^{-2}) und geschätzten Mittelwerte der Masse an SOC (Tg) für alle untersuchten Bodenhorizonte mit ihren Standardabweichungen.

		Holocene River Terrace area: 4,090 km^2			**Active Floodplain Levels** area: 8,830 km^2		
Soil depth (cm)		**Stock** (kg m^{-2}) ± **SD**	**Mass** (Tg)	**SD**	**Stock** (kg m^{-2}) ± **SD**	**Mass** (Tg)	**SD**
0...2	seasonally thawed soil	0.02 ± 0.01	0.07	0.05	0.02 ± 0.01	0.14	0.08
0...10		0.1 ± 0.1	0.35	0.22	0.1 ± 0.1	0.87	0.48
0...30		0.3 ± 0.2	1.26	0.64	0.3 ± 0.1	2.66	1.32
0...50		0.6 ± 0.2	2.31	0.95	0.5 ± 0.2	4.12	1.81
0...75	perma-frost	0.9 ± 0.3	3.51	1.22	0.7 ± 0.3	5.96	2.54
0...100		1.2 ± 0.4	4.81	1.47	0.9 ± 0.4	7.73	3.55

4.5 Discussion

4.5.1 Soil organic carbon pools on the Holocene river terrace and the active floodplains

The mean S_{OC}(100 cm) estimate for the soils of the Holocene river terrace amounts to 29.5 kg m^{-2} and is distinctly higher than some older published estimates of mean organic carbon stocks stored in permafrost-affected tundra soils. Post *et al.* (1982) estimated the average soil organic carbon stock in tundra soils worldwide at 21.8 kg m^{-2}. Kolchugina *et al.* (1995) provided an estimate of 21.4 kg m^{-2} for Russian tundra soils, whereas Matsuura and Yefremov (1995) estimated the soil organic carbon stock in Russian permafrost-affected soils to be between 11 kg m^{-2} and 20 kg m^{-2}. Chestnyck *et al.* (1999) estimated the soil organic carbon stock in East European Russian tundra soil at 17.8 kg m^{-2}. More recent publications, however, provided higher stocks for tundra soils. Gundelwein *et al.* (2007) estimated the soil organic carbon stock in tundra soils of the Taymyr Peninsula at 30.7 kg m^{-2}. For the North American Arctic lowlands, Ping *et al.* (2008) reported soil organic carbon stocks of 25.9 kg m^{-2}. Tarnocai *et al.* (2009) estimated at the organic carbon stocks in *Turbels* and *Orthels* of the circumpolar permafrost at 32.2 kg m^{-2} and 22.6 kg m^{-2}, respectively. Hugelius and Kuhry (2009) estimated the stocks in north-eastern European Russian tundra soils at 38.7 kg m^{-2}. Only Stolbovoi *et al.* (2006) reported a lower stock estimate of 16.6 kg m^{-2} for Russian tundra soils. Ping *et al.* (2011) found a stock of 41 kg m^{-2} in river deltas along the Alaska Beaufort Sea coastline. The estimate provided here for the Holocene river terrace representing the tundra soils (29.5 kg m^{-2}) lies in the range of the more recently reported estimates. The estimate for soils of the active floodplains of 13.6 kg m^{-2} cannot readily be compared with general estimates for tundra regions. Due to their fluvial origin and episodic reworking, the soils of the Lena River Delta floodplains consist of stratified middle to fine sands and silts with layers of allochthonous organic matter as well as autochthonous peat (Boike *et al.* 2012). The regular flooding events enable only sparse vegetation. However, the presented estimate is still notably higher than the mean C stock of sparse tundra (1.4 kg m^{-2}) in the database used by Hugelius and Kuhry (2009), whereas it is also distinctly lower than the C stock the same authors reported for tundra lake sediments (17.5 kg m^{-2}). Hugelius *et al.* (2011) reported a soil organic carbon stock for the sediments of the Rogovaya River in north-

eastern European Russia of 11.7 kg m^{-2} which is very close to the estimate presented for the soils of the active floodplain strongly affected by active fluvial sedimentation by the Lena River.

Generally, the considerable differences in the discussed stocks of soil organic carbon originate in the strong spatial variability of soils on multiple scales. On the one hand, difficult access to remote permafrost-affected areas leads to an inhomogeneous distribution of investigation sites. On the other hand, large spatial heterogeneity within the same biome results in wide ranges and uncertainties, as well as questions of representativeness, of stock estimates and demonstrates the importance of intensive field work to produce more robust stock estimates and more representative data coverage.

4.5.2 Soil organic carbon storage in the patterned ground and the soil subgroups

The estimates for the two characteristic microforms of the polygonal landscape, the polygon centres and polygon rims demonstrated a high micro-scale variability of the soil organic carbon stock within the investigated area. The mean soil organic carbon stocks were 33.3 kg m^{-2} ± 9.7 kg m^{-2} and 19.4 kg m^{-2} ± 3.7 kg m^{-2} for polygon centres and rims, respectively. Polygons within the investigated area are about 15 m wide.

Analyzing the soil organic carbon stock on the soil subgroup level provided stock estimates ranging from 15.2 kg m^{-2} ± 4.6 kg m^{-2} to 32.7 kg m^{-2} ± 10.4 kg m^{-2}. The author therefore suggests that not only the soil organic carbon heterogeneity on the tundra biome scale needs to be captured in upscaling studies but that more detailed field work is necessary to characterize site-scale soil organic carbon stock variations and how these may be successfully translated in upscaling approaches.

4.5.3 Vertical distribution of the soil organic carbon storage within the soil

Vertical distribution of carbon contents considerably differed between the two investigated geomorphic units. The volumetric organic carbon contents in the soils of the Holocene river

terrace were rather uniformly distributed over the profiles' depths whereas volumetric carbon contents in the soils of the floodplains was clearly highest in the uppermost 10 cm from the soil surface. This latter pattern probably is caused by the ongoing regular flooding events of the plains. High intensity of flooding and high current of water of flat plains will not allow plants to grow resulting in low volumetric organic carbon contents in higher profile depth. When a certain elevation of the floodplains is reached caused by regular sedimentation, the intensity of flooding and current of water will decrease and therefore plants will be able to establish. This sparse vegetation at the elevated floodplains is only flooded periodically. As a consequence of these flooding events, the vegetation is covered by a fresh sediment layer which hinders the continuation of plant growth. These sediment layers are then populated by a new generation of plants and incorporate the prior canopy as peat into the top soil horizons resulting in high contents of carbon in the upper parts of soil horizons.

4.5.4 Permafrost soil organic carbon storage

The author assigned estimated soil organic carbon stock data to the landscape units of Samoylov Island, averaged them by land unit and estimated the soil organic carbon pool size within the respective geomorphic unit for the whole Lena River Delta by multiplying with the area of the corresponding unit derived from the land surface classification, particularly the areas of the Holocene river terrace and the active floodplains derived from the satellite image classification. The presented estimates indicate that the Lena River Delta contains in total 241 Tg of soil organic carbon in the upper 1 m of soils within its river terrace and active floodplains. The soil organic carbon stock of the area-dominating active floodplains levels is 120 Tg ± 66 Tg. Despite covering only about half as much area as the active floodplains, soils of the Holocene river terrace have a similar sized total soil organic carbon stock of 121 Tg ± 43 Tg. About one half of the estimated soil organic carbon stock of these two morphological units (127 Tg) occurs in the depth 0...50 cm which is the observed seasonal thaw depth in late summer. This carbon is presumably highly vulnerable to decomposition and mineralization processes resulting in trace gas release to the atmosphere (Dutta *et al.* 2006, Wagner *et al.* 2007, Khvorostyanov *et al.* 2008, Schuur *et al.* 2009, Grosse *et al.* 2011). However, first

results by Höfle *et al.* (2012) indicate that physical protection mechanisms may also limit soil organic carbon decomposition in the active layer.

The other portion of 113 Tg soil organic carbon (ca. 47 %) in the depth from 50...100 cm is currently excluded from intense soil-atmosphere exchange processes in the perennially frozen ground. Permafrost degradation resulting from higher temperatures and changed precipitation patterns leading to a deepening of the seasonally thaw depth are projected by global climate-permafrost models (Sazonova *et al.* 2004, Koven *et al.* 2011). This organic matter which is highly vulnerable to decay (Schuur *et al.* 2008) has so far not undergone significant changes. It is likely to undergo the same biogeochemical processes and to react like the young and relatively fresh organic matter pools from the recent active layer (Waldrop *et al.* 2010). An enhanced mineralisation of this soil organic matter will likely increase the trace gas release to the atmosphere due to its high inherent decomposability (Waldrop *et al.* 2010). It is expected that portions of the near-surface permafrost will disappear by the end of this century (Lawrence *et al.* 2008). For large areas of the Lena River Delta the thickness of the seasonally thawed layer is expected to increase to 120 cm and for some areas even to 180 cm by the end of this century (Sazonova *et al.* 2004).

Tarnocai *et al.* (2009) provide an estimate for soil organic carbon storage in permafrost-affected river deltas. The total of 241 Pg for seven arctic river deltas is based on extrapolation of soil organic carbon stocks from a limited number of samples from the Mackenzie River Delta (5 soil profiles with an average carbon pool of 65 kg m^{-2}) using an estimated average thickness of 50 m for these deposits. For the Lena River Delta, Tarnocai *et al.* (2009) calculate a pool of 131 Pg soil organic carbon (down to 50 m depth). Comparison is difficult, since the presented soil carbon stock data can be attributed to only 43 % of the soil-covered delta, while other portions are not yet quantified (second and third geomorphic terrace, river channels and lakes, small ponds on the Holocene terrace) and may significantly differ from the stocks of the Holocene terrace and the active floodplain. As an extrapolation example, the author used (1) the average carbon stock of 29.5 kg m^{-2} for the Holocene river terrace and 13.6 kg m^{-2} for the active floodplains, and (2) the average carbon stock of 25.7 kg m^{-2}. Applying the set up (thickness and area) used by Tarnocai *et al.* (2009) (1) the carbon storage would amount to 37.76 Pg ± 16.96 Pg or (2) to 51.93 Pg ± 24.25 Pg for the entire Lena River

Delta area. These distinct lower modelled carbon storages result from the here estimated lower carbon pools for the investigated areas.

4.5.5 Nitrogen stocks and nitrogen storage

The mean nitrogen stock estimate for the investigation area and the depth of 100 cm S_N(100 cm) amounted to 1.1 kg m^{-2} or to 0.9 kg m^{-2} and 1.2 kg m^{-2}, respectively, when the active floodplains and the river terrace are separately regarded. Jonasson *et al.* (1999) reported a nitrogen stock for arctic Scandinavian heath of 0.115 kg m^{-2} and a depth of 15 cm, which theoretically can be recalculated for 100 cm depth amounting to 0.8 kg m^{-2}. For the eroding Alaska Beaufort Sea coastline, Ping *et al.* (2011) reported an average total nitrogen storage of 1.4 kg m^{-2}. The nitrogen stocks published by Harden *et al.* (2012) for 300 cm deep soil profiles of Gelisols were 4.6 kg m^{-2}...7.5 kg m^{-2}. Assuming a homogeneous vertical nitrogen stock distribution, the S_N(100 cm) can be estimated at 1.5 kg m^{-2}...2.5 kg m^{-2} which is distinctly higher than the estimates of S_N(100 cm) in the Lena River Delta. The S_N(100 cm) found in this study was in the range of the stock estimates of Jonasson *et al.* (1999) and Ping *et al.* (2011).

The estimates indicate that the Lena River Delta contains 12.5 Tg of nitrogen in the upper 1 m of soils within its Holocene river terrace and the active floodplain levels – reflecting a C/N ratio of about 20 (compare Tab. 7). About 49 % of this nitrogen pool is not available as plant nutrient due to permanent fixation in the perennially frozen ground.

An increased deepening of the seasonally thawed layer (Sazonova *et al.* 2004, Koven *et al.* 2011) is likely to release this frozen storage of nitrogen. As a plant nutrient, this additionally released nitrogen is likely to enhance the net primary production of existing vegetation by reducing the general nitrogen limitation of tundra plant communities (Shaver *et al.* 1986, Schimel *et al.* 1996, Weintraub and Schimel 2003) or triggering a general change of species composition.

4.6 Conclusions

The Lena River Delta, the largest arctic delta extends over an area of 32,000 km². The author investigated soil organic carbon stocks of the Holocene river terrace and the active floodplain levels. Both together are the dominating geomorphic units in the Lena River Delta by area (62% of the soil-covered area). The mean soil organic carbon stocks in the Holocene river terrace and the active floodplain are estimated at 29.5 kg m^{-2} and at 13.6 kg m^{-2}, respectively. The Holocene river terrace stores about 50 % of the estimated soil organic carbon stock while occupying 32 % of the investigated portion of the Lena River Delta. About 127 Tg of the estimated soil organic carbon mass of the river terrace and the active floodplains are stored in the seasonally thawed layer (0...50 cm depth). The soil organic carbon stock stored in permafrost (50...100 cm) and currently excluded from intense biogeochemical exchange with the atmosphere accounts for 113 Tg. Taking into account the projections for deepening of the seasonally thawed active layer and general degradation of permafrost over this century, this large stock is likely to become increasingly available for decomposition and mineralization processes as well as fluvial retransportation and offshore / onshore deposition in future. With this study, the author showed that the soil organic carbon stock in the Lena River Delta is high compared to average values reported for the tundra. However, the stocks are not as high as reported from 5 soil profiles for the Mackenzie River Delta that were used to extrapolate carbon storage in permafrost affected river deltas (Tarnocai *et al.* 2009), indicating that the total carbon storage in permafrost and the seasonally thawed layer of Arctic river deltas is lower than previously estimated, though still of substantial size. Here only the Holocene river terrace and active floodplain levels were investigated, and further correspondent investigations of the other geomorphic terraces that differ in cryostratigraphic composition and soils will be needed. In addition, the author provides a first estimate of the total nitrogen stocks in this arctic river delta for the two investigated geomorphic units - the Holocene river terrace and the active floodplain levels - and the nitrogen pool sizes for the soils up to 100 cm in the corresponding geomorphic units. He also reports the nitrogen stocks on soil subgroup level with their depth distribution. With a mean of 13 Tg, the nitrogen stocks are higher than would be expected by assuming a general C/N ratio of 30 (Jonasson *et al.* 1999, Weintraub and Schimel 2003) and considering the estimated soil organic carbon storage of 241 Tg.

Though not investigated in detail within the investigation area, this large nitrogen pool deserves more consideration in future, particularly with regard to stocks of ammonium, nitrate and dissolved organic nitrogen.

5. Soil Organic Carbon in the Active Layer in Soils from a Latitudinal Transect

Pilot Study: Soil Organic Carbon in the Active Layer in Soils from a Latitudinal Transect - Variability of Soil Organic Carbon Stocks of Different Permafrost-Affected Soils: Initial Results from a North-South Transect in Siberia.

5.1 Introduction

According to climate change projections for the Arctic, organic carbon deposits in permafrost regions are likely to become a future source of atmospheric carbon because increased active-layer depths and changed hydrological conditions (Koven *et al.* 2011) will lead to increased carbon dioxide and methane release from permafrost-affected soils (Dutta *et al.* 2006, Wagner *et al.* 2007, Khvorostyanov *et al.* 2008, Schuur *et al.* 2009). Estimates of the carbon pool of permafrost-affected soils account for between 15 to 50 % of the global soil organic carbon pool (Post *et al.* 1982, Zimov *et al.* 2006, Ping *et al.* 2008, Tarnocai *et al.* 2009, McGuire *et al.* 2009). These soils – principally Gelisols / Cryosols (with respect to either the US Soil Taxonomy by Soil Survey Staff (2010) or the WRB classification by the Food and Agriculture Organization (2006)) – cover 27 % of the terrestrial surface in the territories above 50° N (Jones *et al.* 2010). A significant amount of this carbon pool is presently frozen and currently excluded from intensive interactions with the atmospheric biogeochemical cycles.

Quantitative knowledge of the soil organic carbon pool is still poor, with particularly high uncertainties for cold regions of Russia (Tarnocai *et al.* 2009). During an expedition to Yakutia in August 2009, initial investigations of several soil pedons have been carried out along a north-south climatological gradient (Fig. 57) for a first description of permafrost-affected soils in this rarely investigated region of Siberia (Klemm and Zubrzycki 2009). This study included quantifying the soil organic carbon stock in the top 30 cm of the active layer ($S_{SOC\text{-}30}$) within different vegetation zones from arctic tundra in the North to northern taiga in the South. The northernmost site 10LD1 (Fig. 57) was investigated in 2010. The key objective of this paper is to report the size of top soil organic carbon stocks and to analyze their spatial

variability along a transect in a remote Northeast Siberian permafrost-affected region as a basis for more detailed investigations in the future.

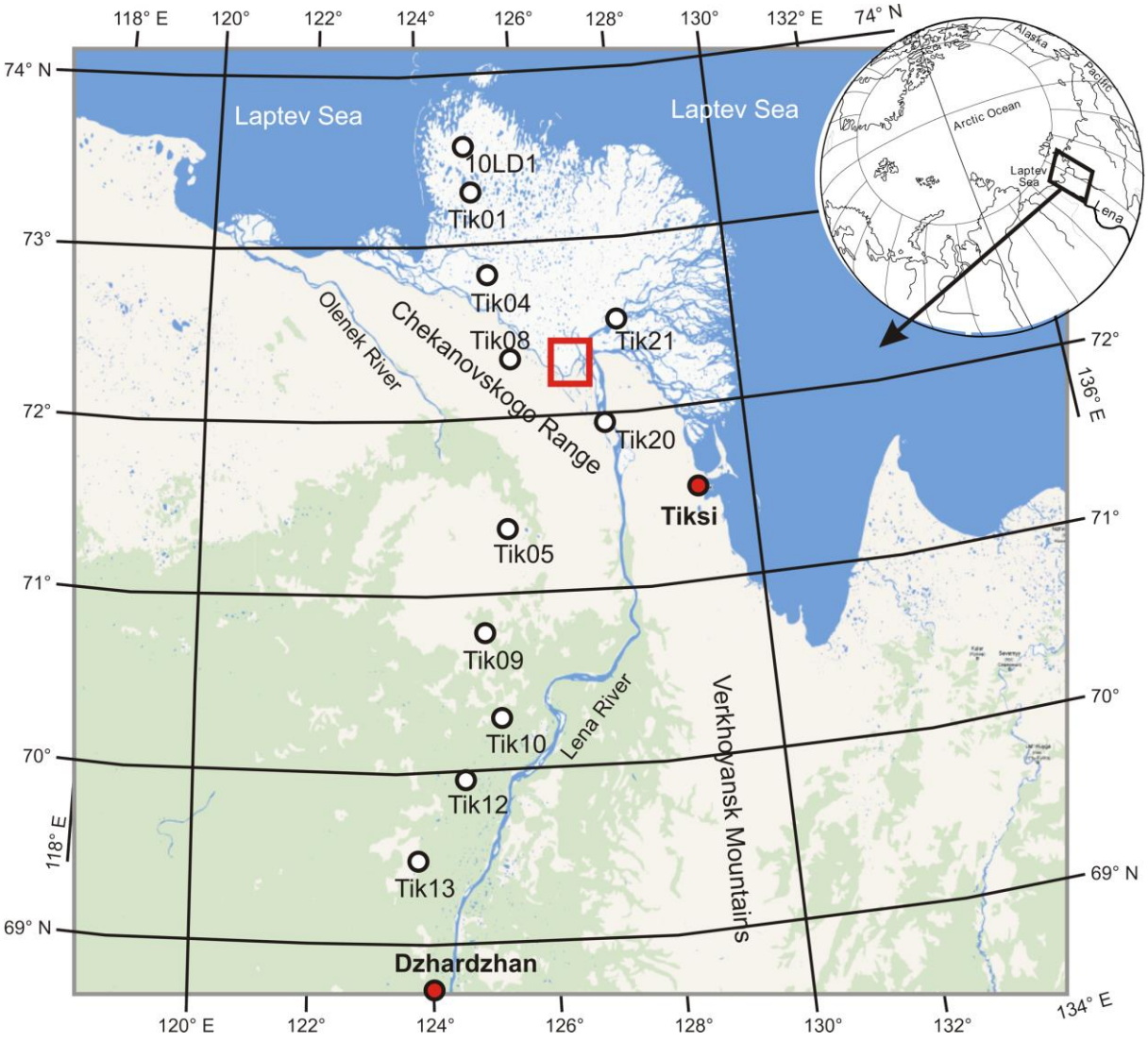

Figure 57: Map of the investigation area in north-east Siberia with locations of study sites. White: delta area (non-forested), yellow: non- forested non-delta area, green: forested non-delta area. Map based on Google & Geocentre Consulting 2011.

Fig. 57: Eine Karte der Untersuchungsregion im Nordosten Sibiriens mit den Lokationen der Arbeitsgebiete. Weiß: Delatgebiet (nicht bewaldet), gelb: nicht bewaldet und kein Deltagebiet, grün: bewaldet und kein Delzagebiet. Die Karte basiert auf Google & Geocentre Consulting 2011.

5.2 Investigation area

The study sites are located along a north-south transect (73.5°...69.5° N) on the western side of the Lena River (Fig. 57). These selected sites cover the main geomorpho-logical units of the investigated area along the transect. In the Lena River Delta, investigations were carried out on Arga Island in the north-west (73.5° N) (field IDs: 10LD1, Tik01, see Fig. 57), on Hardang-Sise Island in the west (Tik04), and in the central part of the delta on Samoylov Island (Tik22) and Sardakh Island (Tik21). One site was on Tit-Ari Island (Tik20), which is located in the main Lena River channel south-east of the Delta and is one of the northernmost places of the tree-limit line in the Russian Arctic. This transect was continued at the north slope of the Chekanovskogo Range where one site was located near to Lake Byluyng-Kyuel' (Tik08). The transect then followed the Lena River to the south (69.5° N) staying on the western side of both the river and the Verkhoyansk Mountains (Tik05, Tik09, Tik10, Tik12, Tik13).

Samoylov Island is a part of the Lena River Delta and consists of a relative young floodplain (0-4 m a.s.r.l. [above summer river level]) and a higher-elevated river terrace (up to 12 m a.s.r.l.) of Late Holocene age (Akhmadeeva *et al.* 1999). This higher-elevated part is termed first terrace (Pavlova and Dorozhkina 1999) and flooded only during extreme high water events (Schwamborn *et al.* 2002, Kutzbach 2006). Arga Island dominates the northwestern part of the Lena River Delta. Its deep deposits are older than 50 kyr (Schirrmeister *et al.* 2011b). This island, also referred to as second terrace, is fluvial sand-dominated (10-30 m a.s.r.l.). The areas of Hardang-Sise Island and Sardakh Island belong to the third river terrace complex (up to 55 m a.s.r.l.) of the Lena River Delta. The third terrace is the oldest terrace in the delta (Grigoriev 1993). It was formed in the Middle and Late Pleistocene (Schwamborn *et al.* 2002, Kuzmina *et al.* 2003). Generally, this terrace forms autonomous islands along the Olenyokskaya and Bykovskaya Channels. The Hardang-Sise Island with Lake Mutnoe is located at the eastern part of Olenyokskaya Channel. Sardakh Island represents a relic of the oldest terrace within the recent delta terrace and is located at the southern part of the Trofimovskaya Channel (Grigoriev 1993). The region surrounding the investigated El'gene-Kyuele Lake at the north slope of the Chekanovskogo Range belongs to the Eurasian landmass but represents a transition zone between the Lena River Delta and the

mainland. The landscape is characterized by rivers draining the mountain ridge and discharging to the northeast into the Olenyokskaya Channel. The remaining southern sites belong to the eastern part of the ancient plain Central Siberian Plateau and are characterized by a continuous change of vegetation type. Pronounced visible differences in vegetation cover can be observed around 70° N. This transitional zone, classified as forest tundra, contains a continuous change from tundra to northern taiga with more and more wooded patches up to densely wooded areas at the southernmost point at Sysy-Kyuele Lake (Tik13).

All investigation sites along the transect are dominated by an arctic-subarctic climate with continental influence and are characterized by low temperatures and low precipitation. The mean annual air temperatures, measured at the climate reference sites in Tiksi (71° 41' N, 128° 42' E) and Dzhardzhan (68° 49' N, 123° 59' E) were -13.5 °C and -12.4 °C, respectively, and the mean annual precipitation was 323 mm and 298 mm, respectively (Fig. 58). The average temperatures of the warmest months in Tiksi (August) and Dzhardzhan (June) were 7.1 °C and 14.9 °C, respectively (Roshydromet 2011, Russia's Weather Server 2013).

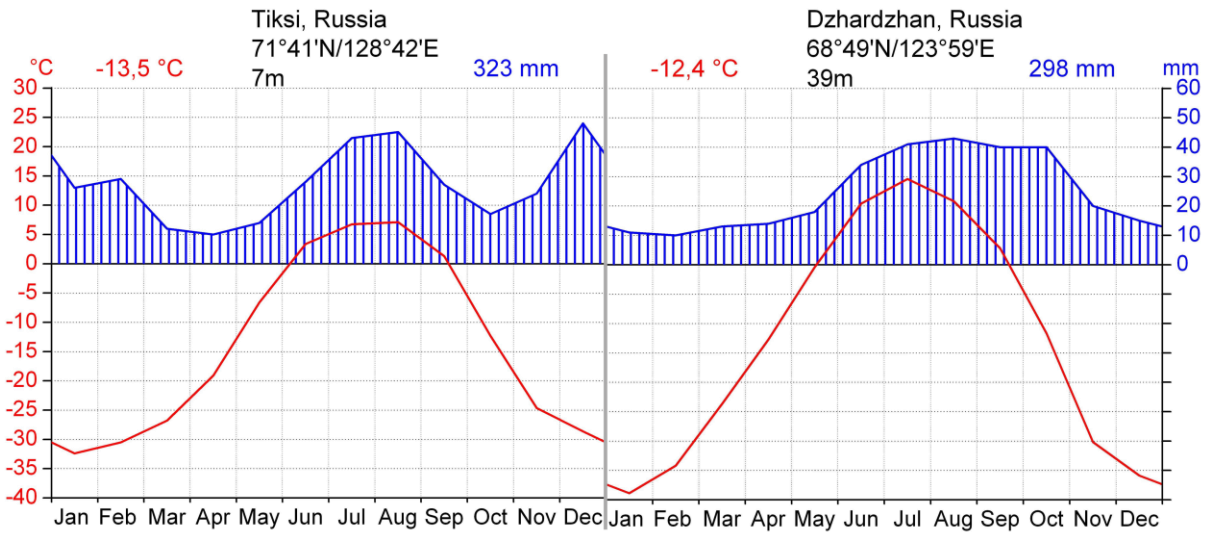

Figure 58: Climate charts for the climate reference sites in Tiksi and Dzardzhan. Based on data by Roshydromet (Tiksi: 1961...1990) and Russia's Weather Server (Dzhardzhan: 1998...2011).

Fig. 58: Klimadiagramme der Referenzstationen in Tiksi and Dzardzhan. Basierend auf Daten von Roshydromet (Tiksi: 1961...1990) und Russia's Weather Server (Dzhardzhan: 1998...2011).

The average temperature and precipitation of both reference climate stations are similar (Fig. 58), but the temperature amplitude is higher at the Dzhardzhan station. The strong continental climate enables longer and warmer summers in the south. This fact and the different precipitation patterns with more rain during the growing season favor more intensive development of soils and more productive vegetation in the south.

5.3 Materials and methods

All investigated soil subgroups were classified according to the US Soil Taxonomy (Soil Survey Staff 2010). Based on the classification system for permafrost soils of Yakutia by Elovskaya (1987), the author determined the soil subtypes for a comparison with Russian literature. Disturbed soil samples (in plastic bags) and undisturbed soil samples (in containers with a volume of 100 cm^3) were collected from each soil horizon down to the surface of frozen ground at the date of sampling. Pedological descriptions of the full soil pits including Munsell soil color, fresh weight, texture, fabric, organic substance, roots and hydromorphic features were performed manually in the field. In Germany, these soil samples were analyzed for acidity (pH) and electrical conductivity (CG820, Schott Geraete GmbH, Germany; Cond 330i, WTW, Germany), gravimetric contents of organic carbon (OC) and total nitrogen (N) (Vario MAX CNS, Elementar Analysesysteme GmbH, Germany), and texture of the <2 mm fraction (Sedimat 4-12, UGT, Germany). The bulk density (BD) was calculated as the ratio of the dry mass of an undisturbed soil sample and the volume of the soil sample container.

The soil organic carbon stock per horizon and area $S_{SOC\text{-}H}$ (kg m^{-2}) was calculated using the formula:

$$S_{SOC\text{-}H} = C \times BD \times d \quad (5)$$

where C is the gravimetric organic carbon content, BD is the bulk density, and d is the thickness of the soil horizon.

The top soil soil organic carbon stock $S_{SOC\text{-}30}$ (kg m^{-2}), defined as the organic carbon mass within the top 30 cm from the soil surface per area was calculated as:

$$S_{\text{SOC-30}} = \int_{0cm}^{30cm} C \times BD \; dh \tag{6}$$

where *h* is soil depth. A depth of 30 cm was the average thaw depth of the investigated sites. Thus, the $S_{\text{SOC-30}}$ can be considered as approximately representative for the soil organic carbon stock in the present-day active layer.

The author analyzed the $S_{\text{SOC-H}}$ of all single horizon types (Eq. 6) and then calculated their contribution to the $S_{\text{SOC-30}}$ for each pedon (cS_{H}) with:

$$cS_{\text{H}} = \frac{\sum_{i=0}^{n_{\text{H}}} S_{\text{SOC-H,i}}}{S_{\text{SOC–30}}} \tag{7}$$

where the index $_{\text{H}}$ indicates the horizon type: A, B, Oi or Oe and n_{H} is the number of horizons of a specific type per pedon up to 30 cm depth. Then, the cS_{H} for each horizon type was averaged over all investigated pedons. An additional calculation following Eq. 8 was conducted where not a specific horizon type was considered but the group of all cryoturbated horizons. Correlation analyses on latitude and $S_{\text{SOC-30}}$ were done using SPSS Package, version 16.0.1.

5.4 Results

All soils classified along the investigated latitudinal transect were Gelisols (Soil Survey Staff 2010). With respect to the soil classification by Elovskaya (1987), the investigated soils belong to the Permafrost type (see also Desyatkin *et al.* 1991, Pfeiffer *et al.* 2000) with the exception of the southernmost one. The soil at Tik13 is a Cryogenic soil. The results of the classification and the physical and chemical soil analyses are summarized by only one representative soil subgroup per site (Tab. 13). The representative soils dominating the twelve transect sites were six *Turbels* and six *Orthels*. No *Histels* were identified. The maximum depth to frozen ground was found to be 57 cm from the surface (min: 18 cm, mean: 30 cm, standard deviation: 10 cm).

Table 13: Classification and properties of dominant soil subtypes at investigated sites. Site identifier with the number of soil pits in parentheses, Soil Subgroup (Soil Survey Staff 2010), Soil Subtype (Elovskaya 1987), Soil Organic Carbon content for the top soil down to 30 cm (S_{SOC-30}), C/N-ratio, Bulk Density (BD), Active Layer depth and the respective standard deviations.

Tab. 13: Klassifikation und Eigenschaften der dominanten Bodensubtypen der Arbeitsgebiete. Gebietskennzeichnunge mit der Anzahl der Bodenprofile in Klammern, Bodenuntergruppe (Soil Survey Staff 2010), Bodensubtyp (Elovskaya 1987), Gehalt an Bodeneigenem organischen Kohlenstoff für die Oberböden bis in die Tiefe von 30 cm (S_{SOC-30}), C/N-Verhältnis, Bodendichte (BD), Tiefe des Auftaubodens und die entsprechenden Standarabweichungen.

Site ID (n)	Soil Subgroup	Soil Subtype	S_{SOC-30} kg m^{-2}	C/N ratio	BD g cm^{-3}	Active Layer depth cm
10LD1 (1)	*Psammentic Aquiturbel*	*Permafrost alluvial turfy typical*	5.4	15.4 ± 1.7	1.19 ± 0.27	52.0
Tik01 (6)	*Typic Psammoturbel*	*Permafrost alluvial primitive sandy*	2.9	19.1 ± 4.1	1.03 ± 0.56	35.0 ± 13.6
Tik04 (1)	*Folistic Haplorthel*	*Permafrost turfness-gley*	12.1	13.5 ± 1.5	1.06 ± 0.20	39.0
Tik21 (1)	*Typic Aquorthel*	*Permafrost silty-peat-gley*	12.4	16.5 ± 0.1	1.11 ± 0.67	24.0
Tik22 (2)	*Glacic Aquiturbel*	*Permafrost peatish-gley*	10.9	26.4 ± 11.0	1.07 ± 0.42	37.0 ± 7.1
Tik08 (2)	*Ruptic Historthel*	*Permafrost peatish*	17.2	18.0 ± 1.4	0.64 ± 0.49	21.5 ± 5.0
Tik20 (1)	*Typic Aquiturbel*	*Permafrost peatish-gley typical*	9.3	18.0 ± 3.9	1.3 3± 0.72	30.0
Tik05 (2)	*Ruptic Historthel*	*Permafrost peat*	32.7	22.5 ± 0.2	1.03 ± 0.10	26.5 ± 3.5
Tik09 (2)	*Ruptic-Histic Aquiturbel*	*Permafrost peat-gley*	27.5	25.8 ± 11.5	0.32 ± 0.42	22.5 ± 3.5
Tik10 (1)	*Typic Histoturbels*	*Permafrost peatish-gleyic*	23.2	22.7 ±8.5	0.34 ± 0.33	19.0
Tik12 (1)	*Fluvaquentic Historthel*	*Permafrost peat*	27.3	26.2 ±4.4	0.18 ± 0.11	30.0
Tik13 (1)	*Typic Haplorthel*	*Cryogenic soil*	10.3	24.4 ± 5.8	1.01 ± 0.63	49.0

The main landscape unit of Arga Island is covered by sparse vegetation, mainly lichens, mosses and *Carex*-species and is dominated by *Psammoturbels* and *Psammorthels* without any rock fragments and with sandy texture within the particle-size control section.

The genesis of these permafrost-affected soils is dominated by the accumulation of fluvial sediments and their dislocation and retransportation by wind. Very often they are cryoturbated.

The main landscape units of the Holocene first as well as the Pleistocene third terrace are covered mainly by vegetation with species like *Carex aquatilis, Dryas punctata, Astragalus umbellatus*. These soils developed as soil complexes which consist of cryoturbated and ice-rich *Aquiturbels* and very wet and organic-rich *Historthels* (Pfeiffer *et al.* 2002, Fiedler *et al.* 2004, Kutzbach *et al*. 2004, Sanders *et al.* 2010). The *Historthels* formed in the centres of low-centred polygons, which are depressed, water-saturated and characterized by high accumulation of organic matter due to anaerobic soil conditions. *Aquiturbels*, which formed at the elevated borders, have gleyic properties and prominent cryoturbation (see also Pfeiffer *et al.* 2002, Fiedler *et al.* 2004, Kutzbach *et al*. 2004, Sanders *et al.* 2010).

Going southward to the continental hinterland of the Lena River Delta, the soils are still dominated by polygonal patterned ground and contain soil complexes of organic-rich *Orthels* within the polygon centres and *Turbels* on the borders. Generally, these soils are drier than those from the delta region due to a different cover of densely rooted vegetation, e.g. *Larix sibirica L.*. The soil at the southernmost site differs in profile composition (*cambic* horizon) and soil structure from the other soils of the Central Siberian Plateau investigated in this study.

The mean BD, C/N ratios and $S_{SOC\text{-}30}$ (0-30 cm depth) calculated for the investigated sites within the north-south transect are given in table 1. Disregarding the southernmost site which is different in genesis, a distinct increase in $S_{SOC\text{-}30}$ following the transect from north to south was found. The Pearson product-moment correlation coefficient for the relationship between latitude and $S_{SOC\text{-}30}$ was $R = 0.85$. The highest calculated $S_{SOC\text{-}30}$ was found at the site Tik05 at the El'gene-Kyuele Lake at 71.3° N and amounted to 32.65 kg m^{-2}. The lowest stock of 2.85 kg m^{-2} was found on Arga Island at the second northernmost site (Tik01). The mean

S_{SOC-30} of the sites amounted to 15.9 kg m^{-2} ± 9.6 kg m^{-2}. The C/N ratios, which are regarded as indicators for decomposability of soil organic matter (van Cleve 1974), varied from 10.4 to 51.4 when every single horizon is considered. Averaged over the soil pedons, they ranged from 13.5 to 26.4 (Tab. 13). Low ratios were found mainly for A (Ø: 18.1±5.2) and sandy B horizons (Ø: 18.7±6.4), whereas water-saturated O horizons were characterized by higher ratios (Oe Ø: 21.8±5.4; Oi Ø 27.3±9.9).

Considering the S_{SOC-H} and taking into account the high variability of OC contents and BD of the different horizons of the same soil pedon, a closer inspection of single horizon types appeared interesting. The highest OC contents were found in the Oi and Oe horizons with 35 to 50 % and 6 to 45 %, respectively (Tab. 14). Generally, an Oi horizon is characterized by a high fiber content and low SOM decomposition. The Oe horizons show intermediate SOM decomposition with fiber contents of 17 to 40 % after rubbing (Soil Survey Staff 2010). On the other hand, due to the high fiber content, these O horizons had low BD values of 0.03 g cm^{-3} to 0.27 g cm^{-3} and 0.12 g cm^{-3} to 0.92 g cm^{-3} for "Oi" and "Oe", respectively (Tab. 14). The A horizons formed at the surface or underneath an O horizon and consisted of organic matter and sandy sediments (mean sand content: 77 %). The high sand content led to relatively high average BD values of 0.79 g cm^{-3}. These horizons showed moderate OC contents of on average 9.5 % with a maximum of 17.7 %. The investigated B horizons had the lowest OC contents (on average 4.1 %) varying from 0.2 % to 17 % and had a relatively high mean BD of 1.33 g cm^{-3}. The moderate OC content of 7.1 % and the high bulk density of horizons showing cryoturbation result in high S_{SOC-H} which ranges between those of Oe and A horizons. Regarding the number of the analyzed horizons, their mean S_{SOC-H} and their mean thickness, it became clear that the Oe horizons had the highest overall contribution to the summed S_{SOC-30} of all investigated soils within the transect (50 % ± 6.41 %) followed by the organic matter-poor B horizons (36 % ± 5.29 %). The Oi horizons showed a low overall contribution of 9 % ± 3.29 % and were undercut only by the A horizons (5 % ± 1.90 %).

Table 14: Average properties of different horizons in sampled permafrost-affected soils. Horizon identifier with sample numbers in parentheses, mean OC content, mean BD, mean S_{SOC-H} per horizon thickness d, mean horizon thickness, and the respective standard deviations. **turb* = cryoturbated horizons.

Tab. 14: Gemittelte Werte der Bodeneigenschaften in verschiedenen Horizonten der permafrostbeeinflußten Böden. Horizontkennzeichnung mit Anzahl der Proben in Klammern, gemittelte Gehalte an orgnischem Kohlenstoff, gemittelte Bodendichte, gemittelte S_{SOC-H} pro Horizont, mittlere Horizontmächtigkeit und die entsprechenden Sandardabweichungen. **turb* = kryoturbierte Horizonte.

Horizon (n)	OC %	BD g cm^{-3}	S_{SOC-H} / d kg m^{-2} cm^{-1}	Thickness cm
Oi (6)	43.9±5.9	0.11±0.08	0.48±0.31	6.2±2.93
Oe (13)	26.7±15.5	0.39±0.21	0.86±0.51	9.3±4.05
A (3)	9.5±7.7	0.79±0.44	0.52±0.25	6.7±0.58
B (13)	4.1±5.1	1.33±0.38	0.39±0.31	14.6±5.72
turb (10)*	*7.1±5.9*	*1.08±0.43*	*0.58±0.31*	*11.5±8.3*

5.5 Discussion and conclusions

The point data of the preliminary exploration presented in this paper give a first impression of the high stocks of organic carbon in the permafrost-affected soils of northern Yakutia. Disregarding the low number of investigated pedons and the uncertainty involved, the results are in the range of comparable studies on permafrost-affected soils recently published (Kuhry *et al.* 2002, Ping *et al.* 2008, Hugelius and Kuhry 2009). Due to the limited database as well as the high natural soil heterogeneity and variability, the author decided neither to prescribe any spatial distribution to the data nor to upscale to any large soil map unit.

Nevertheless, the presented data indicates that the North-Siberian permafrost-affected regions are rich in soil organic carbon. The results show a distinct arrangement into three groups of comparable stocks. The soils of the northern most sites on Arga Island are characterized by the lowest amounts of S_{SOC-30}, and the soils of the permafrost-affected part of the Central Siberian Plateau by the highest amounts of S_{SOC-30}. The soils of the south-central Lena River Delta (i.e., without Arga Island) range between these bounds. Due to its transitioning

appearance, the Tik08 site was included into the "delta group" although it actually belongs to the Siberian main landmass. On the one hand, the big differences between the groups are caused by the varying sources of the parent material and the resulting pedogenetic processes. On the other hand, the climatologic gradient within the N-S transect probably has an additional strong effect on the $S_{SOC\text{-}30}$ of the groups. Arga Island, probably formed by coarse fluvial sediments (Schirrmeister *et al.* 2011b), is covered with sparse vegetation only. The pedogenic processes are strongly related to physical weathering of the sediment and light accumulation of the organic matter provided by the sparse vegetation. A pronounced cryoturbation reworks the sediment and transports small portions of the organic matter to deeper horizons. The other sediments forming the Lena River Delta are of different age and include in this presented case the first Holocene and third Pleistocene terraces (Schwamborn *et al.* 2002, Wetterich *et al.* 2008). These two terraces – despite the differing overall geomorphology – provide comparable conditions for soil genesis. The moderately organic soils of the third terrace developed on top of ice complexes and have mineral sediments of aeolian origin. The vegetation cover is dense and results in a higher accumulation of organic matter than on the Arga Island site. The first terrace, especially the rarely-flooded elevated part is also dominated by high accumulation of organic matter and is composed primarily of fine fluvial sands and silts with additions of aeolian sands. The soil organic matter of the O horizons in the delta region is only slightly decomposed. In contrast, the soil organic matter on the Central Siberian Plateau is more decomposed and shows a higher density. Here, the different vegetation, which includes trees, produces higher amounts of biomass that can be reworked into the soils, accumulates there and is preserved over long time scales.

Regarding the accumulation of organic matter due to the different vegetation covers, the climatologic gradient as an important factor which impacts soil carbon stocks was considered. The pronounced increase of $S_{SOC\text{-}30}$ in the active layer of the soils from north to south is probably caused by the increase of summer length and summer temperatures with decreasing latitude. Though higher temperatures cause accelerated decomposition of the organic matter, the accumulation rates are still high. Additionally, the distribution of precipitation in the south with major summer rains supports more productive plant growth than in the north where a

similar total annual amount is shared between two maxima, one in the summer and one in winter.

The degree of transformation of soil organic material can be described by the ratio of the C and N contents of the organic matter. The C/N ratios of the studied pedons were relatively high and comparable to values reported from other polar regions (Bardgett *et al.* 2007, Knoblauch *et al.* 2008, Sanders *et al.* 2010). The knowledge of the initial botanical composition at the investigated sites is essential for the discussion of C/N ratio (Kuhry and Vitt 1996, Vardy *et al.* 2000). Based on the fact that all sites were dominated by *Carex* species, mosses and lichens (in the south *Larix*) (s. result section) the author assumes that low ratios indicate stronger alteration of the organic material whereas high ratios indicate recalcitrant or only slightly decomposed material. The high C/N ratios observed in the investigation area likely result from a lack of oxygen caused by persistent water saturation and therefore low SOM decomposition. Better aeration of some A and sandy B horizons allows higher decomposition rates which result in lower C/N ratios.

Comparing the presented results with the most-up-to-date carbon stock estimation for northern permafrost soils by Tarnocai *et al*. (2009), which includes the current investigation area, the author wants to point out the importance of further intensive field work within the heterogenic permafrost-affected area, particularly in the rarely researched permafrost regions of Siberia. The calculations by Tarnocai *et al*. (2009) with the best data available overestimated the soil organic carbon stock of the sandy Arga Island by classifying it as a carbon-rich area with stocks of more than 50 kg SOC m^{-2} whereas the stock in the area south to the Lena River Delta with values of 10.01 to 50 kg SOC m^{-2} (both to 1 m depth) was underestimated (Tarnocai *et al*. 2009).

Calculating the $S_{SOC\text{-}H}$ of single soil horizons resulted in interesting insights that should be included into future studies in order to quantify and generalize these observations. Taking into account their low OC contents, high BD, and additionally their abundance, it turned out that the inconspicuous B horizons have a high contribution to the overall $S_{SOC\text{-}30}$ at the presented sites. These mineral horizons are widespread throughout most of the pedons (Tik04, Tik08, Tik13, Tik20, Tik21) and are often cryoturbated with gleyic features. The cryoturbation mixes considerable amounts of organic material into the fine-grained layer (averaged clay

content = 19.4 %). Anaerobic conditions in these zones hinder decomposition and preserve organic matter.

Evaluating the existing data and consulting the preliminary results with all their weaknesses, the author encourages more intensive soil sampling in the Russian Arctic to improve the soil database of this region. This sampling should not be limited to the active layer but should include investigations of deep, currently still permanently frozen soil horizons.

6. Synthesis and conclusions

The soils of permafrost-affected regions have accumulated large amounts of organic carbon and nitrogen during the past. The quantifications are difficult due to the huge extent and limited access to large parts of these regions. Therefore, currently the mass of the organic carbon storage can only be estimated using widely sparse data and upscaling methods. Moreover, disproportionately large shares of these available data were acquired in permafrost regions in Alaska and Northern Canada as well as Northern Scanidinavia and the European part of Russia. Unfortunatelly, the enormous areas of Northeastern Russia capture only a small place within the Northern Circumpolar Soil Carbon Database (Tranocai *et al*. 2007, Hugelius *et al*. 2012) and therefore need an enhancement. The nitrogen storage function of permafrost-affected soils was neglected for long time, and there are only assumptions providing the size as a ratio of the estimated carbon mass (C/N ratio of 30) (Jonasson *et al.* 1999, Weintraub and Schimel 2003).

The overall goal of this interdisciplinary thesis is to enhance the mentioned carbon database by providing new data on soil organic carbon from underrepresented areas of the Russian Arctic, especially the largest arctic delta – the Lena River Delta. An additional goal was to provide first total nitrogen stocks for larger arctic regions. Deltas are expected to store large amounts of carbon and nitrogen in comapartively small areas, due to their high morphologic dynamics resulting in a large thickness of deltaic sediments.

The presented thesis delivers first insights into the huge diversity of soils that developed within the few decimetres of the seasonally thawed ground in the short summer period. This diversity is affected by the soil forming factors, whereupon time and temperature are the limiting and the substrate is the trend-setting factor resulting in the development of one of three major permafrost-affected soil groups in the investigated regions: organic rich soils, organic poor soils and cryoturbated soils. However, these three groups are strongly differentiated by several sublevels. In this study, not all soils could be fully satisfactorily differentiated using the current key for soil classification (Soil Survey Staff 2010). Thus, soils of considerably different appearance and properties sometimes have the same descriptive name given by this classification key. The classification of permafrost-affected soils very

often is problematic due to mimimum depth limits one has to investigate for classification of certain horizons. In this study, some supposedly organic-rich soils as *Histels* were classified as *Orthels* because the diagnostic horizon could not be fully verified due to a shallow thawed layer.

The investigated soils, although only few decimetres thick, have accumulated considerable amounts of soil organic carbon and large nitrogen pools. Therefore, the increased broader attraction is justified and helps fostering an improved assessment of permafrost-affected soils. The analyses of the investigated soils showed that the mean soil organic carbon stock on the Holocene river terrace of the Lena River Delta and the first one-metre of soil account to 29.5 kg m^{-2}. The wiederspread floodplain levels stored 13.6 kg m^{-2}. The nitrogen stocks for these geomorphic units were 1.2 kg m^{-2} and 0.9 kg m^{-2}, respectively. These results prove the importance of spatially distributed field studies prior to large-scale upscaling. This is important due to the enormous error potential when results from one region are prescribed to another, apparent similar, region. In this thesis, an example for the estimation of the soil organic carbon storage of the Lena River Delta using soil investigations from another arctic delta, the Mackenzie River Delta (Tarnocai *et al*. 2009) is demonstrated. This estimate accounts to 131 Pg of carbon for a depth of 50 metres of soil. The author of this thesis used his own results from the Lena River Delta and the published spatial up-scaling model approach of Tarnocai *et al.* (2009) and calculated a significantly lower estimate of 38...52 Pg of carbon in the Lena River Delta!

However, in the presented thesis robust estimates can only be presented for a depth of one metre and only for the Holocene deposits of deltaic origin in the Lena River Delta. The storages of the both dominating geomorphic units, the Holocene river terrace and the active floodplain levels, are similar and amout to 121 and 120 Tg of soil organic carbon as well as 5 and 8 Tg of nitrogen and a depth of one metre. These two dominating geomorphic units occupy more than 60 % of the Lena River Delta area. The results of this thesis prove that the increase of the cumulative soil organic carbon storage with depth is approximately linear and therefore reliable results might be derived from the easy to access samples from the seasonally thawed layer. Within this layer, which has a depth of around 50 cm, one-half of the soil organic carbon and nitrogen stored within the top 1 m of soil was found. Hence, another

one-half of the estimated storage was within the lower 50 cm of still perennially frozen ground. These storages are large, and combined with the projections for deepening the seasonally thawed layer an important factor that should be taken into account when modelling the carbon release from soils, changes in vegetation patterns, and future temperature trends and projections.

The soil organic carbon storages derived from the latitudinal transect conducted as a pilot study in Northeast-Siberia prove an important relationship between the varying soil parent material with the resulting pedogenetic processes and the soil organic carbon stocks within the three groups of investigated soils. This study provides only the soil organic carbon stocks of the seasonally thawed layer. However, a distinct increase of the stock size with decreasing latitude indicates a huge storage of soil organic carbon in the forested tundra and northern taiga. The results from this transect illustrate that the carbon stock of the seasonally thawed layer is double that high in the more southernly located hinterland (24 ± 9 kg m^{-2}) than it is in the Lena River Delta (12 ± 3 kg m^{-2}), when the so-called second river terrace is disregarded. This pilot study indicates that the soil organic carbon stock of the seasonally thawed layer (30 cm thickness on average during the field survey) in the regions of forested tundra (24 ± 9 kg m^{-2}) is comparable to the one meter soil organic carbon stocks investigated in the Lena River Delta amounting to 26 ± 12 kg m^{-2}. These preliminary insights highlight the importance of extended investigations quantifying the carbon for the wide range of vegetation types found in permafrost regions.

Using the linear increase of the cumulative soil organic stock size determined for the Lena River Delta study, the carbon stock of the forested tundra is likely to reach 80 kg m^{-2} within a depth of 100 cm. These places very often are characterised by a great spatial abundance of peatlands. The results of the pilot study encourage continuing carbon quantification studies within this region to gain a more detailed knowledge about the soils of the unique and various landscapes of Northeast-Siberia. Nitrogen quantification studies from these regions are not available and therefore should be included into future investigation strategies. The extent of wetland- and peatland-dominated areas is Northeast-Siberia is large (Fig. 59), and therefore the carbon stock is likely variable but on a high level.

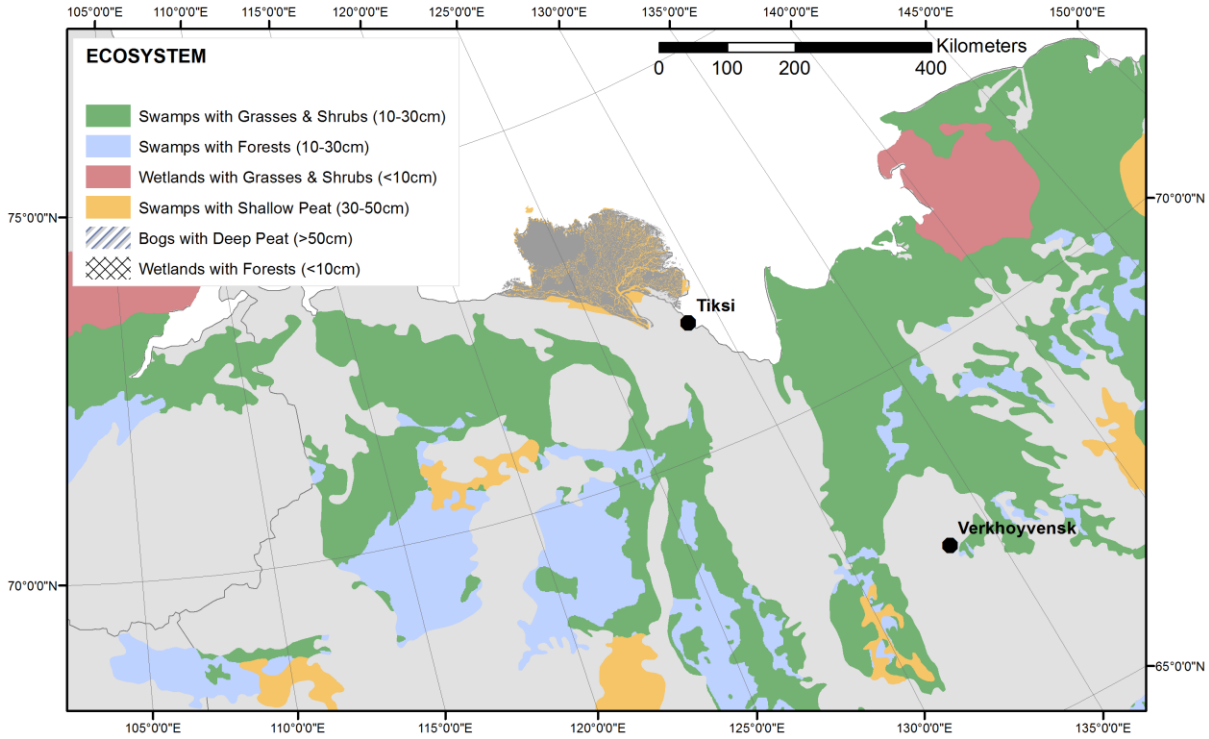

Figure 59: The distribution of wetland ecosystems in Northeast-Siberia. The two dominating types of this region are "swamps with grasses and shrubs" and "swamps with forests". Compiled from data provided by Stolbovoi and McCallum (2002) in Land Resources of Russia database.

Fig. 59: Die Verteilung der Feuchtgebietsökosysteme im Nordosten Sibiriens. Die beiden diese Region dominierenden Arten sind "Sümpfe mit Gräsern und Sträuchern" und "Sümpfe mit Wäldern". Erstellt aus Daten der Land Resources of Russia database von Stolbovoi and McCallum (2002).

Knowledge about the pools of soil organic carbon is of vital importance. However, only its combination with the understanding and quantification of biogeochemical decomposition processes and release of gases like carbon dioxide, methane, and nitrous oxide can provide a carbon lability assessment. Such experiments analysing decomposition rates and decay characteristics are still rare and are needed to be done in future to gain knowledge about the likely vulnerable pool of carbon that could be mineralized within the changing climate. Further future investigations should include long-term *in-situ* monitoring approaches of decay rates of organic matter using e.g. litter bags or minicontainer methods. Doing so, real loss of organic matter can be estimated and mineralization rates could be constrained. Adding laboratory incubation experiments using different temperature settings, future mineralization

rates under a warmer climate could be estimated and compared with the *in-situ* results. Furthermore, it is essential to determine the quality of the organic carbon using e.g. density fractionation methods, and to analyse the mineralization rates for each fraction, since it is known, that different fractions of carbon are characterized by specific vulnerability or recalcitrance. The results of such investigations could help to provide an overview of carbon lability. A combination of carbon storage maps and carbon lability maps would help to figure out the carbon hot spots with high climatic impact.

The knowledge about nitrogen pools as a preliminary insight into this vegetation-limiting factor is extremely important. However, more detailed studies on nitrogen fractions are needed to distinguish among organic and inorganic fractions, e.g. nitrate, nitrite, and ammonia. These nitrogen-related studies should be combined with phosphorous-focused studies to evaluate the two most important elements limiting and therefore regulating the growth of the vegetation.

7. References

AG Boden (2005): Bodenkundliche Kartieranleitung (‚KA5'). E. Schweizerbart´sche Verlagsbuchhandlung, Stuttgart.

Akhmadeeva, I., Becker, H., Friedrich, K., Wagner, D., Pfeiffer, E.-M., Quass, W., Zhurbenko, M., and Zöller, E. (1999): Investigation site 'Samoylov'. Reports on Polar and Marine Research 315: 19-21.

Alabyan, A.M.; Chalov, R.S.; Korotaev, V.N.; Sidorchuk, A.Yu., and Zaitsev, A.A. (1995): Natural and technogenic water and sed- iment supply to the Laptev Sea: In: Kassens, H.; Piepenburg, D.; Thiede, J.; Timokhov, L.; Hubberten, H., and Priamikov, S., (eds.), Reports on Polar Research, 176, 265-271.

Altermann, M., Jäger, K.-D., Kopp, D., Kowalkowski, A., Kühn, D. and Schwanecke, W. (2008): Zur Kennzeichnung und Gliederung von periglaziär bedingten Differenzierungen in der Pedosphäre. In: Waldökologie, Landschaftsforschung und Naturschutz 6, 5-42.

Anisimov, O.A. and Nelson, F.E. (1997): Permafrost zonation and climate change in the northern hemisphere: results from transient general circulation models.Climatic Change, 35(2): 241–258.

Anon, 1986. Classification and Diagnostics of Soils of the USSR. Oxonian Press Pvt. Ltd., New Delhi.

ArcGIS (2012): ArcGIS Resource Center , http://resources.arcgis.com, 2012.05.10.

Are, F., and Reimnitz, E. (2000): An Overview of the Lena River Delta Setting: Geology, Tectonics, Geomorphology, and Hydrology, Journal of Coastal Research, 16, 1083-1093.

Baranov, I. Y. (1959): Geographical distribution of seasonally-frozen ground and permafrost. General Geocryology. Obruchev Institute of Permafrost Studies. Academy of Science Moscow, Part 1, Chapter 7, National Council of Canada. Technical translation. 193-219.

Bardgett, R.D., van der Wal, R., Jónsdóttir, I.S., Quirk, H. and Dutton, S. (2007): Temporal variability in plant and soil nitrogen pools in a high-Arctic ecosystem. Soil Biol. Biochem. 39: 2120-2137.

Barnes, D., L. and Chuvilin, E. (2009): Migration of Petroleum in Permafrost-Affected Regions. In: Margesin, R. (Hrsg.): Permafrost Soils. Berlin: Springer Verlag. 263-278.

Beer, C. (2008): Soil science: The Arctic carbon count. Nature Geoscience, 9: 569-570.

Bliss, N.B. and Maursetter, J. (2010): Soil Organic Carbon Stocks in Alaska Estimated with Spatial and Pedon Data.Soil Sci. Soc. Am. J. 2010, 74: 565–579.

Bockheim, J.G (1979): Relative age and origin of soils in eastern Wright Valley, Antarctica. Soil Science, 128, 142–152.

Bockheim, J. G. (1995): Permafrost Distribution in the Southern Circumpolar Region and its Relation to the Environment – A Review and Recommendations for Further Research. Permafrost Periglac 6 (1), 27–45.

Bockheim, J. G. (2002): Landform and soil development in the McMurdo Dry Valleys, Antarctica: a regional synthesis. Arct Antarct Alp Res 34 (3), 308–317.

Bockheim, J.G. and Tarnocai, C. (1998): Recognition of cryoturbation for classifying permafrost-affected soils. Geoderma 81, 281–293.

Bockheim, J. G. and McLeod, M. (2008): Soil distribution in the McMurdo Dry Valleys, Antarctica. Geoderma 144 (1-2), 43–49.

Boike, J., Kattenstroth, B., Abramova, K., Bornemann, N., Chetverova, A., Fedorova, I., Fröb, K., Grigoriev, M., Grüber, M., Kutzbach, L., Langer, M., Minke, M., Muster, S., Piel, K., Pfeiffer, E.-M., Stoof, G., Westermann, S., Wischnewski, K., Wille, C., and Hubberten, H.-W. (2013): Baseline characteristics of climate, permafrost and land cover from a new permafrost observatory in the Lena River Delta, Siberia (1998–2011), Biogeosciences, 10, 2105-2128, doi:10.5194/bg-10-2105-2013.

Braun-Blanquet, J. (1964); Pflanzensoziologie. Grundzüge der Vegetationskund. Springer Verlag, Wien.

Chestnyck, O. V., Zamolodchikov, D. G., and Karelin, D. V. (1999): Organic matter reserves in the soils of tundra and forest-tundra ecosystems of Russia (in Russian), Ecologia, 6, 426–432.

Cornell, R. M. and Schwertmann, U. (2004): The Iron Oxides. Wiley-VCH, Weinheim. p 703.

Corradi, C., Kolle, O., Walter, K., Zimov S.A. and Schulze E.D. (2005): Carbon dioxide and methane exchange of a north-east Siberian tussock tundra. Global Change Biol 11: 1-16, doi: 10.1111/j.1365-2486.2005.01023.x.

Desyatkin, R. and Teterina, L. (1991): The soils of Lena River Delta. Genesis and melioration of Yakutian soils. 55-66. (in Russian)

Desyatkin, R.V. and Desyatkin, A.R. (2006): Thermokarst transformation of soil cover on cryolithozone flat territories. Hokkaido University Press: 213-223.

DIN 19684-6: Methods of soil investigations for agricultural engineering - Chemical laboratory tests - Part 6: Determination of iron soluble in oxalate solution.

DIN EN ISO 11260: Soil quality - Determination of effective cation exchange capacity and base saturation level using barium chloride solution (ISO 11260:1994+Cor. 1:1996); German version EN ISO 11260:2011.

DIN ISO 10390: Soil quality - Determination of pH (ISO 10390:2005).

DIN ISO 10694: Soil quality - Determination of organic and total carbon after dry combustion (elementary analysis) (ISO 10694:1995).

DIN ISO 11265: Soil quality - Determination of the specific electrical conductivity (ISO 11265:1994 + ISO 11265:1994/Corr.1:1996).

DIN ISO 11277: Soil quality - Determination of particle size distribution in mineral soil material - Method by sieving and sedimentation (ISO 11277:1998 + ISO 11277:1998 Corrigendum 1:2002).

Dutta, K., Schuur, E.A.G., Neff, J.C. and Zimov, S.A. (2006): Potential carbon release from permafrost soils of Northeastern Siberia. Glob. Change Biol. 12, 2336–2351.

Elovskaya, L.G., Petrova, E.I. and Teterina, L.V. (1979): Soils of Northen Yakutia. - Novosibirsk, 303pp.

Elovskaya, L.G. (1987): Classification and diagnosis of permafrost soils of Yakutia. Yakutsk, Russia: 172 pp. (in Russian).

Everett, K.R., Vassiljevskaya, V.D., Brown, J. and Walker, B.D. (1981): Tundra and analogous soils. In Tundra Ecosystems: A Comparative Analysis (L.C. Bliss, O.W. Heal and 1.1. Moore, Eds.). Cambridge: Cambridge University Press, pp.139-179. IBib 35-27051.

FAO - Food and Agriculture Organization (2007): WRB - World reference base for soil resources 2006. First update 2007. FAO, Rom: 128pp.

Fiedler, S., Wagner, D., Kutzbach, L. and Pfeiffer, E.-M. (2004): Element redistribution along hydraulic and redox gradients of low-centred polygons, Lena-Delta, northern Siberia. Soil Sci Soc Am J 68: 1002-1011.

French, H. M. (2007): The periglacial environment. John Wiley and Sons Ltd, West Sussex. 458pp.

Galabala, R.O. (1987): New data on the Lena Delta structure. Quaternary of North-East USSR. Magadan, 152-172.

Gorham, E., Lehman, C., Dyke, A., Janssens, J., and Dyke, L. (2007): Temporal and spatial aspects of peatland initiation following deglaciation in North America, Quat. Sci. Rev., 26, 300–311, doi:10.1016/j.quascirev.2006.08.008.

Goryachkin, S. Tonkonogov, V., Germsimova, M., Lebedeva, I., Shishov, L. and Targulian, V. (2003): Changing Concepts of Soil and Soil Classification in Russia. In: Eswarn, H., Rice, T., Ahrens, R., Stewart, B. (eds.), Soil Classification, A Global Desk Reference. CRC Press, London, pp 187-199.

Goryachkin, S.V. and Ignatenko, I.V. (2004): Cryosols of the Russian European North. In: Kimble, J.M. (Hrsg.). Cryosols. Permafrost-Affected Soils. Berlin: Springer Verlag. 185-208.

Gracheva, R.G. (2004): Cryosols of the Mountains of Southern Siberia and Far Eastern Russia. In: Kimble, J.M. (Hrsg.). Cryosols. Permafrost-Affected Soils. Berlin: Springer Verlag. 231-252.

Grigoriev, M.N. (1960): The temperature of permafrost in the Lena delta basin – deposit conditions and properties of the permafrost in Yakutia. Yakustk 2, 97-101.

Grigoriev, M.N. (1993): Criomorphogenesis in the Lena Delta. Yakutsk: Permafrost Institute Press, p 176.

Grosse, G., Harden, J., Turetsky, M., McGuire, A.D., Camill, P., Tarnocai, C., Frolking, S., Schuur, E.A.G., Jorgenson, T., Marchenko, S., Romanovsky, V., Wickland, K.P., French, N., Waldrop, M., Bourgeau-Chavez, L. and Striegl, R.G. (2011): Vulnerability of high-latitude soil organic carbon in North America to disturbance. Journal of Geophysical Research-Biogeosciences. 116, G00K06, 23 pp.

Gubin, S. V. and Lupachev, A. V. (2008): Soil Formation and the Underlying Permafrost. Eurasian Soil Science, 2008, Vol. 41, No. 6, pp. 574–585.

Gundelwein, A., Müller-Lupp, T., Sommerkorn, M., Haupt, E.T., Pfeiffer, E.-M. and Wiechmann, H., (2007): Carbon in tundra soils in the Lake Labaz region of arctic Siberia. Eur J Soil Sci doi: 10.1111/j.1365-2389.2007.00908.x.

Harden, J. W., Sundquist, E. T., Stallard, R. F., and Mark, R. K. (1992): Dynamics of soil carbon during the deglaciation of the Laurentide ice sheet, Science, 258, 1921–1924, doi:10.1126/science.258.5090.1921.

Harden, J. W., Koven, C. D., Ping, C.-L., Hugelius, G., McGuire, A. D., Camill, P., Jorgenson, T., Kuhry, P., Michaelson, G. J., O'Donnell, J. A., Schuur, E. A. G., Tarnocai, C., Johnson, K. and Grosse, G. (2012): Field information links permafrost carbon to physical vulnerabilities of thawing, Geophys. Res. Lett., 39, L15704, doi:10.1029/2012GL051958.

Höfle, S., Rethemeyer, J., Mueller, C. W., and John, S. (2012): Organic matter composition and stabilization in a polygonal tundra soil of the Lena-Delta. Biogeosciences Discuss., 9, 12343–12376.

Hugelius, G and Kuhry, P. (2009): Landscape partitioning and environmental gradient analyses of soil organic carbon in a permafrost environment. Global Biogeochem. Cycles 23: GB3006. DOI:10.1029/2008GB003419

Hugelius, G., Kuhry, P., Tarnocai, C. and Virtanen, T. (2010): Soil Organic Carbon Pools in a Periglacial Landscape: a Case Study from the Central Canadian Arctic. Permafrost and Periglacial Processes 21, 1: 16–29.

Hugelius, G., Virtanen, T., Kaverin, D., Pastukhov, A., Rivkin, F., Marchenko, S., Romanovsky, V. and Kuhry, P. (2011): High-resolution mapping of ecosystem carbon storage

and potential effects of permafrost thaw in periglacial terrain, European Russian Arctic. Journal of Geophysical Research-Biogeosciences. 116, G03024, 14pp.

Hugelius, G., Tarnocai, C., Broll, G., Canadell, J. G., Kuhry, P., and Swanson, D. K. (2012): The Northern Circumpolar Soil Carbon Database: spatially distributed datasets of soil coverage and soil carbon storage in the northern permafrost regions. Earth Syst. Sci. Data Discuss., 5, 707-733.

Hugelius, G. (2012): Spatial upscaling using thematic maps: An analysis of uncertainties in permafrost soil carbon estimates. Global Biogeochem. Cycles 26: GB2026. DOI: 10.1029/2011GB004154.

IPCC - Intergovernmental Panel on Climate Change (2007): Climate Change 2007 – IPCC Fourth Assessment Report. Cambridge University Press, Cambridge, United Kingdom and New York, NY, USA

Ivanova, E.N. (1965): Taiga cryogenic soils of Northen Yakutia. Pochvovedenie (Soil Science) No.7.

Ivanova, E.N. (1971): Soils of Central Yakutia. Pochvovedenie (Soil Science) No.9, 3-18.

Ivanova, T. I., Kuz'mina, N. P. and Isaev, A. P. (2012): A microbiological characterization of the permafrost soil of Tit-Ary Island (Yakutia). Contemporary Problems of Ecology, Vol. 5, Issue 6, DOI 10.1134/S1995425512060078, 589-596.

Jonasson, S., Michelsen, A. and Schmidt, I. K. (1999): Coupling of nutrient cycling and carbon dynamics in the Arctic, integration of soil microbial and plant processes. Applied Soil Ecology 11:135-146.

Jones, A., Stolbovoy, V., Tarnocai, C., Broll, G., Spaargaren, O. and Montanarella, L. (Hrsg.) (2010): Soil Atlas of the Northern Circumpolar Region. European Commission, Publications Office of the European Union, Luxembourg: 144 pp.

Karavaeva, N.A. (1969): Tundra soils of Northern Yakutia. - Moscow: Nauka (Science), 206pp.

Karavaeva, N. (2004): Cryosols of Western Siberia. In: Kimble, J.M. (Hrsg.). Cryosols. Permafrost-Affected Soils. Berlin: Springer Verlag. 209-230.

Khvorostyanov, D.V., Krinner, G. and Ciais, P. (2008): Vulnerability of permafrost carbon to global warming. Part I. Model description and role of heat generated by organic matter decomposition. Tellus, 60B: 343-358.

Kimble, J.M. (Hrsg.) (2004): Cryosols. Permafrost-Affected Soils. Berlin: Springer Verlag. 726pp.

Klemm, J. and Zubrzycki, S. (2009): Investigation on soil and vegetation units along a North-South transect in Northeast Siberia and central part of Lena Delta, Yakutia. Reports on Polar and Marine Research 600: 28-29.

Knoblauch, C., Zimmermann, U., Blumenberg, M., Michaelis, W. and Pfeiffer, E.-M. (2008): Methane turnover and temperature response of methane-oxidising bacteria in permafrost-affected soils of northeast Siberia. Soil Biology and Biochemistry 40: 3004-3013.

Kolchugina, T. P., Vinston, T. S., Gaston, G. G. Rozhkov, V. A., and Shwidenko, A. Z. (1995): Carbon pools, fluxes and sequestration potential in soils of the former Soviet Union, in Soil Management and Greenhouse Effect, edited by R. Lal et al., pp. 25– 40, Lewis, Boca Raton, Fla.

Konishchev, V.N., Rogov, V.V. (1993): Investigations of cryogenic weathering in Europe and Northern Asia. Permafrost and Periglacial Processes 4, 49–64.

Korotaev, V.N. (1991): The geomorphology of river deltas. Moscow State University Press, p 224.

Koven, C.D., Ringeval, B., Friedlingstein, P., Ciais, P., Cadule, P., Khvorostyanov, D., Krinner, G. and Tarnocai, C. (2011): Permafrost carbon-climate feedbacks accelerate global warming. PNAS, 108, 36: 14769–14774.

Krasuk, A.A. (1927): Soils of Lensk-Amginsk drainage-basin (Yakutsk district). Materials of the committee of Yakutsk ASSR. Issue of Academy of Science SSR, Moscow, 176pp.

Kuhry, P. and Vitt, D.H. (1996): Fossil carbon/nitrogen ratios as a measure of peat decomposition. ECOLOGY 77, 1: 271–275.

Kuhry, P., Mazhitova, G. G., Forest, P.-A., Deneva, S. V., Virtanen, T. and Kultti, S. (2002): Upscaling soil organic carbon estimates for the Usa Basin (northeast European Russia) using GIS-based landcover and soil classification schemes. Dan. J. Geogr. 102: 11–25.

Kuhry, P., E. Dorrepaal, G. Hugelius, E. A. G. Schuur and C. Tarnocai (2010): Potential Remobilization of Belowground Permafrost Carbon under Future Global Warming. Permafrost and Periglac. Process. 21: 208–214.

Kutzbach, L. (2000): Die Bedeutung der Vegetation und bodeneigener Parameter für die Methanflüsse in Permafrostböden. Dipl. Arb. Universität Hamburg, p 105.

Kutzbach, L. (2006): The exchange of energy, water and carbon dioxide between wet arctic tundra and the atmosphere at the Lena River Delta, Northern Siberia. Bremerhaven: Reports on Polar and Marine Research, 141 pp.

Kutzbach, L., Wagner, D. and Pfeiffer, E.-M. (2004): Effect of microrelief and vegetation on methane emission from wet polygonal tundra, Lena-Delta, Northern Siberia. Biogeochem 69: 341-362.

Kutzbach, L., Wille, C. and Pfeiffer, E.-M. (2007): The exchange of carbon dioxide between wet arctic tundra and the atmosphere at the Lena River Delta, Northern Siberia. Biogeosciences 4: 869-890.

Kuzmina, S., Wetterich, S. and Meyer, H. (2003): Paleoecological and sedimentological studies of Permafrost deposits in the Central Lena Delta (Kurungnakh and Samoylov Islands). Reports on Polar and Marine Research 466: 71-81.

Lantuit, H., Overduin, P.P., Couture, N., Wetterich, S., Are, F., Atkinson, D., Brown, J., Cherkashov, G., Drozdov, D., Forbes, D., Graves-Gaylord, A., Grigoriev, M., Hubberten, H.-W., Jordan, J., Jorgenson, T., Ødegård, R. S., Ogorodov, S., Pollard, W., Rachold, V., Sedenko, S., Solomon, S., Steenhuisen, F., Streletskaya, I. and Vasiliev, A. (2011): The Arctic Coastal Dynamics database. A new classification scheme and statistics on arctic permafrost coastlines, Estuaries and Coasts, doi:10.1007/s12237-010-9362-6.

Laplace, P.-S. (1774): Memoir on the Probability of the Causes of Events, Statistical Science 1(3):364–378, translated (1986) by Stigler, S. M.

Lawrence, D. M., Slater, A. G., Romanovsky, V. E., and Nicolsky, G. J. (2008): Sensitivity of a model projection of near-surface permafrost degradation to soil column depth and representation of soil organic matter, J. Geophys. Res., 113, F02011, doi:10.1029/2007JF000883.

Lembke, P., Ren, J., Alley, R.B., Allison, I., Carrasco, J., Flato, G., Fujii, Y., Kaser, G., Mote, P., Thomas, R.H. and Zhang, T. (2007): Observations: Changes in Snow, Ice and Frozen Ground. In: Solomon, S., Qin, D., Manning, M., Chen, Z., Marquis, M., Averyt, K.B., Tignor M. and Miller, H.L. (Hrsg.): Climate Change 2007: The Physical Science Basis. Contribution of Working Group I to the Fourth Assessment Report of the Intergovernmental Panel on Climate Change. Cambridge University Press, Cambridge, United Kingdom and New York, NY, USA.

Lenton, T.M. and Schellnhuber, H.J. (2010): Tipping elements: Jokers in the pack. In: Richardson K. et al. (Hrsg.), Climate Change: Global Risks, Challenges, and Decisions. Cambridge University Press, Cambridge, UK.

Liebner, S., Zeyer, J., Wagner, D., Schubert, C., Pfeiffer, E.-M. and Knoblauch, C. (2011): Methane oxidation associated with submerged brown mosses reduces methane emissions from Siberian polygonal tundra. Journal of Ecology, 99: 914–922.

Loveland, T. R., Reed, B. C., Brown, J. F., Ohlen, D. O., Zhu, Z., Yang, L., and Merchant, J. W. (2000): Development of a global land cover characteristics database and IGBP DISCover from 1 km AVHRR data. International Journal of Remote Sensing, 21, 6-7: 1303-1330.

Margesin, R. (Hrsg.) (2009): Permafrost Soils. Berlin: Springer Verlag. 348pp.

Matsuura, Y. and Yefremov, D.P. (1995): Carbon and nitrogen storage of soils in a forest-tundra area of northern Sakha, Russia. In: Proceedings of the Third Symposium on the Joint Siberian Permafrost Studies between Japan and Russia in 1994,97–101. Forest and Forest Products Research Unit, University of Sapporo, Sapporo, Japan.

Maximovich, S.V. (2004): Geography and Ecology of Cryogenic Soils of Mongolia. In: Kimble, J.M. (Hrsg.). Cryosols. Permafrost-Affected Soils. Berlin: Springer Verlag. 253-274.

Mazhitova, G. G., Kazakov, V. G., Lopatin, E. V. and Virtanen, T. (2003): Geographic information system and soil carbon estimates for the Usa River basin, Komi Republic, EURASIAN SOIL SCIENCE, 36: 123–135.

McGuire, AD., Anderson, LG., Christensen, TR., Dallimore, S., Guo, L., Hayes, DJ., Heimann, M., Lorenson, TD., Macdonald, RW. and Roulet N. (2009): Sensitivity of the carbon cycle in the Arctic to climate change. Ecological Monographs, 79:523-555

Mehra, O.P. and Jackson, M.L. (1960): Iron oxide removal from soils and clays by dithionite-citrate systems buffered with sodium bicarbonate. 7th National Conference on Clays and Clay Minerals, S. 317.

Mikhailov, V.N. (1997): The river mouths of Russia and contiguous countries: past, present, and future. Moscow: GEOS, p 413.

Morgenstern, A., Grosse, G., and Schirrmeister, L. (2008): Genetic, Morphological, and Statistical Characterization of Lakes in the Permafrost-Dominated Lena Delta. In: Kane, D.L. and Hinkel, K.M. (eds.) Proceedings of the 9th International Conference on Permafrost, University of Alaska Fairbanks, Institute of Northern Engineering: 1239-1244.

Morgenstern, A., Grosse, G., Günther, F., Fedorova, I., Schirrmeister, L. (2011): Spatial analyses of thermokarst lakes and basins in Yedoma landscapes of the Lena Delta. The Cryosphere 5, 849-867.

Mueller, K. (1997): Oberflächenstrukturen und Eigenschaften von Permafrostböden im nordsibirieschen Lena-Delta. Z. Pflanzenernähr. Bodenk., 160, 497-503.

Munsell (1988): Soil color charts. Bolitmore: Kollmogen Corporation

Nadelhoffer, K.J., Shaver, G.R., Giblin, A. and Rastetter, E.B. (1997): Potential impacts of climate change on nutrient cycling, decomposition and productivity in Arctic ecosystems. In: Global Change and Arctic Terrestrial Ecosystems (Ecological Studies 124): 349–364. Springer, Berlin.

Naumov, Ye.M. (2004): Soils and Soil Cover of Northeastern Eurasia. In: Kimble, J.M. (Hrsg.). Cryosols. Permafrost-Affected Soils. Berlin: Springer Verlag. 161-184.

Oechel, W.C. and Billings, W.D. (1992): Effects of global change on the carbon balance of Arctic plants and ecosystems. In: Arctic Ecosystems in a Changing Climate: 139–168. Academic Press, San Diego, CA.

Oechel, W.C., Hastings, S.J., Vourlrtis, G., Jenkins, M., Riechers, G. and Grulke, N. (1993): Recent change of Arctic tundra ecosystems from a net carbon dioxide sink to a source. Nature 361: 520-523.

Oechel, W.C., Vourlitis, G.L., Hastings, S.J., Zulueta, R.C., Hinzman, L. and Kane, D. (2000): Acclimation of ecosystem CO2 exchange in the Alaskan Arctic in response to decadal climate warming. Nature 406: 978-981.

Okoneshnikova, M.V. (1994): Humus of alas soils of Lena-Amginsk interfluves. Dissertation abstract, Novosibirsk, 147pp.

Orlov, D.S., Biryukova and, O.N. and Sakhanova N.I. (1996): Soil organic matter of Russia, Nauka, ISBN 5-02-003643-9, 256pp. (in Russian)

Ovenden, L. (1990): Peat accumulation in northern wetlands. Quaternary Research 33, 377-386.

Ozerskaya, S., Kochkina, G., Ivanushkina, N. and Gilichinsky, D. (2009): Fungi in Permafrost. In: Margesin, R. (Hrsg.): Permafrost Soils. Berlin: Springer Verlag. 85-96.

Panikov, N., S. (2009): Microbial Activity in Frozen Soils. In: Margesin, R. (Hrsg.): Permafrost Soils. Berlin: Springer Verlag. 119-148.

Pavlova, E., and Dorozhkina, M. (1999): Geological-geomorphological studies in the northern Lena river delta. Reports on Polar and Marine Research 315: 112-126.

Pfeiffer, E.-M. and Janssen, H., (1992): C-isotope analysis of permafrost soil samples of NE-Siberia. In Joint Russian-American Seminar on Cryopedology and Global Change. Gilichinsky, D.A. (ed). Pushchino: Pushchino Research Center, Russian Academy of Science.

Pfeiffer, E.-M. (1998): Methanfreisetzung aus hydromorphen Böden verschiedener naturnaher und genutzter Feuchtgebiete (Marsch, Moor, Tundra, Reisanbau). Hamburg bodenkundliche Arbeiten 37, 208pp.

Pfeiffer, E.-M., Gundelwein, A., Becker, H. and Mueller-Lupp, T. (1997): Soil organic matter (SOM) studies at Taimyr Peninsula. Polar Res 237: 113-126.

Pfeiffer, E.-M., Wagner, D., Becker, H., Vlasenko, A., Kutzbach, L., Boike, J., Quass, W., Kloss, W., Schulz, B., Kurchatova, A., Pozdnyakov, V. and Akhmadeeva, I. (2000): Modern processes in permafrost affected soils. Reports on Polar and marine Research 354: 22-54.

Pfeiffer, E.-M., Wagner, D., Kobabe, S., Kutzbach, L., Kurchatova, A., Stoof, G. and Wille, C. (2002): Modern processes in permafrost affected soils. Reports on Polar and Marine Research 426: 21-41.

Ping, C. L., Michaelson, G. J. and Kimble, J. M. (1997): Carbon storage along a latitudinal transect in Alaska. Nutrient Cycling in Agroecosystems 49: 235–242.

Ping, C.L., Bockheim, J.G., Kimble, J.M., Michaelson, G.J. and Walker, D.A. (1998): Characteristics of cryogenic soils along a latitudinal transect in Arctic Alaska. Journal of Geophysical Research, 103 (D22): 28917-28928.

Ping, C.-L., Clark, M.H. and Swanson, D.K. (2004a): Cryosols in Alaska. In: Kimble, J.M. (Hrsg.). Cryosols. Permafrost-Affected Soils. Berlin: Springer Verlag. 71-94.

Ping, C.-L., Qiu, G. and Zhao, L. (2004b): The Periglacial Environment and Distribution of Cryosols in China. In: Kimble, J.M. (Hrsg.). Cryosols. Permafrost-Affected Soils. Berlin: Springer Verlag. 275-290.

Ping, C. L., Michaelson, G. J., Packee, E. C., Stiles, C. a., Swanson, D. K., and Yoshikawa, K. (2005): Soil Catena Sequences and Fire Ecology in the Boreal Forest of Alaska. Soil Science Society of America Journal, 69(6), 1761. doi:10.2136/sssaj2004.0139.

Ping, C. L., Michaelson, G. J., Jorgenson, M. T., Kimble, J. M., Epstein, H., Romanovsky, V. E. and Walker, D. A. (2008): High stocks of soil organic carbon in the North American Arctic region. Nature Geoscience. 1: 615-619.

Ping, C. L., Michaelson, G. J., Kane, E. S., Packee, E. C., Stiles, C. A., Swanson, D. K. and Zaman, N. D. (2010): Carbon Stores and Biogeochemical Properties of Soils under Black Spruce Forest, Alaska. Soil Sci Soc Am J 2010, 74: 969-978.

Ping, C.-L., Michaelson, G.J., Guo, L., Jorgenson, M.T., Kanevskiy, M., Shur, Y., Dou, F., and Liang, J. (2011): Soil carbon and material fluxes across the eroding Alaska Beaufort Sea coastline. J. Geophys. Res. 116, G02004.

Post, W.M., Emanuel, W.R., Zinke, P.J. and Stangenberger, A.G. (1982): Soil carbon pools and world life zones. Nature. 298: 156-159.

Post, W.M. (2006): Organic matter, global distribution in world ecosystems. In: Encyclopedia of Soil Science, 2nd edn (Hrsg. R. Lal), pp.1216–1221. Taylor and Francis, New York.

Rivkina, E., Shcherbakova, V., Laurinavichius, K., Petrovskaya, L., Krivushin, K., Kraev, G., Pecheritsina, S. and Gilichinsky, D. (2007): Biogeochemistry of methane and methanogenic archaea in permafrost. FEMS Microbiology Ecology, 61: 1-15.

Roshydromet (2011): Russian Federal Service for Hydrometeorology and Environmental Monitoring. http://www.worldweather.org, 2011.08.08.

Rozhkov, V.A., Wagner, V. B., Kogut, B. M., Konyushkov, D. E., Nilsson, S., Sheremet, V. B. and Shvidenko, A. Z. (1996): Soil Carbon Estimates and Soil Carbon Map for Russia. Working Paper WP-96-60. International Institute for Applied Systems Analysis, Laxenburg, Austria.

Russia's Weather Server (2013): Weather Archive for Sakha. http://meteo.infospace.ru, 2013.08.08.

Sachs, T., Wille, C., Boike, J. and Kutzbach, L. (2008): Environmental controls on ecosystem-scale CH4 emission from polygonal tundra in the Lena River. . Journal of Geophysical Research-Biogeosciences, 113, G00A03: 12pp.

Sachs, T., Giebels, M., Boike, J. and Kutzbach, L. (2010): Environmental controls on CH4 emission from polygonal tundra on the micro-site scale in the Lena River Delta, Siberia. Global Change Biol, 16(11), 3096-3110. doi:10.1111/j.1365-2486.2010.02232.x.

Sanders, T., Fiencke, C. and Pfeiffer, E.-M. (2010): Small-Scale Variability of Dissolved Inorganic Nitrogen (DIN), C/N Ratios and Ammonia Oxidizing Capacities in Various Permafrost Affected Soils of Samoylov Island, Lena River Delta, Northeast Siberia. Polarforschung 80 (1): 23-35.

Sanders, T. (2011): Charakterisierung Ammoniak oxidierender Mikroorganismen in Böden kalter und gemäßigter Klimate und ihre Bedeutung für den globalen Stickstoffkreislauf. Diss. Universität Hamburg, p 155.

Sazonova, T. S., Romanovsky, V. E., Walsh, J. E., Sergueev, D. O. (2004): Permafrost dynamics in the 20th and 21st centuries along the East Siberian transect. J. Geophys. Res., 109, D01108, doi:10.1029/2003JD003680.

Schaefer, K., Zhang, T., Bruhwiler, L. and Barrett, A. P. (2011): Amount and timing of permafrost carbon release in response to climate warming. Tellus B, 63: 165–180. doi: 10.1111/j.1600-0889.2011.00527.x.

Schimel, J. P., Reynolds, J. F., Tenhunen, J. D., Kielland, K. and Chapin F. S. III. (1996): Nutrient availability and uptake by tundra plants. In: Ecological studies analysis and synthesis, vol 120: landscape function and disturbance in arctic tundra. New York: Springer-Verlag. pp 203–221.

Schirrmeister, L., Grosse, G., Wetterich, S., Overduin, P.P., Strauss, J., Schuur, E.A.G. and Hubberten, H.-W. (2011a): Fossil organic matter characteristics in permafrost deposits of the northeast Siberian Arctic. Journal of Geophysical Research, Vol 116: G00M02, 16pp.

Schirrmeister, L., Grosse, G., Schnelle, M., Fuchs, M., Krbetschek, M., Ulrich, M., Kunitsky, V., Grigoriev, M., Andreev, A., Kiensat, F., Meyer, H., Babiy, O., Klimova, I., Bobrov, A., Wetterich, S. and Schwamborn, G. (2011b): Late Quaternary paleoenvironmental records from the western Lena Delta, Arctic Siberia. Paleogeography, Paleoclimatology, Paleoecology 299: 175-196.

Schneider, J., Grosse, G., and Wagner, D. (2009): Land cover classification of tundra environments in the Arctic Lena Delta based on Landsat 7 ETM+ data and its application for upscaling of methane emissions. Remote Sens. Environ. 113, 380–391.

Schuur, E., Bockheim, J., Canadell, J., Euskirchen, E., Field, C. and Goryachkin, S. (2008): Vulnerability of permafrost carbon to climate change: Implications for the global carbon cycle. In: Biogeoscience 58 (8): 701-714.

Schuur, E., Vogel, J., Crummer, K., Lee, H., Sickman, J. and Osterkamp, T. (2009): The effect of permafrost thaw on old carbon release and net carbon exchange from tundra. Nature, 459 (7246). 556-559.

Schwamborn, G., Rachold, V., and Grigoriev, M.N. (2002): Late quaternary sedimentation history of the Lena Delta. Quaternary International 89: 119-134.

Schwertmann, U. (1964): Differenzierung der Eisenoxide des Bodens durch photochemische Extraktion mit saurer Ammoniumoxalat-Lösung. In: Zeitschrift für Pflanzenernährung, Düngung und Bodenkunde. Bd. 105, S. 194.

Shaver, G. R., Chapin, F. S. III and Gartner, B. L. (1986): Factors limiting seasonal growth and peak biomass accumulation in Eriophorum vaginatum in Alaskan [USA] tussock tundra. J Ecol 74: 257–278.

Shi Y. (ed) (1988): Map of Snow, Ice and Frozen Ground in China (1:4000000), with explanatory notes. China Cartographic Publishing House. Peking.

Shishov, L., Tonkonogov, V., Lebedeva, I., Gerasimova, M. and Krasilnikov, P. (1997): Russian Soil Classification System. Moscow.

Shishov, L., Tonkonogov, V., Lebedeva, I., Gerasimova, M. and Krasilnikov, P. (2004): Russian Soil Classification System: Second Approximation. Moscow.

Shcherbakova, V., Rivkina, E., Pecheritsyna, S., Laurinavichius, K., Suzina, N. and Gilichinsky, D. (2011): Methanobacterium arcticum sp. nov., a methanogenic archaeon from Holocene Arctic permafros. International Journal of Systematic and Evolutionary Microbiology, 61: 144-147.

Shur, Y. L., and Ping, C. L. (1994): Permafrost dynamics and soil formation. In “Proceedings of the Meeting of the Classification, Correlation, and Management of Permafrost-Affected Soils, July, 1993” (J. M. Kimble and R. J. Ahrens, Eds.), pp. 112–117. USDA, Soil Conservation Service, National Soil Survey Center, Lincoln, NE.

Simkin, T., Tilling, R. I., Vogt, P. R., Kirby, S. H., Kimberly, P. and Stewart, D. B. (2006): This dynamic planet; world map of volcanoes, earthquakes, impact craters, and plate tectonics: U.S. Geological Survey Geologic Investigations Series Map I-2800.

SIPRE auger. Jon's Machine Shop (http://jonsmachine.com/); 350 Goldstream Rd; Fairbanks, Alaska 99712-1007.

Smith, C.A.S. and Veldhuis, H. (2004): Cryosols of the Boreal, Subarctic, and Western Cordillera Regions of Canada. In: Kimble, J.M. (Hrsg.). Cryosols. Permafrost-Affected Soils. Berlin: Springer Verlag. 119-138.

Smith, L. C., MacDonald, G. M., Velichko, A. A., Beilman, D. W., Borisova, O. K., Frey, K. E., Kremenetski, K. V., and Sheng, Y. (2004): Siberian peatlands a net carbon sink and global methane source since the early Holocene, Science, 303(5656), 353–356, doi:10.1126/science.1090553.

Soil Survey Staff (2010): Keys to Soil Taxonomy. United States Department of Agriculture and Natural Resources Conservation Service, Washington, D.C: 329pp.

Sokolov, I.A., Ananko, T.V. and Konyushkov, D.Ye. (2004): The Soil Cover of Central Siberia. In: Kimble, J.M. (Hrsg.). Cryosols. Permafrost-Affected Soils. Berlin: Springer Verlag. 303-338.

Solomonov, N. G. and Larionov, C. V. (1994): Ust-Lensky Zapovednik. Institute of Biology of the University of Yakutsk, Report, p 4.

STIHL BT 121. ANDREAS STIHL AG and Co. KG. 2006. Instruction Manual.

Stolbovoi, V. (2002): Carbon in Russian soils. Climatic change, 55: 131-156.

Stolbovoi, V. (2006): Soil carbon in the forests of Russia, Mitig. Adapt. Strategies Glob. Change, 11, 203– 222, doi:10.1007/s11027-006-1021-7.

Stolbovoi and McCallum (2002): Land Resources of Russia database. http://webarchive.iiasa.ac.at/Research/FOR/russia_cd/guide.htm

Targulyan, V.O. (1971): Soil formation and weathering in cold humid zones. Moscow, 267pp.

Tarnocai, C. and Smith, C.A.S. (1992): The formation and properties of soils in the permafrost regions of Canada. In: Cryosols: the Effect of Cryogenesis on the Processes and Peculiarities of Soil Formation. Proceedings of the 1st International Conference on

Cryopedology. November 10-16, Pushchino, Russia (Hrsg. D.A. Gilichinsky): 21-42. Russian Academy of Sciences, Pushchino, Russia.

Tarnocai, C. and Ballard, M. (1994): Organic carbon in Canadian soils. In: Soil Processes and Greenhouse Effect (Hrsg. R. Lal, J.M. Kimble and E. Levine): 31-45. USDA Soil Conservation Service, Lincoln, NE.

Tarnocai, C., Kimble, J. and Broll, G. (2003): Determining carbon stocks in Cryosols using the Northern and Mid Latitudes Soil Database, in Permafrost, vol. 2, edited by M. Philips, S. Springman, and L. U. Arenson: 1129-1134.

Tarnocai, C. (2004): Cryosols of Arctic Canada. In: Kimble, J.M. (Hrsg.). Cryosols. Permafrost-Affected Soils. Berlin: Springer Verlag. 95-118.

Tarnocai C., Swanson D., Kimble J. and Broll G. (2007): Northern Circumpolar Soil Carbon Database, Digital Database. Research Branch, Agriculture and Agri-Food Canada, Ottawa, Canada.

Tarnocai, C., Canadell, J.G., Schuur, E.A.G., Kuhry, P. Mazhitova, G. and Zimov, S. (2009): Soil organic carbon pools in the northern circumpolar permafrost region. Global Biogeochemical Cycles 23, GB2023: 11pp.

Ulrich, M., Grosse, G., Chabrillat, S., and Schirrmeister, L. (2009): Spectral characterization of periglacial surfaces and geomorphological units in the Arctic Lena Delta using field spectrometry and remote sensing. Remote Sensing of Environment, 113(6), 1220–1235. doi:10.1016/j.rse.2009.02.009.

van Cleve, K. (1974): Organic matter quality in relation to decomposition. Proceedings of the Microbiology, Decomposition and Invertebrate Working Groups Meeting (IBP), Fairbanks 1973: 311-324.

van der Molen, M.K., van Huissteden, J., Parmentier, F.J.W., Petrescu, A.M.R., Dolman, A.J., Maximov, T.C., Kononov, A.V., Karsanaev, S.V. and Suzdalov, D.A. (2007): The growing season greenhouse gas balance of a continental tundra site in the Indigirka lowlands, NE Siberia. Biogeosciences 4: 985-1003.

van Everdingen, R.O. (Hrsg.) (1998, revised 2005): Multi-Language Glossary of Permafrost and Related Ground-Ice Terms. National Snow and Ice Data Center/World Data Center for Glaciology.

Vardy, S.R., Warner, B.G., Turunen, J. and Aravena, R. (2000): Carbon accumulation in permafrost peatlands in the Northwest Territories and Nunavut, Canada. The Holocene 10, 2: 273–280.

VDLUFA - Verband Deutscher Landwirtschaflicher Untersuchungs- und Forschungsanstalten, V. (1991): Methodenbuch 1: Untersuchung von Böden. Lose Blattsammlung. VDLUFA-Verlag, Darmstadt.

Vieira, G., Bockheim, J., Guglielmin, M., Balks, M., Abramov, A. and Boelhouwers, J. (2010): Thermal State of Permafrost and Active-layer Monitoring in the Antarctic: Advances During the International Polar Year 2007-2009. Permafrost Periglac 21 (2): 182-197.

Wagner, D., Gattinger, A., Embacher, A., Pfeiffer, E.-M., Schloter, M. and Lipski, A. (2007): Methanogenic activity and biomass in Holocene permafrost deposits of the Lena Delta, Siberian Arctic and its implication for the global methane budget. Global Change Biology 13: 1089-1099.

Wagner, D., Kobabe, S. and Liebner, S. (2009): Bacterial community structure and carbon turnover in permafrost-affected soils of the Lena Delta, northeastern Siberia. Canadian Journal of Microbiology, 55: 73-83.

Wagner, D. and Liebner, S. (2009): Global Warming and Carbon Dynamics in Permafrost Soils: Methane Production and Oxidation. In: Margesin, R. (Hrsg.): Permafrost Soils. Berlin: Springer Verlag. 219-236.

Waldrop, M. P., Wickland, K. P., White III, R., Berhe, A. A., Harden, J. W., and Romanovsky, V.(2010): Molecular investigations into a globally important carbon pool: permafrost-protected carbon in Alaskan soils, Global Change Biology, 16, 2543–2554, doi: 10.1111/j.1365-2486.2009.02141.x.

Walker, H. J.: Arctic Deltas, Journal of Coastal Research, 14(3), 718-738, 1998.

Washburn, A. L. (1980): Geocryology: a survey of periglacial processes and environments. Wiley, 01.01.1980, 406 pp.

Weintraub, M. N. and Schimel, J. P. (2003): Interactions between carbon and nitrogen mineralization and soil organic matter chemistry in arctic tundra soils. Ecosystems 6:129-143.

Wetterich, S., Kuzmina, S., Kuznetsova, T., Andreev, A.A., Kienast, F., Meyer, H., Schirrmeister, L. and Sierralta, M. (2008): Paleoenvironmental dynamics inferred from late Quaternary permafrost deposits on Kurungnakh Island, Lena Delta, Northeast Siberia, Russia. Quaternary Science Reviews 27: 1523-1540.

Wille, C., Kutzbach, L., Sachs, T., Wagner, D. and Pfeiffer, E.-M. (2008): Methane emission from Siberian arctic polygonal tundra: eddy covariance measurements and modeling. Global Change Biology. 14, 6: 1395-1408.

Wüthrich, C., Möller, I. and Thannheiser, D. (1999): CO2-fluxes in different plant communities of a high-Arctic tundra watershed (Western Spitsbergen). In Journal of Vegetation Science 10 (3): 413-420.

Yershov, E. D., Kondrat'yeva, K. A., Loginov, V. F. and Sychev, I. K. (1991): Geocryological Map of Russia and Neighbouring Republics, Faculty of Geology, Chair of Geocryology, Lomonosov Moscow State University.

Zhang, T., Barry, R.G., Knowles, K., Ling, F. and Armstrong, R.L. (2003): Distribution of seasonally and perennially frozen ground in the Northern Hemisphere. In: Swets and Zeitlinger (Hrsg.) Permafrost. Phillips, Springman, and Arenson.

Zhang, T., Barry, R.G. Knowles. K., Heginbottom. J.A. and Brown, J. (1999): Statistics and characteristics of permafrost and ground ice distribution in the Northern Hemisphere. Polar Geography 23(2): 147-169.

Zimov, S.A., Voropaev, Y.V., Semiletov, I.P., Davidov, S.P., Prosiannikov, S.F., Chapin, F.S., Chapin, M.C., Trumbore, S. and Tyler, S. (1997): North Siberian lakes: A methane source fuelled by Pleistocene carbon, Science 277: 800-802.

Zimov, S.A., Schuur, E.A.G. and Chapin, F.S. III. (2006a): Permafrost and the Global Carbon Budget. Science. 312: 1612-1613.

Zimov, S.A., Davydov, S.P., Zimova, G.M., Davydova, A.I., Schuur, E.A.G., Dutta, K. and Chapin III, F.S. (2006b): Permafrost carbon: Stock and decomposability of a globally significant carbon pool, Geophys. Res. Lett., 33, L20502, doi:10.1029/2006GL027484.

Zubrzycki, S. (2009): Geographisch-bodenkundliche Untersuchungen zur Charakterisierung von rezenten und Paläoböden des sibirischen Permafrostes im Bereich der Laptewsee. University of Hamburg, 112 pp.

Zubrzycki, S. (2012): Drilling frozen soils in Siberia. Polarforschung 81(2): 151-153.

Zubrzycki, S., Wetterich, S., Schirrmeister, L., Germogenova, A. and Pfeiffer, E.-M. (2008): Iron-Oxides and Pedogenesis of Modern Gelisols and Paleosols of the Southern Lena Delta, Siberia, Russia., In: Kane, D.L. and Hinkel, K.M. (Hrsg.) Proceedings of the 9th International Conference on Permafrost, University of Alaska Fairbanks, Institute of Northern Engineering: 2095-2100.

Zubrzycki, S., Kutzbach, L. and Pfeiffer, E.-M. (2012a): Böden in Permafrostgebieten der Arktis als Kohlenstoffsenke und Kohlenstoffquelle (Soils in arctic permafrost regions as carbon sink and source). Polarforschung 81(1): 33-46.

Zubrzycki, S., Kutzbach, L., Vakhrameeva, P. and Pfeiffer, E.-M. (2012b): Variability of Soil Organic Carbon Stocks of Different Permafrost Soils: Initial Results from a North-South Transect in Siberia. In: Hinkel, K.M. (Eds.) Proceedings of the 10th International Conference on Permafrost. Salekhard, pp. 485-490.

Zubrzycki, S., Kutzbach, L., Grosse, G., Desyatkin, A. and Pfeiffer, E.-M. (2013): Organic Carbon and Total Nitrogen Stocks in Soils of the Lena River Delta. Biogeosciences, 10, 3507-3524, doi:10.5194/bg-10-3507-2013.

8. Acknowledgements

I am particularly grateful to my supervisors Professor Dr. Eva-Maria Pfeiffer and Professor Dr. Lars Kutzbach who gave me the opportunity and a lot of freedom to develop and to work on this project. I am especially thankful to Eva-Maria Pfeiffer who several years ago gave the incredibly interesting lesson series “Böden der kalten Klimate” at the Institute of Soil Science. By these lessons, I was infected by her enthusiasm for the permafrost regions and permafrost-affected soils. I am very grateful to Lars Kutzbach for his continuous support during this project and the motivating scientific discussions. His ability to transfer thoughts into mathematical equations is incredible!

Working at the Institute of Soil Science contains a lot of laboratory work. This time only was bearable due to the great technical personnel. For their help in the laboratory I would like to thank all technicians and Hiwi-students. Special thanks are due to Susanne Kopelke who always was eager to answer questions on improving work and on reasons for any not comprehensible step during the laboratory work.

The author would like to thank the Lena Delta Reserve, especially Aleksander Gukov for the possibility to perform the study within the nature reserve. I thank the Alfred-Wegener-Institute in Potsdam and the “Hydro-Base” in Tiksi for logistical support. Special thanks go to Dmitri Bolshiyanov from the Arctic and Antarctic Research Institute, Irina Federova and Vladimir Churun from the Otto-Schmidt-Laboratory in St. Petersburg for using their laboratory facilities and help. I am thankful to Aleksander Derevyagin from the Moscow State University. He provided giant help with organizing of a last minute cargo transport for my permafrost augers and therefore directly contributed to the success of this thesis! Mikhail Grigiriev from the Institute for Permafrost provided not only great logistical support. He always was willing to discuss about the “so called” river terraces of non-river origin. Thank you Misha!

Special thanks are due to Günter Stoof and Waldemar Schneider who have always been supportive with technical and logistical ideas during the expeditions to the Lena River Delta. These expeditions always were great times due to terrific participants. I want to thank all of you! There was one extraordinary expedition in April 2011, which earns a special

consideration. Without Moritz Langer and Pete Schreiber I would never had tried neither flambéed fries nor Samoylov pizza. Thank you guys for the best expedition ever! The preparations for this special spring expedition were done in Yakutsk and surroundings where I received great help by my colleagues from the Institute for Permafrost and the Institute for Biological Problems of the Cryolithozone. Special thanks go to Anna Urban and Aleksey Desyatkin. We three drilled the first cores of the season!

Special thanks go to my parents for their great support during the last three years. My most special thanks go to Katja for the continuous encouragement especially during the last work-intensive months of finishing this thesis.

This study was supported through (1) a dissertation fellowship funded through the University of Hamburg (HmbNFG), (2) the Cluster of Excellence "CliSAP" (EXC177), University of Hamburg, funded through the German Research Foundation (DFG), and (3) a grant founded through the German Academic Exchange Service "DAAD" PKZ: D/10/01863.